ISSN 0021-9673

VOL. 606 NO. 2 AUGUST 14, 1992

THIS ISSUE COMPLETES VOL. 606

JOURNAL OF CHROMATOGRAPHY

INCLUDING ELECTROPHORESIS AND OTHER SEPARATION METHODS

ELSEVIER

JOURNAL OF CHROMATOGRAPHY

INCLUDING ELECTROPHORESIS AND OTHER SEPARATION METHODS

Scope. The *Journal of Chromatography* publishes papers on all aspects of chromatography, electrophoresis and related methods. Contributions consist mainly of research papers dealing with chromatographic theory, instrumental development and their applications. The section *Biomedical Applications*, which is under separate editorship, deals with the following aspects: developments in and applications of chromatographic and electrophoretic techniques related to clinical diagnosis or alterations during medical treatment; screening and profiling of body fluids or tissues with special reference to metabolic disorders; results from basic medical research with direct consequences in clinical practice; drug level monitoring and pharmacokinetic studies; clinical toxicology; analytical studies in occupational medicine.

Submission of Papers. Manuscripts (in English; *four* copies are required) should be submitted to: Editorial Office of *Journal of Chromatography*, P.O. Box 681, 1000 AR Amsterdam, Netherlands, Telefax (+31-20) 5862 304, or to: The Editor of *Journal of Chromatography, Biomedical Applications*, P.O. Box 681, 1000 AR Amsterdam, Netherlands. Review articles are invited or proposed by letter to the Editors. An outline of the proposed review should first be forwarded to the Editors for preliminary discussion prior to preparation. Submission of an article is understood to imply that the article is original and unpublished and is not being considered for publication elsewhere. For copyright regulations, see below.

Publication. The *Journal of Chromatography* (incl. *Biomedical Applications*) has 39 volumes in 1992. The subscription prices for 1992 are:

J. Chromatogr. (incl. *Cum. Indexes, Vols. 551–600*) + *Biomed. Appl.* (Vols. 573–611):
Dfl. 7722.00 plus Dfl. 1209.00 (p.p.h.) (total *ca.* US$ 4880.25)

J. Chromatogr. (incl. *Cum. Indexes, Vols. 551–600*) only (Vols. 585–611):
Dfl. 6210.00 plus Dfl. 837.00 (p.p.h.) (total *ca.* US$ 3850.75)

Biomed. Appl. only (Vols. 573–584):
Dfl. 2760.00 plus Dfl. 372.00 (p.p.h.) (total *ca.* US$ 1711.50).

Subscription Orders. The Dutch guilder price is definitive. The US$ price is subject to exchange-rate fluctuations and is given as a guide. Subscriptions are accepted on a prepaid basis only, unless different terms have been previously agreed upon. Subscriptions orders can be entered only by calender year (Jan.–Dec.) and should be sent to Elsevier Science Publishers, Journal Department, P.O. Box 211, 1000 AE Amsterdam, Netherlands, Tel. (+31-20) 5803 642, Telefax (+31-20) 5803 598, or to your usual subscription agent. Postage and handling charges include surface delivery except to the following countries where air delivery via SAL (Surface Air Lift) mail is ensured: Argentina, Australia, Brazil, Canada, China, Hong Kong, India, Israel, Japan*, Malaysia, Mexico, New Zealand, Pakistan, Singapore, South Africa, South Korea, Taiwan, Thailand, USA. *For Japan air delivery (SAL) requires 25% additional charge of the normal postage and handling charge. For all other countries airmail rates are available upon request. Claims for missing issues must be made within three months of our publication (mailing) date, otherwise such claims cannot be honoured free of charge. Back volumes of the *Journal of Chromatography* (Vols. 1–572) are available at Dfl. 217.00 (plus postage). Customers in the USA and Canada wishing information on this and other Elsevier journals, please contact Journal Information Center, Elsevier Science Publishing Co. Inc., 655 Avenue of the Americas, New York, NY 10010, USA, Tel. (+1-212) 633 3750, Telefax (+1-212) 633 3990.

Abstracts/Contents Lists published in Analytical Abstracts, Biochemical Abstracts, Biological Abstracts, Chemical Abstracts, Chemical Titles, Chromatography Abstracts, Clinical Chemistry Lookout, Current Contents/Life Sciences, Current Contents/Physical, Chemical & Earth Sciences, Deep-Sea Research/Part B: Oceanographic Literature Review, Excerpta Medica, Index Medicus, Mass Spectrometry Bulletin, PASCAL-CNRS, Pharmaceutical Abstracts, Referativnyi Zhurnal, Research Alert, Science Citation Index and Trends in Biotechnology.

US Mailing Notice. *Journal of Chromatography* (main section ISSN 0021-9673, *Biomedical Applications* section ISSN 0378-4347) is published (78 issues/year) by Elsevier Science Publishers (Sara Burgerhartstraat 25, P.O. Box 211, 1000 AE Amsterdam, Netherlands). Annual subscription price in the USA US$ 4880.25 (subject to change), including air speed delivery. Application to mail at second class postage rate is pending at Jamaica, NY 11431. **USA POSTMASTERS:** Send address changes to *Journal of Chromatography*, Publications Expediting, Inc., 200 Meacham Avenue, Elmont, NY 11003. Airfreight and mailing in the USA by Publication Expediting.

See inside back cover for Publication Schedule, Information for Authors and information on Advertisements.

0021-9673/92/$05.00

Printed in the Netherlands

CONTENTS

(Abstracts/Contents Lists published in Analytical Abstracts, Biochemical Abstracts, Biological Abstracts, Chemical Abstracts, Chemical Titles, Chromatography Abstracts, Current Awareness in Biological Sciences (CABS), Current Contents/Life Sciences, Current Contents/Physical, Chemical & Earth Sciences, Deep-Sea Research/Part B: Oceanographic Literature Review, Excerpta Medica, Index Medicus, Mass Spectrometry Bulletin, PASCAL-CNRS, Referativnyi Zhurnal, Research Alert and Science Citation Index)

REGULAR PAPERS

Column Liquid Chromatography

Gas Chromatography

Electrophoresis

SHORT COMMUNICATIONS

Column Liquid Chromatography

Continued overleaf

Discover new solutions . . .

"Dr. Jones, this is Retriever™ 500. . . the smallest hundred-tube fraction collector.

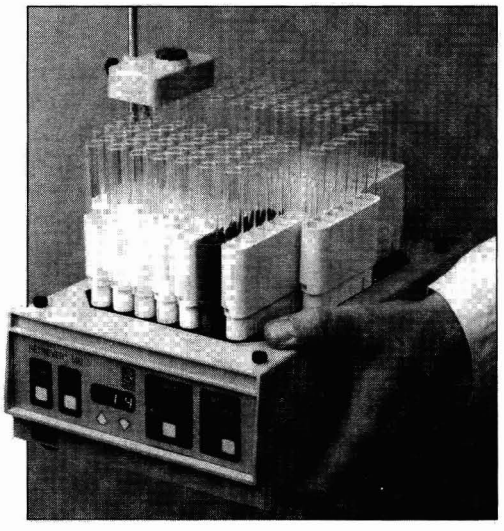

And the most affordable."

Here's the solution to crowded labs – the all-new Retriever 500. It fits right into your HPLC or low- pressure LC system, and hides anywhere in a cramped coldroom. Its multiple-rack, linear-movement configuration lets you remove filled tube groups at any time.

Only the size of this page, Retriever 500 still holds 102 thirteen mm test tubes; 68 large tubes or MiniVials; or 24 full-size scintillation vials. Time, drop, or pumped-volume control is standard. If an Isco Wiz peristaltic pump is used, you can even set the fraction size on the Retriever 500 directly in 1 ml or 0.1 ml increments. Accurate peak collection is available when used with a UA-6 detector.

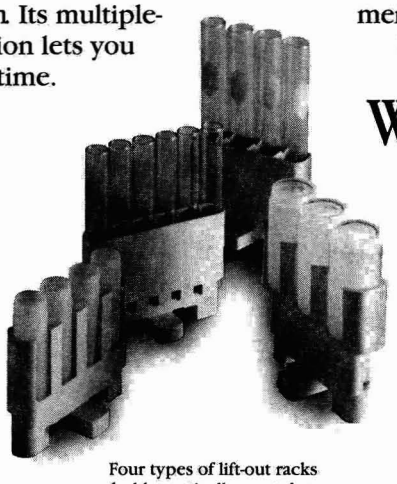

Four types of lift-out racks hold practically any tube.

Retriever 500 has coldroom-proof electronics, thorough spill protection, and a mechanism proven in over 30,000 similar Isco instruments. It's designed to give you reliable performance year after year.

With Retriever 500, you can stay within your budget and still keep up with Dr. Jones.

Order Now!

In the U.S., call **(800)228-4250.** Outside the U.S., contact your Isco distributor.

Isco, Inc., P.O. Box 5347
Lincoln NE 68505, U.S.A.

Isco Europe AG, Brüschstr. 17
CH8708 Männedorf, Switzerland
Fax (41-1)920 62 08

ISCO

Distributors • Australia: Australian Chromatography Co. • **Austria:** INULA • **Belgium:** Mettler-Toledo S.A. • **Canada:** Canberra Packard Canada, Ltd.• **Denmark:** Mikrolab Aarhus • **Finland:** ETEK OY • **France:** Ets. Roucaire, S.A. • **Germany:** Colora Messtechnik GmbH • **Italy:** Analytical Control Italia S.p.A. • **Japan:** JSI Co. Ltd. • **Korea:** Sang Chung, Ltd. • **The Netherlands:** Beun-de Ronde B.V. • **Norway:** Dipl. Ing. Houm A.S. • **Spain:** VARIAN-CHEMICONTROL, S.L. • **Sweden:** Spectrochrom AB • **Switzerland:** IG Instrumenten-Gesellschaft AG • **UK:** Jones Chromatography Ltd. •

Wilson and Wilson's Comprehensive Analytical Chemistry Volume XXIX

Chemiluminescence Immunoassay

by **I. Weeks**, *University of Wales, College of Medicine, Cardiff, UK*

Series editor: **Prof. G. Svehla**, *Department of Chemistry, University College, Cork, Ireland*

Chemiluminescence immunoassay is now established as one of the best alternatives to conventional radioimmunoassay for the quantitation of low concentrations of analytes in complex samples. During the last two decades the technology has evolved into analytical procedures whose performance far exceeds that of immunoassays based on the use of radioactive labels. Without the constraints of radioactivity, the scope of this type of analytical procedure has widened beyond the confines of the specialist clinical chemistry laboratory to other disciplines such as microbiology, veterinary medicine, agriculture, food and environmental testing. This is the first work to present the topic as a subject in its own right.

In order to provide a complete picture of the subject, overviews are presented of the individual areas of chemiluminescence and immunoassay with particular emphasis on the requirements for interfacing chemiluminescent and immunochemical reactions. The possible ways of configuring chemiluminescence immunoassays are described. State-of-the-art chemiluminescence immunoassay systems are covered in detail together with those systems which are commercially available.

The book is aimed at researchers and routine laboratory staff in the life sciences who wish to make use of this high-performance analytical technique and also at those interested in industrial applications of the technology in the food, agricultural and environmental sciences.

1992 xvi + 294 pages
Price: US $ 151.50 / Dfl. 295.00
Subscription price:
US $ 136.00 / Dfl. 265.00
ISBN 0-444-89035-1

Elsevier Science Publishers

P.O. Box 211, 1000 AE Amsterdam, The Netherlands
P.O. Box 882, Madison Square Station, New York, NY 10159, USA

FOR ADVERTISING INFORMATION PLEASE CONTACT OUR ADVERTISING REPRESENTATIVES

USA/CANADA

Weston Media Associates

Mr. Daniel S. Lipner
P.O. Box 1110, GREENS FARMS, CT 06436-1110
Tel: (203) 261-2500, Fax: (203) 261-0101

GREAT BRITAIN

T.G. Scott & Son Ltd.

Tim Blake
Portland House, 21 Narborough Road
COSBY, Leicestershire LE9 5TA
Tel: (0533) 753-333, Fax: (0533) 750-522

Mr. M. White or Mrs. A. Curtis
30-32 Southampton Street, LONDON WC2E 7HR
Tel: (071) 240 2032, Fax: (071) 379 7155,
Telex: 299181 adsale/g

JAPAN

ESP - Tokyo Branch

Mr. S. Onoda
20-12 Yushima, 3 chome, Bunkyo-Ku
TOKYO 113
Tel: (03) 3836 0810, Fax: (03) 3839-4344
Telex: 02657617

REST OF WORLD

ELSEVIER SCIENCE PUBLISHERS

Ms. W. van Cattenburch
P.O. Box 211, 1000 AE AMSTERDAM,
The Netherlands
Tel: (20) 515.3220/21/22, Telex: 16479 els vi nl
Fax: (20) 683.3041

Capillary Electrophoresis

Principles, Practice and Applications

by **S.F.Y. Li**, *National University of Singapore, Singapore*

Journal of Chromatography Library Volume 52

Capillary Electrophoresis (CE) has had a very significant impact on the field of analytical chemistry in recent years as the technique is capable of very high resolution separations, requiring only small amounts of samples and reagents. Furthermore, it can be readily adapted to automatic sample handling and real time data processing. Many new methodologies based on CE have been reported. Rapid, reproducible separations of extremely small amounts of chemicals and biochemicals, including peptides, proteins, nucleotides, DNA, enantiomers, carbohydrates, vitamins, inorganic ions, pharmaceuticals and environmental pollutants have been demonstrated. A wide range of applications have been developed in greatly diverse fields, such as chemical, biotechnological, environmental and pharmaceutical analysis.

This book covers all aspects of CE, from the principles and technical aspects to the most important applications. It is intended to meet the growing need for a thorough and balanced treatment of CE. The book will serve as a comprehensive reference work and can also be used as a textbook for advanced undergraduate and graduate courses. Both the experienced analyst and the newcomer will find the text useful.

Contents:

1992 xxvi + 586 pages
Price: US$ 225.50 / Dfl. 395.00
ISBN 0-444-89433-0

TO ORDER

Contact your regular supplier or:

ELSEVIER SCIENCE PUBLISHERS
P.O. Box 211
1000 AE Amsterdam
The Netherlands

Customers in the USA & Canada:

ELSEVIER SCIENCE PUBLISHERS
Attn. Judy Weislogel
P.O. Box 945
Madison Square Station
New York, NY 10160-0757, USA

No postage will be added to prepaid book orders. US $ book prices are valid only in the USA and Canada. In all other countries the Dutch guilder (Dfl.) price is definitive. Customers in The Netherlands please add 6% BTW. In New York State please add applicable sales tax. All prices are subject to change without prior notice.

ELSEVIER
SCIENCE PUBLISHERS

Announcement from the Publisher

ELSEVIER SCIENCE PUBLISHERS

prefers the submission of electronic manuscripts

Electronic manuscripts have the advantage that there is no need for the rekeying of text, thereby avoiding the possibility of introducing errors and resulting in reliable and fast delivery of proofs.

The preferred storage medium is a $5\frac{1}{4}$ or $3\frac{1}{2}$ inch disk in MS-DOS format, although other systems are welcome, e.g. Macintosh.

Your disk and (**exactly matching**) printed version (printout, hardcopy) should be submitted together to the accepting editor. In case of revision, the same procedure should be followed such that, on acceptance of the article, the file on disk and the printout are **identical**. Both will then be forwarded by the editor to Elsevier.

Please follow the general instructions on style/arrangement and, in particular, the reference style of this journal as given in 'Instructions to Authors'.

Please label the disk with your name, the software & hardware used and the name of the file to be processed.

Further information can be found under 'Instructions to Authors - Electronic manuscripts'.

Contact the Publisher for further information.

ELSEVIER SCIENCE PUBLISHERS B.V.
P.O. Box 330, 1000 AH Amsterdam
Netherlands
Fax: (+31-20) 5862-304

4/92

Journal of Chromatography, 606 (1992) 153–163
Elsevier Science Publishers B.V., Amsterdam

CHROM. 24 300

Plate-height equation for non-linear chromatography

Wen-Chien Lee

Department of Chemical Engineering, Chung Yuan Christian University, Chung-Li (Taiwan)

(First received June 11th, 1991; revised manuscript received April 14th, 1992)

ABSTRACT

A height equivalent to a theoretical plate (HETP) equation for non-linear chromatography was derived analytically based on an equilibrium–non-equilibrium theory. The band-broadening factors including non-linear behaviour of the adsorption isotherm and kinetics of adsorption–desorption and mass transfer were all considered. The contributions of sample concentration, inhibitor concentration and sample size to plate height were explicitly expressed. Some significant advantages of the proposed plate-height equation were demonstrated by the agreement between the experimental data from a concanavalin A–sugar system and the calculated results. In a limiting case, this plate-height equation can reduce to the HETP expression for linear chromatography. It is easier to use this HETP equation in scaling-up a non-linear chromatographic process and in determining the thermodynamic and kinetic constants characterizing non-linear chromatography.

INTRODUCTION

The theory of non-linear chromatography has been well developed during the last few years. Excellent reviews of theoretical analyses and modelling methods of non-linear chromatography include the works of Lin *et al.* [1], Lee *et al.* [2], Cowan *et al.* [3] and Liapis [4]. The concept of non-linear chromatography takes into account the non-linear isotherm of equilibrium between the solute in the mobile phase and the solute on the inner surface of the adsorbent. Experimentally, samples with a very large volume and/or mass have to be considered in preparative chromatography, which can rarely be regarded as a linear process as interactions between solute molecules are unavoidable. Preparative chromatography is therefore sometimes called non-linear chromatography [1]. In non-linear chromatography, peak shapes and band spreading are affected by the solute's competition for adsorbent sites, sample size and various mass transfer resistances. As a result, peak shape and band spreading are complex functions of the equilibrium isotherm, mass transfer parameters, packing properties and operating conditions [2]. Unfortunately, no theory of non-linear chromatography that encompasses all the usual chromatographic broadening factors is available. For the past few decades, the height equivalent to a theoretical plate (HETP) has been used to characterize the chromatographic efficiency and band broadening of the elution peak [5]. Typical HETP equations for linear chromatography explicitly contain terms contributed by eddy diffusion, longitudinal molecular diffusion, film mass transfer, pore diffusion and surface adsorption resistances [6]. However, the plate-height equations generally found in the literature are limited to linear chromatography. In this work, a novel, closed-form plate-height equation for non-linear chromatography was developed based on an equilibrium–non-equilibrium theory. The focos was placed on the effects of isotherm non-linearity.

THEORY

Equilibrium–non-equilibrium theory

In this work the plate-height equation for non-linear chromatography is based on equilibrium–

Correspondence to: Dr. W.-C. Lee, Department of Chemical Engineering, Chung Yuan Christian University, Chung-Li, Taiwan.

0021-9673/92/$05.00

non-equilibrium theory. In this theory, the capacity factor is regarded as a thermodynamic invariant and can be predicted by the local equilibrium model, whereas the plate-height is obtained from both the isotherm non-linearity and the departure from equilibrium. To obtain a plate-height expression we used the same assumption as made by Knox and Pyper [7] and Golshan-Shirazi and Guiochon [8] that the column HETP is the sum of two independent contributions:

$$H = H_{\text{ther}} + H_{\text{kin}} \tag{1}$$

The thermodynamic contribution to the plate-height, H_{ther}, results from the non-linear behaviour of the equilibrium isotherm. On the other hand, the contribution H_{kin} is attributed to the non-equilibrium due to a finite rate of adsorption–desorption and mass transfer. Eqn. 1 is not exactly correct as the convolution theorem used to sum the contributions for plate-height is only valid for a linear system. It is nevertheless a reasonable approximation which is often used by investigators working in overload chromatography [7–10]. Lucy and Carr [11] recently demonstrated that eqn. 1 is valid under a wide range of chromatographic conditions. The derivation of each contribution in eqn. 1 is given as the follows.

Solution of local equilibrium model and capacity factor

The local equilibrium model (theory), also called the ideal model [8], has been thoroughly studied for non-linear chromatography in the measurement of association and inhibition constants [12]. Golshan-Shirazi and Guiochon [8,13] used this model for the simulation of band profiles in chromatography in the case of a Langmuir isotherm. In a local equilibrium model, the mass transfer resistances due to axial dispersion, film mass transfer and pore diffusion are assumed to be negligible and the adsorption–desorption interaction is assumed to be very rapid. As a result, the concentrations of the solute in the pore and in the bulk fluid are all the same and denoted by C. If equilibrium prevails throughout the column, the concentration of the solute in the mobile phase, C, and the concentration of the solute on the inner surface of the solid, q, is related by an equilibrium isotherm. The governing equations for a single solute pulse and Langmuir equilibrium are

$$u_0 \cdot \frac{\partial C}{\partial z} + \varepsilon_t \cdot \frac{\partial C}{\partial t} + (1 - \varepsilon)\rho_p \cdot \frac{\partial q}{\partial t} = 0 \tag{2}$$

$$q = \frac{q_s K_L C}{1 + K_L C} \tag{3}$$

The solutions for this local equilibrium model with a rectangular input which has concentration C_0 and width t_0 are obtainable by applying the method of characteristics. The concentrations of the solute at the outlet of a column of length L are given by [12,14]

$$C = \begin{cases} \dfrac{1}{K_L}\left[\sqrt{\dfrac{(1-\varepsilon)\rho_p q_s K_L L}{u_0(t - t_0) - \varepsilon_t L}} - 1\right], & t_f \leqslant t \leqslant t_e \\ 0, \quad \text{otherwise} \end{cases} \tag{4}$$

where t_f and t_e are the retention times of the shock front and the tailing edge, respectively, and given by

$$t_f = t_0 + \frac{L}{u_0}\left[\varepsilon_t + \left(\sqrt{(1-\varepsilon)\rho_p q_s K_L} - \sqrt{t_0 u_0 K_L C_0 / L}\right)^2\right] \tag{5}$$

and

$$t_e = t_0 + \frac{L}{u_0}\left[\varepsilon_t + (1-\varepsilon)\rho_p q_s K_L\right] \tag{6}$$

If

$$t_0 > (1-\varepsilon)\rho_p q_s K_L \left(\frac{L}{u_0}\right) \frac{K_L C_0}{(1 + K_L C_0)^2}$$

then the concentrations are given by

$$C = \begin{cases} C_0, & t_f \leqslant t \leqslant t_x \\ \dfrac{1}{K_L}\left[\sqrt{\dfrac{(1-\varepsilon)\rho_p q_s K_L L}{u_0(t - t_0) - \varepsilon_t L}} - 1\right], & t_x \leqslant t \leqslant t_e \\ 0, \quad \text{otherwise} \end{cases} \tag{7}$$

where

$$t_x = t_0 + \frac{L}{u_0}\left[\varepsilon_t + \frac{(1-\varepsilon)\rho_p q_s K_L}{(1 + K_L C_0)^2}\right] \tag{8}$$

t_e is defined as in eqn. 6, but t_f is given by

$$t_f = \frac{L}{u_0}\left[\varepsilon_t + \frac{(1-\varepsilon)\rho_p q_s K_L}{(1 + K_L C_0)}\right] \tag{9}$$

Substituting the concentration profiles, eqns. 4–9, into the definition of the first moment,

$$\mu_1 = \int_0^\infty Ct\mathrm{d}t / \int_0^\infty C\mathrm{d}t \qquad (10)$$

an expression for the first moment can be obtained. The capacity factor, k', is thus given by $k' = (\mu_1 - t_m)/t_m$, where t_m is the retention time of the unretained solute. After taking the integration for μ_1 (*i.e.*, eqn. 10) and assuming that the injection volume of the sample is relatively small compared with the retention volume, *i.e.*, $(u_0 t_0/L\varepsilon_t)/k'_0 \ll 1$, we obtain the capacity factor as

$$k' = k'_0 \Phi(a) \qquad (11)$$

where $\Phi(a)$ is a universal function presented in Table I and a is defined as

$$a = \sqrt{\left(\frac{t_0 u_0}{L}\right)\frac{C_0}{(1-\varepsilon)\rho_p q_s}}$$

The value of a reflects the amount of relative feed concentration and sample size. The parameter a can be defined as

$$a = \sqrt{\left(\frac{t_0 u_0}{L\varepsilon_t}\right)\left(\frac{K_L C_0}{k'_0}\right)}$$

a combination of three non-dimensional factors, k'_0, $(t_0 u_0/L\varepsilon_t)$ and $K_L C_0$, where the last two represent the non-dimensional quantities of sample size and sample concentration, respectively. The quantity k'_0 represents the capacity factor in the case of zero concentration, *i.e.*, the capacity factor when the chromatographic process is linear and no interaction occurs between solutes. As shown in eqn. 11, the capacity factor in non-linear chromatography is no longer a constant as it is in linear chromatography. The Langmuir isotherm derives from the linear isotherm by a universal function Φ of a, due to the overload effect of sample concentration. This universal function $\Phi(a)$ is obtained directly by integration of the first moment using the concentration profiles, eqns. 4–9. As listed in Table I, the universal function is simply $1 - 4a/3 + a^2/2$ for $a \leqslant 1$ and $1/(6a^2)$ for $a > 1$.

TABLE I

UNIVERSAL FUNCTIONS OF LOADING FACTOR IN NON-LINEAR CHROMATOGRAPHY

Universal function			Application
$\Phi(a) =$	$1 - \frac{4}{3}a + \frac{a^2}{2}$	$a \leqslant 1$[a]	Capacity factor: $k' = k'_0\Phi(a)$
	$\frac{1}{6a^2}$	$a \geqslant 1$	
$\Psi(a) =$	$\frac{\frac{2}{9}a^2 - \frac{4}{15}a^3 + \frac{1}{12}a^4}{\left(1 - \frac{4}{3}a + \frac{1}{2}a^2\right)^2}$	$a \leqslant 1$	Thermodynamic contribution to HETP: $H_{ther} = \left(\frac{k'}{1+k'}\right)^2 L\Psi(a)$
	$\frac{36}{15}a^2 - 1$	$a \geqslant 1$	
$\theta(a) =$	$\frac{a^2}{2a - a^2}$	$a \leqslant 1$	Average equilibrium concentration: $K_L C^* = \theta(a)$
	a^2	$a \geqslant 1$	

[a] The universal function $\Phi(a)$ in ref. 25 was derived based on the solution with a printed error presented in ref. 12, it should be corrected to that in this table.

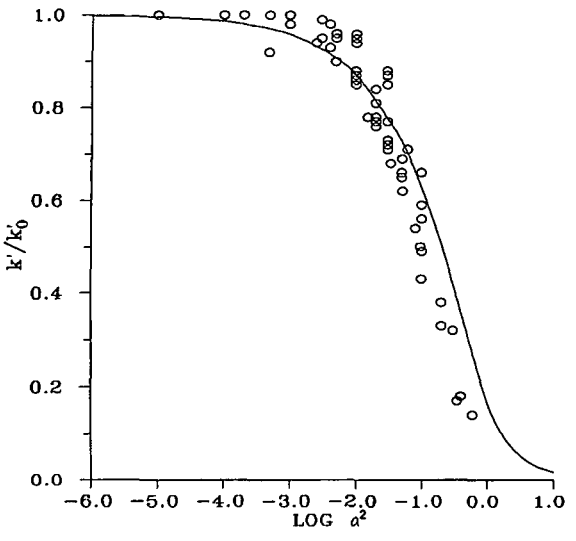

Fig. 1. Comparison of capacity factors calculated by eqn. 11 (solid line) and obtained from Craig model simulation given by Eble *et al.* [15] (data points).

To confirm the validity of eqn. 11, we compared the calculated results using eqn. 11 with the data from Craig simulation of overload separations. The "band" values of the capacity factor k' from Craig simulation are read from Table I in the paper by Eble *et al.* [15]. Fig. 1 shows that the data from Craig simulations cluster about the curve predicted by eqn. 11. As the Craig simulations for these data are carried out for a broad range of conditions, we believe that eqn. 11 is valid not only for local equilibrium but also for the cases with a finite rate of adsorption–desorption and mass transfer. Fig. 1 also shows that the onset of the concentration overload effect seems to occur at $a \approx 0.08$ (10% deviation from linear theory).

The capacity factor can be regarded as a thermodynamic property only when the elution time is independent of various mass transfers, *i.e.*, flow velocity. Wade *et al.* [16] have shown, in the case of infinitesimal sample volume, that the slow kinetics of mass transfer and adsorption–desorption tend to delay the decrease in elution time with increasing solute concentration. However, the kinetic dependence of the capacity factor is a trivial problem since the effect of mass transfers on capacity factor is relatively small, as Wade *et al.* [16] concluded. With the support of Fig. 1, we may conclude that the capacity factor can be regarded as a thermodynamic invariant. Eqn. 11 shows that k'/k'_0 also can be represented as a function of non-dimensional sample concentration $K_L C_0$ and relative sample volume, denoted by $(t_0 u_0/L\varepsilon_t)/k'_0$. In contrast to the effect of slow kinetics, an increase in relative sample volume promotes a decrease in capacity factor (and elution time) beginning at lower solute concentration, as shown in Fig. 2.

Thermodynamic contribution to the plate height

Golshan-Shirazi and Guiochon [8] used the concentration profiles (eqns. 4, 5 and 6) to obtain the column height equivalent to a theoretical plate. They called the "thermodynamic" contribution the plate height, H_{ther}, which results from the non-linear behaviour of the equilibrium isotherm. Accordingly, they derived two equations for the plate number of an ideal model band, *i.e.*, eqns. 38 and 40 in their work. Actually, the non-linear isotherm effect is coupled with that of concentration overload through the loading factor, denoted a^2 in this paper. The pure volume overload due to a larger injection interval is negligible. Other similar plate-height equations for the contribution of non-linear isotherms are summarized in Table II.

Using the concentration profiles given by eqns. 4–9 and the following definition of plate height [11]:

$$H = \frac{\mu'_2}{\mu_1^2} \cdot L \tag{12}$$

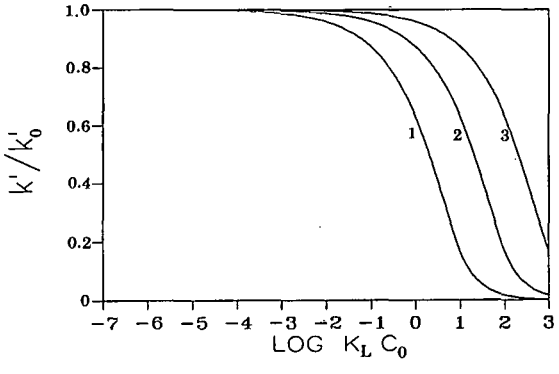

Fig. 2. Effects of sample size on the dependence of capacity factor on concentration, $\left(\frac{t_0 u_0}{L\varepsilon_t}\right)\Big/k'_0$ = (1) 0.1, (2) 0.01 and (3) 0.001.

TABLE II

EXPRESSIONS FOR THE THERMODYNAMIC CONTRIBUTION TO PLATE HEIGHT

Source	H_{ther}
Golshan-Shirazi and Guiochon, eqn. 38 [8]	$L\left[5.54\frac{(2-a)^4}{(4a-a^2)^2}\right]^{-1}\left[1+\frac{1}{(1-a)^2}\left(\frac{a^2}{K_L C_0}+\frac{1}{k'_0}\right)\right]^{-2}$
Golshan-Shirazi and Guiochon, eqn. 40 [8]	$L\left[\frac{16}{(2a-a^2)^2}\right]^{-1}\left[\frac{1}{k'_0}+a^2/(K_L C_0)+(1-a)^2\right]^{-2}$
This work	$L\left[\frac{k'_0\Phi(a)}{1+k'_0\Phi(a)}\right]^2\Psi(a)$
Knox and Pyper [7]	$\frac{L}{4}\left(\frac{k'_0}{1+k'_0}\right)^2 a^2$
Snyder *et al.* [17]	$\frac{3}{8}L\left(\frac{k'_0}{1+k'_0}\right)^2 a^2$
Jenke [18]	$\frac{c}{k'}La^2$ (c is an experimental constant)

in which μ'_2 is the second central moment, we obtained the thermodynamic contribution to the plate height as

$$H_{ther} = L\left[\frac{k'_0\Phi(a)}{1+k'_0\Phi(a)}\right]^2\Psi(a) \qquad (13)$$

where $\Psi(a)$ and $\Phi(a)$, resulting from the integrations for the first moment and the second central moment with the application of the concentration profiles given by eqns. 4–9, are universal functions of the loading factor in non-linear chromatography as shown in Table I. A calculation not shown here revealed that eqn. 13 gives values in the middle of those predicted by eqns. 38 and 40 of Golshan-Shirazi and Guiochon [8] with the parameter values for typical affinity chromatography.

The plate height defined by eqn. 12 takes advantage of the fact that the plate height can be calculated from the experimental chromatogram or from the profile predicted by the mass balance model. In addition, the assumption of a Gaussian chromatographic peak is not needed in applying this definition. With the aid of computer calculations and data acquisition, it becomes easier to characterize a peak by its statistical moments, which can be measured from the chromatogram.

The other expressions in Table II are either empirical or experimental. It should be noted that the notation a^2 used in this paper is exactly the same as that of L_f in Golshan-Shirazi and Guiochon's work [8]. The loading factor a^2 also is equal to w_x/w_s, the ratio of the mass of solute injected to the saturation capacity of the column [7,17,18]. The larger is a^2, the greater is the concentration overload effect. We may conclude that the plate height resulting from the non-linear behaviour of the equilibrium isotherm is the contribution of concentration overload through a loading factor.

Plate height due to non-equilibrium

To obtain H_{kin} in eqn. 1, we should reconsider the mass balance model as represented by eqns. 2 and 3. When a Langmuir kinetics relationship is used to account for a finite rate of adsorption–desorption kinetics, eqn. 3 should be replaced by

$$\frac{\partial q}{\partial t} = k^*_a(q_s - q)C - k^*_d q \qquad (14)$$

while eqn. 2 remains unchanged. If adsorption–desorption processes are slow compared with all diffusion processes, the rate parameters k^*_a and k^*_d in eqn. 14 are the true adsorption and desorption rate constants, respectively. Experimentally, Chase [19] and Arnold and Blanch [20] used the model eqns. 2

and 14 successfully to interpret the results of affinity chromatography for protein purification.

Whenever the mass transfer contribution is comparable to the adsorption–desorption contribution, the rate constants k_a^* and k_d^* should be regarded as the effective overall rate constants that combine the effects of mass transfer and chemical kinetic limitations of the binding interaction. For this reason, the model including eqns. 2 and 14 is called the lumped rate constants model. Based on the "linear driving force" concept of Hiester and Vermeulen [21], as noted by Arnold and Blanch [20], combination of the mass transfer rate constant k_{mass} and the true desorption rate constant k_d yields the following effective desorption rate constant:

$$\frac{1}{k_d^*} = \frac{1}{k_d} + \frac{(1-\varepsilon)\rho_p q_s K_L}{2k_{mass}}\left(\frac{2 + K_L C_0}{1 + K_L C_0}\right) \quad (15)$$

where

$$k_{mass} = \frac{6(1-\varepsilon)}{d_p}\left(\frac{1}{k_f} + \frac{1}{10}\cdot\frac{d_p}{D_i}\right)^{-1} \quad (16)$$

Wade *et al.* [16] also obtained a similar relationship between true and effective rate constants. However, in the following derivation of plate height, k_d^* is regarded as independent of concentration, which is believed to be realistic in ion-exchange and affinity chromatography.

The lumped rate constants model (eqns. 2 and 14) has often been used for the simulation of chromatography operated in the frontal mode and in the zonal mode. Although the lumped rate constants model with different kinds of boundary conditions has been solved and reported by Thomas [22], Hiester and Vermeulen [21], Goldstein [23], Aris and Amundson [14], Chase [19], Arnold and Blanch [20] and Wade *et al.* [16], the calculations for the moments can only be done numerically and an explicit form of the plate-height expression is not possible.

In this work, an extension of the non-equilibrium theory developed originally by Giddings [24] was made to obtain the plate height due to the non-equilibrium by starting from the lumped rate constants model (eqns. 2 and 14). According to the non-equilibrium theory [24], the solute in a chromatographic zone is slightly out of equilibrium owing to the moving concentration gradient and the inability of equilibration to keep up with it. Plate height can be related to the extent of departure from equilibrium, as the departure is found to be directly responsible for zone (band) spreading. By following the approach developed by Giddings, the plate height resulting from non-equilibrium for non-linear chromatography with a Langmuir isotherm was derived as eqn. A10 in the Appendix. It is a function of equilibrium concentration in the mobile phase, C^*. A detailed derivation is given in the Appendix. An average equilibrium concentration was then introduced to express C^* by taking the average value of solute concentrations between the elution times for the shock front and the tailing edge when the chromatographic process is in equilibrium, *i.e.*,

$$C^* = \int_{t_f}^{t_e} C\,dt \Big/ \int_{t_f}^{t_e} dt \quad (17)$$

where the concentration profile C is given by eqns. 4 and 7. Eqn. 17 results in the third universal function $\theta(a)$ as presented in Table I. Accordingly, the kinetic contribution to the plate height is given by

$$H_{kin} = \frac{2u_0}{\varepsilon_t}\cdot\frac{1}{k_d^*}\cdot\frac{k_0'[1+\theta(a)]}{\{k_0' + [1+\theta(a)]^2\}^2} \quad (18)$$

Plate-height equation for non-linear chromatography

Finally, substituting eqns. 13 and 18 into eqn. 1 we obtained the following plate-height equation for non-linear chromatography:

$$H = L\left[\frac{k_0'\Phi(a)}{1 + k_0'\Phi(a)}\right]^2 \Psi(a) + \frac{2u_0}{\varepsilon_t}\cdot\frac{1}{k_d^*}\cdot\frac{k_0'[1+\theta(a)]}{\{k_0' + [1+\theta(a)]^2\}^2} \quad (19)$$

Clearly, when the feed concentration C_0 approaches zero, both $\theta(a)$ and $\Psi(a)$ vanish, and eqn. 19 becomes the plate height due to slow kinetics in linear chromatography. It is noted that eqn. 19 is so far the only explicit expression of plate height for non-linear chromatography. Further, it seems useful in optimizing and scaling up non-linear chromatographic processes.

In eqn. 19, we used an effective rate constant k_d^* to lump the effects of slow adsorption–desorption and all mass transfers but not axial dispersion, and assumed that k_d^* is independent of sample concentration. This assumption is realistic when the

adsorption–desorption contribution to the peak spreading outweighs the mass transfer contribution, as in ion-exchange and affinity chromatography. We may let N_0 denote the plate number determined under linear conditions, and rewrite eqn. 19 as

$$\frac{1}{N} = \frac{1}{N_{\text{ther}}} + \frac{1}{N_0}\left(\frac{H_{\text{kin}}}{H_0}\right) \tag{20}$$

where

$$\frac{H_{\text{kin}}}{H_0} = \frac{[1 + k'_0]^2[1 + \theta(a)]}{\{k'_0 + [1 + \theta(a)]^2\}^2} \tag{21}$$

In eqn. 20, $H_0 = L/N_0$ and $H_{\text{ther}} = L/N_{\text{ther}}$. The plate number predicted by eqns. 20 and 21 is comparable to that obtained from the lumped rate constants model and calculated by Craig simulation. A general agreement was found from the plot of N/N_0 values calculated by eqns. 20 and 21 *versus* the simulated N/N_0 by the Craig model as shown in Fig. 3. The Craig simulation data are read from the "band" values of N/N_0 in Table I in the paper by Eble *et al.* [15].

Obviously, eqn. 20 is slightly different from that given in the literature by a factor H_{kin}/H_0. The contribution of this factor is significant provided that the plate height due to kinetic non-equilibrium is much greater than that due to isotherm non-linearity. This case occurs when the rate of adsorption and desorption kinetics are slow. In all instances, the plots of N *versus* the loading factor a^2

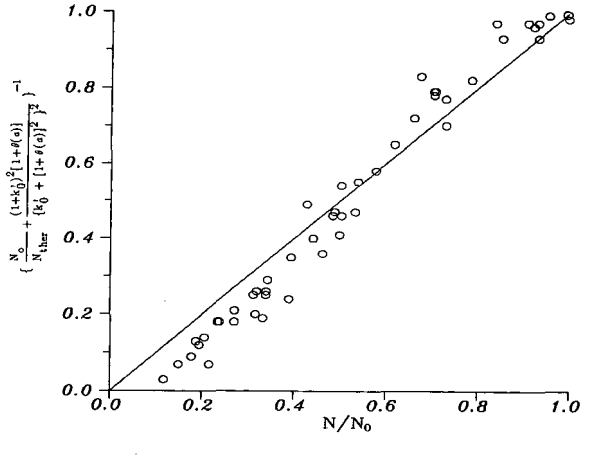

Fig. 3. Comparison of N/N_0 simulated from Craig model, as in Table I in the paper by Eble *et al.* [15] (abscissa) and the values calculated by eqns. 20 and 21 (ordinate).

according to eqns. 20 and 21 will reveal that the plate number decreases with increasing loading factor in a manner very similar to that previously published by Colin [10] and Golshan-Shirazi and Guiochon [8].

For multi-component systems, the afore-mentioned plate-height equations and the universal functions presented in Table I are still useful with minor modification. For example, consider a competing free (soluble) inhibition system in an affinity process [25,26]. A solute inhibitor (I), which competes with an immobilized ligand for the desired macromolecular compound, is present in the sample solution pre-equilibrated buffer. Assuming a constant concentration of I throughout the column during elution stage, all the above-mentioned equations are valid when the limiting capacity factor for the desired solute k'_0 is replaced by $k'_0/(1 + K_I C_I)$, where C_I and K_I are the concentration and the binding constant, respectively, of inhibitor I. According to ref. 25, the limiting capacity factor in the definition of a should also be changed to $k'_0/(1 + K_I C_I)$.

EXAMPLE

The use of this plate-height equation is demonstrated by the following example. Consider the adsorption of sugar, *p*-nitrophenyl-α-D-mannopyranoside (pNp)-mannoside, on to the inner surface of 50-μm concanavalin A (Con A)–silica packed in a column (5.0 cm × 0.3 cm I.D., 38 mg/g Con A, pore diameter 42 nm, $\varepsilon = 0.5$, $\varepsilon_p = 0.6$). The chromatographic system is operated at a flow-rate of 1 ml/min with an injection volume of 25 μl ($t_0 = 1.5$ s, $u_0 = 0.236$ cm/s). Variation of the experimental capacity factor and total plate height with injected concentration has been reported by Muller and Carr [27]. Using the equations derived in the previous section by assuming the capacity factor k' to be independent of mass transfer, the best fitting of the experimental and calculated capacity factors yielded $k'_0 = 13$ and $K_L = 1.6 \cdot 10^4$ lmol^{-1}. It was found that this fitted value of the binding constant K_L is identical with that reported by Muller and Carr [28]. The calculated plate height is obtained using eqn. 19 with a constant effective desorption constant $k_d^* = 0.1$ s^{-1}. The assumption employed here that the kinetics of adsorption–desorption are rate limiting is realistic in affinity chromatography, especially when

TABLE III

EXPERIMENTAL AND THEORETICAL VALUES OF THE CAPACITY FACTOR AND PLATE HEIGHT FOR THE EXAMPLE AS DESCRIBED IN THE TEXT[a]

C_0 (mM)	Experimental		k' calculated using eqn. 11 ($k'_0 = 13, K_L = 1.6 \cdot 10^4$ lmol^{-1})	Equilibrium–non-equilibrium theory			Lumped rate constants model: HETP (μm)
	k'	HETP (μm)		H_{ther}	H_{kin}	HETP (μm)	
0.1	11.4	4050	11.26	119	4063	4182	3980
0.2	10.6	4280	10.58	253	4127	4380	4110
0.4	9.7	5400	9.67	551	4219	4770	4350
0.6	9.2	4710	8.99	882	4292	5174	4560
0.8	8.4	5630	8.45	1243	4354	5597	4850
1.0	8.0	6090	7.99	1633	4409	6042	5180

[a] Theoretical values were generated from the best-fit parameters.

the immobilized ligand is a macromolecule such as Con A in this example. As suggested by Hethcote and DeLisi [29] and Arnold and Blanch [20], the mass transfer contribution can be reduced by immobilizing the macromolecular species and allowing the small molecules to diffuse to the binding site. The results are summarized in Table III for comparison. Obviously, the calculated HETP agrees with the experimental data. Also, this rate constant k_d^* is close to the value of k_d reported by Muller and Carr [28] (0.3 s^{-1}), but unfortunately they incorrectly took the HETP equation of linear chromatography from a paper by Horváth and Lin [6] for this nonlinear system. Table III indicates that the equilibrium–non-equilibrium theory is comparable to the lumped rate constants model in obtaining HETP to take account of band spreading. However, the lumped rate constants model predicted lower HETP values than the experimental values. The advantage of the proposed HETP equation based on the equilibrium–non-equilibrium theory, however, is very clear: it is simpler and easier to use.

Plots of the experimental and calculated HETP *versus* concentration are shown in Fig. 4. The calculated HETP is generated by eqn. 19 with the parameter values from the best fitting. It is clear that the HETP starting from a limiting value in the linear region at zero concentration increases with sample concentration. This is because at higher sample concentration, the fraction of unbound solutes increases and tends to be eluted rapidly. Further, the solute concentrations are scattered over the entire column and serious mixing is induced by concentration gradients, which increase the plate height. Plots of HETP *versus* linear velocity u_0 with various sample concentrations are shown in Fig. 5. A higher plate height accounts for much of the inefficiency of the chromatographic column when a higher concentration is applied. It is clear that the effect of concentration cannot be ignored even when the concentration is not really high. The larger is K_L, the much pronounced is the contribution of concentration overload. However, at very high concentrations, the concentration effect on the plate height may be traded off by the high flow velocity. The reason may be that a large fraction of the solute does not adsorb immediately, and elutes together at the

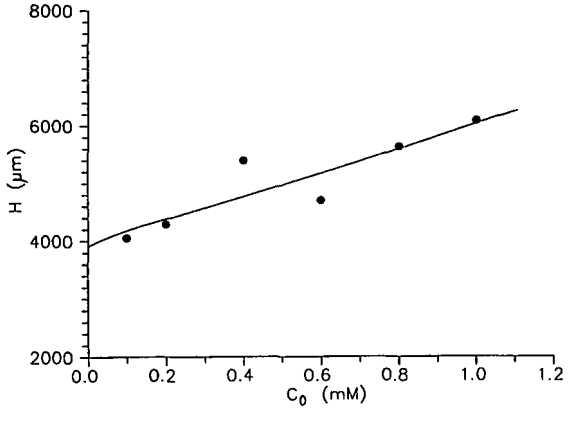

Fig. 4. Effects of sample concentration on plate height with $k'_0 = 13$, $K_L = 1.6 \cdot 10^6$ lmol^{-1}, $L = 5$ cm, $\varepsilon_t = 0.8$, $u_0 = 0.236$ cm/s, $t_0 = 1.5$ s and $k_d^* = 0.1$ s^{-1}. Calculated values were generated by eqn. 19.

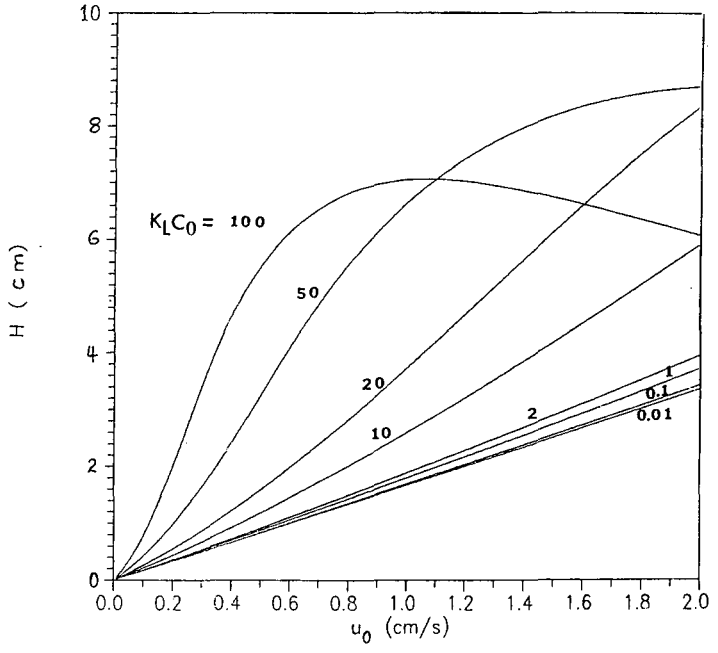

Fig. 5. Plate height as a function of flow velocity in non-linear chromatography. Parameter values are $L = 5$ cm, $\varepsilon_t = 0.8$, $t_0 = 1.5$ s, $k'_0 = 13$ and $k_d^* = 0.1\ s^{-1}$

dead volume under the condition of heavy concentration overload. Regardless the variation of plate height at high flow velocities, it is suggested that the effective desorption rate constant can be measured from the slope of these plots in the region of low velocity.

As shown in this example, one of the greatest advantages of the equations obtained in this work is that they provide a easier way for the determination of the thermodynamic constant K_L and rate constants. Experimentally, by varying the amount of sample mass or sample concentration, one can easily obtain measurements of the site density (k'_0/K_L) and equilibrium binding constant by using eqn. 11. Further, eqn. 19 provides a theory for the estimation of the effective desorption rate constant.

CONCLUSIONS

In non-linear chromatography, the sample concentration tends to sharpen the front of the sample pulse and to prolong the tailing. If the time interval of sample injection is relatively small compared with the total retention time, the effect of sample concentration on the capacity factor can be estimated using the local equilibrium model. The contribution of concentration to plate height due to the isotherm non-linearity is also obtainable from the same model. In the limiting case of zero sample concentration, the plate height due to a non-linear isotherm vanishes. This thermodynamic plate height contributed by isotherm non-linearity is given by eqn. 13.

A plate-height equation for non-linear chromatography (under isocratic condition) has been derived based on the equilibrium–non-equilibrium theory. With this theory, the retention time is assumed to be identical with that of the local equilibrium model and the capacity factor is calculated from this retention time. Both the departure from equilibrium contributed by slow adsorption–desorption and mass transfer and the self-sharpening and tailing effect of concentrations due to non-linear isotherms are responsible for band broadening (zone spreading). The overall plate-height equation, eqn. 19, accounts for this band broadening. For a multi-component inhibition system, the con-

tribution of competing inhibitor concentration to plate height is via the limiting capacity factor of the desired solute k'_0 and the loading factor a.

An example of non-linear chromatography has been used to demonstrate the application of the plate-height equation derived in this work. A comparison of calculated HETP and simulation results from the Craig model and the lumped rate constants model showed general agreement. Finally, it should be noted that the plate-height equation derived in this work can be easily used in scaling-up chromatography of biomolecules and in determining the thermodynamic and kinetic constants characterizing non-linear chromatography.

SYMBOLS

C Concentration of solute in bulk fluid phase, mol l^{-1}
C_0 Sample concentration, mol l^{-1}
C_I Concentration of inhibitor, mol l^{-1}
C_m Total concentration of solute in mobile phase, $= \varepsilon_t C$
C_s Total concentration of solute in stationary phase, $= (1 - \varepsilon)\rho_p q$
$\bar{C}$ $= C_m + C_s$
d_p Diameter of adsorbent particle, cm
D^* Apparent diffusion coefficient, $cm^2\ s^{-1}$
D_i Pore diffusivity of solute, $cm^2\ s^{-1}$
H HETP, plate height, cm
k' Capacity factor
k'_0 Capacity factor at zero sample concentration, $= (1 - \varepsilon)\rho_p q_s K_L/\varepsilon_t$
k_a Adsorption rate constant, $l mol^{-1}\ s^{-1}$
k_d Desorption rate constant, s^{-1}
k_d^* Effective desorption rate constant, s^{-1}
k_f Fluid film mass transfer coefficient of solute, cm s^{-1}
K_I Inhibition constant, $l mol^{-1}$
K_L Equilibrium binding constant, $= k_a/k_d$, $l mol^{-1}$
L Length of the column, cm
N Plate number, $= L/H$
q Sorbate concentration, mmol (g particle)$^{-1}$
q_s Maximum number of available binding sites, mmol (g particle)$^{-1}$
t Time, s
t_m Retention time of the unretained solute, $= \varepsilon_t L/u_0$, s
t_0 Time interval of sample injection, s
u Chromatographic velocity, $= u_0/\varepsilon_t$, cm s^{-1}
u^* Velocity of solute in local equilibrium, cm s^{-1}
u_0 Fluid superficial velocity, cm s^{-1}
z Linear coordinate along the packed bed, cm

Greek letters

ε Void fraction of packed bed, equal to the volume outside the particles divided by the empty column volume
ε_t Total void fraction in column
ρ_p Particle density, the density of packed stationary phase in column, g (cm^3 particle)$^{-1}$
μ_1 First moment, s
μ'_2 Second central moment, $= \int_0^\infty C(t - \mu_1)^2 dt / \int_0^\infty C dt$, s^2
$\in$ Parameter of departure from equilibrium

Superscript

* Value estimated at equilibrium

ACKNOWLEDGEMENT

This study was supported in part by the National Science Council of the Republic of China under contract NSC 80-0402-E033-03.

APPENDIX

Define C_m and C_s as the total concentrations of the solute in the mobile phase and the stationary phase, respectively. We can rewrite eqns. 2 and 14 as

$$\frac{\partial C_m}{\partial t} + u \cdot \frac{\partial C_m}{\partial z} \equiv S_m = k_d^* \left\{ C_s - \left[\frac{(1 - \varepsilon)\rho_p q_s - C_s}{\varepsilon_t} \right] K_L C_m \right\} \quad \text{(A1)}$$

where $u = u_0/\varepsilon_t$ and $K_L = k_a^*/k_d^*$.

When the net rate of mass transfer between phases through adsorption and desorption approaches zero, we have

$$0 = k_d^* \left\{ C_s^* - \left[\frac{(1 - \varepsilon)\rho_p q_s - C_s^*}{\varepsilon_t} \right] K_L C_m^* \right\} \quad \text{(A2)}$$

Obviously, the isotherm is Langmuiran. If we substitute $C_m^*(1 + \in_m)$ for C_m and $C_s^*(1 + \in_s)$ for C_s, we then have

$$S_m = k_d^* C_s^* \epsilon_s - \frac{k_d^* K_L}{\varepsilon_t} [(1-\varepsilon) q_s C_m^* + C_m^{*2} - C_s^* C_m^*] \epsilon_m \quad \text{(A3)}$$

where the ϵ terms represent the departures from equilibrium. In eqn. A3, the higher order term $\epsilon_s \epsilon_m$ has been ignored and ϵ_s relates to ϵ_m by $\epsilon_s = -\epsilon_m \cdot C_m^*/C_s^*$. With eqns. A2 and A3, we have

$$S_m = -k_d^* \left\{ C_m^* + \frac{K_L}{\varepsilon_t} [(1-\varepsilon)\rho_p q_s C_m^* + C_m^{*2} - C_s^* C_m^*] \right\} \epsilon_m \quad \text{(A4)}$$

When the near-equilibrium approximation applied, S_m can also given by

$$S_m \approx \frac{\partial C_m^*}{\partial t} + u \cdot \frac{\partial C_m^*}{\partial z} = (u - u^*) \frac{\partial C_m^*}{\partial z} \quad \text{(A5)}$$

where we have used the relationship of mass balance in local equilibrium:

$$\frac{\partial C_m^*}{\partial t} + u^* \cdot \frac{\partial C_m^*}{\partial z} = 0 \quad \text{(A6)}$$

In eqn. A6, u^* is given by $u^* = u/[1 + k'_0(1 + K_L C_m^*/\varepsilon_t)^{-2}]$. It is noted that $k'_0 = (1-\varepsilon)\rho_p q_s K_L/\varepsilon_t$.

Following the preceding formulation of plate height by Giddings [24], we define a mass flux related to u, $J = C_m u$. The zone spreading originates in the ΔJ term and $\Delta J = J - J^* = C_m^* \epsilon_m u$. Let $\bar{C}$ denote the sum of C_m and C_s. Applying the equilibrium relationship of C_m^* and C_s^*, we have

$$\frac{\partial \bar{C}}{\partial z} = \left[1 + \frac{k'_0}{(1 + K_L C_m^*/\varepsilon_t)^2} \right] \frac{\partial C_m^*}{\partial z} = \frac{u}{u^*} \cdot \frac{\partial C_m^*}{\partial z} \quad \text{(A7)}$$

For the total concentration $\bar{C}$, we may make a mass balance with an additional dispersion term:

$$\frac{\partial \bar{C}}{\partial t} + u \cdot \frac{\partial C_m}{\partial z} \approx \frac{\partial \bar{C}}{\partial t} + u^* \cdot \frac{\partial \bar{C}}{\partial z} \equiv D^* \cdot \frac{\partial^2 \bar{C}}{\partial z^2} \quad \text{(A8)}$$

where D^* is the apparent diffusion coefficient and is given by $D^* = -\Delta J/(\partial \bar{C}/\partial z)$. By definition, the plate height is related to the apparent diffusion coefficient D^* by

$$H = \frac{2D^*}{u^*} = \frac{-2C_m^* \epsilon_m u}{u^*(\partial \bar{C}/\partial z)} \quad \text{(A9)}$$

Solving for ϵ_m by equating eqns. A4 and A5 and substituting it into eqn. A9, we finally obtain the plate height H as a function of equilibrium concentration and lumped rate constant:

$$H = \frac{2(u - u^*)}{k_d^*[1 + k'_0 + (K_L C_m^*/\varepsilon_t) - (K_L C_s^*/\varepsilon_t)]} \quad \text{(A10)}$$

It is noted that $C_m^* = \varepsilon_t C^*$ and $C_s^* = (1-\varepsilon)\rho_p q_s K_L C^*/(1 + K_L C^*)$.

REFERENCES

1 B. Lin, Z. Ma, S. Golshan-Shirazi and G. Guiochon, *J. Chromatogr.*, 500 (1990) 185.
2 C. K. Lee, Q. Yu, S. U. Kim and N.-H. L. Wang, *J. Chromatogr.*, 484 (1989) 29.
3 C. H. Cowan, I. S. Gosling and W. P. Sweetenham, *J. Chromatogr.*, 484 (1989) 187.
4 A. I. Liapis, *J. Biotechnol.*, 11 (1989) 143.
5 J. A. Jonsson, *Chromatography Theory and Basic Principles*, Marcel Dekker, New York, 1987.
6 Cs. Horváth and H.-J. Lin, *J. Chromatogr.*, 149 (1978) 43.
7 J. H. Knox and H. M. Pyper, *J. Chromatogr.*, 363 (1986) 1.
8 S. Golshan-Shirazi and G. Guiochon, *Anal. Chem.*, 60 (1988) 2364.
9 S. Golshan-Shirazi and G. Guiochon, *J. Chromatogr.*, 506 (1990) 495.
10 H. Colin, *Sep. Sci. Technol.*, 24 (1987) 1933.
11 C. A. Lucy and P. W. Carr, *J. Chromatogr.*, 556 (1991) 159.
12 F. H. Arnold, S. A. Schofield and H. W. Blanch, *J. Chromatogr.*, 355 (1986) 1.
13 S. Golshan-Shirazi and G. Guiochon, *Anal. Chem.*, 61 (1989) 462.
14 R. Aris and N. R. Amundson, *Mathematical Methods in Chemical Engineering*, Prentice-Hall, Englewood Cliffs, NJ, 1973.
15 J. E. Eble, R. L. Grob, P. E. Antle and L. R. Snyder, *J. Chromatogr.*, 384 (1987) 25.
16 J. L. Wade, A. F. Bergold and P. W. Carr, *Anal. Chem.*, 59 (1987) 1286.
17 L. R. Snyder, G. B. Cox and P. E. Antle, *Chromatographia*, 24 (1987) 82.
18 D. R. Jenke, *J. Chromatogr.*, 479 (1989) 387.
19 H. A. Chase, *J. Chromatogr.*, 297 (1984) 179.
20 F. H. Arnold and H. W. Blanch, *J. Chromatogr.*, 355 (1986) 13.
21 N. K. Hiester and T. Vermeulen, *Chem. Eng. Prog.*, 48 (1952) 505.
22 H. C. Thomas, *J. Phys. Chem.*, 66 (1944) 1664.
23 S. Goldstein, *Proc. R. Soc. London*, Ser. A, 219 (1953) 151.
24 J.C. Giddings, *Dynamics of Chromatography*, Marcel Dekker, New York, 1965.
25 W.-C. Lee, G.-J. Tsai and G. T. Tsao, *J. Chromatogr.*, 504 (1990) 55.
26 R. R. Walters, *J. Chromatogr.*, 249 (1982) 19.
27 A. J. Muller and P. W. Carr, *J. Chromatogr.*, 357 (1986) 11.
28 A. J. Muller and P. W. Carr, *J. Chromatogr.*, 284 (1984) 33.
29 H. W. Hethcote and C. DeLisi, in I. M. Chaiken, M. Wilchek and I. Parikh (Editors), *Affinity Chromatography and Biological Recognition*, Academic Press, Orlando, FL, 1983, p. 119.

Journal of Chromatography, 606 (1992) 165–170
Elsevier Science Publishers B.V., Amsterdam

CHROM. 24 282

Multiple peak formation from reversed-phase liquid chromatography of recombinant human platelet-derived growth factor

E. Watson and W. C. Kenney

Amgen Inc., Amgen Center, Thousand Oaks, CA 91320 (USA)

(First received November 5th, 1991; revised manuscript received April 16th, 1992)

ABSTRACT

Reversed-phase liquid chromatography of recombinant platelet-derived growth factor (PDGF) results in the appearance of at least four distinguishable peaks. The relative areas of these peaks are, in part, dependent upon the gradient time and the temperature. Isolation and reinjection of each peak gave chromatographic profiles comparable to that obtained from unfractionated PDGF. Increasing the temperature above 60°C resulted in a single peak that, when isolated and reinjected at ambient temperature, produced a chromatogram comparable to PDGF which had not been exposed to elevated temperature. Sodium dodecyl sulfate–polyacrylamide gel electrophoresis showed that all four peaks had the same molecular mass as PDGF and were active as determined by a PDGF mitogenic bioassay. These results indicate that multiple conformations of PDGF are present and we postulate that their appearance may be a result of isomeric structures arising from the presence of Pro–Pro bonds within the primary structure of the protein.

INTRODUCTION

PDGF is one of a growing number of growth factors produced by recombinant protein techniques for possible use in wound healing. It has a molecular mass of *ca.* 28 000 and consists of two polypeptide chains denoted A and B which are about 50% similar in amino acid composition. These chains are linked by interchain disulfide bonds. The dimeric structure is essential for biological activity since upon reduction, PDGF is inactivated. In addition to the heterodimer, homodimers of the A and of the B chains have also been found in nature [1]. The amino acid sequence for PDGF-B monomer is shown in Fig. 1.

Recombinant derived proteins are often subjected to a variety of electrophoretic and chromatographic techniques in order to show that they are homogeneous and devoid of impurities. Commonly used techniques include: sodium dodecyl sulfate–polyacrylamide gel electrophoresis (SDS-PAGE), isoelectric focusing, and ion-exchange, hydrophobic-interaction and reversed-phase chromatography. The latter chromatographic technique has been the subject of numerous studies aimed at defining column and eluent parameters in order to better understand the retention process involved in these separations [2–11].

Ser- Leu- Gly- Ser- Leu- Thr- Ile- Ala- Glu- Pro-	10
Ala- Met- Ile- Ala- Glu- Cys- Lys- Thr- Arg- Thr-	20
Glu- Val- Phe- Glu- Ile- Ser- Arg- Arg- Leu- Ile-	30
Asp- Arg- Thr- Asn- Ala- Asn- Phe- Leu- Val- Trp-	40
Pro- Pro- Cys- Val- Glu- Val- Gln- Arg- Cys- Ser-	50
Gly- Cys- Cys- Asn- Asn- Arg- Asn- Val- Gln- Cys-	60
Arg- Pro- Thr- Gln- Val- Gln- Leu- Arg- Pro- Val-	70
Gln- Val- Arg- Lys- Ile- Glu- Ile- Val- Arg- Lys-	80
Lys- Pro- Ile- Phe- Lys- Lys- Ala- Thr- Val- Thr-	90
Leu- Glu- Asp- His- Leu- Ala- Cys- Lys- Cys- Glu-	100
Thr- Val- Ala- Ala- Ala- Arg- Pro- Val- Thr- Arg-	110
Ser- Pro- Gly- Gly- Ser- Gln- Glu- Gln- Arg	120

Fig. 1. Amino acid sequence of recombinant human PDGF-BB.

Correspondence to: Dr. E. Watson, Amgen Inc., Amgen Center, Thousand Oaks, CA 91320, USA.

0021-9673/92/$05.00

While developing a reversed-phase liquid chromatography (RPLC) method for PDGF, multiple peak formation was routinely observed regardless of the column source or gradient elution scheme used. This paper describes this unusual behavior for this protein. A proposed explanation for this observation is based upon *cis–trans* isomerization of peptide bonds containing Pro residues taking place within the time course of the chromatographic separation.

MATERIALS AND METHODS

The liquid chromatographic equipment consisted of a Model 8700 pump (Spectra-Physics), a Model SPG 6A variable-wavelength UV detector (Shimadzu) and a Chromjet integrator (Spectra-Physics). The columns used included a C_4 Vydac (250 × 4.6 mm I.D.; The Separations Group) and a TSK gel Octadecyl-NPR (35 × 4.6 mm I.D.; Toso Haas). The flow-rate was 1.0 ml/min in all experiments. Temperature control during the heating and cooling experiments was carried out using a column temperature controller (Anspec). Cooling experiments used an independent Nesslab Model RTE110 to regulate the temperature. PDGF used in this study is a homodimer of the B chain (human sequence, Fig. 1) and is derived from a bacterial expression system. SDS-PAGE was performed in 15% gels according to Laemmli [12]. A mitogenic assay was used to detect bioactivity of PDGF [13].

RESULTS

A number of procedures were used to established the homogeneity of PDGF and to aid in its characterization. These included SDS-PAGE, hydrophobic interaction chromatography, and size exclusion chromatography. Under these conditions a single component was obtained. When PDGF was chromatographed under RPLC conditions, however, a heterogeneous elution profile with typically four peaks, was present regardless of the source of the column, pore size, length, or whether the ligand was C_4 or C_{18} and was reproducible over a prolonged period. Fig. 2A and B show the chromatograms obtained when Toso Haas NPR C_{18} and Vydac C_4 columns were used. Peak ratios were dependent on the length of time for the gradient with longer gradient times favoring an increase in the slowest eluting peak.

The Toso Haas C_{18} column allowed for greater flexibility in manipulating conditions of gradient time and temperature, and all subsequent studies

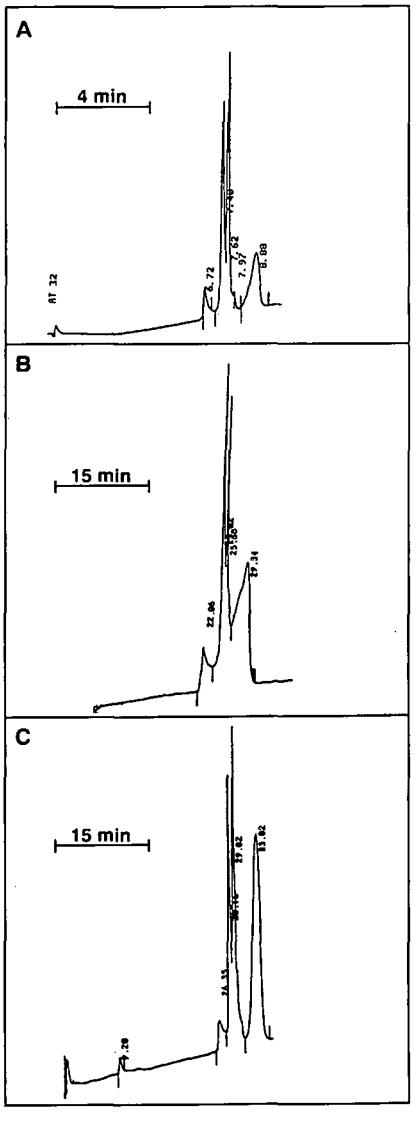

Fig. 2. RPLC profiles of PDGF-BB as a function of column type and length of gradient. (A) Toso Haas NPR C_{18}, gradient time 10 min; (B) Vydac C_4, gradient time 40 min; (C) Toso Haas NPR C18, gradient time 40 min. eluent A, 0.1% trifluoroacetic acid in water; B, 0.1% trifluoroacetic acid in acetonitrile, gradient from 12% to 15% B.

were carried out using this column. The Toso Haas C_{18} column is a polymer based micropellicular support with a relatively low binding capacity for proteins. A series of increasing amounts of PDGF from 5 to 23 μg did not affect the elution profile to any significant extent establishing that column overloading was not a contributing factor to multiple peak formation.

To examine the effect of column contact time, PDGF was injected and after a period of 30 s the flow-rate was maintained isocratically for 60 min at which time the gradient elution was started. The results showed that the relative amount of peak 4 increased by a factor of two while both peak 1 and peak 2 almost decreased in half. The influence of the column eluent on PDGF was also evaluated. This was performed in several ways. First, PDGF was incubated in 0.1% TFA for periods up to 24 h. Comparable chromatograms were obtained at all times examined indicating that acidic conditions did not effect the chromatographic behavior of PDGF. Second, PDGF was incubated in trifluoroacetic acid–water–acetonitrile (0.1:62.9:37), corresponding to the eluent composition where peak 4 eluted. After a period of 60 min, the sample was treated in one of two ways. In the first, dilution with 0.1% trifluoroacetic acid was made to achieve approximate initial eluent composition. In the second, the sample was injected directly. Evaluation of the elution profiles showed that no change had occurred.

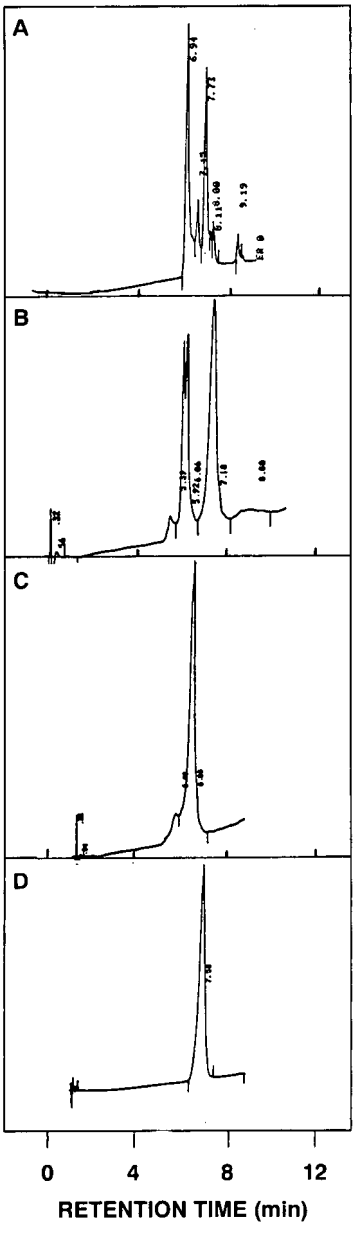

Fig. 3. RPLC profiles of PDGF-BB as a function of temperature. (A) −5°C, (B) 40°C, (C) 60°C, (D) 99°C.

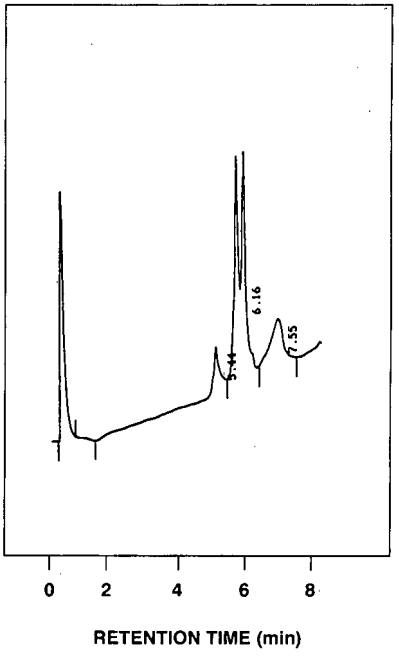

Fig. 4. Elution profile of PDGF-BB peak collected from 60°C chromatography (see Fig. 2C).

More dramatic changes were observed when temperature was varied. At −5°C, the profile shifted in favor of early eluting peaks. Because of the shifts in retention times, it was difficult to ascertain which of the early eluting peaks present at room temperature was increasing in intensity. As temperatures increased to 25, 40 and 60°C, there was a slight decrease in the retention times of the peaks with the peak profile shifting in favor of the later eluting peaks until at 60°C, a single peak was present and at 99°C this peak sharpened considerably (Fig. 3). Throughout these temperature evaluations, the total peak area remained essentially constant. The major peak remaining at 60°C was isolated and the eluent removed under vacuum. The material was dissolved in 0.1% TFA and injected into a column at room temperature. The peak profile observed (Fig. 4) was comparable to that obtained from unfractionated PDGF.

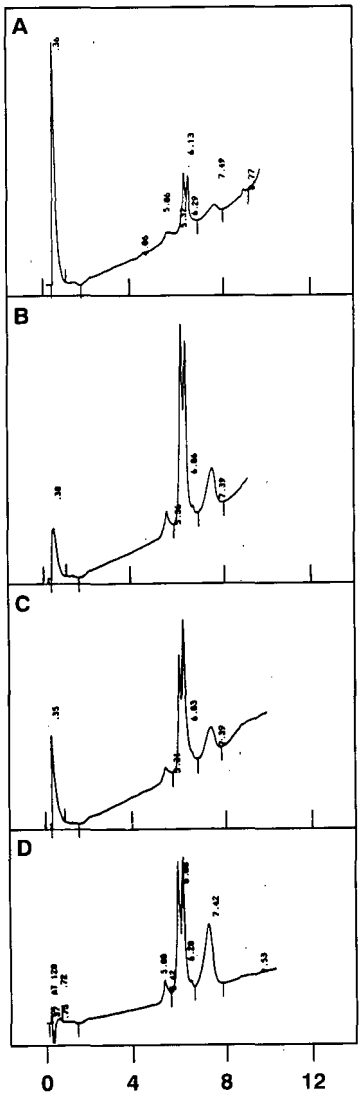

Fig. 5. Elution profile of isolated four peaks present in Fig. 2A. Elution conditions as in Fig. 2A. (A) Peak at 6.72 min; (B) peak at 7.40 min; (C) peak at 7.62 min; (D) peak at 8.88 min.

TABLE I

RELATIONSHIP OF BIOACTIVITY TO PEAK AREA FOR PDGF FRACTIONATED BY RPLC

Peak No.	t_R[a] (min)	Units bioactivity	Peak area	Bioactivity/area
1	6.72	44	1000	0.044
2	7.40	124	3550	0.035
3	7.62	116	3010	0.039
4	8.88	126	3660	0.034

[a] Retention times.

Four individual peaks obtained from RPLC of PDGF at room temperature were isolated, dried under vacuum, and redissolved in 0.1% TFA. Reinjection resulted in essentially the same elution profile as present in unfractionated PDGF (Fig. 5). From SDS-PAGE, it was determined that all four fractions had the same molecular mass as each other and with PDGF. The mitogenic bioassay showed that all fractions were active and when these results were expressed on an area basis, as determined from the RPLC chromatogram, the activity per unit area was essentially equal in all fractions (Table I).

DISCUSSION

In the majority of instances involving RPLC of proteins, a single peak is present which is accepted as complementary evidence for product purity. In recent years, it has been shown that a seemingly pure protein can give rise to multiple peaks for a variety of reasons, a quite common one being due to the existence of conformational changes caused by the hydrophobic column matrix disrupting the native protein structure. This effect has been demon-

stated to occur with papain [14], ribonuclease [15] and lysozyme [16] amongst others.

When PDGF was examined by SDS-PAGE, hydrophobic-interaction and size-exclusion chromatography the data showed that a single component was present. RPLC, on the other hand, consistently showed that at least four species were present with a wide range of hydrophobicities. Similar results were obtained from two quite dissimilar columns, Vydac C_4 and Toso Haas NPR C_{18} indicating that the effect was caused by the reversed-phase process and was not specifically related to a single column source. Increased column contact time favored a shift in peak profiles toward the later eluting peak, peak 4. Results from incubation studies and magnitude of the peak shift indicated that these were not the major cause leading to the formation of multiple peaks. Raising and lowering the temperature produced more dramatic changes in elution profiles. When the temperature was raised, the number of peaks decreased until a single peak existed. Isolation and reinjection of this peak resulted in the appearance of the same initial four peaks when RPLC was performed at ambient temperature. Lowering the temperature has the opposite effect on peak profiles favoring the presence of early eluting peaks. Isolation of the four peaks present at room temperature followed by their reinjection resulted in the reappearance of the same four initial peaks from unfractionated PDGF. In addition, SDS-PAGE demonstrated that all four peaks had the same migration as each other and with intact PDGF. The activity data indicated that all four fractions had essentially the same activity when corrected for relative amounts present (Table I). Taken together, these results suggest that PDGF exists in a variety of conformational states which are separable during the time course of chromatography.

What might give rise to these conformational states? While PDGF contains a number of proline residues, a Pro–Pro sequence at positions 41–42 [1] stands out as a possible site for *cis–trans* isomerization (Fig. 1). The presence of a Pro–Pro sequence is more likely than any single Pro containing sequence to elicit *cis–trans* isomerization. In PDGF, these residues are located in a hydrophobic region of the primary structure (...Ala–Asn–Phe–Leu–Val–Trp–Pro–Pro–Cys–Val...) and are bounded by a Trp residue and a Cys residue involved in a disulfide linkage. In such an environment, *cis–trans* isomerization of Pro residues might be expected to be relatively slow and the various forms could be observed in real time, *e.g.*, during the RPLC process. The multiple Pro residues in PDGF together with the results from heating and cooling chromatographic processes provide possible explanation for the presence of the multiple forms of PDGFduring reversed phase chromatography. The ...Trp–Pro–Pro-Cys... sequence is also found in human angiogenin [17]. This protein gives rise to a doublet peak on RPLC on a C_{18} column presumably a result of a reversible conformational change in the protein (see footnote in ref. 17). A tryptic fragment containing this sequence also gives rise to two peaks on reversed phase chromatography, however, the interpretation for this duplex is complicated in part by the presence of two peptides joined by a disulfide linkage.

Jacobsen *et al.* [18] has shown that the *cis* isomer of Pro has a more hydrophobic surface area than the *trans* isomer and can interact to a much greater extent with hydrophobic ligands on columns. As a result, *cis–trans* conformers of proline containing peptides can be separated by RPLC [19]. The existence of multiple peaks from proline containing peptides has been explained as being directly related to the slow kinetics of isomerization of *cis–trans* conformers that occurred during the time course of the chromatographic separation. Peptide bonds that include proline are characterized by their relative rigidity as compared with other amino acids. Melander *et al.* [20] showed that temperature, pH and flow velocity were involved in affecting the peak shape of these proline containing peptides upon RPLC.

Many studies have suggested that proline *cis–trans* isomerism plays a central role in the folding of proteins. As a result, proline *cis–trans* isomerism has been directly implicated in the formation of multiple conformations of protein in solution [21–25]. Using conformational energy calculations, Levitt [26] demonstrated the existence of three types of proline residues in the folded, native state of bovine pancreatic trypsin inhibitor. In the first type, proline residues can isomerize freely; in the second type, proline isomerization destabilizes the native conformation, but not enough to disrupt the overall conformation; in the third type, isomerization is so disruptive as to prevent the proper protein confir-

mation without the proper proline isomer. Definitive evidence for proline *cis–trans* isomerism is readily achieved with small peptides, however, for larger proteins such information is much more difficult to obtain. *cis–trans* isomerism of proline in staphylococcal nuclease and in calbindin D_{9k} have been recently shown by two-dimensional ^1H NMR to be the source of conformational heterogeneity in the folded form of these proteins [27]. The use of NMR for demonstrating distinct conformations is not a realistic option of DGF at the present time. PDGF contains multiple prolines of which Pro–Pro at positions 41–42 is proposed to be a likely site for *cis–trans* isomerization. Replacement of these proline residues, either individually or together could provide indirect evidence for the presence of proline *cis–trans* isomerization should the resulting RPLC profile be simplified. While it is not presently possible to prove definitively that the existence of Pro–Pro bonds are a direct cause of the multiple peak formation observed with PDGF, the experimental evidence, nevertheless, provides some indication that such a possibility exists.

REFERENCES

1 T. F. Deuel, *Ann. Rev. Cell Biol.*, 3 (1987) 443–492.
2 M. T. W. Hearn and W. S. Hancock, *Trends Biochem. Sci.*, 4 (1978) 58–62.
3 C. E. Dunlap, S. Gentlemen and L. I. Lowney, *J. Chromatogr.*, 160 (1978) 191–198.
4 M. Rubenstein, *Anal. Biochem.*, 98 (1979) 1–7.
5 J. E. Revier, *J. Chromatogr.*, 202 (1980) 211–222.
6 F. E. Regnier and K. M. Gooding, *Anal. Biochem.*, 103 (1980) 1–25.
7 H. P. J. Bennet, C. A. Browne and S. Soloman, *J. Liq. Chromatogr.*, 3 (1980) 1353–1365.
8 W. C. Mahoney and M. A. Hermodson, *J. Biol. Chem.*, 255 (1980) 11199–11203.
9 J. D. Pearson, W. C. Mahoney, M. A. Hermondson and F. E. Regnier, *J. Chromatogr.*, 207 (1981) 325–332.
10 R. V. Lewis, A. Fallon, S. Stein, K. D. Gibson and S. Udenfriend, *Anal. Biochem.*, 104 (1980) 153–159.
11 J. D. Pearson, N. T. Lin and F. E. Regnier, in M. T. W. Hearn, F. E. Regnier and C. T. Wehr (Editors), *High Performance Liquid Chromatography of Proteins and Peptides*, Academic Press, New York, 1983, pp. 81–94.
12 U. K. Laemmli, *Nature (London)*, 227 (1970) 680–685.
13 G. F. Pierce, T. A. Mustoe, R. M. Senior, J. Reed, G. L. Griffin, A. Thomason and T. F. Deuel, *J. Exp. Med.*, 167 (1988) 974–987.
14 S. A. Cohen, K. P. Benedek, S. Dong, Y. Tapuhi and B. L. Karger, *Anal. Chem.*, 56 (1984) 217–221.
15 S. A. Cohen, K. Benedek, Y. Tapuhi, J. C. Ford and B. L. Karger, *Anal. Biochem.*, 144 (1985) 275–284.
16 K. A. Cohen, K. Schellenberg, K. P. Benedek, B. L. Karger, B. Grego and M. T. W. Hearn, *Anal. Biochem.*, 140 (1984) 223–232.
17 R. Shapiro, D. J. Strydom, K. A. Olson and B. L. Vallee, *Biochemistry*, 26 (1987) 5141–5146.
18 J. Jacobsen, W. Melander, G. Vaisnys and Cs. Horváth, *J. Phys. Chem.*, 88 (1984) 4536–4542.
19 J. C. Gesquiere, E. Diesis, M. T. Chung and A. Tartar, *J. Chromatogr.*, 478 (1989) 121–129.
20 W. Melander, H.-J. Lin, J. Jacobson and Cs. Horváth, *J. Phys. Chem.*, 88 (1984) 4527–4536.
21 R. Grafl, K. Lang, A. Wrba and F. Schmid, *J. Mol. Biol.*, 191 (1986) 281–293.
22 P. A. Evans, C. M. Dobson, R. A. Kautz, G. Hatfull and R. Fox, *Nature (London)*, 327 (1987) 266–268.
23 R. Kelley and F. M. Richards, *Biochemistry*, 26 (1987) 6765–6774.
24 M. Adler and H. A. Scheraga, *Biochemistry*, 29 (1990) 8211–8216.
25 C. M. Deber, B. J. Sorrel and G.-Y. Yu, *Biochem. Biophys. Res. Commun.*, 172 (1990) 862–869.
26 M. Levitt, *J. Mol. Biol.*, 145 (1981) 251–263.
27 W. J. Chazin, J. Kordel, T. Drakenberg, E. Thulin, P. Brodin, T. Grundstrom and S. Forsen *Proc. Natl. Acad. Sci. USA* 86 (1989) 2195–2198.

Journal of Chromatography, 606 (1992) 171–177
Elsevier Science Publishers B.V., Amsterdam

CHROM. 24 347

Isolation, trace enrichment and liquid chromatographic analysis of diacetylphloroglucinol in culture and soil samples using UV and amperometric detection

Phil Shanahan and Alex Borro

Analytical Chemistry, Chemistry Department, University College, Cork (Ireland)

Fergal O'Gara

Microbiology Department, University College, Cork (Ireland)

Jeremy D. Glennon

Analytical Chemistry, Chemistry Department, University College, Cork (Ireland)

(First received January 30th, 1992; revised manuscript received May 4th, 1992)

ABSTRACT

A reversed-phase approach is described for the preparative-scale isolation of the biotechnologically important antibiotic compound 2,4-diacetylphloroglucinol (DAPG), using solid-phase extraction and medium-pressure liquid chromatography. Using the purified sample, a high-performance liquid chromatographic assay was developed for the determination of DAPG in complex matrices such as growth media and soil. A sample pretreatment procedure involving solid-phase extraction on octadecyl silica prior to analytical high-performance liquid chromatography, removed endogenous peaks from the chromatogram when UV (254 nm) and amperometric detection (1.1 V *vs.* Ag/AgCl) were used. The reversed-phase chromatographic method is used to monitor the production of DAPG by a strain of *Pseudomonas* in culture media. The proven higher sensitivity and selectivity of amperometric detection for phenols and catechols are continued here in the analysis of phloroglucinols. Demonstrated selectivity improvements using amperometric detection for the analysis of DAPG in soil samples are however dependent on soil type.

INTRODUCTION

The quest for new and improved antibiotics from microbial sources is an important area of modern biotechnological research. Antibiotics are generally considered to be organic compounds of low molecular mass produced by microbes and are capable of killing bacteria or preventing their growth at low concentrations [1]. Approximately fifty such antibiotic substances have been isolated from pseudomonads [2,3], the largest percentage of these supplied by the sub-species *Pseudomonas fluorescens*. The majority of these antibiotic compounds isolated from *Pseudomonas* culture filtrates are N-containing heterocycles. They include such compounds as phenazines [4–6], pyrrole-type antibiotics [7–9], pyocompounds [10] and indole derivatives [11].

However, there are a small number of non-nitrogen-containing antibiotic compounds produced by *Pseudomonas fluorescens*. 2,4-Diacetylphloroglucinol (DAPG) (2,4-diacetyl-1,3,5-trihydroxybenzene) is one such compound and is one of just three phloroglucinols which have been isolated from the *Pseu-*

Correspondence to: J. D. Glennon, Analytical Chemistry, Chemistry Department, University College, Cork, Ireland.

0021-9673/92/$05.00

domonas species [12]. This compound has been characterised previously in this laboratory [13] and by a number of other workers [14–16]. However, literature contains no method of harvesting large quantities of DAPG chromatographically nor are there any reported chromatographic methods of analysis for microbially derived phloroglucinols.

A large number of naturally occurring phloroglucinols from the plant genera *Dryopteris, Hagenia* and *Malotus* have already been studied chromatographically by reversed-phase high-performance liquid chromatography (HPLC) using absorption detection at 254 nm [17] and also by gas–liquid chromatography (GLC) [18]. However, these phloroglucinols of plant origin are structurally more complex than those of bacterial origin, existing mostly as large polycyclic molecules.

Phloroglucinols are classified according to the presence of a 1,3,5-trihydroxybenzene group which places them in the structural sequence; phenols, catechols and phloroglucinols (Fig. 1).

Much work has appeared in the literature on phenols and catechols and on how well they lend themselves towards electrochemical detection [19–23]. In many cases electrochemical detection of the above molecules has proven to be the favoured method of analysis, demonstrating higher sensitivity and increased selectivity over UV methods of detection. Results from this laboratory have also demonstrated the usefulness of amperometric detection to the analysis of microbial siderophores, many of which can contain catecholate groups [24].

Recent efforts to define the role of antibiotics in soil have been greatly impeded by a lack of direct evidence that antibiotics are present in soil. The physical and biological factors influencing antibiotic production and detection in soil have been reviewed [25,26] and although some success has been achieved in soil with amended nutrient sources, soil still proves to be a very complex matrix for the detection of antibiotics which are by definition produced in trace amounts [1]. Recently Thomashow *et al.* [6] successfully developed a HPLC method for the detection of the antibiotic phenazine 1-carboxylic acid in the rhizosphere of wheat. This paper reports on the development of a HPLC assay for the detection of a naturally occurring phloroglucinol and demonstrates how electrochemical detection shows enhanced sensitivity and selectivity over UV detection of DAPG. Advantage is taken of a sample pretreatment method involving solid-phase extraction of the antibiotic on octadecylsilica (ODS) prior to chromatographic analysis. The paper also outlines a method for the harvesting of large quantities of DAPG from a *Pseudomonas fluorescens* strain grown on sucrose–asparagine (SA) minimal media [27]. The technique involves preparative chromatography at medium pressures where the precolumn (guard column) is adapted to permit large-scale trace enrichment of DAPG from culture supernate.

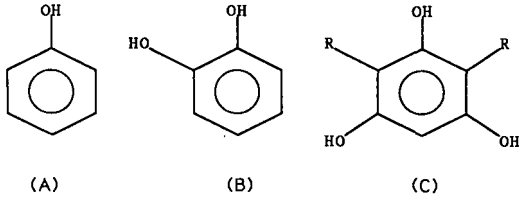

Fig. 1. Chemical structures of electroactive analytes. (A) Phenol; (B) catechol; (C) phloroglucinol (R = H), 2,4-diacetylphloroglucinol (R = CH_3CO-).

EXPERIMENTAL

Medium-pressure liquid chromatography

The preparative medium-pressure liquid chromatography (MPLC) system consisted of a Buchi 681 MPLC pump which can operate up to 40 bar backpressure. The sample was injected using a 10-ml syringe (Segma) directly through a septum into the top of Buchi B-685 chromatographic column (230 mm × 26 mm I.D.) operating at a flow-rate of 6 ml/min. The mobile phase consisted of methanol–water (25:75, v/v). The column was previously packed with LiChroprep RP-18, particle size 5–20 μm, using a standardised dry-packing method with vacuum and nitrogen over-pressure [28]. UV detection was carried out using a Buchi UV-Vis filter photometer at 254 nm equipped with a 2-mm superpreparative flow-through cell. The recorder output was recorded on a Perkin-Elmer 023 strip chart recorder and the fractions were collected manually.

Isolation of diacetylphloroglucinol using off-line solid-phase extraction prior to MPLC

A *Pseudomonas fluorescens* strain (code named

F113) was cultured on minimal SA medium [27] incorporating 0.35% agar and incubated at 28°C for 8 days. Prior to inoculation the medium was sterilized by autoclaving and *ca.* 25-ml aliquots were poured into sterile petri dishes. The bacterial cells and agar gel were sedimented by centrifugation at 16 000 *g* on a Beckmann JA-10 rotor for 20 min at 10°C creating a pellet of the agar and cells. A 1-l volume of supernate was collected, filtered through a 0.45-μm filter and concentrated five-fold by rotary evaporation at 35°C. The concentrated supernate was again filtered through a 0.45-μm filter before commencing solid-phase extraction. The guard column (100 mm × 10 mm I.D.) of the MPLC system was fitted with a porous PTFE frit and packed under gravity using a wet slurry technique. The packing material consisted of LiChroprep RP-18 (Merck) of particle size 25–40 μm. The column was then conditioned by passing methanol and water through it at a flow-rate of 6 ml/min.

By switching the pump inlet, 100 ml of the concentrated supernate was pumped through the guard column. It was then washed with 200 ml of water, followed by 300 ml of methanol, to elute all retained material. The latter washings were collected separately, taken to dryness *in vacuo* and reconstituted in 2 ml of methanol. The sample was then applied to the preparative column for final purification, employing a mobile phase of methanol–water (25:75, v/v). The chromatographic peak corresponding to the antibiotic eluted at a retention time of 32 min. Following solvent evaporation the purity of the isolated product was checked using analytical HPLC where it gave a single peak. An elemental analysis was also performed and the experimental values of C = 57.0%, H = 4.8% and N = 0% compared favourably with the theoretical values of 57.13%, 4.76% and 0% for C, H and N respectively.

HPLC apparatus

The HPLC system consisted of a Waters pump Model 510 attached to a Rheodyne injection valve with a 20-μl loop. The column used was an analytical column (150 mm × 6 mm O.D. × 4.5 mm I.D.) packed with Hypersil ODS (particle size 5 μm). The detector used was a Waters Lambda-Max Model 481 variable-wavelength spectrophotometer. The amperometric detector was an LC4B model from Bioanalytical Systems (BAS, West Lafayette, IN, USA). This was coupled with a BAS column adaptor housing model CC4. The electrode cell was of thin film design with a working electrode of glassy carbon, a platinum auxiliary electrode and a Ag/AgCl reference electrode. The detector was attached to a Philips 8251 strip chart recorder.

Mobile phase composition

Reagents for mobile phase preparation were of AnalaR grade and all mobile phases were filtered and degassed on a Millipore HPLC filtration system using 0.45-μm filters. Unless otherwise stated the HPLC mobile phase consisted of (water–methanol–tetrahydrofuran (THF) (40:45:15) at a flow-rate of 1 ml/min. For electrochemical analysis, 0.05 *M* sodium chloride was incorporated as a background electrolyte.

Preparation of standard solutions and soil samples

Purified antibiotic 2.010 mg was accurately weighed into 25 ml of methanol using a Mettler Me22 electronic balance coupled to a Mettler control unit BA 25. Standard solutions of DAPG were prepared by dilution with methanol to give concentrations in the range of $3.8 \cdot 10^{-4}$ to $1.0 \cdot 10^{-8}$ *M*. Experiments were carried out on a sandy soil sample (pH 6.9) (chemical composition: Ca = 532, K = 203, P = 78, N = 20, Mg = 31, Mn = 0.84, mg/kg soil) taken from a nearby location in Ovens, County Cork, Ireland. The soil was collected from the upper 5 cm of the soil profile, sieved through a 0.5 cm mesh screen and air dried prior to use. Purified DAPG dissolved in diethyl ether (10 ml) was mixed into the soil to yield concentrations of 100, 50 and 25 μg/g of soil. The ether was removed *in vacuo* at 35°C to ensure a uniform dispersion of DAPG throughout the soil.

Pretreatment of growth culture liquid media

A second medium commonly used for the growth of pseudomonads is the complex Luria–Bertani (LB) medium [29]. The production of a range of secondary metabolites by the growing microorganism, as well as the large number of constituents in the media necessitates the use of an efficient sample clean-up step when analysing for DAPG. The following procedure was developed. A Waters Sep-Pak C_{18} cartridge was first wetted with 10 ml of methanol followed by 10 ml water. The antibitiotic

was retained on the cartridge when applied in water. Filtered supernate samples (5 ml) were injected onto the cartridge. The cartridge was then washed with 30 ml of water followed by 20 ml of methanol to elute the retained constituents. The methanol eluate was taken to dryness and the residue reconstituted in 5 ml of mobile phase. The sample was again filtered and 20-μl aliquots injected into the HPLC system. Sample pretreatment of growth cultures on SA minimal media is carried out in the same way; however, the clean-up effect is not as pronounced as that observed in LB media.

Monitoring in vitro DAPG production

To monitor *in vitro* DAPG production over a period of eight days, sixteen 100-ml Erlenmeyer flasks containing 5 ml of SA liquid medium were inoculated to give *ca.* 10^3 colony-forming units (cfu[a])/ml of strain F113 and incubated without shaking at 28°C. At 12-h intervals, a flask was removed from the incubator and a cfu value recorded. The cells were pelleted by centrifugation at 3000 *g* for 10 min at room temperature. The supernate was decanted off and assayed for DAPG production by HPLC. All samples analysed for antibiotic production were pretreated using the outlined solid-phase extraction procedure.

Analysis of spiked soil samples

Spiked soil samples (1 g) were washed three times with 100-ml quantities of diethyl ether. The washings were pooled and rotary evaporated to dryness at 30°C. The residual material was taken up in mobile phase (5 ml) and filtered through 0.45-μm filters. Aliquots (20 μl) were injected into the HPLC system and analysed with UV and amperometric detection. Non-spiked soil samples were washed in the same way and their chromatographic profiles recorded as blanks.

RESULTS AND DISCUSSION

The obvious advantage in employing microbes to produce specific compounds, some of which can be very exotic and chemically difficult to synthesise, lies in the speed and ease of microbial production as opposed to what may involve a multi-step chemical synthesis of the same compound. However this is dependent on whether it is possible to isolate the desired product from what can often be a complex microbial growth matrix. The antibiotic DAPG has been previously synthesised [30], but with the new method of isolation proposed in this paper, from a species of *Pseudomonas* a ready and easily accessible source of DAPG is provided. The purified antibiotic supplied a parent molecular ion in the mass spectrum at *m/z* 210.053 (calculated for $C_{10}H_{10}O_5$:210.0528), a melting point at 167–170°C (Lit. [30] 168–170°C); IR bands (KBr) (*inter alia*) at 3650–2100, 1645–1575, 1435, 1365 and 1200 cm^{-1} and ^1H NMR ($C^2H_3O^2H$) chemical shifts at δ2.63 (S 6H), 5.76 (S 1H) (hydroxyls exchanged).

A sensitive and selective assay for the monitoring of DAPG levels in culture media and in soil samples is required to assist with the optimisation of microbial production of the antibiotic and with its detection in complex matrices such as soil for biotechnological applications including biocontrol. The sensitivity requirements vary with the nature of the application as well as with environmental and time dependent factors. For example, when the microbe is grown under nutritionally stressed conditions such as created by a particular choice of temperature or growth medium [13], only trace amounts of DAPG are present. Selectivity requirements are greatly determined by the microbial sample matrix. These studies examine these attributes of UV and amperometric detection when HPLC is used for the analysis of DAPG in culture media (*i.e. in vitro*) and soil samples.

Optimisation of HPLC assay

Standard solutions of DAPG were used to study the effect of the nature and percentage organic modifier concentration on the capacity factors and peak shapes. The chosen mobile phase containing 15% THF and 45% methanol in water improved the peak shape for DAPG. Hydrodynamic voltammetry was carried out to determine the optimum applied potential for DAPG detection (Fig. 2). A value of 1.10 V *vs.* Ag/AgCl was chosen for amperometric and 254 nm for UV detection.

[a] cfu is the cell count unit providing a representation of the number of viable bacterial cells present in a culture, normally expressed per ml of that culture.

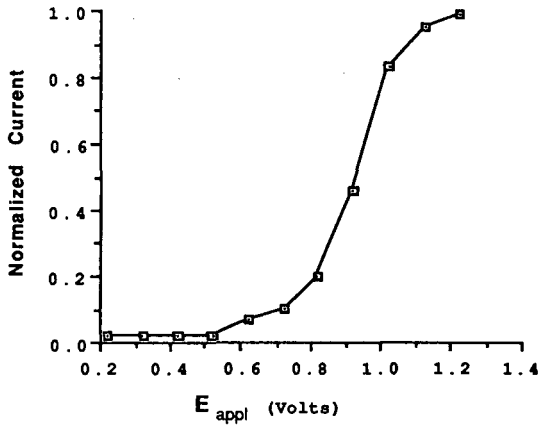

Fig. 2. Hydrodynamic voltammogram of 2,4-diacetylphloroglucinol.

Linearity and precision

The amperometric and UV responses were studied in the ranges $8.86 \cdot 10^{-5}$ to $5.32 \cdot 10^{-6}$ *M* DAPG, each standard being injected five times. Table I summarises a statistical evaluation of the results. Overall, UV detection emerges as being slightly more precise. The mean relative standard deviations were taken as a measure of the precision of the methods with intra-assay values of 2.96 and 3.01% for UV and amperometric detection respectively. Correlation coefficients of 0.9997 and 0.9993 were obtained for amperometric and UV detection respectively.

Limits of detection

The limit of detection (LOD) is defined as the concentration of analyte that will produce a signal-to-noise ratio of 2 and is considered to be the minimum concentration that can be detected [31]. The limit of detection was calculated from a series of measurements made at concentrations close to the blank level and was determined to be $2.309 \cdot 10^{-9}$ *M* at an applied amperometric potential of 1.1 V and $9.767 \cdot 10^{-7}$ *M* at a wavelength of 254 nm. The limit of detection using amperometry is over 400 times lower than with UV detection, and with trace enrichment using the solid-phase extraction procedure described in the experimental section limits of detection in the region of 10^{-12} *M* can be achieved.

Analysis of DAPG in microbial culture media

The monitoring of *in vitro* DAPG production by the *Pseudomonas* bacteria when cultivated on the complex LB growth media clearly benefits from improved chromatographic resolution when the sample pretreatment step is employed. On passing the sample through a cartridge containing octadecylsilica, the poorly retained constituents are washed off, thus eliminating the problem of column overloading caused by the high concentration of media substituents in the analyte sample and allowing for excellent resolution of DAPG (Fig. 3). Similar improvements in chromatographic profile were obtained for UV detection at 254 nm. Furthermore, the recovery of DAPG from culture media was found to be quantitative.

TABLE I

INTRA-ASSAY PRECISION OF THE HPLC ASSAY OF DAPG USING UV AND AMPEROMETRIC DETECTION

HPLC conditions were the same as in Fig. 3. Injection volume, 20 μl; $n = 5$; R.S.D. = relative standard deviation.

Concentration added (10^{-6} *M*)	Concentration found			
	UV		Amperometric	
	Mean ± S.D. (10^{-6} *M*)	R.S.D. (%)	Mean ± S.D. (10^{-6} *M*)	R.S.D. (%)
0.88	0.88 ± 0.04	3.98	0.89 ± 0.02	2.74
1.33	1.18 ± 0.05	3.89	1.41 ± 0.06	4.26
1.77	1.70 ± 0.06	3.58	1.76 ± 0.05	2.84
2.66	3.01 ± 0.06	1.93	2.59 ± 0.06	2.31
5.32	5.22 ± 0.08	1.43	5.39 ± 0.16	2.97

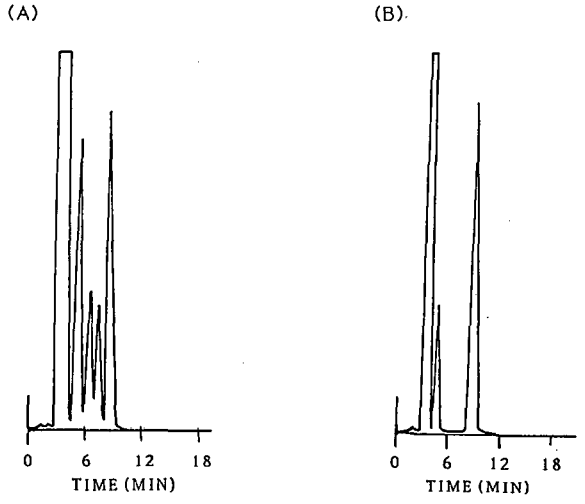

Fig. 3. Chromatograms obtained using amperometric detection from supernates of the pseudomonad grown on complex LB medium (A) without and (B) with sample pre-treatment. Retention time DAPG = 9.15 min. HPLC conditions: mobile phase, water–methanol–THF (40:45:15); flow-rate 1-0 ml/min; detection at 254 nm.

Microbial growth is measured as the change in optical density of the growth media with time and the growth curve obtained shows the characteristic lag, exponential and stationary phases (Fig. 4A). The outlined HPLC assay was employed to investigate the onset and rate of microbial production of DAPG in SA medium (Fig. 4B). DAPG is first detected in the growing culture after 36 h, when the growing microbe has reached its stationary growth phase. In measuring DAPG production, the cell count remained constant in the stationary phase at approximately 10^9 cfu/ml. Thus changes in DAPG production are attributed to an increase in the metabolism of DAPG rather than an increase in cell number. DAPG production increases linearly with time; however, this effect did not continue indefinitely, suggesting that there is a minimum time of approximately four days growth required for optimum DAPG production.

The selectivity of analysis of DAPG in sandy soil samples is enhanced by the use of electrochemical detection. As shown in Fig. 5A the injected sample contained a number of long-retained components together with a component that overlapped the DAPG peak (retention time 8.6 min) when analysed

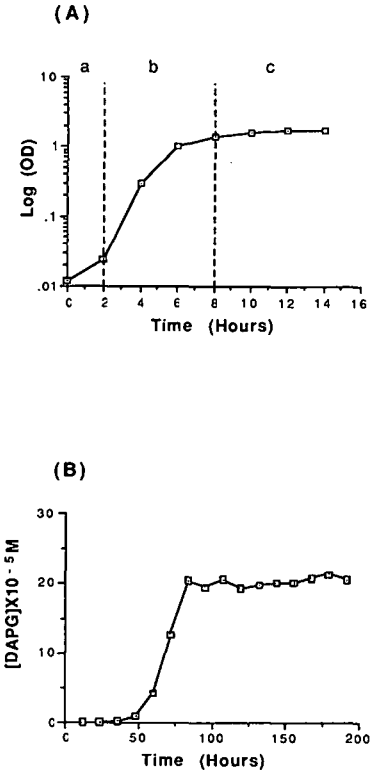

Fig. 4. (A) Growth curve of *Pseudomonas* strain in SA culture medium obtained from optical density measurements at 600 nm showing (a) lag, (b) exponential and (c) stationary phases of growth and (B) DAPG production in SA culture medium monitored by HPLC.

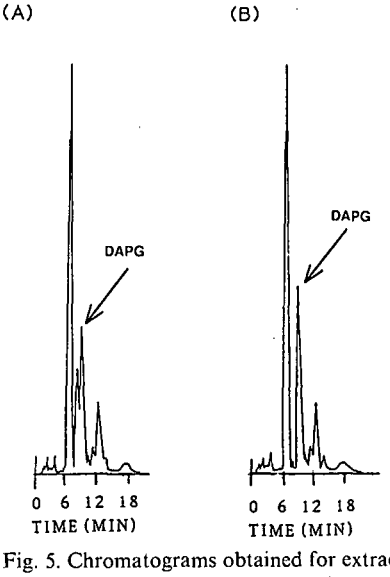

Fig. 5. Chromatograms obtained for extracts of sandy soil samples using (A) UV detection at 254 nm and (B) amperometric detection at + 1.1 V.

with UV detection. When studied with amperometric detection the latter contaminating peak is conveniently absent (Fig. 5B). This improved selectivity was not, however, observed in DAPG analysis of peat soils, highlighting the problem posed by the variation in chemical composition of different soils. Recoveries of DAPG from soil samples were also low, in the range of 60–70%. Further studies are required to optimize selectivity and recovery for detection of microbial antibiotics in these more complex soil matrices.

CONCLUSIONS

The new reversed-phase approach described above for the isolation of DAPG on a preparative scale provides easy access to appreciable amounts of a compound which is already known to be inhibitory to many plant deleterious bacteria. Biological assays for the detection of this compound involve observing the capacity of the DAPG producing strain to inhibit growth of susceptible bacteria or fungi. However, this method presents problems as typical bioassay plates or tubes must be incubated for about 18 h before results can be obtained. There is also the further disadvantage that the technique has no ability to quantify the inhibitory compound produced. The developed HPLC assay employing solid-phase extraction for sample clean-up in conjunction with amperometric detection provides an efficient means of sensitively and selectively monitoring the antibiotic production in complex matrices such as culture media and soil samples.

REFERENCES

1 R. C. Fravel, *Ann. Rev. Phytopathol.*, 26 (1988) 75–91.
2 T. Leisinger and R. Magraff, *Microbiol. Rev.*, 43 (1979) 422–442.
3 E. A. Kipirianova and V. V. Smirnov, *Antibiotiki*, 26 (1981) 135–143.
4 P. G. Brisbane, L. K. Janik, M. E. Tate and R. O. F. Warren, *Antimicrob. Agents Chemother.*, 31 (1987) 1967–1971.
5 N. N. Gerber, *J. Heterocyclic Chem.*, 6 (1969) 297–300.
6 L. S. Thomashow, D. M. Weller, R. F. Bonsall and L. S. Pierson, *Appl. Environ. Microbiol.*, 56 (1990) 908–912.
7 M. Hashimoto and K. Hattori, *Bull. Chem. Soc.*, 39 (1966) 410.
8 M. Hashimoto and K. Hattori, *Chem. Pharm. Bull.*, 14 (1966) 1314–1316.
9 H. Imanaka, M. Kowsaka, G. Tamura and K. Arima, *J. Antibiot., Ser. A*, 18 (1965) 207–210.
10 C. R. Howell and R. O. Stipanovic, *Phytopathology*, 70 (1980) 712–175.
11 S. J. Wratten, M. S. Wolfe, R. J. Anderson and D. J. Faukner, *Antimicrob. Agents Chemother.*, 11 (1977) 411–414.
12 T. K. Redi, Y. P. Khuclyakov and A. V. Borokov, *Mikrobiologiyia*, 38 (1969) 909–913.
13 P. Shanahan, D. J. O'Sullivan, P. Simpson, J. D. Glennon and F. O'Gara, *Appl. Environ. Microbiol.*, 58 (1992) 353–358.
14 D. Broadbent, R. P. Mabelis and H. Spencer, *Phytochemistry*, 15 (1976) 1785.
15 G. M. Strunz, R. E. Wall and D. J. Kelly, *J. Antibiot.*, 31 (1978) 1201–1202.
16 C. Keel, P. H. Wirthner, T. H. Oberhansli, C. Voisard, U. Burger, D. Haas and G. Defago, *Symbiosis*, 9 (1990) 327–341.
17 C. J. Widen, H. Pyysalo and p. Salovaara, *J. Chromatogr.*, 188 (1980) 213–220.
18 H. Pyysalo and C. J. Widen, *J. Chromatogr.*, 168 (1979) 246–249.
19 D. A. Roston and P. T. Kissinger, *Anal. Chem.*, 53 (1981) 1695–1699.
20 W. A. Mac Crehan and J. M. Brown-Thomas, *Anal. Chem.*, 59 (1987) 477–479.
21 G. Chiarvari and V. Concialini, *Analyst (London)*, 113 (1988) 91–94.
22 G. Eisenhofer, K. L. Kirk, I. J. Kopin and D. S. Goldstein, *J. Chromatogr.*, 431 (1988) 156–162.
23 C. L. Davies and S. G. Molneux, *J. Chromatogr.*, 231 (1982) 41–51.
24 J. D. Glennon, M. R. Wolfe, A. T. Senior and N. NiChoileain, *Anal. Chem.*, 61 (1989) 1474–1478.
25 S. T. Williams, *Pedobiologica*, 23 (1982) 427–435.
26 D. M. Weller and L. S. Thomashow, in R. Baker and P. Dunn (Editors), *New Directions in Biological Control*, A. R. Liss, New York, 1990, pp. 703–711.
27 F. M. Scher and R. Baker, *Phytopathology*, 72 (1982) 1567–1573.
28 C. G. Zogg, S. Z. Nyiredy and O. Sticher, *J. Liq. Chromatogr.*, 12 (1989) 2031–2048.
29 T. Maniatis, E. F. Fritsch and J. Sambrook, *Molecular Cloning: A Laboratory Manual*, Cold Spring Harbor Laboratory, Cold Spring Harbor, New York, 1982.
30 T. W. Campbell and G. M. Coppinger, *J. Am. Chem. Soc.*, 73 (1951) 2708–2712.
31 P. C. White, *Analyst (London)*, 109 (1984) 677–697.

Journal of Chromatography, 606 (1992) 179–185
Elsevier Science Publishers B.V., Amsterdam

CHROM. 24 299

Determination of sterols, erythrodiol, uvaol and alkanols in olive oils using combined solid-phase extraction, high-performance liquid chromatographic and high-resolution gas chromatographic techniques

Mauro Amelio, Renzo Rizzo and Flavio Varazini

Fratelli Carli SpA, Via Garessio 11/13, 18100 Imperia (Italy)

(First received December 11th, 1991; revised manuscript received April 6th, 1992)

ABSTRACT

A method is described for the determination of the sterol, erythrodiol, uvaol and alkanol content in olive oils by means of solid-phase extraction and high-performance liquid chromatography, instead of liquid–liquid and thin-layer chromatographic separations, the following step being high-resolution gas chromatographic separation. This type of procedure allows the simultaneous analysis of a larger number of samples and a substantial reduction in manual operations. Comparisons were made between the two methods on 100 different olive oils and with a statistical analysis of the results (Student's *t*-test).

INTRODUCTION

The sterol, erythrodiol, uvaol and alkanol contents are very important for the investigation of the quality of olive oil. The recent EEC Regulation No. 2568/91 requires analyses for this type of investigation and fixes the physico-chemical characteristics of the product. Sterols, erythrodiol, uvaol and alkanols are present in the unsaponifiable fraction and are separated from it by suitable techniques. Unfortunately, they are very time consuming and require substantial manual operations, which limits the number of samples that can be analysed daily.

Several papers have described alternative methods to replace the official methods. In particular, solid-phase extraction (SPE) and high-performance liquid chromatography (HPLC) have been proposed for the determination of both free and combined sterols and for the total sterols in unsaponifiable matter.

The use of SPE to separate sterols from biological matter has been applied for a long time [1]. In contrast, it is not very common in fat analysis and most official methods do not take into account this type of separation.

Worthington and Hitchcock [2] used semi-preparative HPLC to separate free and combined sterols from seed oils. The collected fractions were then separated and analysed by means of thin-layer (TLC) and gas chromatography (GC). Horstmann and Montag [3] suggested the use of silica gel cartridges and different eluents of increasing polarity to obtain sterols from fats or unsaponifiable matter. They achieved a better separation by HPLC (direct phase) and discussed some instrumental problems. Schuster [4] suggested a multi-component analysis (triglycerides, hydroperoxides, sterols and vitamins) by means of HPLC with diode-array detection.

More recently, Grob *et al.* [5] used an "on-line" LC–GC system to determine the sterol (free and

Correspondence to: Dr. Mauro Amelio, Fratelli Carli SpA, Via Garessio 11/13, 18100 Imperia, Italy.

0021-9673/92/$05.00

combined), alkanol and wax contents in olive oil. However, the quality control routine requires sterol and alkanol contents to be determined in the unsaponifiable matter. In this case, they must be separated from the soap solution. This separation is normally performed by means of a liquid–liquid extraction.

Cortesi and co-workers [6,7] used HPLC to separate sterols, alkanols, erythrodiol and uvaol in the unsaponifiable matter from olive oil. Further, they investigated the possibility of determining these analytes directly by HPLC.

In order to collect a suitable amount of samples from HPLC for further analyses and achieve good separations, Iatride *et al.* [8] chose repeated cycles of separation of unsaponifiable from rapeseed oil, using an analytical column, automated injection and a fraction collector. Further, sterols were well separated from triterpenic alcohols. Holen [9] optimized the isolation and identification by reversed-phase HPLC of eight sterols from rapeseed oil and mayonnaise. Mordret *et al.* [10] compared separations of unsaponifiable matter carried out by means of TLC and HPLC. They obtained comparable results and investigated the advantages of the HPLC method. Homberg [11] carried out rapid separations of sterols and other non-polar compounds in the unsaponifiable matter from the soap solution using aluminia columns. Perrin and Raoux [12] investigated the effects of the mobile phase and temperature on the reversed-phase HPLC separation of unsaponifiable matter. They achieved good separations of sterols from different oils.

Nowadays disposable SPE cartridges are available that absorb large amounts of solutions that allow liquid–liquid extractions to be replaced. For this reason, we used SPE cartridges (3 ml) only for the clean-up of the unsaponifiable solutions. We tried to develop a single procedure that would combine the advantages of SPE, HPLC and high-resolution GC (HRGC) to allow us to perform the largest possible number of analyses daily. Further, if the laboratory is equipped with an automatic HPLC injector and collector, it is possible to perform the separation and collection automatically. Each component is then determined using HRGC, as it is when using the conventional method described in the NGD collection [13]. The aim of this work was to verify that the suggested method gives results that are not significantly different from those given by the NGD method. Comparisons were made on numerous different olive oils: crude olive oil (45), extravirgin oil (30), refined oil (20) and crude pomace olive oil (5).

EXPERIMENTAL

Apparatus and materials

The extraction columns used were a Bakerbond SPE, quaternary amine (N^+) No. 7091-03 (3 ml) (40 μm average particle diameter, 60 Å) and a Varian Chem Elut 2050 (50 ml). Suitable flasks for the saponification of about 2 g of olive oil were used.

For HPLC separations the following were used: gradient pump, LDC Analytical CM 4000; UV detector, Milton-Roy SpectroMonitor 3100; column, Supelcosil LC-Si, 15 cm × 4.6 mm I.D., 5 μm (Supelco); flow-rate, 1.00 ml/min; detection wavelength, 210 nm; range, 0.10 a.u.f.s.; response time, 0.10 s; loop, 10 μl; chart speed, 0.5 cm/min; and elution gradient (Fig. 1) with *n*-hexane–diethyl ether, 0 min 80:20, 15–20 min 60:40, 20.1–30 min 80:20 and 30 min ready for next run.

For HRGC separations, the following were used: gas chromatograph, Carlo Erba Mega Series HRGC 5300; capillary column, SPB-5 (5% diphenyl–94% dimethyl–1% vinylpolysiloxane), fused silica, 30 m × 0.25 mm I.D., 0.25 μm film thickness (Supelco) oven temperature, for sterols isothermal at 263°C, for alkanols programmed from 180°C (5 min) to 260°C (25 min) at 5°C/min; injector temperature, 290°C; detector (flame ionization) temper-

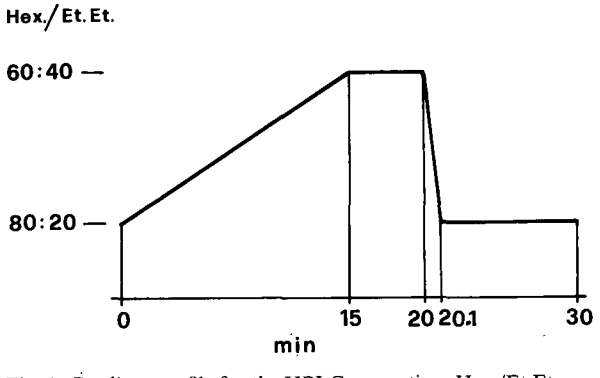

Fig. 1. Gradient profile for the HPLC separation. Hex./Et.Et. = *n*-Hexane–diethyl ether.

ature, 300°C; carrier gas, hydrogen at 4.5 ml/min; split ratio, 2.8; and injection volume, 1–2 μl.

Computing was performed using Maxima 820 software (Water Dynamic Solutions, Millipore) installed on an IBM PS2/H21 personal computer.

Reagents

Analytical reagent-grade chemicals were used unless indicated otherwise.

Diethyl ether, methanol, chloroform, pyridine, anhydrous sodium sulphate and potassium hydroxide were obtained from Fluka. *n*-Hexane (HPLC grade) and diethyl ether (HPLC grade) from Fluka were used for HPLC separations. Trimethylchlorosilane (TMCS) and hexamethyldisilazane (HMDS) were supplied by Supelco.

The saponification solution [20% (w/v) potassium hydroxide in methanol] was prepared by dissolving potassium hydroxide (40 g) in distilled water (24 ml) and diluting 200 ml with methanol in a volumetric flask.

Internal standard solutions were 2 mg/ml 5α-cholestan-3β-ol (cholestanol) (>99%, Fluka) in chloroform and 1 mg/ml 1-eicosanol (C_{20}) (>98%, Fluka) in chloroform.

The derivatization reagent was pyridine–hexamethyldisilazane (HMDS)–trimethylchlorosilane (TMCS) (9:3:1).

Procedure

As regards the NGD methods, we refer to the NGD method collection for sterols, method No. C71-1989 and C72-1989; alkanols, C75-1989 and C76-1989; and erythrodiol and uvaol, C52-1985.

The method tested was the following. Add 200 μl of each internal standard solution to the saponification flask (if pomace oil has to be tested, add 600 μl) and evaporate the solvent. Weight exactly a sample of about 2.000 g, add 5 ml of saponification solution, fit the condenser and boil over a water-bath or another suitable device for 25 min. Add 15 ml of distilled water, pour the hot solution into the Chem Elut 2050 column, wait for about 15 min, add 50 ml of diethyl ether, wait for about 15 min, add 20–25 ml of diethyl ether and collect the solution in a 50-ml flask containing about 1 g of anhydrous sodium sulphate. Purify the solution by passing it through a Bakerbond quaternary amine (N^+) column, already "conditioned" with 3 ml of diethyl ether. Collect the solution in a 50-ml flask containing about 1 g of anhydrous sodium sulphate. Filter the solution through paper into a small flask, evaporate the solvent, weight the unsaponifiable matter and dissolve it in chloroform to give a 10% solution. Inject the solution into the HPLC system and collect the fractions which are of interest, evaporate the solvent, derivatize and inject into the HRGC system.

RESULTS AND DISCUSSION

Several methods for performing the saponification and separation of unsaponifiable material have been suggested, as surveyed by Homberg [11]. However, saponification is usually carried out using a suitable alkali solution.

We preferred not to change the method, but to choose the saponification conditions in order to minimize the solution volumes and to decrease the reaction time. For this reason, the concentration of the KOH solution was increased and, consequently, the reaction time was investigated.

First, we waited only 1 min after the disappearance of the phases (10 min in all). This period is too short and erythrodiol and uvaol were wrongly determined. To solve this problem, four tests using 10, 20, 40, 60 min were carried out and the results were compared with the results obtained with the conventional method (NGD). Table I shows that at least 20 min are needed to determine the erythrodiol and uvaol contents exactly.

Homberg [11] replaced the liquid–liquid extraction with a separation on a laboratory-filled alumina column. For the reasons mentioned earlier, we used the "ready-for-use" Chem Elut 2050 column.

TABLE I

RECOVERY OF ERYTHRODIOL + UVAOL WITH DIFFERENT SAPONIFICATION TIMES

Saponification time (min)	Erythrodiol + uvaol (%)[a]
10	1.9
20	2.8
40	2.7
60	2.8

[a] Value obtained using NGD = 2.8%.

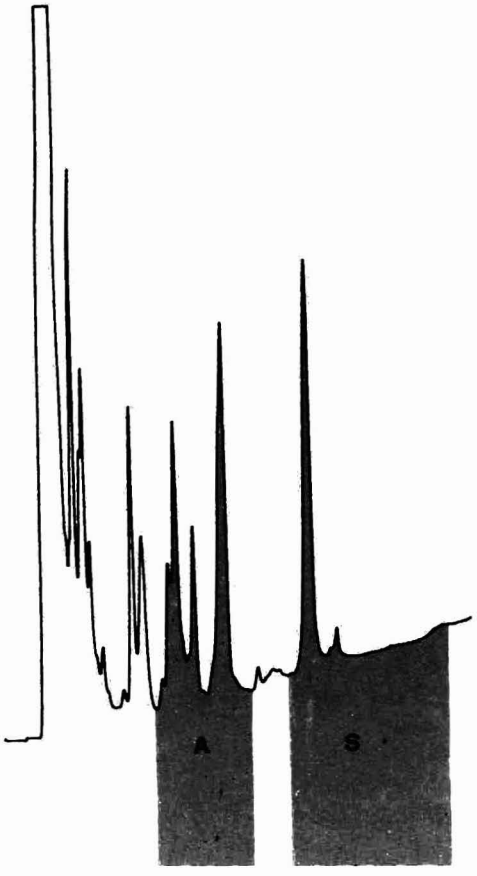

Fig. 2. HPLC of extra-virgin olive oil unsaponifiable and collected fractions. A = Fraction containing alkanols (6 and 9 min); S = fraction containing sterols (10 and 18 min).

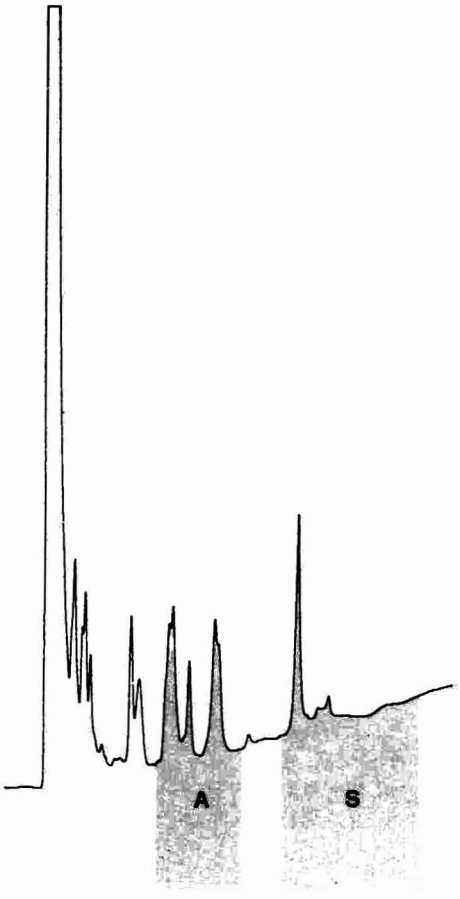

Fig. 3. HPLC of crude olive oil unsaponifiable and collected fractions. A and S as in Fig. 2.

This type of highly efficient, disposable column is made for rapid and easy sample preparation for HPLC or HRGC analyses. It allowed emulsions and several manual operations to be avoided. This is why it is possible to process numerous samples at the same time.

After saponification, it is necessary to add water and to pour the hot solution into the Chem Elut 2050 column at once, in order to facilitate the solid-phase adsorption. It is advisable to wait for about 15 min, instead of 3–5 min as suggested in the instructions, because of the high soap concentration.

The collected solution contains water, which is partially absorbed by sodium sulphate, and a small amount of soaps that has to be removed as it could interfere in the following steps. In order to do this, the solution is passed through the Bakerbond quaternary amine (N^+) column, which removes all the remaining soaps (clean-up). A small amount of water is again separated and absorbed by sodium sulphate.

The subsequent HPLC separation is carried out in a way similar to that described by Cortesi and co-workers [6,7]. We chose gradient elution to achieve complete separation of the less polar compounds from alkanols and sterols and, at the same time, to keep the analysis time short.

The collection of sterols and alkanols is very easy; the fractions which have to be collected are clearly shown in Figs. 2–5. These fractions give sufficient analytes for the subsequent HRGC determinations. Hence it is not necessary to perform repeat-

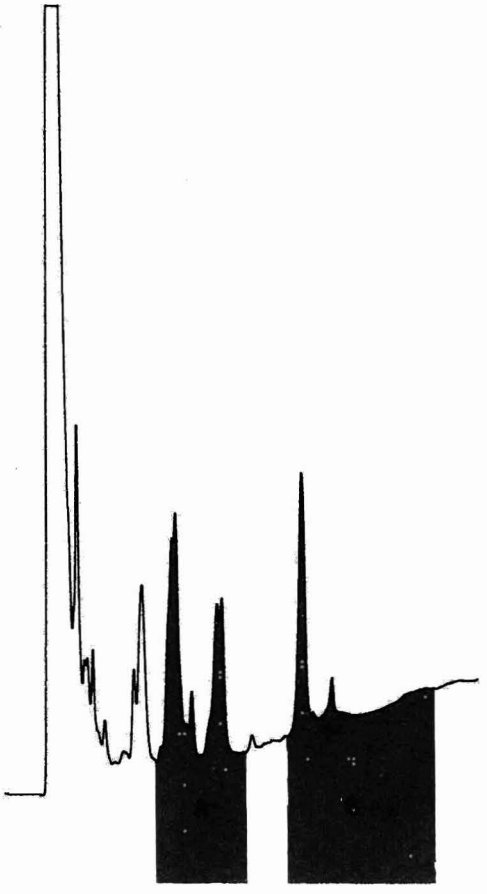

Fig. 4. HPLC of refined olive oil unsaponifiable and collected fractions. A and S as in Fig. 2.

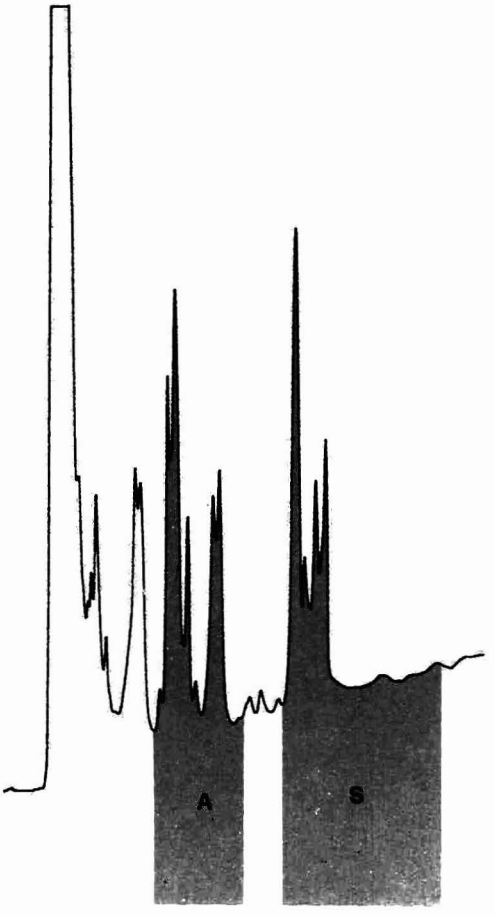

Fig. 5. HPLC of crude pomace oil unsaponifiable and collected fractions. A and S as in Fig. 2.

ed cycles of injections as was done by Iatrides *et al.* [8]. This allows us to choose a gradient profile that gives a good separation of unsaponifiable material (useful, for instance, for future applications) instead of very fast, but worse, separations. The resolution achieved by several workers [9,10,12] is not necessary here because the quantification is to be performed by HRGC. In our case, alkanols are eluted between about 6 and 9 min and sterols and erythrodiol + uvaol between 10 and 18 min.

Each fraction is then evaporated and the solutes are derivatized with a suitable reagent and injected for HRGC separation.

CONCLUSION

As mentioned above, official methods are very time consuming, but a faster method can be chosen only if it gives results that are not significatively different from those obtained using the official methods.

Tables II and III compare the mean values and the standard deviations of the results obtained by the two methods. In order to verify whether the differences between the results are random or not, Student's t-test was applied to check the H_0 hypothesis, *i.e.*, random differences [17,18]. For a 95% confidence level and $N - 1 = 99$ degrees of freedom, the t-value is 1.984. The t values calculated from the

TABLE II

STATISTIC ANALYSIS OF STEROL DATA (STUDENT'S *t*-TEST)

Method	Parameter	Compound[a]													
		a	b	c	d	e	f	g	h	i	l	m	n	o	p
Conventional (NGD method)	Mean (%)	0.328	0.117	3.630	1.769	0.090	0.855	80.391	0.817	10.057	0.658	0.299	0.465	3.020	1576.530
	S.D. (%)	0.131	0.619	2.724	1.047	0.226	0.185	5.820	0.486	5.991	0.331	0.154	0.137	2.221	928.450
This work	Mean (%)	0.375	0.123	3.491	1.761	0.074	0.818	80.455	0.835	9.992	0.704	0.299	0.462	3.015	1580.950
	S.D. (%)	0.210	0.620	2.571	0.989	0.218	0.151	5.837	0.455	5.876	0.335	0.180	0.145	2.153	919.588
	t	−1.888	−0.068	0.369	0.055	0.506	1.540	−0.077	−0.268	0.077	−0.972	0.000	0.149	0.016	−0.033

[a] a = Cholesterol; b = brassicasterol; c = campesterol; d = stigmasterol; e = $\Delta^{5,23}$-stigmastadienol; f = clerosterol; g = β-sitosterol; h = sitostanol; i = Δ^{5}-avenasterol; l = $\Delta^{5,24}$-stigmastadienol; m = Δ^{7}-stigmastenol; n = Δ^{7}-avenasterol; o = erythrodiol + uvaol; p = total sterols (mg/kg).

TABLE III

STATISTICAL ANALYSIS OF ALKANOL DATA (STUDENT'S *t*-TEST)

Method	Parameter	Alkanol[a]							
		a	b	c	d	e	f	g	h
Conventional (NGD method)	Mean (mg/kg)	83.695	7.190	142.187	9.362	130.476	6.992	50.584	429.456
	S.D. (mg/kg)	187.982	12.896	269.367	15.099	214.025	10.581	75.458	780.711
This work	Mean (mg/kg)	82.691	7.183	137.675	9.183	128.109	6.251	51.296	422.313
	S.D. (mg/kg)	175.717	11.945	249.974	13.236	198.039	8.943	65.204	718.363
	t	0.038	0.003	0.121	0.088	0.080	−0.184	−0.070	0.066

[a] a = 1-Docosanol (C_{22}); b = 1-tricosanol (C_{23}); c = 1-tetracosanol (C_{24}); d = 1-pentacosanol (C_{25}); e = 1-hexacosanol (C_{26}); f = 1-heptacosanol (C_{27}); g = 1-octacosanol (C_{28}); h = total alkanols.

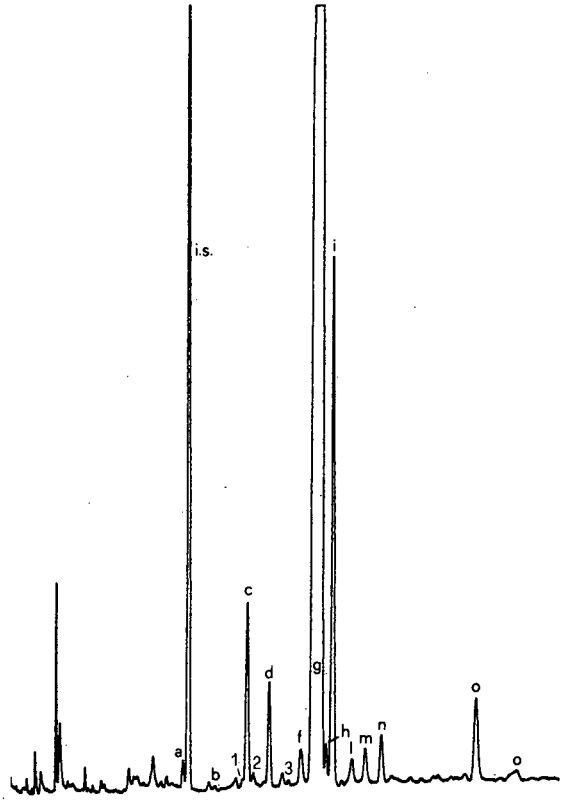

Fig. 6. Gas chromatogram showing olive oil sterol, erythrodiol and uvaol composition. Peaks: 1 = 24-methylenecholesterol; [retention time (t_R) = 10.6 min]; 2 = campestanol (t_R = 11.0 min); 3 = Δ^7-campesterol (t_R = 12.2 min); i.s. = internal standard (cholestanol) (t_R = 8.8 min). See Table II for the identification of the other sterols.

experimental data are less than 1.984 for each component; this means that H_O is always true (random differences).

The statistical analysis does not take into account 24-methylenecholesterol, campestanol and Δ^7-campesterol (Fig. 6) because, as is known [14,15], severe interferences can occur which make it difficult to determine these sterols. Further, we have never observed interference at the retention time of Δ^7-stigmastenol, due to 24-methylenecycloartanol not being well separated by TLC [16]. The examination of the t values shows $| t | = 1.888$ for cholesterol, which is quite close to 1.984.

We suspect that sometimes interferences occurred during the cartridge separation of the unsaponifiable matter from the soap solution. In these cases we "washed" the cartridge using diethyl ether and dried it at room temperature before use.

With regard to the erytrodiol, uvaol and alkanols, the examination of the t values shows good agreement between the two methods.

Overall we believe that the tested method gives the same results as the NGD method and can replace it, especially when many samples have to be analysed daily. On the other hand, we think the method could be improved; for instance, a more suitable elution solvent for the Chem Elut 2050 column is desirable, and the HPLC separations could be performed more efficiently with a significant decrease in the sampling time.

ACKNOWLEDGEMENTS

We thank Mr. R. Vago (Service T. L., Milan, Italy) and Mr. L. Traverso (Pro.D.E.St., Genoa, Italy) for their kind collaboration.

REFERENCES

1 Application Notes SS-AN020, 1982, PH-009 and PH-010, 1989, J. T. Baker Chemicals, Phillipsburgh, NJ.
2 R. E. Worthington and H. L. Hitchcock, *J. Am. Oil Chem. Soc.*, 61 (1984) 1085.
3 P. Horstmann and A. Montag, *Fette Seifen Anstrichm.*, 88 (1986) 262.
4 R. Schuster, *HPLC Application Note No. 12-5954-6269*, Hewlett-Packard, Avondale, PA, 1987.
5 K. Grob, M. Lanfranchi and C. Mariani, *J. Am. Oil Chem. Soc.*, 67 (1990) 626.
6 N. Cortesi, E. Fedeli, A. Gasparoli and E. Tiscornia, *Riv. Ital. Sostanze Grasse*, 54 (1977) 16.
7 N. Cortesi, E. Fedeli and E. Tiscornia, *Riv. Ital. Sostanze Grasse*, 55 (1978) 168.
8 M. C. Iatrides, J. Artaud and M. Derbesy, *Analusis*, 12 (1984) 205.
9 B. Holen, *J. Am. Oil Chem. Soc.*, 62 (1985) 1344.
10 F. Mordret, H. Ajana and C. Gauchet, *Rev. Fr. Corps Gras*, 32 (1985) 305.
11 E. Homberg, *Fat Sci. Technol.*, 89 (1987) 215.
12 J. L. Perrin and R. Raoux, *Rev. Fr. Corps Gras*, 35 (1988) 329.
13 NGD, *Norme Grassi e Derivati*, Stazione Sperimentale per le Industrie degli Oli e dei Grassi, Milan, 1976, and subsequent revisions.
14 G. Morchio, G. Amelotti, A. Bocca, V. Bocio, L. Conte, O. Cozzoli, L. Cremonesi, R. Fascioli, L. Giro, D. Grieco, G. Lercker, C. Mariani, G. Pierattine, E. Sarti and P. Zunin, *Riv. Ital. Sostanze Grasse*, 66 (1989) 531.
15 G. Amelotti, *Riv. Ital. Sostanze Grasse*, 62 (1985) 337.
16 G. Amelotti, A. Griffini, M. Bergna and P. Montorfano, *Riv. Ital. Sostanze Grasse*, 62 (1985) 459.
17 G. Bussetti, *Esercitazioni Pratiche di Fisica*, Univ. Levrotto e Bella, Turin, 1980, p. 669.
18 M. R. Spiegel, *Statistica*, ETAS Libri, Milan, 1982, p. 357.

Journal of Chromatography, 606 (1992) 187–193
Elsevier Science Publishers B.V., Amsterdam

CHROM. 24 318

Chemiluminescent detection of thymine hydroperoxides by high-performance liquid chromatography*

Rie Saeki

Research Development Corporation of Japan, Biophoton Project, c/o Kohjinkai Hospital, Tsutsujigaoka, Miyagino-ku, Sendai 980 (Japan)

Humio Inaba

Research Institute of Electrical Communications, Tohoku University, Katahira, Aoba-ku, Sendai 980 (Japan)

Toshihide Suzuki and Teruo Miyazawa

Department of Food Chemistry, Faculty of Agriculture, Tohoku University, Tsutsumidori, Aoba-ku, Sendai 981 (Japan)

(First received June 20th, 1991; revised manuscript received April 21st, 1992)

ABSTRACT

High-performance liquid chromatography (HPLC) with chemiluminescence detection was used to detect thymine hydroperoxides, which are expected to occur in biological tissues as primary products in free radical-mediated DNA damage. The thymine hydroperoxides were chemically prepared by the acid-catalysed hydrogen peroxide oxidation of thymine and 5-hydroxymethyluracil and their hydroperoxide products were identified as *trans*- or *cis*-5-chloro-6-hydroperoxy-5,6-dihydrothymine and 5-hydroperoxymethyluracil, respectively, by means of NMR, IR and mass spectrometry. The results confirmed that these thymine hydroperoxides are specifically detectable at picomole levels by the described HPLC method with high reproducibility.

INTRODUCTION

It is well known that ionizing radiation or chemical oxidation causes DNA damage [1–7], and thus results in strand breakage in cellular DNA and modification of DNA bases. Among the DNA bases, thymine is the most susceptible to these modifying effects [8], and the detection and characterization of the modified thymine may be of considerable importance in studying the mechanism of DNA damage.

Correspondence to: Dr. T. Miyazawa, Department of Food Chemistry, Faculty of Agriculture, Tohoku University, Tsutsumidori, Aoba-ku, Sendai 981, Japan.

* Part of this study was presented at the *5th Biennial General Meeting of the International Society of the Free Radical Research, Pasadena, CA, November 14–20th, 1990.*

Ionizing and near-ultraviolet irradiation of DNA causes modification of thymine with the formation of saturated ring compounds [1,8–12]. The *cis*- or *trans*-5,6-dihydroxy-5,6-dihydrothymine (thymine glycol) was found to be formed in aqueous thymine medium by permanganate oxidation [13,14] and irradiation [15,16], and also formed in DNA by the action of ionizing and near-ultraviolet irradiation [9] and by chemical oxidation with potassium permanganate [1,8,17] and osmium tetraoxide [9]. These compounds are suggested to be removed from irradiated cellular DNA in repairing processes and yielded from the oxidized DNA by endonucleases. It has been reported that *Escherichia coli* endonuclease III contains N-glycosylase activity which can release oxidized thymine [11,18–22].

On the other hand, irradiation of DNA solutions

0021-9673/92/$05.00

in the presence of oxygen was shown to lead to the formation of stable hydroperoxides on the pyrimidine base moieties of the nucleic acid molecule [23–25] and the formation of several thymine hydroperoxides by irradiation or chemical oxidation has been suggested (Fig. 1). It is known that 5- or 6-hydroperoxy-6- or -5-hydroxy-5,6-dihydrothymine (Fig. 1a–d) are formed by X-irradiation, gamma-irradiation [26–30], photo-excitation at 1849 Å [16] and chemical oxidation with OsO_4 in aerated aqueous solutions of nucleic acids, pyrimidine nucleotides and pyrimidine bases [31,32], and these are also known to have mutagenic activity [33,34]. 5-Hydroperoxymethyluracil (Fig. 1e) was formed from 5-hydroxymethyluracil by acid-catalysed oxidation with H_2O_2–HCl [35] and also has mutagenic activity [34]. 5,6-Dihydroperoxydihydrothymine (Fig. 1f) was formed from 6-hydroxy-5-bromothymine by chemical oxidation with H_2O_2–H^+–Ag_2O [32].

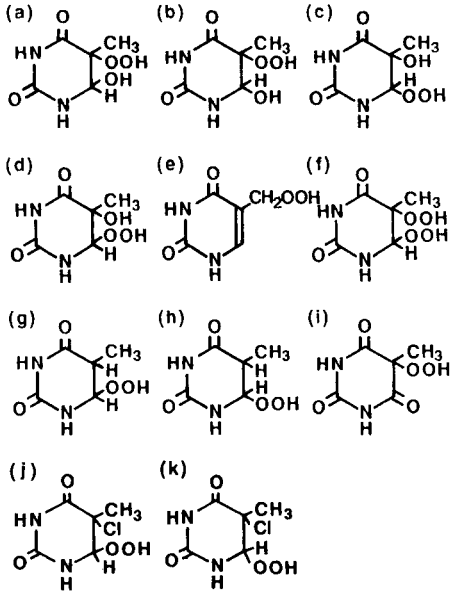

Fig. 1. Structures of thymine hydroperoxides. a = *trans*-5-hydroperoxy-6-hydroxy-5,6-dihydrothymine; b = *cis*-5-hydroperoxy-6-hydroxy-5,6-dihydrothymine; c = *cis*-6-hydroperoxy-5-hydroxy-5,6-dihydrothymine; d = *trans*-6-hydroperoxy-5-hydroxy-5,6-dihydrothymine; e = 5-hydroperoxymethyluracil; f = *trans*-5,6-dihydroperoxy-5,6-dihydrothymine; g = *cis*-6-hydroperoxy-5,6-dihydrothymine; h = *trans*-6-hydroperoxy-5,6-dihydrothymine; i = 5-hydroperoxy-5-methylbarbituric acid; j = *trans*-5-chloro-6-hydroperoxy-5,6-dihydrothymine; k = *cis*-5-chloro-6-hydroperoxy-5,6-dihydrothymine.

6-Hydroperoxy-5,6-dihydrothymine (Fig. 1g and h) and 5-hydroperoxy-5-methylbarbituric acid (Fig. 1i) were also formed from 6-hydroxy-5-bromothymine by H_2O_2–H^+–Zn and H_2O_2–H_2O–Ag_2O–Br_2 oxidation, respectively [32]. *trans*-5-Chloro-6-hydroperoxy-5,6-dihydrothymine (Fig. 1j) was formed from thymine by acid-catalysed oxidation with H_2O_2–HCl [36].

Thin-layer chromatography, paper chromatography, gas chromatography–mass spectrometry with selected-ion monitoring [5–7] and high-performance liquid chromatography (HPLC) with UV detection have been used for the detection of thymine glycols and hydroperoxides. However, the hydroperoxide group-specific determination of thymine hydroperoxide has not been accomplished. Chromatographic determination of thymine hydroperoxides as primary intermediates in the oxidation reaction would be the most direct and useful approach in the study of DNA damage, in both *in vitro* and *in vivo* systems.

In this study, we used chemiluminescence (CL) detection for the hydroperoxide group-specific determination of thymine hydroperoxides by HPLC. The chemiluminescent nature of thymine hydroperoxides is not generally known. The CL assay based on detecting photon emission in the oxidation of luminol during the interaction of hydroperoxides and cytochrome *c*-haeme has high sensitivity and specificity for determining hydroperoxide groups [37,38].

EXPERIMENTAL

Oxidation of thymine

Ten milligrams of thymine (Wako, Osaka, Japan) were dissolved in 1.5 ml of 30% hydrogen peroxide containing 25 μl of concentrated hydrochloric acid and oxidized for 96 h at room temperature [35,36]. After oxidation, the reaction mixture was diluted twentyfold with distilled water and a 10-μl portion was injected directly into the HPLC system.

Luminescence reagent

The post-column luminescence reagent for the assay of hydroperoxide groups was prepared by dissolving 10 μg/ml of cytochrome *c* (from horse heart, type IV) (Sigma, St. Louis, MO, USA) and 1 μg/ml of luminol (3-aminophthaloyl hydrazine) (Wako) in

50 m*M* borate buffer (pH 9.3), as described by Miyazawa *et al.* [37].

Instruments and chromatographic conditions

A schematic diagram of the HPLC system used for determining thymine hydroperoxides is shown in Fig. 2. It consisted of a JASCO HPLC instrument and reversed-phase column (Finepak SIL C_{18}, 10 μm, 250 × 4.6 mm I.D.) (Japan Spectroscopic, Tokyo, Japan). The flow-rate of the mobile phase (distilled water) was 1.0 ml/min with a JASCO 880-PU pump. The column eluate was introduced into a JASCO 875-UV detector set at 210 nm, and the eluate was then mixed with the luminescence reagent at a mixing joint attached close to the entrance to the flow cell of the CL detector. The CL generated by the reaction of hydroperoxide and the luminescence reagent was monitored with a CLD-100 single-photon counting CL detector (Tohoku Electronic, Sendai, Japan) equipped with a PTFE flow cell (200 μl) [38]. The chromatograms detected by CL were recorded by a microcomputer and saved on a diskette. The chromatograms detected at 210 nm were recorded with a SIC Chromatocoder 12.

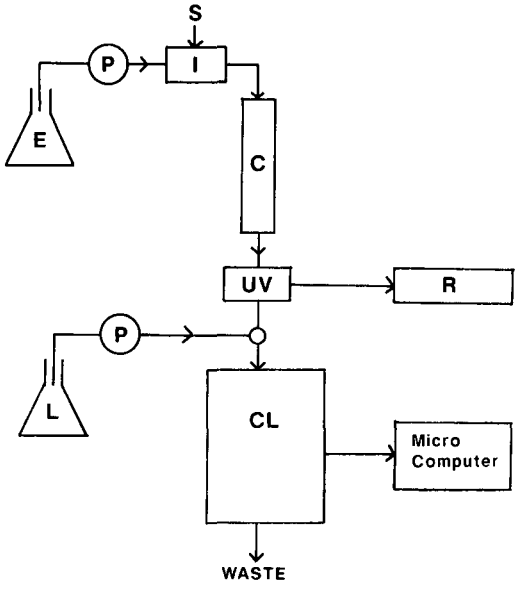

Fig. 2. Schematic diagram of HPLC system. P = Pump (JASCO 880-PU); I = injection valve (Rheodyne 7125); C = column (JASCO Finepak SIL C_{18} or Megapak SIL C_{18}); UV = UV detector (JASCO 875-UV); CL = chemiluminescence detector (Tohoku Electronic, CLD-100); R = recorder (SIC Chromatocoder 12); E = eluate (distilled water, flow-rate 1.0 ml/min); L = luminescence reagent containing cytochrome *c* and luminol in borate buffer (pH 9.3, flow-rate 0.5 ml/min).

Structural characterization of thymine hydroperoxides

The experiments were carried out on a larger scale in order to isolate the oxidation products by using a reversed-phase column (Megapak SIL C_{18}, 10 μm, 250 × 7.5 mm I.D.) (JASCO). The isolated fractions were then lyophilized with an EYELA FD-1 lyophilizer (Tokyo Rikakikai, Tokyo, Japan). NMR spectra were determined in tetramethylsilane (TMS) as an internal standard by using a JEOL JNM-FX100 instrument. Infrared analyses were performed on KBr pellets with a JASCO IR Report-100 instrument. Mass spectra were recorded with a JEOL JMS-DX303 mass spectrometer in the fast atom bombardment mode.

Preparation of 5-hydroperoxymethyl uracil

A 114-mg amount of 5-hydroxymethyluracil (Sigma) was dissolved in 20 ml of 15% hydrogen peroxide, then 100 μl of concentrated hydrochloric acid in 10 ml of hydrogen peroxide were added dropwise. After standing at room temperature for 48 h with stirring, the reaction mixture was lyophilized. The residue was washed with cold water and the purified product, 5-hydroperoxymethyluracil, was obtained by recrystallization from 10% methanol solution [35].

RESULTS AND DISCUSSION

Fig. 3 shows a typical HPLC pattern of the H_2O_2–HCl oxidation products of thymine. Oxidized thymine gave two sharp CL peaks, peak 1 (9 min) and peak 2 (21 min), with good reproducibility together with a CL H_2O_2 peak. These two CL peaks were completely eliminated by $NaBH_4$ reduction (OOH → OH), indicating that both the peak 1 and 2 compounds possess a hydroperoxide group in their thymine molecules [38].

Our structural assignment of the peak 1 and 2 compounds yielded by H_2O_2–HCl oxidation of thymine was further corroborated by the spectral data after their isolation. Fig. 4 shows the time-dependent change in the UV spectra of the oxidized thymine reaction mixture. The time-dependent de-

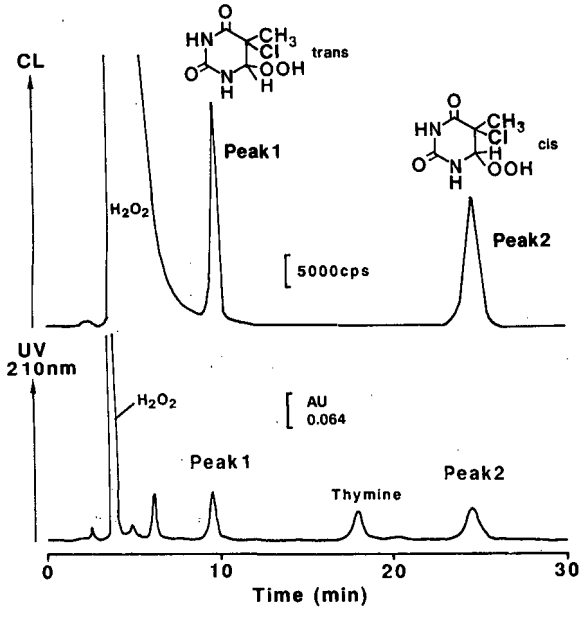

Fig. 3. HPLC of thymine oxidized by H_2O_2–HCl.

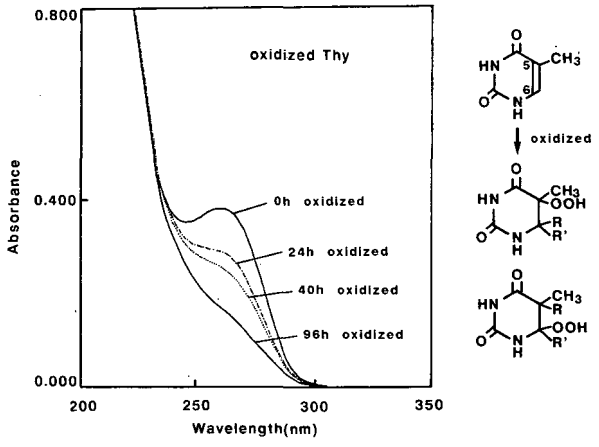

Fig. 4. Changes in UV absorption spectra of thymine (Thy) during H_2O_2–HCl oxidation.

crease in absorption at 265 nm suggests that thymine is oxidized and changed to a ring-saturated compound.

Fig. 5 shows the NMR spectra of the peak 1 and peak 2 compounds in $(CD_3)_2SO$ at 100 MHz with

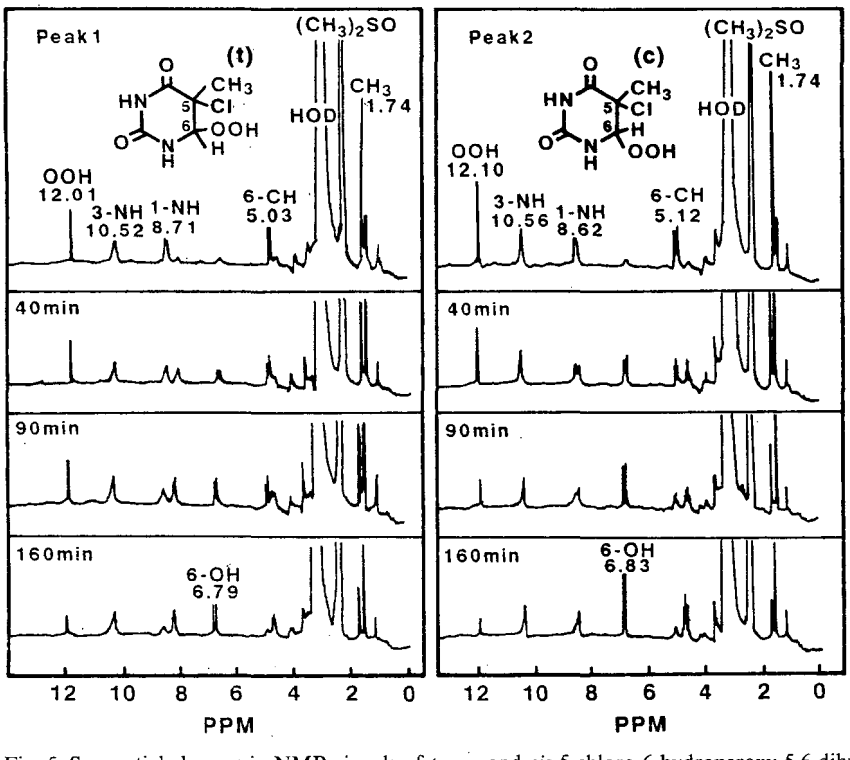

Fig. 5. Sequential changes in NMR signals of *trans*- and *cis*-5-chloro-6-hydroperoxy-5,6-dihydrothymine.

TMS as an internal standard. Peak 1 compound has signals for CH_3 (1.74), C(6)H (4.97), C(6)OH (6.83), N(1)H (8.70), N(3)H (10.51) and OOH (12.00 ppm). Peak 2 compound has signals for CH_3 (1.73), C(6)H (5.06), C(6)OH (6.82), N(1)H (8.62), N(3)H (10.55) and OOH (12.09 ppm). As time progressed, the signals for OOH decreased and the signals for C(6)OH increased. No signals for C(5)OH were present.

In the IR spectra, peak 1 compound had bands for NH (3400), νOH (3300), νCH_3 (3100), $\nu C=O$ (1730, 1685), νCH_3 (1480) and νC–O (1115, 1100, 1065 cm^{-1}), and peak 2 compound had bands for NH (3400), νOH (3300), νCH_3 (3100), $\nu C=O$ (1720), νCH_3 (1480, 1385) and νC–O (1130, 1070 cm^{-1}). A peak at m/z 195 corresponding to $[M+H]^+$, the molecular ion of 5-chloro-6-hydroperoxy-5, 6-dihydrothymine, was confirmed in the mass spectra of both peak 1 and 2 components.

From a comparison of these data with previous findings reported for the spectral characteristics of thymine peroxides [28,36], it is concluded that both the peak 1 and 2 compounds were 5-chloro-6-hydroperoxy-5,6-dihydrothymine, and that the difference between the spectra was solely dependent on their geometrical isomerism. Structurally, *trans* compounds must have a multiple signal for C(6)H and *cis* compounds have a triplet signal for C(6)H [28] in NMR spectra. Peak 1 showed multiple signal patterns for C(6)H and peak 2 showed triplet signals (Fig. 6). From these results, it is concluded that the peak 1 and 2 compounds were *trans*- and *cis*-6-hydroperoxy-5,6-dihydrothymine, respectively.

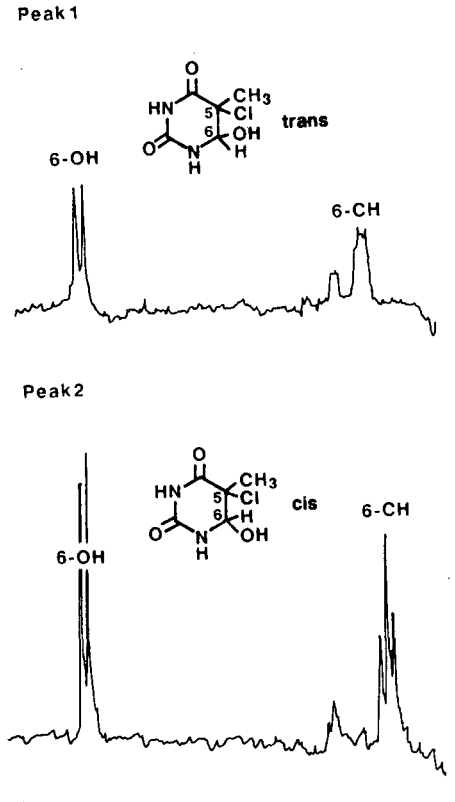

Fig. 6. Expanded NMR signals for 6-CH of reduced derivative of peak 1 and 2 components.

In previous paper [36], it was reported that only a *trans*-compound (Fig. 1j) was produced by the oxidation of thymine with H_2O_2–HCl. However, from the present results, it was confirmed that the *cis* compound (Fig. 1k) was also produced in this oxidation system.

The calibration lines for *trans*- and *cis*-5-chloro-6-hydroperoxy-5,6-dihydrothymine showed that the CL counts integrated for the peak area corresponding to thymine hydroperoxides after subtraction of the background counts were proportional to the amount present at least in the range 30–500 pmol that was examined.

Fig. 7 shows the HPLC pattern of 5-hydroperoxymethyluracil that was prepared by acid-catalised oxidation with H_2O_2–HCl [35]. A single, sharp CL peak was detected with good reproducibility and was also eliminated after $NaBH_4$ reduction (OOH $\rightarrow$ OH).

The calibration line for 5-hydroperoxymethyluracil (HPMU) showed that the CL counts integrated for the peak area were proportional to the amount present at least in the range 50–250 pmol that was examined.

The present results indicate that thymine hydroperoxides, such as *trans*- and *cis*-5-chloro-6-hydroperoxy-5,6-dihydrothymine and 5-hydroperoxymethyluracil, could be hydroperoxide-specifically determined by the proposed HPLC method. High sensitivity, specificity and reproducibility were confirmed.

HPLC incorporating the luminol reaction has attracted particular interest recently for the detection of trace amounts of biological hydroperoxidic constituents [37–43]. For example, biological lipid hydroperoxides have been determined by this method

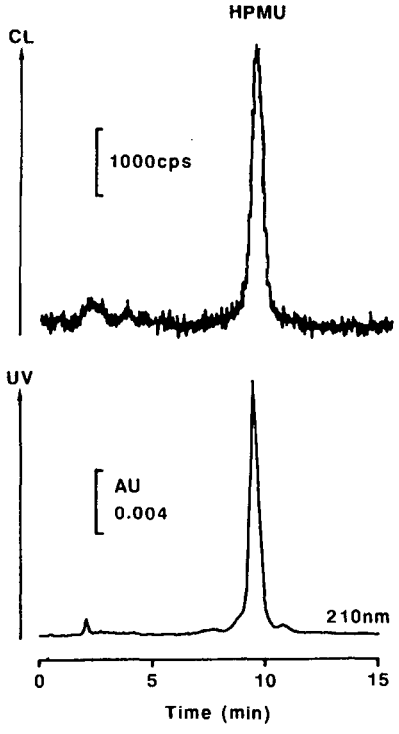

Fig. 7. HPLC of isolated 5-hydroperoxymethyluracil (HPMU).

[38–43]. The present results show that this method is also useful for detecting nucleic acid–base hydroperoxides.

The thymine hydroperoxides that we prepared at low pH were fairly stable under physiological conditions. On preparing thymine hydroperoxide, oxygen and nitrogen did not gave any effect on the hydroperoxide yields, and the yield was solely dependent on the H_2O_2 concentration. Under the present conditions for preparing thymine hydroperoxides, the product possessing a hydroperoxide group in the molecule was only thymine hydroperoxide. Several very minor products were observed with UV detection, but they were not chemiluminescent, thus indicating they were not hydroperoxides.

Thymine hydroperoxides formed by irradiation and chemical oxidation have been characterized in many *in vitro* systems (Fig. 1) and also detected from damaged DNA by irradiation or chemical oxidation [1–12]. The oxidation of denatured DNA with permanganate under certain mild conditions does not result in the selective degradation of its thymine residues [8,13]. Thymine glycol formation in DNA by several oxidizing agents and ionizing and near-UV radiation has also been detected by using radiometric analysis [1,9]. Excision of thymine glycol and thymidine glycols by DNA repair enzymes and their excretion into urine have also been performed by radiometric analysis [44]. However, the hydroperoxide derivatives were not detected especially in biological samples, because of the lack of a suitable method.

The use of sensitive CLD-100 and CLD-110 CL detectors (Tohoku Electronic) that have been improved by Miyazawa's group [38] enables the sensitivity to be increased further down to femtomole levels of hydroperoxides. Thymine hydroperoxide determination would be very important useful for establishing how damage occurs to DNA. Further investigations on the formation of these compounds in various biological systems are needed.

REFERENCES

1 K. Frenkel, M. S. Goldstein, N. J. Duker and G. W. Teebor, *Biochemistry*, 20 (1981) 750.
2 G. W. Teebor, K. Frenkel and M. S. Goldstein, *Proc. Natl. Acad. Sci. U.S.A.*, 81 (1984) 318.
3 J. F. Ward and I. Kuo, *Radiat. Res.*, 66 (1976) 485.
4 E. Gajewski, G. Rao, Z. Nackerdien and M. Dizdaroglu, *Biochemistry*, 29 (1990) 7876.
5 O. I. Aruoma, B. Halliwell and M. Dizdaroglu, *J. Biol. Chem.*, 264 (1989) 13024.
6 O. I. Aruoma, B. Halliwell, E. Gajewski and M. Dizdaroglu, *J. Biol. Chem.*, 264 (1989) 20509.
7 M. Dizdaroglu, O. I. Aruoma and B. Halliwell, *Biochemistry*, 29 (1990) 8447.
8 S. Iida and H. Hayatsu, *Biochim. Biophys. Acta*, 240 (1971) 370.
9 K. Frenkel, M. S. Goldstein and G. W. Teebor, *Biochemistry*, 20 (1981) 7566.
10 P. V. Hariharan and P. A. Cerutti, *J. Mol. Biol.*, 66 (1972) 65.
11 P. V. Hariharan and P. A. Cerutti, *Proc. Natl. Acad. Sci. U.S.A.*, 71 (1974) 3532.
12 P. V. Hariharan and P. A. Cerutti, Biochemistry, 16 (1977) 2791.
13 S. Iida and H. Hayatsu, *Biochim. Biophys. Acta*, 213 (1970) 1.
14 H. Hayatsu and T. Ukita, *Biochem. Biophys. Res. Commun.*, 29 (1967) 556.
15 B. S. Hahn and S. Y. Wang, *J. Am. Chem. Soc.*, 94 (1972) 4764.
16 M. Daniels and A. Grimison, *Biochim. Biophys. Acta*, 142 (1967) 292.
17 G. K. Darby, A. S. Jones, J. R. Tittensor and R. T. Walker, *Nature (London)*, 216 (1967) 793.

18 T. Lindahl, S. Ljungquist, W. Siegert, B. Nyberg and B. Sperens, *J. Biol. Chem.*, 252 (1977) 3286.
19 C. J. Chetsanga and T. Lindahl, *Nucleic Acids Res.*, 6 (1979) 3673.
20 L. H. Breimer and T. Lindahl, *Nucleic Acids Res.*, 8 (1980) 6199.
21 L. H. Breimer and T. Lindahl, *J. Biol. Chem.*, 259 (1984) 5543.
22 L. H. Breimer and T. Lindahl, *Biochemistry*, 24 (1985) 4018.
23 G. Scholes, J. Weiss and C. M. Wheeler, *Nature (London)* 4525 (1956) 157.
24 G. Scholes, J. F. Ward and J. Weiss, *J. Mol. Biol.*, 2 (1960) 379.
25 S. Tofigh and K. Frenkel, *Free Radical Biol. Med.*, 7 (1989) 131.
26 G. Scholes and J. Weiss, *Nature (London)*, 185 (1960) 305.
27 J. Cadet and R. Teoule, *Tetrahedron Lett.*, 31 (1972) 3225.
28 B. S. Hahn and S. Y. Wang, *Biochem. Biophys. Res. Commun.*, 54 (1973) 1224.
29 L. Stelter, C. von Sonntag and D. Schulte-Frohlinde, *Z. Naturforsch., B: Anorg. Chem., Org. Chem.*, 30 (1975) 609.
30 F. Beesk, M. Dizdaroglu, D. Schulte-Frohlinde and C. von Sonntag, *Int. J. Radiat. Biol.*, 36 (1979) 565.
31 B. Ekert and R. Monier, *Nature (London)*, 184 (1959) B.A. 58.
32 J. Cadet and R. Teoule, *Biochim. Biophys. Acta*, 238 (1971) 8.
33 S. Y. Wang, B. S. Hahn, R. P. Batzinger and E. Bueding, *Biochem. Biophys. Res. Commun.*, 89 (1979) 259.
34 H. F. Thomas, R. M. Herriott, B. S. Hahn and S. Y. Wang, *Nature (London)*, 259 (1976) 341.
35 B. S. Hahn and S. Y. Wang, *J. Org. Chem.*, 41 (1976) 567.
36 T. Itahara, *Chem. Lett.*, (1987) 841.
37 T. Miyazawa, K. Yasuda and K. Fujimoto, *Anal. Lett.*, 20 (1987) 915.
38 T. Miyazawa, *Free Radical Biol. Med.*, 7 (1989) 209.
39 T. Miyazawa, R. Saeki and H. Inaba, *J. Biolumin. Chemilumin.*, 4 (1989) 475.
40 L. S. Yoshida, T. Miyazawa, K. Fujimoto and T. Kaneda, *Lipids*, 25 (1990) 565.
41 T. Miyazawa, K. Yasuda, K. Fujimoto and T. Kaneda, *J. Biochem.*, 103 (1988) 744.
42 T. Miyazawa. K. Fujimoto and S. Oikawa, *Biomed. Chromatogr.*, 4 (1990) 131.
43 T. Miyazawa, T. Suzuki, K. Fujimoto and T. Kaneda, *J. Biochem.*, 107 (1990) 689.
44 R. Adelman, R. L. Saul and B. N. Ames, *Proc. Natl. Acad. Sci. U.S.A.*, 85 (1988) 2706.

Journal of Chromatography, 606 (1992) 195–201
Elsevier Science Publishers B.V., Amsterdam

CHROMSYMP. 2568

Applications of high-performance ion chromatography in the mineral processing industry☆

D. J. Barkley, L. A. Bennett☆☆, J. R. Charbonneau and L. A. Pokrajac☆☆

Mineral Sciences Laboratories, Canada Centre for Mineral and Energy Technology, Ottawa, Ontario, K1A 0G1 (Canada)

(First received December 23rd, 1991; revised manuscript received April 4th, 1992)

ABSTRACT

A reversed-phase column, coated with a permanently sorbed ion exchanger ("permanent coating" ion-interaction chromatography), was used for the separation of anions in ground water samples from a hydrometallurgical processing plant. Optimization of the capacity of the anion exchanger and wide linear range calibration curves obtained with these columns permitted the direct determination of Cl^-, NO_2^-, NO_3^-, and SO_4^{2-} in the presence of large amounts of ammonium and metal ions.

Dynamic ion exchange ("dynamic coating" ion-interaction chromatography) was investigated for the separation of rare earths in samples from an aluminum processing operation. Data is presented to illustrate that with appropriate adjustment of pH of the eluent it is possible to optimize conditions to resolve rare earth metals from interfering metal ions.

The selective sorption of Th(IV) and U(VI) on to reversed phases as their α-hydroxyisobutyric complexes, formed in situ in the eluent, was used for the analysis of samples from bacterial leaching of uranium ores. By minimizing the baseline noise of the post-column reaction the detection limit for Th(IV) is 5 μg/l and for U(VI) is 15 μg/l (3 × baseline noise) for a 100-μl sample injection.

INTRODUCTION

Canada Centre for Mineral and Energy Technology research activities include increased productivity in mineral processing and development of technologies to reduce the environmental impact of process residues. To analyze the wide range of sample matrices generated by this research, much effort has been focused on the application of high-performance ion chromatography.

In this paper we will discuss some of the ion chromatographic (IC) techniques used and show examples to illustrate the application of these separation systems. This will include the separation of anions in ground waters, and the determination of rare earths in metallurgical processing samples by ion-interaction chromatography. This chromatographic technique offers advantages over the use of fixed-site ion-exchangers in that there is a wide range of variables which can be used to manipulate the retention of solutes. For this reason, ion-interaction chromatography is applied in our laboratory to the resolution of difficult sample matrices. Also presented is the separation of thorium and uranium as their α-hydroxyisobutyric acid complexes by reversed-phase chromatography. In the strict sense, this approach may not be defined accurately as IC, yet it is applicable to the retention of inorganic ions.

EXPERIMENTAL

Instrumentation

Several different systems were used in this work. Solvent delivery pumps included Waters M-625 and M-45 (Waters, Milford, MA, USA), Spectra-

Correspondence to: Dr. D. J. Barkley, 59 Ridgefield Crs., Nepean, Ontario K2H 6S6, Canada (present address).

☆ Presented at the *International Ion Chromatography Symposium 1991, Denver, CO, October 6–9, 1991.* The majority of the papers presented at this symposium were published in *J. Chromatogr.*, Vol. 602 (1992).

☆☆ Present address: University of Waterloo, Waterloo, Ontario, Canada.

0021-9673/92/$05.00

Physics 8100 and 8800 (Spectra-Physics, Santa Clara, CA, USA), Dionex 4000i (Dionex, Sunnyvale, CA, USA). Autosamples were Spectra-Physics 8100 and 8200. For absorbance detection, Spectra-Physics 2000, Linear 100 and Kratos 770 variable-wavelength detectors were used. Data handling was done by Spectra-Physics ChromJet integrators and a Spectra Station.

The eluted metal ions were monitored after a post-column reaction with 2,7-bis[(*o*-arsenophenyl)azo]-1,8-dihydroxynaphthalene-3,6-disulphonic acid (Arsenazo III) and the post-column reagent was added to the eluate via a low-volume T-mixer [6] with a modified syringe pump (ISCO M-645, Lincoln, NE, USA), or He-pressurized delivery system.

Analytical columns used were Supelcosil LC-18-DB (5 μm, 150 cm × 4.6 mm) (Supelco Canada, Oakville, Canada).

Reagents

All eluents, standard and sample solutions were prepared using water pretreated via ion-exchange and distillation, then passed through a Milli-Q water-purification system (Millipore, Bedford, MA, USA).

Determination of anions. A stock solution (5 m*M*) of the eluent acid, 1,3,5-benzenetricarboxylic, was dissolved in water by adding NaOH to pH of *ca.* 5. Eluents were prepared by diluting the stock solution and adjusting the pH to 6.5 with tris(hydroxymethyl)aminomethane (THAM). Salts of cetyltrimethylammonium bromide (cetrimide) and cetylpyridinium bromide (CTP) were used for coating the columns and these reagents were used as received from the supplier (Sigma, St. Louis, MO, USA).

Determination of rare earths and thorium. Standard solutions (1000 μg/ml) of the rare earths were prepared from 99.999% pure oxides (Aldrich, Milwaukee, WI, USA). These oxides were ignited to constant weight at 950°C and dissolved in dilute nitric acid. Reagent-grade sodium 1-octanesulphonate and α-hydroxyisobutyric acid (HIBA) were obtained from Sigma and from Aldrich. Stock solutions of 2 *M* α-hydroxyisobutyric acid and of 0.1 *M* sodium 1-octanesulphonate were purified by passing them through a column packed with a strong cation-exchange resin (AG 50W-X4); resins in the H^+ from were used for HIBA and the Na^+ form for 1-octanesulphonate. Eluents were prepared by weighing the calculated amounts of stock solution and diluting to approximately 900 ml with water, after which the pH was adjusted to the desired value by addition of 5 *M* sodium hydroxide, and the solution diluted to 1 l. All vessels used to prepare and store eluents were of polypropylene plastic. A stock solution (0.5 g/l) of Arsenazo III was made 5 *M* in acetic acid. The post-column reagent solution was prepared by dilution of 100 ml of the Arsenazo III stock solution to 1 l and filtered through a 0.45-μm filter. Acids used for sample dissolution were commercially available high-purity reagents.

Procedure for coating columns

Solutions containing the coating reagent, CTP or cetrimide, were prepared in water–acetonitrile mixtures (0.5 m*M*) of reagent with 15–30% of acetonitrile. The solutions were adjusted with THAM to pH 6.5. The analytical column was first washed with a solution of the desired acetonitrile concentration without the reagent, then the reagent containing solution with the same percentage of acetonitrile was pumped through the column. The breakthrough curve was recorded by monitoring the bromide ion with a UV detector at 210 nm. To determine the capacity, a 1.0 m*M* salicylic acid solution (5% acetonitrile and pH 6.5) was pumped through the column until breakthrough of the salicylic anion was recorded at 290 nm. This was followed by equilibrating the column with the eluent. To remove the sorbed coating reagent a solution of 0.1 *M* potassium bromide containing 70% acetonitrile was passed through the column for at least for 1 h followed by washing with acetonitrile for 10 min.

Sample preparation

Aluminum processing solution. To a 20-ml sample, 5 ml of $HClO_4$ and 5 ml of HNO, were added and the solution evaporated to near dryness at low hot plate temperature to remove excess $HClO_4$. The salts were then dissolved in 10 ml of water and the solution transferred to a 50-ml volumetric flask and diluted to volume with eluent.

RESULTS AND DISCUSSION

Separation of anions by "permanent coating" ion-interaction chromatography

Studies have been conducted [1,2] with reversed-

phases that are permanently coated with a large hydrophobic quaternary amine to give a charged surface. Results have shown that such systems can offer several advantages over either dynamically coated or fixed-site ion-exchange columns. These exchangers give greater chromatographic efficiency and greater flexibility with regard to choice of column capacity and eluent for optimum anion separations.

Of these factors the ability to control the anion-exchange capacity is important. Fig. 1 shows the variation of amount of sorbed CTP and cetrimide on Supelcosil LC-18-DB reversed-phase columns. The amount of sorbed quaternary amine, and therefore the capacity of a column, is a function of the concentration of acetonitrile in the coating solution. As can be seen there was little difference in the number of moles of the two quaternary amines sorbed for a given percentage of acetonitrile. This indicates that the cetyl group, which is common to both compounds, is the main contributor in the hydrophobic interactions with the octadecyl group of the C_{18} column. The effects of these coated columns on analyte retention were studied using an eluent of 0.5 m*M* 1,3,5-benzenetricarboxylic acid, neutralized to pH 6.5 with THAM. For both columns, the peak shape and the retention times of the anions Cl^-, NO_2^-, NO_3^- and SO_4^{2-} were similar.

The application of a permanently coated column system is shown in Fig. 2. This chromatogram shows the separation of anions in a sample of ground water from a metallurgical processing plant in Western Canada. Attempts at determining the anions by a non-suppressed column technique were unsuccessful. The high concentrations of ammonium and other cations in the sample eluted near the solvent front and interfered with the separation of chloride. Also the high concentration of sulphate in the injected sample gave a broad and tailing peak which resulted in run times of 30 min to allow for column re-equilibration. Preseparation of the cations and analyzing the sample at different dilutions to solve the problem was unacceptable to the analytical operations in this plant. By adjusting the capacity of a permanently coated column, the retention of the chloride was increased to allow a separation from

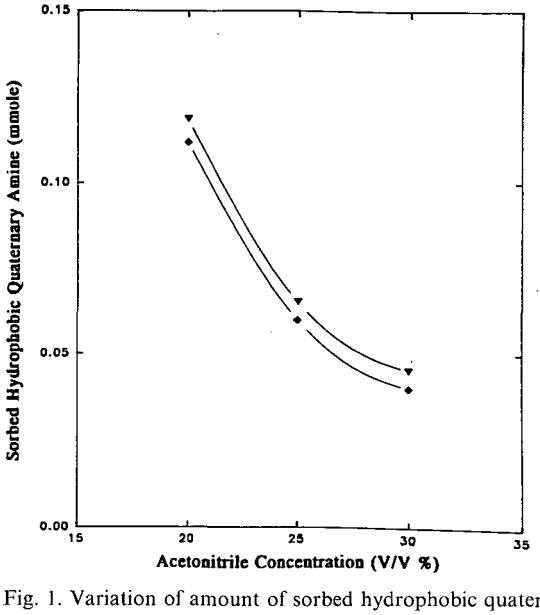

Fig. 1. Variation of amount of sorbed hydrophobic quaternary amine with the concentration of acetonitrile in coating solution. ◆ = Cetyltrimethylammonium; ▼ = cetylpyridinium; column, 5-μm Supelcosil LC-18-DB reversed-phase.

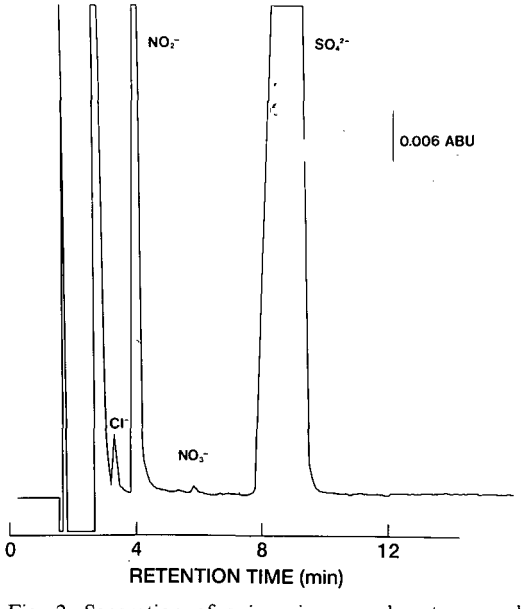

Fig. 2. Separation of anions in ground water sample on a permanent coated anion-exchange column with detection by indirect UV adsorption. Conditions: Supelcosil LC-18-DB column coated with $5 \cdot 10^{-4}$ *M* cetyltrimethylammonium ion in 20% acetonitrile; eluent, $0.5 \cdot 10^{-3}$ *M* 1,3,5-benzenetricarboxylic acid, neutralized to pH 6.8 with THAM; flow-rate, 1 ml/min; detection by indirect UV at 254 nm (ABU = absorbance units); sample injected, 50 μl; sample dilution, 5 ml diluted to 100 ml with eluent.

the early eluting interferences, and good peak shape was obtained for sulphate because of the excellent efficiency of these columns. The eluent used here was 1,3,5-benzenetricarboxylic acid (0.5 mM) neutralized to pH 6.8, and detection was by indirect UV absorbance at 254 nm.

Our studies have shown that wide linear range calibration curves are obtained with these permanently coated systems. Standards of sulphate were prepared at the 5, 10, 25, 50, 100, 150 and 200 μg/ml levels, and the linearity of the calibration curve for sulphate over this range showed a correlation coefficient equal to 0.9998. The peak for sulphate in Fig. 2 is equivalent to 8.25 μg of SO_4^{2-} in the injected 50-μl sample. Results obtained for this sample were 28 mg/l Cl^-, 214 mg/l NO_2^-, 7 mg/l NO_3^-, and 3300 mg/l SO_4^{2-}

Separation of rare earths by "dynamic coating" ion-interaction chromatography

Dynamic ion-exchange chromatography [3,4] is used in our Laboratory to determine rare earths in a variety of samples. This includes mine tailings, metallurgical processing solutions, sediments, steels, and alloys. In this technique a hydrophobic ion (such as octanesulphonate), which is present in the eluent, is dynamically sorbed onto the hydrophobic surface of a reversed-phase to provide a charged surface that can be used for ion-exchange separations. The eluent also contains a complexing agent such as HIBA to elute the rare earths. The advantages of this approach includes rapid mass transfer characteristics, good reproducibility, and the ability to vary ion-exchange capacity. Changes in capacity along with eluent pH and addition of an organic modifier can be used to adjust the selectivity of the separation. With an on-line post-column reaction, using Arsenazo III and monitored at 658 nm, detection limits are in the low nanogram range.

An example of the application of dynamic ion-exchange chromatography for the direct separation of rare earths is shown in Fig. 3. The sample was a sodium hydroxide leach solution from an aluminium processing operation and contained high concentrations of sodium, iron and aluminium. Due to matrix interference, these solutions could not be accurately analyzed by inductively coupled plasma emission spectroscopy. Fig. 3A shows the chromatogram when the sample was separated by dynamic

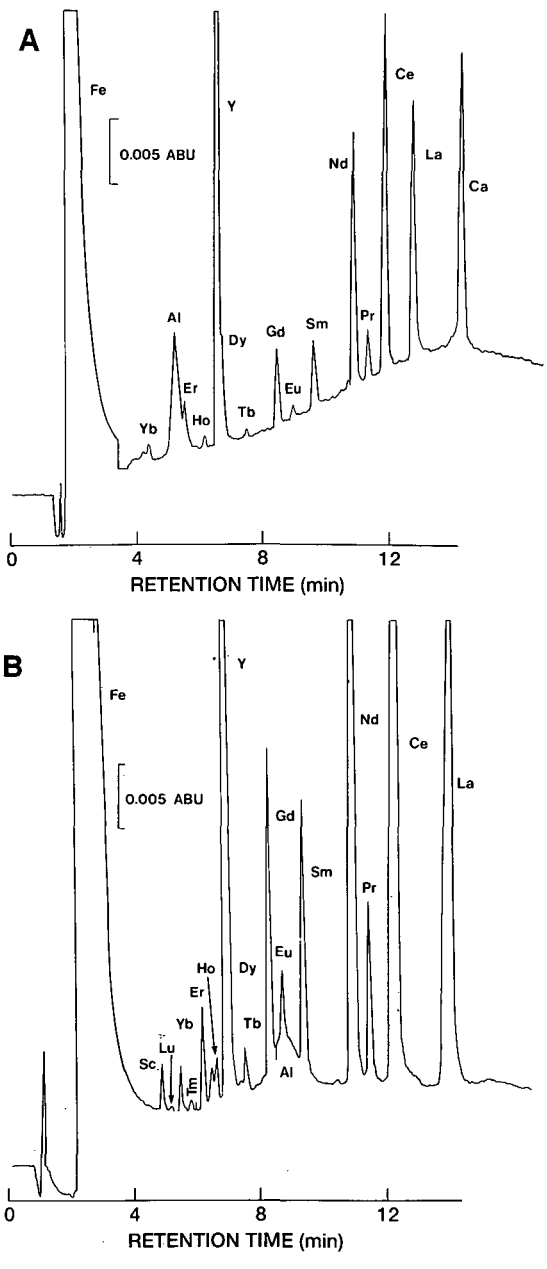

Fig. 3. Direct injection of aluminium processing solution. Conditions: Supelcosil LC-18-DB column; gradient programme at a flow-rate of 1.0 ml/min from 0.05 M HIBA to 0.4 M HIBA over 10 min and held at 0.4 M for 5 min; modifier, 1-octanesulphonate at 0.01 M; (A), eluents at pH 4.5; (B), eluents at pH 3.8; detection at 658 nm after post-column reaction with Arsenazo III; sample injected, 50 μl; sample dilution, (A) 10 ml to 100 ml, (B) 20 ml to 50 ml.

ion-exchange at an eluent pH of 4.5. The rare earths are well resolved except for Tm and Er which are masked by aluminium. By changing the eluent pH to 3.8 (Fig. 3B) the relative time for aluminium is quite different and appears as a broad peak under Eu and allows the determination of Tm and Eu. With this approach all the rare earths were resolved. In this system iron elutes near the solvent front. The difference in aluminium peak shape between A and B is probably due to its weak complexing properties with HIBA at pH 3.8. The range of results found for rare earths in this sample by dynamic ion-exchange was from <0.05 mg/l for Tm to 10.0 mg/l for Y. A solution simulating the matrix composition and containing 2.0 mg/l of the rare earths was analyzed, and the recoveries of the rare earths were 2.0 ± 0.05 mg/l.

The above results illustrate that the eluent pH can influence retention. The effect of pH on the retention of rare earths and metal complexes of HIBA was tested on a gradient programme from 0.05 *M* to 0.4 *M* HIBA for 10 min. Fig. 4 shows data we obtained for the retention of the rare earths, and the results for the metals tested are shown in Fig. 5. By comparison it can be seen that a change in pH can cause significant differences in the relative retention between a rare earth and a transition metal. This parameter can be very useful for optimizing selectivity.

Separation of thorium and uranium by reversed-phase

Samples of drainage from uranium tailing deposits and from studies into bacterial leaching of uranium ores are analysed on a regular basis in our laboratory for thorium and uranium. The method used to determine these elements is based on the retention of Th(IV) and U(VI) as their HIBA complexes on a reversed-phase. It has been shown that with only HIBA added to an eluent the rare earths are unretained and the transition metals only weakly sorbed on a reversed-phase, while Th(IV) and U(VI) are strongly retained [4]. Fig. 6 shows the chromatogram obtained for a bacterial leach liquor. Detection was by a post-column reaction with Arsenazo III. This chromatogram illustrates the rapid analysis time and good selectivity obtained with this method. Transition metal ions and the rare earths elute near the solvent front.

The parameters used to optimize separation of

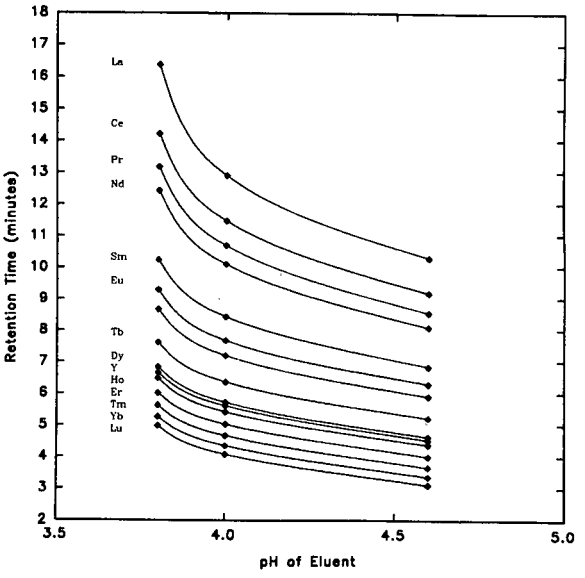

Fig. 4. Effect of pH on the retention time of the rare earths. Conditions: Supelcosil LC-18-DB column; gradient programme at a flow-rate of 1.0 ml/min from 0.05 *M* HIBA to 0.4 *M* HIBA over 10 min and held at 0.4 *M* for 5 min; modifier, 1-octanesulphonate at 0.01 *M*; detection as in Fig. 3.

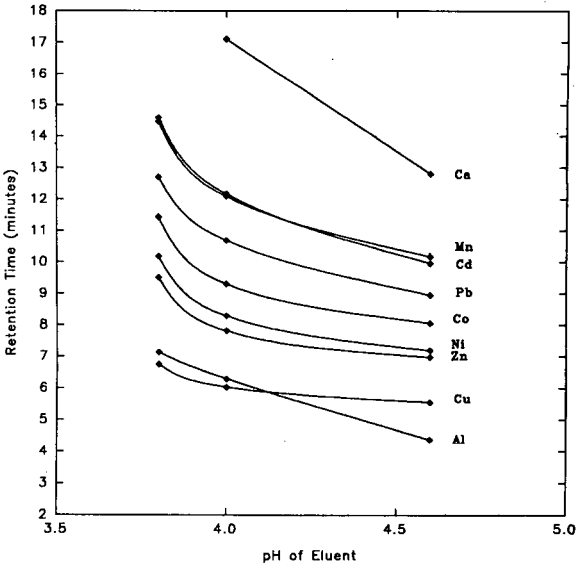

Fig. 5. Effect of pH on the retention time of metal ions. Conditions: Supelcosil LC-18-DB column; gradient programme at a flow-rate of 1.0 ml/min from 0.05 *M* HIBA to 0.4 *M* HIBA over 10 min and held at 0.4 *M* for 5 min; modifier, 1-octanesulphonate at 0.01 *M*; detection as in Fig. 3.

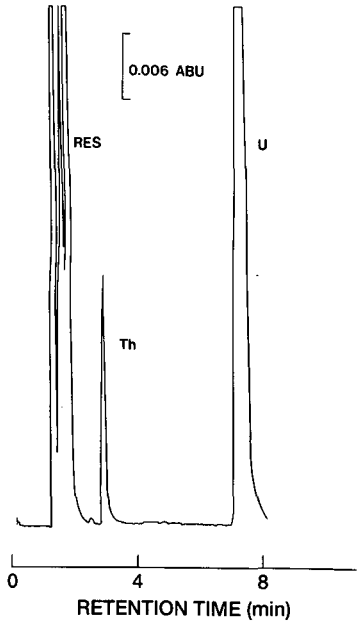

Fig. 6. Separation of thorium and uranium in bacterial leach liquor. Conditions: column, 5-μm Supelcosil LC-18-DB; eluent, 0.2 mol/l HIBA at pH 4.2; modifier, 10% (v/v) methanol; flow-rate, 1 ml/min; detection at 658 nm after post-column reaction with Arsenazo III; sample injected, 50 μl; sample dilution, 5 ml of leach liquor diluted to 50 ml with eluent.

Th(IV) and U(VI) from transition metals and rare earths were eluent pH, HIBA concentration, and amount of organic modifier in the eluent [5]. Addition of an organic solvent such as methanol or acetonitrile to the HIBA eluent decreased retention times of U(VI) and Th(IV). Increases in the concentration of HIBA had only a slight effect on increasing the retention times, while decreases in pH caused large decreases in retention of U(VI) and Th(IV).

Optimizing detection

Minimizing the baseline noise (BLN) level of the post-column reaction is important in achieving low limits of detection in this chromatographic technique. Factors that contribute to detector cell noise are the effectiveness of the post-column reactor system at mixing the column eluent with the colorimetric reagent and stability in the flow-rates of the eluent and reagent solutions. We have found that pump pulsation remained the largest source of BLN in a post-column system. Tests were conducted to evaluate flow pulsations for some eluent pumps and for both gas-pressurized and syringe delivery of the Arsenazo III reagent. Fig. 7 shows the noise levels observed for systems studied. The newer eluent pumps (the Dionex 4000i and Waters M-625) with more effective pulse dampening and gas-pressurized delivery of the colour reagent, resulted in very low levels of BLN. For the Waters M-625 pump the peak-to-peak BLN level under the conditions was $3 \cdot 10^{-5}$ ABU. The back-pressure system used with the ISCO M-645 pump was a 7.5 cm $\times$ 4.6 mm column of 10 μm styrene–divinylbenzene inserted between the mixing tee and the syringe pump, which gave a back-pressure of *ca.* 400 p.s.i. This system in combination with older eluent pumps was found to be

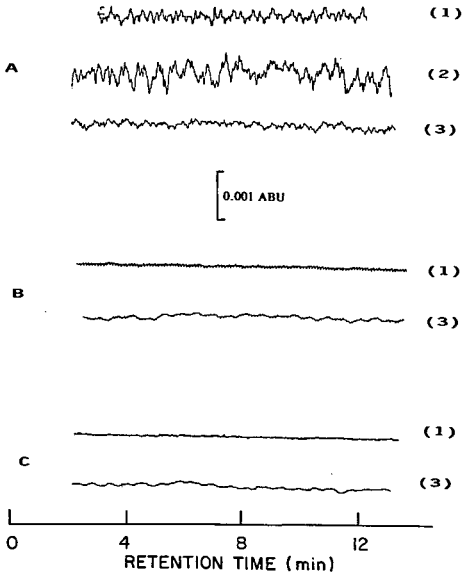

Fig. 7. Comparison of baseline noise for some eluent pumps with gas-pressure and syringe pumping for colour reagent. (A) Spectra-Physics SP8700 eluent pump and colour reagent delivery with (1) He-pressurized, (2) ISCO M314 syringe and (3) ISCO M314 syringe with back-pressure device. (B) Dionex Advanced Gradient eluent pump and colour reagent delivery with (1) He-pressurized and (3) ISCO M314 syringe with back-pressure device. (C) Waters Model M-625 eluent pump and colour reagent delivery with (1) He-pressurized and (3) ISCO M314 syringe with back-pressure device. Back-pressure device used with the ISCO syringe pump is a 7-cm column of 10 μm styrene–divinylbenzene (400 p.s.i.). Instrumentation used in these tests: for absorbancy detection, a Spectra-Physics 2000; data handling was done by Spectra-Physics ChromJet integrator, and the post-column reagent was added to the eluent via a low-volume T-mixer [6]. Conditions: column, 5-μm Supelcosil LC-18-DB at 32°C; eluent, 0.20 *M* HIBA at pH 4.6 and flow-rate of 1 ml/min; Arsenazo III, $1.5 \cdot 10^{-4}$ *M* at flow-rate of 0.5 ml/min; detection at 658 nm.

more effective in reducing BLN than when a gas-pressurized reagent pump is used. The post-column reactor used was a version of the screen-tee type as used by Cassidy [6]. By minimizing the BLN level of the post-column reaction the detection limit for Th(IV) is 5 μg/l and for U(VI) is 15 μg/l (3 $\times$ BLN) for a 100-μl sample injection.

REFERENCES

1 D. J. Barkley, T. E. Dahms and K. N. Villeneuve, *J. Chromatogr.*, 395 (1987) 631.
2 K. Ito, Y. Ariyoshi, F. Tanabili and H. Sunahara, *Anal. Chem.*, 63 (1991) 273.
3 C. H. Knight, R. M. Cassidy, B. M. Recoskie and L. W. Green, *Anal. Chem.*, 56 (1984) 474.
4 R. M. Cassidy and M. Frarer, *Chromatographia*, 18 (1984) 370.
5 D. J. Barkley, M. Blanchette, R. M. Cassidy and S. Elchuk, *Anal. Chem.*, 58 (1986) 2222.
6 R. M. Cassidy, S. Elchuk and P. K. Dasgupta, *Anal. Chem.*, 59 (1987) 85.

Journal of Chromatography, 606 (1992) 203–209
Elsevier Science Publishers B.V., Amsterdam

CHROM. 24 302

Manipulation of ion trap parameters to maximize compound-specific information in gas chromatographic–mass spectrometric analyses

Charles K. Huston

Varian Chromatography Systems, Research and Engineering, WC-14, 2700 Mitchell Drive, Walnut Creek, CA 94598 (USA)

(First received February 18th, 1992; revised manuscript received April 21st, 1992)

ABSTRACT

The most effective way to conduct trace analyses of complex samples is to couple a high-resolution separation method to a sensitive, information-rich detector. The latest generation quadrupole ion trap uses an automatic gain control (AGC) scan function and an axial modulation voltage to achieve maximum sensitivity. With these capabilities, an ion trap gas chromatography–mass spectrometry system can separate, quantitate, and identify low picogram quantities of trace analytes present in a complex sample.

The AGC scan function uses a target value (AGC-TV) during analysis to maximize signal intensity by varying ionization time. Filament emission current (FEC) is also a major affector of ion trap signal intensity when electron ionization (EI) is used. Maximum sensitivity was achieved when AGC-TV and FEC were optimized. Additionally, useful information about selected types of compounds were also obtained from analyses conducted with non-optimum AGC-TV and FEC settings. In these specific cases, the effects seen when non-optimal AGC-TV or FEC settings were used could be explained in terms of the inherent ion chemistries of the compounds.

INTRODUCTION

The power of mass spectrometry (MS) as a detection method lies in the enormous amount of useful information it provides [1]. In routine use, searching a library of "known" spectra allows for rapid identification of unknowns in a capillary gas chromatogram. For trace analysis, this technique is limited only by the ability of the instrument to obtain a characteristic spectrum from a small amount of sample. This ability is affected primarily by instrument design limitations and by variations in ion chemistry.

The ion trap mass spectrometer has rapidly developed into an extremely valuable analytical tool [2,3] and the earliest versions of commercial ion traps were valued for their sensitivity. However, they exhibited certain instrumental design limitations that were often incorrectly attributed to ion chemistry [4]. Continued development of the ion trap corrected these early design limitations [5] and its latest generation (Saturn) provides maximum sensitivity. The remaining affector of spectral characteristics, thus, is inherent ion chemistry. Specific compounds naturally undergo ion-neutral reactions under electron ionization (EI) conditions which are independent of instrument type [6]. This behavior can provide useful information [7] as long as the spectra are consistent enough for library searching. For example, significant M+1 formation in the spectra of fatty acid methyl esters (FAMEs) allowed identification of the molecular ion in addition to library confirmation [8].

In addition to sample concentration, major variables of ion trap EI-MS are automatic gain control-target value (AGC-TV) and filament emission current (FEC). These parameters were characterized in this work to optimize library identification capa-

Correspondence to: Dr. Charles K. Huston, Varian Chromatography Systems, Research and Engineering, WC-14, 2700 Mitchell Drive, Walnut Creek, CA 94598, USA.

0021-9673/92/$05.00

bilities and to allow additional information about inherent ion chemistries to be obtained.

EXPERIMENTAL

The ion trap system [Varian Saturn gas chromatography (GC)–MS System] utilized a temperature-programmable, cold on-column injector (Varian SPI) and a 25 m × 220 μm, HT5 capillary column (SGE) with a 0.25-μm film thickness to separate analytes of interest. The carrier gas velocity (helium) was approximately 30 cm/s and various column oven programs were used to achieve suitable separation of selected test samples (PolyScience). The transfer line was held at 280°C and the ion trap manifold was set at 260°C. The ion trap was first tuned using default software settings to obtain suitable mass calibrations and electron multiplier responses. FEC and AGC-TV settings were subsequently manipulated as indicated below. For all analyses, the injector used a high-performance insert and was programmed as follows: 0.1 min at 40°C, 150°C/min ramp to 280°C, hold until end of column program.

RESULTS AND DISCUSSION

Quadrupole ion traps use an AGC scan function (Fig. 1) to conduct mass analyses. Ions are trapped and subsequently ejected by ramping the radio frequency (RF) voltage applied to the ring electrode. Ions with low m/z sequentially eject before higher m/z ions as the RF voltage increases. Before a "spectrum" scan occurs, the system first uses a fixed ionization time and a rapid RF scan to get a gross measurement of the sample size [the "base" total ion current (TIC) measurement]. Using both the "base" TIC measurement and the AGC-TV, the ionization time for the mass analysis can then be adjusted by the system in real time to achieve the desired signal level. Thus, the higher the AGC-TV for a given sample size, the longer the actual ionization time. Because longer ionization times allow more ions to be produced from a given sample, increasing the AGC-TV is an effective way to increase signal intensity. FEC also affects signal intensity, but does so independent of time. A higher FEC causes more electrons to be injected into the trap during ionization, and this increases the production of sample ions (and their signal intensity). In this situation, if the AGC-TV remains unchanged, the AGC scan function will respond to the increased signal by shortening the ionization time.

In this system, changing FEC had a greater effect on signal intensity than did changing the AGC-TV (Fig. 2). The relative relationships shown for m/z 69 of DFTPP were generally found in all other analyses. Increasing AGC-TV was a practical way to in-

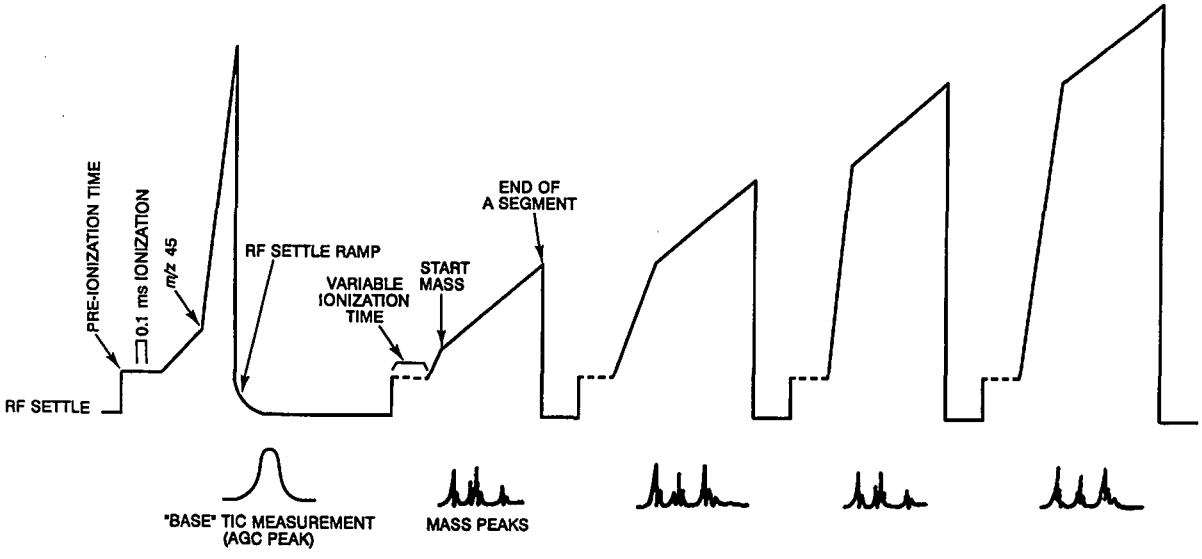

Fig. 1. The AGC scan function.

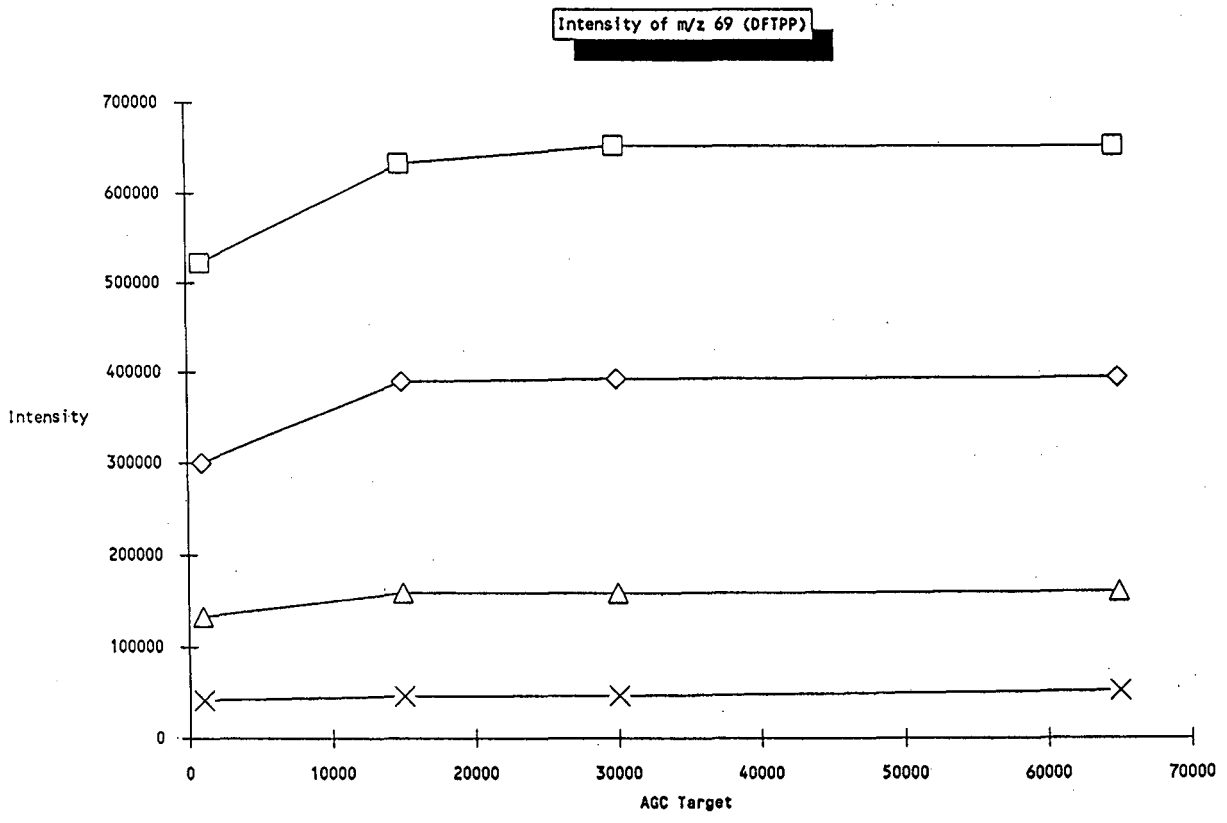

Fig. 2. Effects of AGC-TV and FEC on ion intensity. FEC: × = 10 μA; △ = 25 μA; ◇ = 50 μA; □ = 100 μA.

crease signal intensities, however, the greatest effects were seen for changes below 30 000. The major affector of signal intensity was FEC and its effects were significant throughout the instrument's operational range. In practical terms, a FEC of 50 μA and an AGC-TV of 25 000 provided excellent sensitivity without excessive loss in filament lifetime. Under these conditions, low picogram quantities of sample gave library searchable spectra (*e.g.*, with commercial EI spectral libraries).

In the spectra of certain analytes, M + 1 ions were observed which resulted from ion-neutral interactions. Compounds that were prone to M + 1 formation could be grouped into two categories based on both their spectral characteristics and their reaction to AGC-TV and FEC manipulation. "Type 1" compounds had "weak" molecular ions (*i.e.*, of low relative abundance) and included FAMEs, amphetamines, benzodiazepines, and barbiturates. The spectra of "Type 1" compounds were generally unaffected by changes in AGC-TV or FEC. "Type 2" compounds had "stronger" molecular ions (*i.e.*, of greater relative abundance) and included atrazine, ketones, imides and triazines. AGC-TV and FEC could be used to affect the relative extent of M + 1 formation for "Type 2" compounds. The inherent

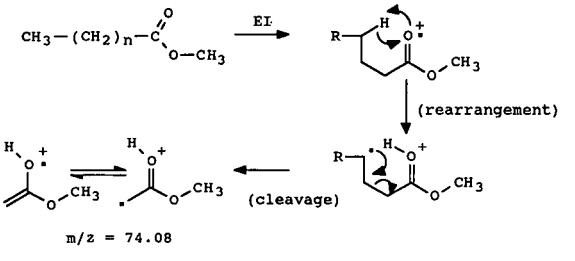

Fig. 3. Formation of the major proton-donating ion in electron ionization of fatty acid methyl esters.

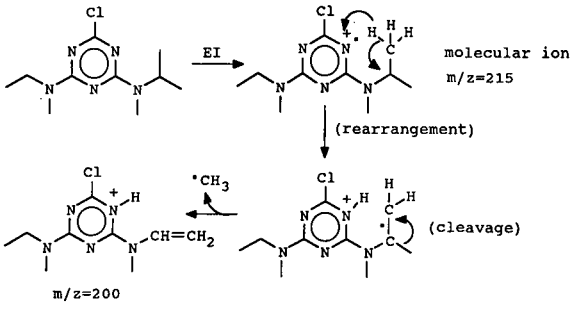

Fig. 4. Formation of the major proton-donating ion in electron ionization of atrazine (molecular mass 215).

ion chemistries of both types of compounds caused them to produce significant amounts of proton donating ion fragments under EI conditions. These fragments protonated the neutral molecules to form M + 1 ions. The general sequence could be described as follows:

$$AB \xrightarrow{(1)} AB+$$

$$AB+ \xrightarrow{(2)} AH+ \text{ and } B$$

$$AH+ \text{ and } AB \xrightarrow{(3)} ABH+ \text{ and } A$$

(1) Electron ionization of the neutral compound (AB) produced the molecular ion (AB+).

(2) Rearrangement and cleavage of the molecular ion (AB+) produced the proton donating ion (AH+).

(3) The proton donating ion (AH+) protonated a neutral sample molecule (AB) which became the M + 1 ion (ABH+).

For example, the base peak (most abundant ion) for many FAMEs ("Type 1") is an ion with *m/z* 74. This ion is a strong proton donor which is formed as shown in Fig. 3. The base peak (*m/z* 200) for atrazine ("Type 2") is also a strong proton donor (Fig. 4). The mechanisms of EI for all the ion-neutral reactive compounds were similar, and major ions (proton donators) responsible for M + 1 formation in other samples are shown in Fig. 5.

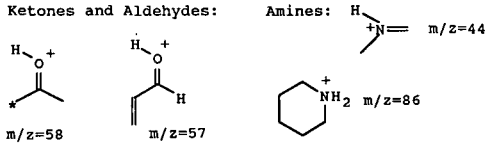

Fig. 5. Examples of proton-donating ions produced by electron ionization of ketones, aldehydes and amines.

Generally, AGC-TV and FEC had little or no effect on compounds with weak molecular ions. However, this was not considered a limitation because M + 1 was useful (in these cases) for molecular ion identification. For example, the M + 1 ion (*m/z* 187) for C-10 FAME was the only ion that significantly changed with concentration (Fig. 6). These spectra gave good library search results and demonstrated that the molecular mass for this compound was 186.

The effects of AGC-TV and FEC on compounds with stronger molecular ions was clearly seen in the spectra (Figs. 7–10) taken from 1-ng samples of atrazine (molecular mass 215). At a low FEC (10 μA), the relative abundance of the ion at *m/z* 216 (M + 1) was much lower at a low AGC-TV of 5000 (Fig. 4) than with an AGC-TV of 40 000 (Fig. 5). When a high FEC (50 μA) was used, relatively less M + 1 was formed (Figs. 9 and 10) and the effects of AGC were much less dramatic.

Differences seen in how AGC-TV and FEC affected the formation of M + 1 could be explained in terms of the relative rates of the previously described steps (1), (2), and (3). For weak molecular ion compounds (Type 1), reactions 1–3 occurred very rapidly and could be considered to be "spontaneous" relative to each other. In other words, they all rapidly approached a pseudo-equilibrium within the variable time frame of the AGC scan. The absence of a rate-limiting step for Type 1 compounds, then, is why the relative amounts of M + 1 [ABH+] was almost independent of AGC-TV (reaction time) and FEC (number of ionization electrons). These instrumental variables did affect the "amount" of total EI reactions, but not the "relative amounts" of individual products from reactions 1–3. The only way to affect the relative amount of M + 1 [ABH+] was to alter the relationships between reactions 1–3. This could be accomplished by varying the amount of sample [AB] as demonstrated in Fig. 6.

A "rate limiting step" was present for "Type 2" compounds, conversely, and their stronger molecular ion (relative to Type 1 compounds) pointed towards possible differences in how a Type 2 molecule [AB] might have reacted. Reaction 3 (protonation) was affected by reaction time (AGC-TV) and the number of ionization electrons (FEC) and, thus, was "slow" relative to the "spontaneous" reactions

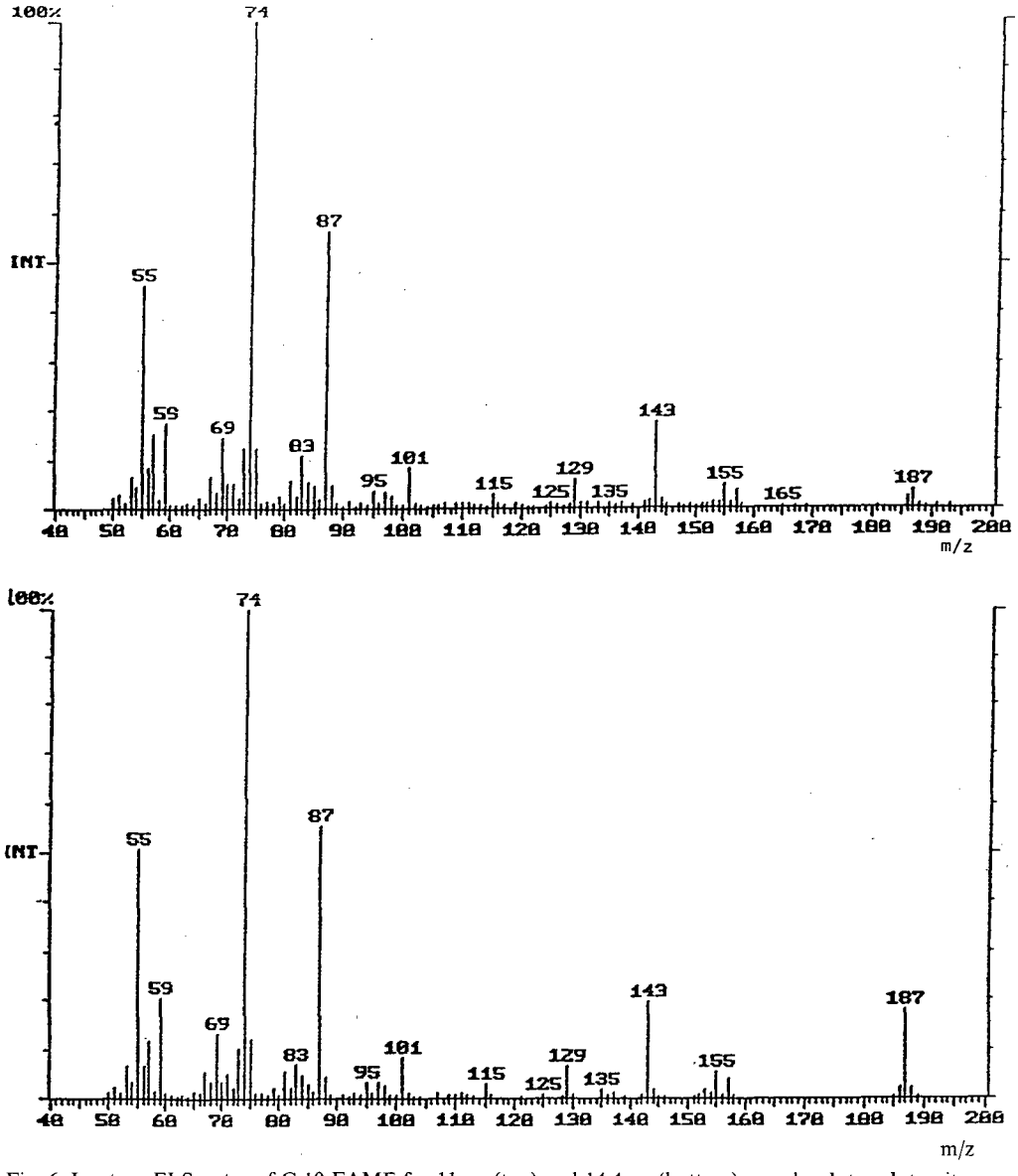

Fig. 6. Ion trap EI Spectra of C-10 FAME for 11 pg (top) and 14.4 ng (bottom) samples. Int = Intensity.

1 (EI) and 2 (rearrangement and cleavage). A change in AGC-TV affected the amount of time available for M + 1 formation. The longer reaction times at high AGC-TV created a situation similar to the Type 1 case where the three reactions were spontaneous (equilibrated) within the time frame of the AGC scan. When the rate limiting step was given more time, more of its product (M + 1) was produced relative to the other "equilibrated" products from reactions 1 and 2.

When FEC was high for Type 2 compounds, the relative amounts of M + 1 [ABH +] was lower. FEC affected reactions 1 and 2 just like it did for Type 1 compounds; it increased the total amount of their products without any relative differences. Because reaction 3 was a slower, secondary reaction, how-

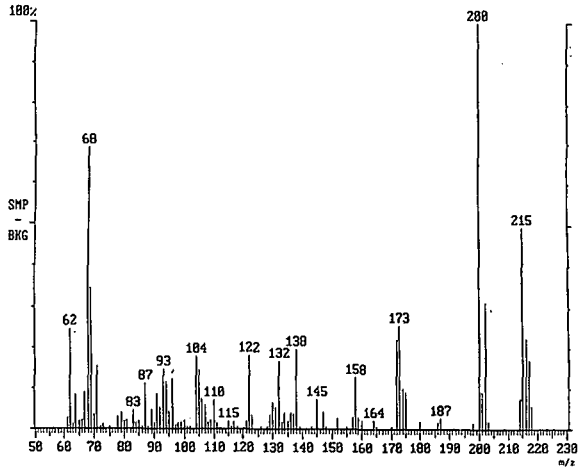

Fig. 7. Atrazine spectrum obtained using a FEC of 10 μA and an AGC-TV of 5000. (SMP-BKG means that this is a background-subtracted spectrum.)

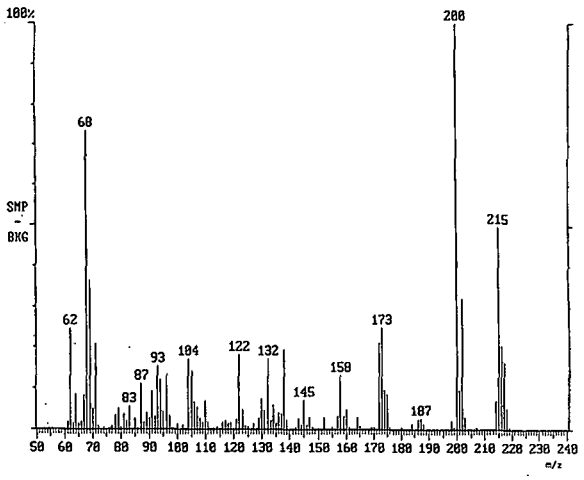

Fig. 9. Atrazine spectrum obtained using a FEC of 50 μA and an AGC-TV of 5000.

ever, FEC did not increase M + 1 formation as much as it did the formation of [AB+] and [AH+]. Although more actual M + 1 was formed at higher FEC, relative to the other EI reaction products, [ABH+] appeared to go down. Last, M + 1 formation in Type 2 compounds was also affected by sample concentration [AB] for the same reasons as previously described for Type 1 compounds.

CONCLUSIONS

For all analytes of interest, a "working optimum" of 50 μA for the FEC and 25 000 for the AGC-TV could be used. These instrumental settings gave ion signal intensities which allowed acquisition of characteristic mass scans at low sample concentrations. These same conditions were also effective for analysis of ion neutral reactive compounds because they minimized the relative abun-

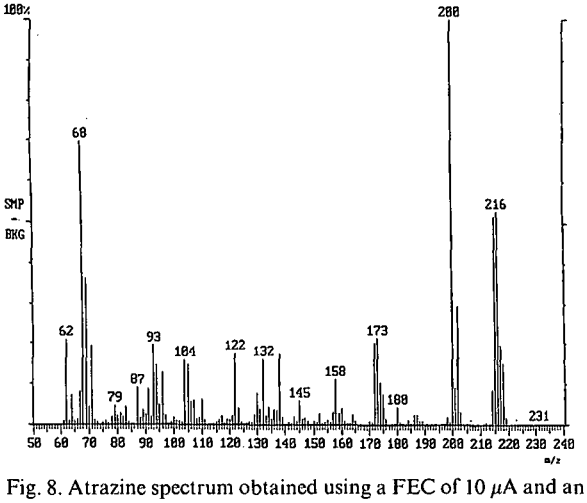

Fig. 8. Atrazine spectrum obtained using a FEC of 10 μA and an AGC-TV of 40 000.

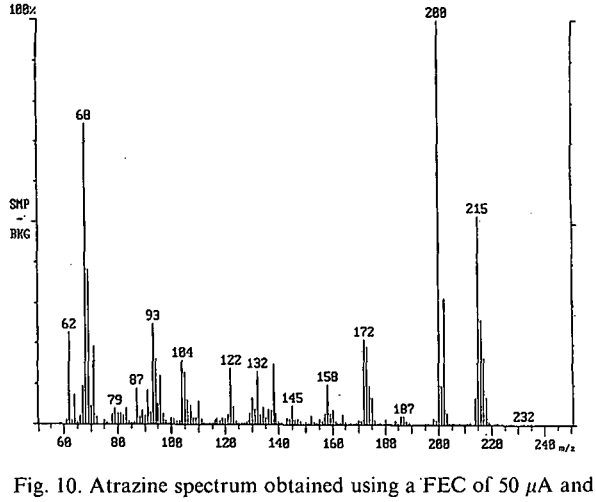

Fig. 10. Atrazine spectrum obtained using a FEC of 50 μA and an AGC-TV of 40 000.

dance of M + 1 ions in Type 2 compounds. A Type 2 unknown could be confirmed by varying either AGC-TV or FEC. Sample concentration effects were common to both Type 1 and Type 2 compounds.

REFERENCES

1 F. W. McLafferty, *Interpretation of Mass Spectra*, University Science Books, Mill Valley, CA, 3rd ed., 1980.
2 J. F. J. Todd, *Mass Spectrom. Rev.*, 10 (1991) 3–52.
3 R. G. Cooks, G. L. Glish, S. A. McLuckey and R. E. Kaiser, *Chem. Eng. News*, 69 No. 2 (1001) 26–41.
4 J. W. Eichelberger, W. L. Budde and L. E. Slivon, *Anal. Chem.*, 59 (1987) 2730–2732.
5 L. K. Pannell, Q.-L. Pu, H. M. Fales, R. T. Mason and J. L. Stephenson, *Anal. Chem.*, 61 (1989) 2500–2503.
6 S. A. McLucky, G. L. Glish, K. G. Asano and G. J. van Berkel, *Anal. Chem.*, 60 (1988) 2312–2314.
7 I. Horman and H. Traitler, *Anal. Chem.*, 61 (1989) 1983–1984.
8 C. K. Huston, J. Sullivan and R. Simon, presented at the *11th International Symposium on Capillary Chromatography, Monterey, CA, May 14–19, 1990.*

Journal of Chromatography, 606 (1992) 211–220
Elsevier Science Publishers B.V., Amsterdam

CHROM. 24 287

Identification of C_2–C_4 alkylated benzenes in flash pyrolysates of kerogens, coals and asphaltenes☆

W. A. Hartgers, J. S. Sinninghe Damsté and J. W. de Leeuw

Delft University of Technology, Faculty of Chemical Technology and Materials' Science, Organic Geochemistry Unit, De Vries van Heystplantsoen 2, 2628 RZ Delft (Netherlands)

(First received January 16th, 1992; revised manuscript received April 21st, 1992)

ABSTRACT

Pseudo-Kováts indices were determined for all positional isomers of C_2–C_4 alkylated benzenes using a non-polar capillary column (CP Sil-5). These indices were applied in combination with mass spectral data to identify these compounds in complex mixtures of a relatively non-polar nature generated upon flash pyrolysis of macromolecular sedimentary organic matter (kerogens, asphaltenes and coals). Alkylbenzene distribution patterns were constructed by integration of appropriate mass chromatograms. Generally, toluene is the major pyrolysis product. Other specific alkylated benzenes (*e.g.* 1,2,3,4-tetramethylbenzene and 1-methyl-4-isopropylbenzene) were found to be enhanced in flash pyrolysates of different samples. Flash pyrolysates of asphaltene and kerogen fractions isolated from the same oil shale exhibit similar alkylbenzene distributions.

INTRODUCTION

Complex mixtures of relatively non-polar organic compounds are commonly encountered in the analysis of the composition of soils, sediments and fossil fuels. High-resolution gas chromatography (GC) is nowadays commonly used to separate such complex mixtures, to enable the identification of the individual compounds present with mass spectrometry (MS). Similar complex mixtures are obtained by analytical pyrolysis (controlled thermal dissociation in an inert atmosphere) of high-molecular-weight, relatively non-polar material. Flash pyrolysis (Py) coupled on-line with GC–MS is frequently applied to characterize natural, high-molecular-weight substances present in kerogens and coals, and to screen polluted soil and sediment samples for anthropogenic substances [1,2].

Owing to the complexity of the mixtures [generally mixtures of *n*-alkenes, *n*-alkanes, saturated and aromatic (poly)cyclic hydrocarbons as well as heteroatom-containing compounds], it is often not possible to identify all compounds present using only mass spectral data. For example, isomeric alkylbenzenes have similar mass spectra and require additional retention time data for unequivocal identification.

The GC retention behaviour of aromatic hydrocarbons, including alkylbenzenes, has been the subject of many studies [3–7]. Many relatively polar stationary phases (Carbowax 20M; UCON-LB 550X; Tris-cyanoethoxypropane) and various temperature programmes have been used to achieve optimal GC separation and to determine accurate, reproducible retention indices [8]. However, to separate complex mixtures in extracts of soils, sediments and fossil fuels as well as pyrolysates of kerogens and coals, non-polar stationary phases (*e.g.* CP Sil-5; Squalane; DB-5; OV-101) are preferred. It is, therefore, apparent that retention indices for alkylbenzenes on non-polar stationary phases are essential for the reliable identification of these com-

Correspondence to: Dr. W. A. Hartgers, Delft University of Technology, Faculty of Chemical Technology and Materials' Science, Organic Geochemistry Unit, De Vries van Heystplantsoen 2, 2628 RZ Delft, Netherlands.

☆ Delft Organic Geochemistry Unit Contribution No. 273.

0021-9673/92/$05.00

pounds in complex mixtures such as those obtained from pyrolysis of natural materials.

In this paper we report the relative retention indices of C_2–C_4 alkylated benzenes determined with a capillary column coated with CP Sil-5. These data enabled the full identification of these compounds in pyrolysates of kerogens, coals and asphaltenes. The samples described in this paper are representative examples of different types of organic matter ranging from aliphatic-rich substances to those mainly composed of condensed polyaromatic material (kerogen types I, II and III) [9]. The geochemical applications of this work will be discussed elsewhere [10].

EXPERIMENTAL

Origin and preparation of kerogen samples

The Mulhouse kerogen was isolated from a marl layer (No. 6) from the Mi_1-bed of the Salt IV unit from the Lower Oligocene Mulhouse Potash Basin (Alsace, France). The sample was selected from a suite of rock layers sampled in the Amélie Concession, Gallery 830 [11]. The Jurf ed Darawish Oil Shale (Jordan) is a Cretaceous deposit of immature bituminous calcareous marl stones [12]. The sample investigated is a composite sample from 156–157 m taken from a core. The organic matter present in this sample has a high sulphur content [13] and is marine-derived. The Estonian kerogen is from an Ordovician deposit [14], mainly comprising fossil remains of the extinct alga *Gloeocapsomorpha prisca*. The Beulah Zap coal is selected from the Argonne Premium coal set [15]. This coal sample was taken from the upper Palaeocene Sentinel Butte Formation (North Dakota, USA) [16].

The Mulhouse and Jurf ed Darawish kerogen samples were grounded in a rotary disc mill and extracted for 24 h in a soxhlet apparatus with methanol–toluene (3:1, v/v). The powdered Estonian kerogen was extracted for 12 h at room temperature by chloroform–methanol (2:1, v/v). The carbonate minerals present in the Mulhouse residue after extraction were removed by treatment with 6 *M* hydrochloric acid at room temperature. The neutralized and dried residue was re-extracted ultrasonically with methanol and dichloromethane to yield the concentrated Mulhouse kerogen fraction. All kerogen samples were dried in a vacuum stove at 40°C overnight. The asphaltene fraction of the Jurf ed Darawish sample was isolated from the corresponding bitumen by precipitation with *n*-heptane [17]. The coal sample was powdered and used without further treatment for pyrolysis.

Authentic standards

Twenty-four alkylbenzene standards were commercially available from Aldrich. Ten C_4 alkylated benzenes were obtained from the collection of standards of the Organic Chemistry Division of Delft University (Delft, Netherlands).

The ethyldimethyl-substituted C_4 alkylated benzenes were kindly provided by Dr. T. Tóth (University of Budapest, Budapest, Hungary) and Dr. J. P. E. M. Rijks (Technical University Eindhoven, Eindhoven, Netherlands). The standards provided by Dr. Tóth were synthesized via a Friedel Crafts ethylation of the appropriate dimethylbenzene [18]. Fractional distillation of mixtures of alkylbenzenes was performed by Rijks [19] to obtain the pure isomers. Structural assignments were made by chromatographic and spectroscopic studies.

The synthesis of 1-methyl-3-propylbenzene and 1-methyl-4-propylbenzene was performed via a Grignard reaction. Two equivalents of ethylbromide were converted to the corresponding alkylmagnesiumhalide and subsequently coupled to 3-methylbenzaldehyde and 4-methylbenzaldehyde, respectively, in diethyl ether under reflux. The resulting secondary alcohol function was removed by ionic hydrogenolysis with triethylsilane in trifluoracetic acid [20,21]. The products were obtained in 80% overall yield.

Gas chromatography

GC was performed with a Hewlett-Packard 5890 Series II instrument, using an on-column injector. Detection was accomplished using a flame ionization detector. Helium was used as the carrier gas. Separation was achieved using a fused-silica capillary column (25 m × 0.32 mm I.D.) coated with CP Sil-5 (film thickness 0.45 μm). The alkylbenzene standards were injected at 0°C in hexane (*ca.* 0.05 μl/ml), except for benzene, which was injected in *n*-pentane. The gas chromatograph, equipped with a cryogenic unit, was held at its initial temperature of 0°C for 5 min and then programmed at a rate of 3°C/min to 320°C, at which temperature it was held for 10 min.

Gas chromatography–mass spectrometry

GC–MS was carried out using a Hewlett-Packard 5890 Series II gas chromatograph connected to a VG-70S mass spectrometer by direct insertion of the capillary column into the ion source. Electron-impact spectra were obtained at 70 eV using the following conditions: cycle time 1.8 s; resolution 1000; mass range *m/z* 50–900. Separation was achieved using the same capillary column and temperature programme as described for GC analyses.

Curie point pyrolysis–gas chromatography

Flash pyrolysis experiments were performed using a FOM-3LX Curie point pyrolysis unit [22] directly connected to the injector of a Hewlett-Packard 5890 Series II gas chromatograph. Samples were pressed on flattened ferromagnetic wires (iron–nickel alloy; Curie temperature 610°C) as described by Venema and Veurink [23]. The on-line flash pyrolysis was performed by inductive heating of the wire in 0.15 s to its final temperature using a high-frequency generator (Fischer, Model 9425). Separation of the pyrolysis products was achieved using a fused-silica column (25 m × 0.32 mm I.D.) coated with CP Sil-5 (film thickness 0.45 μm). Helium was used as the carrier gas. The oven was programmed from 0°C (5 min) to 320°C (10 min) at a rate of 3°C/min.

Curie point pyrolysis–gas chromatography–mass spectrometry

Curie point Py–GC–MS analysis was performed using the same conditions as described for Py–GC, using a similar Curie point device and gas chromatograph connected to a magnetic sector mass spectrometer (VG-70S) as described above. Alkylbenzenes present in the kerogen pyrolysates were analysed by constructing accurate mass chromatograms using *m/z* values of 78, 92, 106, 120 and 134 (window 0.03).

Retention index measurements

The retention indices of all alkylbenzene standards were determined by co-injection of each indi-

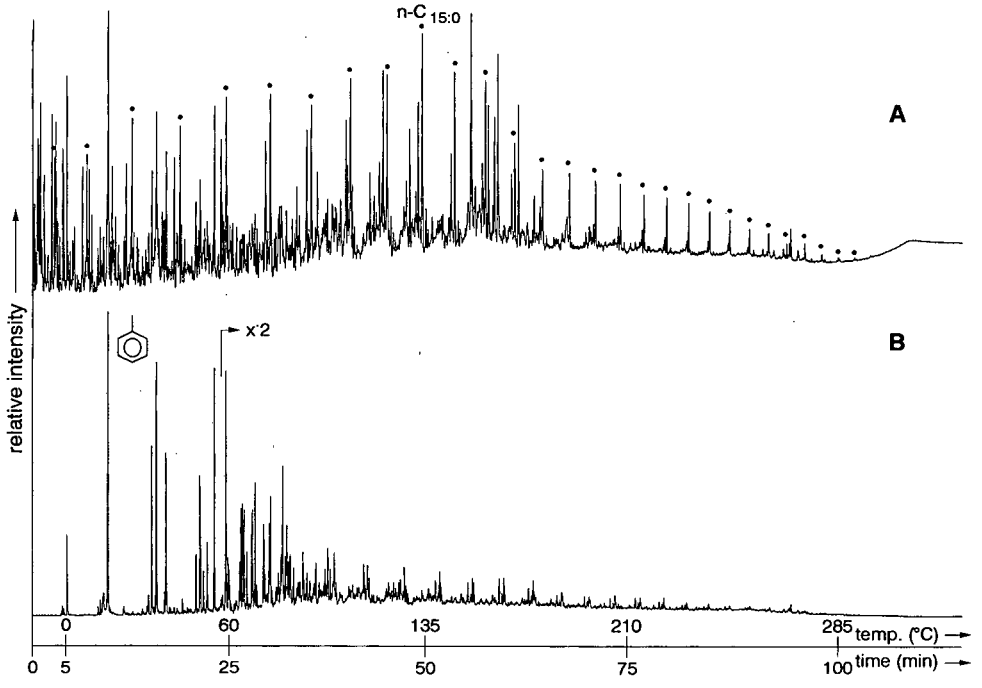

Fig. 1. (A) Total ion current of the flash pyrolysate (Curie temperature 610°C) of the Mulhouse kerogen and (B) summed accurate mass chromatogram (*m/z* 78.12 + 91.13 + 92.14 + 105.16 + 106.17 + 119.18 + 120.19 + 133.21 + 134.22 + 147.23 + 148.24) showing the distribution of akylbenzenes. Dots indicate *n*-alkanes.

vidual standard with a mixture of *n*-alkanes (C_6–C_{15}) using a non-isothermal temperature programme of the GC oven from 0°C (5 min) to 320°C at a rate of 3°C/min. A function was obtained by fitting a third-order polynomial equation to the data points (retention times) of the homologous series of *n*-alkanes. Subsequently, the pseudo-Kováts indices of the alkylbenzene standards were calculated using this regression function. The measurements were performed four times to determine the standard deviation.

Calculation of the retention indices of alkylbenzenes present in flash pyrolysates was performed using the scan number of peaks in the reconstructed total ion current or mass chromatogram corresponding to these alkylbenzenes and the regression function generated using the homologous series of *n*-alkanes present in the pyrolysates.

RESULTS AND DISCUSSION

Fig. 1A shows the total ion current (TIC) trace of the flash pyrolysate of the Mulhouse kerogen. Accurate mass chromatograms of relevant *m/z* values show that the complex mixture of compounds generated is dominated by *n*-alkenes, *n*-alkanes and alkylbenzenes. Branched alkanes are also present in relatively high abundance. Alkylcyclohexanes, alkylnaphthalenes, alkylthiophenes and alkylbenzo[*b*]thiophenes are minor constituents of the pyrolysate.

Fig. 1B shows an accurate, summed mass chromatogram (*m/z* 78 + 91 + 92 + 105 + 106 + 119 + 120 + 133 + 134) to illustrate the complex distribution of the alkylbenzenes. The ions used to generate this mass chromatogram are the most abundant ions in the mass spectra of the alkylbenzenes. Therefore, this summed mass chromatogram provides a quantitatively representative picture of the alkylbenzene distribution present in the flash pyrolysate of the Mulhouse kerogen. An accurate mass chromatogram was constructed because a mass chromatogram using nominal *m/z* values also contains contributions from alkylated benzothiophenes. Although toluene is the single most abundant pyrolysis product, alkylbenzenes of higher molecular weight are also abundant. Mass chromatography using *m/z* values of the molecular ions is a useful tool to analyse individual clusters of alkylbenzenes with the same molecular weight in the pyrolysate of the Mulhouse kerogen. Fig. 2 has been constructed on this basis and shows the accurate mass chromatograms of *m/z* values 78, 92, 106, 120 and 134. Each individual cluster of alkylbenzenes with the same molecular weight has been normalized to the most abundant isomer present. This approach provides insight into the internal distribution of isomeric alkylbenzenes present in the pyrolysate.

Mass spectra of low-molecular-weight alkylbenzenes have been reported [24,25]. The base peak for most alkylated alkylbenzenes results from cleavage of the benzylic bond and loss of the largest alkyl substituent. Exceptions to this general rule are tri- and tetramethylated alkylbenzenes (*e.g.* Fig. 3F), which show base peaks at $M^+ - 15$. A rearrangement involving neighbouring methyl groups which leads to the stabilized tropylium ion explains this fragmentation behaviour [26]. Mass spectra of positional isomers are often very similar (*e.g.* compare Fig. 3D and E). As a result, it is possible to discriminate only isomers with different alkyl substituent(s) (Fig. 3). Complementary relative retention time data, therefore, are required to identify all positional isomers.

Determination of the retention indices of the C_0–C_4 alkylated benzenes was performed by co-injection of each individual alkylbenzene standard with a mixture of *n*-alkanes on a CP Sil-5 capillary column using a non-isothermal temperature programme of the GC oven (see Experimental section). It was decided to study the distribution of alkylated members only upon to C_4 because of the large number of isomers involved above C_4. For example, it is possible to have 51 isomers for C_5 alkylated benzene. Table I shows a list of the measured pseudo-Kováts indices of all isomers of the C_0–C_4 alkylated benzenes. The maximum standard deviation (calculated from four measurements) is 0.4 index units. The pseudo-Kováts indices of alkylbenzenes were in good agreement with those obtained from the pyrolysate, which were calculated using the scan numbers in the mass chromatograms of these compounds and the regression function generated using the scan numbers of the homologous series of C_6–C_{12} *n*-alkanes present in the pyrolysate.

The complete qualitative identification enabled a detailed quantitative investigation of the distribu-

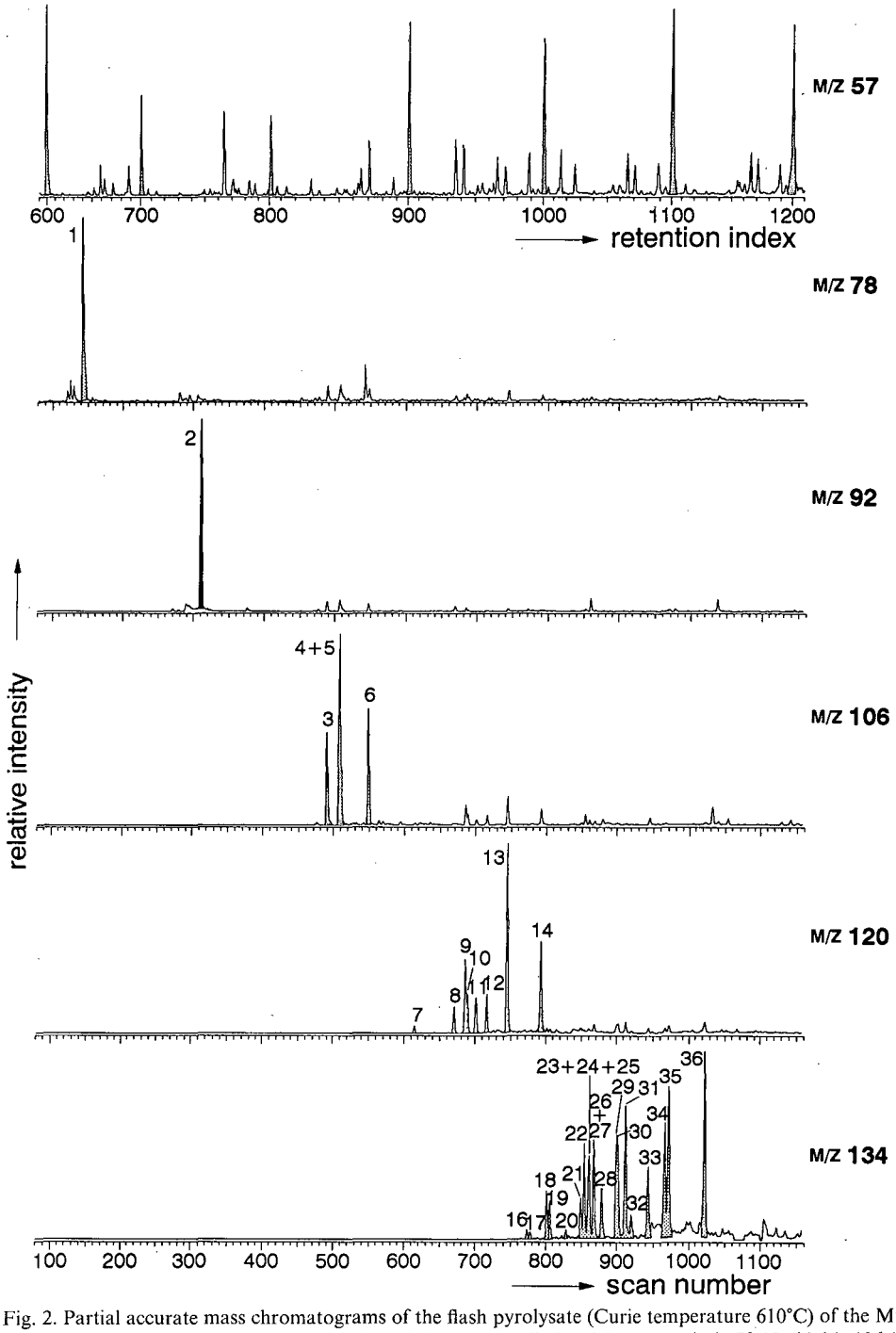

Fig. 2. Partial accurate mass chromatograms of the flash pyrolysate (Curie temperature 610°C) of the Mulhouse kerogen showing the distribution of C_6–C_{12} *n*-alkanes (*m/z* 57) and the C_0–C_4 alkylated benzenes (*m/z* 78.12, 92.14, 106.17, 120.19 and 134.22). Peak numbers refer to compounds listed in Table I.

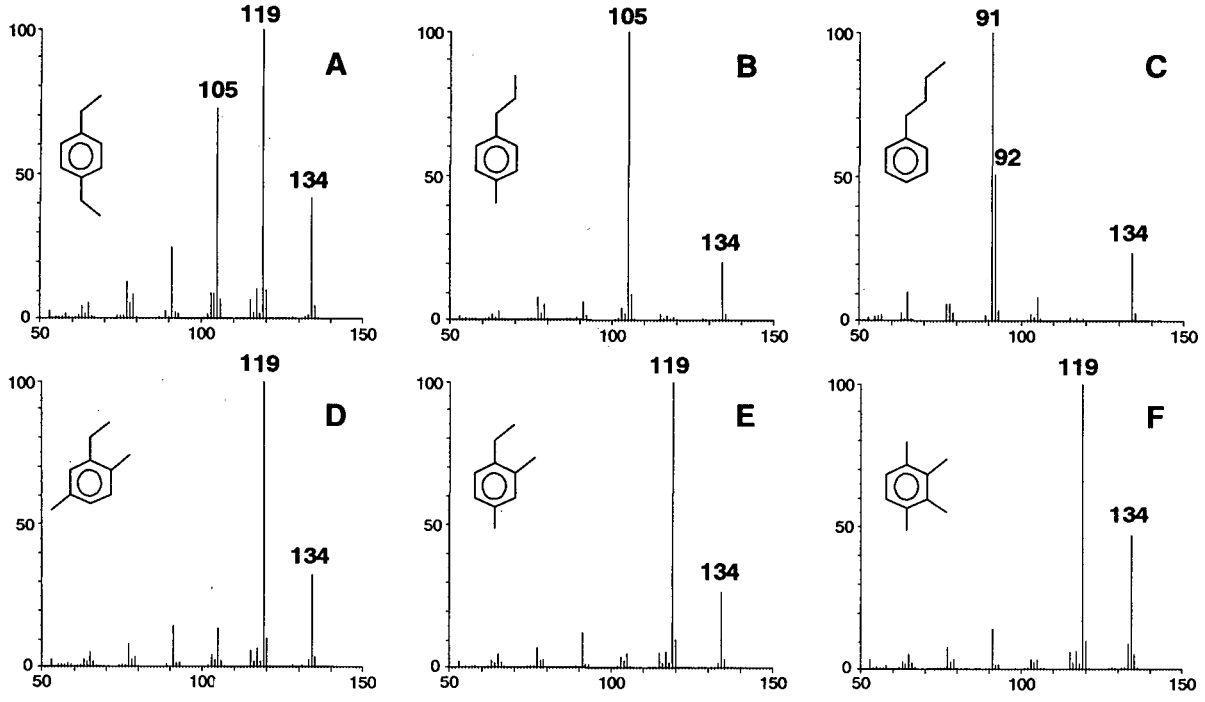

Fig. 3. Mass spectra of authentic C_4 alkylated benzenes: (A) 1,4-diethylbenzene, (B) 1-methyl-4-propylbenzene, (C) *n*-butylbenzene, (D) 1,4-dimethyl-2-ethylbenzene, (E) 1,3-dimethyl-4-ethylbenzene, (F) 1,2,3,4-tetramethylbenzene.

tion patterns of these compounds in flash pyrolysates by integration of peak areas from partial mass chromatograms (Fig. 2), taking into account different abundances of molecular ion peaks in the mass spectra of different alkylbenzenes (Fig. 3). These differences were taken into account by multiplying the obtained peak areas by a correction factor, calculated from the mass spectra of the authentic standards by taking the inverse of the percentages of the total ion current (Table I) of the relevant *m/z* value and multiplying it by 100. This approach was successfully applied for non-coeluting compounds.

To calculate peak areas of coeluting compounds, differences in their mass spectra were used. 1,4-Diethylbenzene, 1-methyl-4-propylbenzene and *n*-butylbenzene exhibit similar retention behaviour (see Table I).

Relative concentration of 1-methyl-4-propylbenzene and 1,4-diethylbenzene were calculated by integration of the peak areas in the partial mass chromatograms of *m/z* 105 and 119 separately. Mass fragment *m/z* 119 is almost absent in the mass spectrum of 1-methyl-4-propylbenzene (Fig. 3B). As a result, the corresponding peak area in the partial mass chromatogram of *m/z* 119 is derived almost exclusively from 1,4-diethylbenzene. The peak area of 1-methyl-4-propylbenzene was calculated by correcting the peak area obtained from the partial mass chromatogram *m/z* 105 for the contribution of 1,4-diethylbenzene.

The relative concentration of *n*-butylbenzene was determined by integrating the peak area in the partial mass chromatogram of *m/z* 92. This characteristic mass fragment, resulting from a McLafferty rearrangement, can be attributed almost entirely to *n*-butylbenzene (Fig. 3C). Afterwards, the results of the calculation method used were checked. Calculated peak areas of 1,4-diethylbenzene, 1-methyl-4-propylbenzene and *n*-butylbenzene were converted to their corresponding peak areas of *m/z* 134 using their mass spectral data and subsequently summed. Comparison of this summed area with the peak area obtained by integration of the appropriate peak in the partial mass chromatogram *m/z* 134 showed a good match (error within 1%). In a similar manner the peak areas of 1,3-dimethyl-5-ethyl-

TABLE I

RETENTION INDICES OF LOW-MOLECULAR-WEIGHT ALKYLBENZENES IDENTIFIED IN KEROGEN PYROLYSATES

No.[a]	Compound	Mol.wt.	I^b	S.D. (n = 4)	Characteristic ions[c]
1	Benzene	78	640.0	0.0	77(7), 78(38)
2	Toluene	92	746.4	0.0	91(40), 92(29)
3	Ethylbenzene	106	841.8	0.1	91(44), 105(3), 106(14)
4	1,3-Dimethylbenzene	106	851.1	0.2	91(32), 105(9), 106(21)
5	1,4-Dimethylbenzene	106	851.3	0.1	91(33), 105(10), 106(21)
6	1,2-Dimethylbenzene	106	871.6	0.1	91(35), 105(6), 106(14)
7	Isopropylbenzene	120	906.2	0.2	91(3), 105(49), 120(13)
8	*n*-Propylbenzene	120	936.0	0.3	91(65), 105(2), 120(13)
9	1-Methyl-3-ethylbenzene	120	944.0	0.3	91(5), 105(43), 120(14)
10	1-Methyl-4-ethylbenzene	120	945.9	0.2	91(5), 105(46), 120(13)
11	1,3,5-Trimethylbenzene	120	951.8	0.3	105(35), 119(5), 120(21)
12	1-Methyl-2-ethylbenzene	120	960.2	0.1	91(5), 105(46), 120(14)
13	1,2,4-Trimethylbenzene	120	975.5	0.4	105(38), 119(5), 120(19)
14	1,2,3-Trimethylbenzene	120	1000[d]	–	105(40), 119(5), 120(19)
15	*tert.*-Butylbenzene	134	975.4	0.4	91(21), 119(37), 134(8)
16	Isobutylbenzene	134	991.5	0.4	91(44), 92(23), 134(11)
17	*sec.*-Butylbenzene	134	994.0	0.3	91(7), 105(51), 134(9)
18	1-Methyl-3-isopropylbenzene	134	1005.6	0.3	91(8), 119(45), 134(12)
19	1-Methyl-4-isopropylbenzene	134	1008.4	0.3	91(8), 119(46), 134(11)
20	1-Methyl-2-isopropylbenzene	134	1020.7	0.3	91(9), 119(44), 134(11)
21	1,3-Diethylbenzene	134	1032.1	0.3	105(24), 119(26), 134(12)
22	1-Methyl-3-propylbenzene	134	1034.5	0.3	105(51), 134(12)
23	1,4-Diethylbenzene	134	1038.0	0.3	105(20), 119(28), 134(12)
24	1-Methyl-4-propylbenzene	134	1038.1	0.4	105(58), 134(12)
25	*n*-Butylbenzene	134	1038.9	0.1	91(43), 92(22), 134(10)
26	1,3-Dimethyl-5-ethylbenzene	134	1041.6	0.2	119(40), 134(15)
27	1,2-Diethylbenzene	134	1042.5	0.3	105(23), 119(23), 134(11)
28	1-Methyl-2-propylbenzene	134	1048.6	0.3	105(55), 134(12)
29	1,4-Dimethyl-2-ethylbenzene	134	1059.5	0.3	119(43), 134(14)
30	1,3-Dimethyl-4-ethylbenzene	134	1060.7	0.3	119(49), 134(13)
31	1,2-Dimethyl-4-ethylbenzene	134	1066.7	0.3	119(43), 134(13)
32	1,3-Dimethyl-2-ethylbenzene	134	1071.7	0.3	119(44), 134(12)
33	1,2-Dimethyl-3-ethylbenzene	134	1085.2	0.3	119(42), 134(13)
34	1,2,4,5-Tetramethylbenzene	134	1097.8	0.3	119(39), 134(20)
35	1,2,3,5-Tetramethylbenzene	134	1100[d]	–	119(40), 134(20)
36	1,2,3,4-Tetramethylbenzene	134	1130.4	0.4	119(40), 134(19)

[a] Numbers refer to Figs. 3, 4, 5 and 6.
[b] Pseudo-Kováts index.
[c] Percentages of the total ion current are given in parentheses.
[d] Coelution with *n*-alkane.

benzene and 1,2-diethylbenzene were calculated.

It was not possible to determine mathematically the relative concentrations of 1,3-dimethylbenzene and 1,4-dimethylbenzene because of almost identical retention behaviour and mass spectral data of these compounds.

This mathematical procedure enables the full identification of all C_0–C_4 alkylated benzene iso-

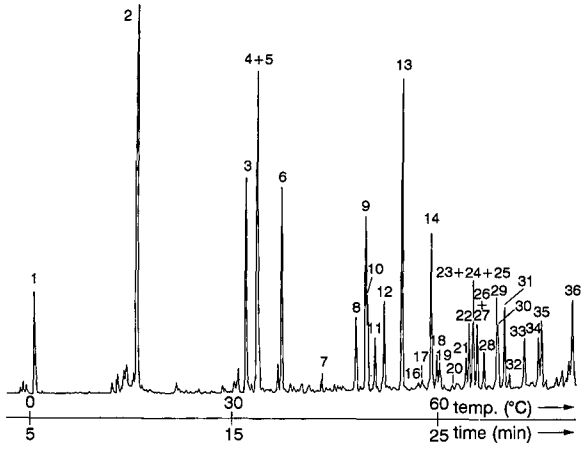

Fig. 4. Partial summed accurate mass chromatogram (m/z 78.12 + 91.13 + 92.14 + 105.16 + 106.17 + 119.18 + 120.19 + 133.21 + 134.22) of the flash pyrolysate (Curie temperature 610°C) of the Mulhouse kerogen illustrating the distribution of benzene, toluene and the C_2–C_4 alkylated benzenes. Peak numbers refer to the compounds listed in Table I.

mers present in complex mixtures of hydrocarbons. Fig. 4 shows a partial accurate mass chromatogram illustrating the distribution of the C_0–C_4 alkylated benzenes in the pyrolysate of the Mulhouse kerogen. Peak numbers refer to Table I. All alkylbenzene isomers were found to be present, except *tert.*-butylbenzene (compounds 15), the concentration of which is below the detection level of the method used.

In the way described above, distribution patterns of C_0–C_4 alkylated benzenes of kerogen, asphaltenes and coal pyrolysates can be obtained. Significant differences in distribution patterns were observed. For example, the alkylbenzene distribution of the pyrolysate of the Mulhouse kerogen (Fig. 5A) compared with the Estonian kerogen (Fig. 5B) shows considerable differences. The pyrolysate of the Estonian kerogen is dominated by a relatively higher abundance of homologous series of monosubstituted and *ortho*-disubstituted *n*-alkylbenzenes (compounds 6, 8, 12, 25 and 28). Also the relative abundance of C_4 alkylated benzenes in the pyrolysate is lower than that in the Mulhouse pyrolysate. The C_4 alkylated benzene distribution present in the pyrolysate of the Beulah Zap coal (Fig. 5C) is dominated by 1-methyl-4-isopropylbenzene and 1,2,3,4-tetramethylbenzene (compounds 19 and 36). Also noteworthy is the higher abundance of benzene and toluene relative to C_2–C_4 alkylated benzenes in the pyrolysate of Estonian Kukersite compared with that of Mulhouse kerogen and Beulah Zap coal.

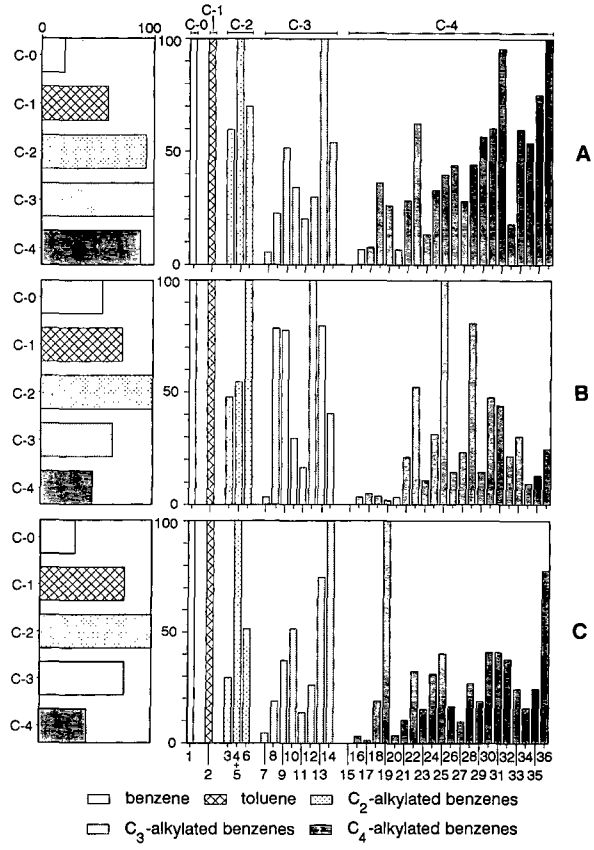

Fig. 5. Bar plots showing the carbon number distributions of benzene, toluene and the C_2–C_4 alkylated benzenes (left bar graphs) and the distribution of isomers (right bar graphs) generated upon flash pyrolysis (Curie temperature 610°C) of the Mulhouse kerogen (A), Estonian kerogen (B) and Beulah Zap coal (C). The distributions of the alkylated benzenes were normalized to the most abundant component. Numbers refer to compounds listed in Table I.

Fig. 6 shows the distributions of alkylbenzenes generated by flash pyrolysis of the asphaltene and the extracted kerogen fractions of the Jurf ed Darawish Oil Shale. The similarity of the alkylbenzene distributions is striking, although an enhanced relative abundance of the C_3 and C_4 alkylated benzenes in the pyrolysate of the asphaltene is observed. The observed similarity supports the idea that asphaltenes are structurally related to kerogen [27–30]. It

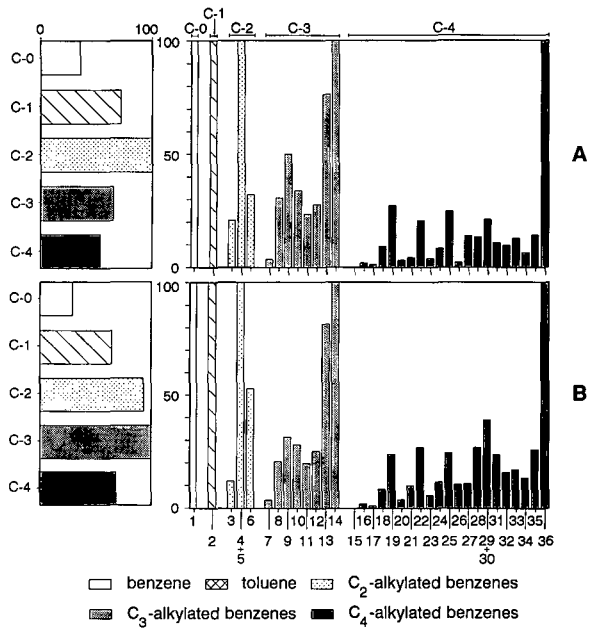

Fig. 6. Bar plots showing the carbon number distribution of benzene, toluene and the C_2–C_4 alkylated benzenes (left bar graphs) and the distribution of isomers (right bar graphs) generated upon flash pyrolysis (Curie temperature 610°C) of the asphaltenes (A) and kerogen (B) of the oil shale of Jurf ed Darawish. The internal distributions of the alkylated benzenes were normalized to the most abundant component. Numbers refer to compounds listed in Table I.

appears, therefore, that analysis of alkylbenzene distributions in pyrolysates of asphaltenes may be a useful tool for oil–source rock correlations. The full identification of alkylbenzenes in flash pyrolysates enables a comparative study of alkylbenzene distributions in order to give more information about the presence and origin of their natural precursors.

CONCLUSIONS

Pseudo-Kováts indices have been determined for all isomers of C_2–C_4 alkylated benzenes using a non-polar capillary column coated with CP Sil-5. In combination with mass spectral data, the identification of these compounds in flash pyrolysates of kerogens, coals and asphaltenes was achieved. To investigate in more detail the variations in the internal distributions of alkylbenzenes present in these flash pyrolysates, appropriate mass chromatograms were integrated and corrected for different MS responses. Benzene and toluene are generally the most abundant products. Significant differences were observed owing to the relatively high abundances of specific alkylbenzenes (*e.g.* 1,2,3,4-tetramethylbenzene and 1-methyl-4-isopropylbenzene). A higher abundance of "linear" alkylbenzenes was found in the pyrolysate of Estonian Kukersite. The alkylbenzene distributions present in flash pyrolysates of the asphaltene and kerogen fractions of the Jurf ed Darawish oil shale are very similar, confirming their structural relationship.

ACKNOWLEDGEMENTS

The authors want to thank Drs. T. Tóth and J. A. Rijks for providing some alkylbenzene standards. The samples used in this study were kindly donated by Drs. H. Wehner (Jurf ed Darawish sample) and S. Derenne (Estonian kerogen). The Mulhouse sample studied has been made available by the ENOG (European Network of Organic Geochemistry) funded by the European Economic Community under Contract No. SCI-0021-C(TT). Mr. W. Pool and Mrs. A. Knol are acknowledged for technical support. We greatly appreciate the constructive remarks given by the reviewers which significantly benefitted the manuscript.

REFERENCES

1 J. W. de Leeuw, E. W. B. de Leer, J. S. Sinninghe Damsté and P. J. W. Schuyl, *Anal. Chem.*, 58 (1986) 1852.
2 E. Matisová, E. Juranyiová, P. Kurán, E. Brandsteterová, A. Kocan and S. Holotic, *J. Chromatogr.*, 552 (1991) 301.
3 M. L. Lee, D. L. Vassilaros, C. M. White and M. Novotny, *Anal. Chem.*, 51 (1979) 768.
4 C. E. Döring, D. Estel and R. Fischer, *J. Prakt. Chem.*, 316 (1974) 1.
5 W. Engewald, I. Topalova, N. Petsev and C. Dimitrov, *Chromatographia*, 23 (1987) 561.
6 K. Heberger, *Chromatographia*, 25 (1988) 725.
7 N. Dimov and O. Mekenyan, *J. Chromatogr.*, 471 (1989) 227.
8 L. Soják and J. A. Rijks, *J. Chromatogr.*, 119 (1976) 505.
9 B. P. Tissot and D. H. Welte, *Petroleum Formation and Occurence*, Springer, Heidelberg, 2nd ed., 1984.
10 W. A. Hartgers, J. S. Sinninghe Damsté and J. W. de Leeuw, *Geochim. Cosmochim. Acta*, (1992) submitted for publication.
11 M. M. Blanc-Valleron and J. P. Gely, *IFP Report No. 36790*, 1989.
12 J. S. Sinninghe Damsté, W. I. C. Rijpstra, A. C. Kock-van Dalen, J. W. de Leeuw and P. A. Schenck, *Geochim. Cosmochim. Acta*. 53 (1989) 1343.

13 W. L. Orr, *Org. Geochem.*, 10 (1986) 499.
14 S. Derenne, C. Largeau, E. Casadevall, J. S. Sinninghe Damsté, E. W. Tegelaar and J. W. de Leeuw, *Org. Geochem.*, 16 (1990) 873.
15 K. S. Vorres, *Energy Fuels*, 4 (1990) 420.
16 S. C. Teerman and R. J. Whang, *Org. Geochem.*, 17 (1991) 749.
17 M. E. L. Kohnen, J. S. Sinninghe Damsté, A. C. Kock-van Dalen and J. W. de Leeuw, *Geochim. Cosmochim. Acta*, 55 (1991) 1375.
18 T. Tóth, *J. Chromatogr.*, 279 (1983) 157.
19 J. A. Rijks, Personal communication.
20 D. N. Kursanov, Z. N. Parnes, G. I. Bolestova and L. I. Belen'kii, *Tetrahedron*, 31 (1975) 311.
21 Z. N. Parnes, G. I. Bolestova and D. N. Kursanov, *J. Org. Chem. USSR*, 13 (1977) 434.
22 J. J. Boon, A. D. Pouwels and G. B. Eijkel, *Biochem. Soc. Trans.*, 15 (1987) 251.
23 A. Venema and J. Veurink, *J. Anal. Appl. Pyrol.*, 7 (1985) 207.
24 H. M. Grubb and S. Meyerson, in F. W. McLafferty (Editor), *Mass Spectrometry of Organic Ions*, Academic Press, New York, 1963.
25 E. E. Kingston, J. V. Eichholzer, P. Lyndon, J. K. MacLeod and R. E. Summons, *Org. Mass Spectr.*, 23 (1988) 42–47.
26 F. W. McLafferty, *Interpretation of Mass Spectra*, W. A. Benjamin, London, 2nd ed., 1973, p. 106.
27 F. Behar and R. Pelet, *J. Anal. Appl. Pyrol.*, 7 (1985) 121.
28 E. Bandurski, *Energy Sources*, 6 (1982) 47.
29 R. P. Philp and T. D. Gilbert, *Geochim. Cosmochim. Acta*, 49 (1985) 1421.
30 J. S. Sinninghe Damsté, T. I. Eglinton, J. W. de Leeuw and P. A. Schenck, *Geochim. Cosmochim. Acta*, 53 (1989) 873.

Journal of Chromatography, 606 (1992) 221–228
Elsevier Science Publishers B.V., Amsterdam

CHROM. 24 269

Recovery of diesel fuel from clays by supercritical fluid extraction–gas chromatography

A. P. Emery, S. N. Chesler and W. A. MacCrehan

Organic Analytical Research Division, Chemical Science and Technology Laboratory, National Institute of Standards and Technology, Gaithersburg, MD 20899 (USA)

(First received December 20th, 1991; revised manuscript received April 8th, 1992)

ABSTRACT

Supercritical fluid extraction (SFE) coupled with gas chromatography was used to analyze diesel fuel oil adsorbed on montmorillonite, kaolinite and illite clays. Adsorptive differences in the clays were reflected in the SFE desorption conditions required. However, in all instances the diesel hydrocarbon recovery was greater than 75% with an extraction precision of 2–3%. The short extraction times of 20 min and the other benefits of SFE make this method attractive over classical methods used to extract diesel oil quantitatively from soils.

INTRODUCTION

Supercritical fluid extraction (SFE) promises to provide rapid, automated extractions of organic analytes from various matrices without the use of hazardous solvents. These benefits suggest that SFE may be an attractive alternative to solvent extraction techniques which require large volumes of such solvents (*e.g.*, Soxhlet extraction and sonication). However, unlike the commonly used Soxhlet extraction and sonication procedures, the SFE conditions required for quantitative recovery are particularly dependent on the analyte and its matrix, and also on how the analyte is incorporated in the matrix.

Soil and associated groundwater contamination resulting from diesel oil spills and leaks from underground storage tanks are pressing environmental issues [1–3]. Because of its advantage, SFE was investigated as an alternative method to remove hydrocarbon contaminants from soil samples. As a first step in developing this method, the recovery of diesel fuel from clay was studied because clay is one of the major adsorptive fractions of soils. The three clays that were studied, each being a relatively well characterized material, were also used as model matrices to investigate SFE recovery processes.

Clay minerals are composed of layered aluminosilicate sheets which are bound to each other by van der Waals and electrostatic forces. Typically, the clays possess anionic charge on the surfaces of the sheets and to a small extent at edges of the clay particle surfaces. This charge is the result of isomorphous substitution throughout the clay lattice structure and is compensated for by the sorption of exchangeable cations. The nature of the cation (valence, size, energy of hydration, etc.) is important in defining the structure and stability of the interlayer which, in turn, affects the sorptive ability of the clay. Interaction of organic molecules with clay occurs either through weak physical adsorption or through actual penetration and intercalation in the interlayers, or basal spacings, of the clay matrix [4,5].

Correspondence to: Dr. A. P. Emery, Organic Analytical Research Division, Chemical Science and Technology Laboratory, National Institute of Standards and Technology, Gaithersburg, MD 20899, USA.

0021-9673/92/$05.00

The recovery of diesel oil from illite, kaolinite and montmorillonite (sodium and calcium forms) was studied. By using these clays, commonly found in North American soil, it was possible to determine diesel recovery from clays having different basal spacings and counter ions. The effect of added water on the SFE recovery of diesel oil from sodium montmorillonite clay was also investigated.

EXPERIMENTAL

Preparation of diesel-contaminated clay samples

Montmorillonite (sodium and calcium forms), kaolinite and illite clays were obtained from Ward's Natural Science Establishment (Rochester, NY, USA). Each clay was ground using an agate mortar and pestle and then sieved through wire-mesh screens. The 40–60 mesh fraction of the clay was used for all of the experiments. National Institute of Standards and Technology Standard Reference Material (SRM) 1624, a distillate fuel oil comparable to a commercial diesel oil, was used to contaminate the samples. Although SRM 1624 was not certified for any organic analytes, it was chosen because it is a homogeneous liquid and is a readily available source for diesel fuel oil. Five types of samples were investigated: SRM 1624 spiked on to filter-paper, unspiked/uncoated clays (blanks), SRM 1624 spiked on to each clay and SRM 1624 coated on to each clay with and without added water. Three 1-g aliquots of each sample type were extracted.

Spiked filter paper samples. Spiked filter paper samples were prepared by placing a *ca.* 1-cm thick bed of 1.1-cm diameter discs of filter paper in the top portion of the extraction cell as described below, and then injecting a weighed amount (*ca.* 50 mg) of a 50% (w/w) solution of SRM 1624 in toluene into the middle of the filter paper bed.

Blank clay samples. Blank samples were prepared by extracting 1.0 g of each of the clays. The clay bed was placed between two pieces of filter paper in the top portion of the extraction cell.

Spiked clay samples. Spiked clay samples were prepared by positioning 1.0 g of clay, sandwiched between two discs of filter paper, in the top portion of the extraction cell. A weighed portion (*ca.* 20 m g) of SRM 1624 was then injected through the top filter paper disc mid-way into the clay layer.

Coated clay samples. A 10-g portion of the 40–60-mesh fraction of clay was weighed into a 250-ml round-bottomed flask. Approximately 260 mg of SRM 1624 were weighed into a 100-ml flask and diluted with 50 ml of a solution of 5% (v/v) methylene chloride in hexane. The diluted SRM solution and two solvent rinses were transferred into the 250-ml flask containing the clay. The flask was attached to a rotary evaporator and the solvent was removed in 20 min under a 25 mm water vacuum (3.3 kPa) at 40°C. The resulting material, a homogeneous-appearing, free-flowing powder, was stored in glass jars with Teflon-lined caps prior to extraction. Samples were found to be stable for 3 months at room temperature (20°C). Coated clay samples were prepared by placing a weighed portion (1.0 g) of the coated clay between filter papers in the top portion of the extraction cell.

Water wet-coated clay samples. The wet samples were prepared by injecting a weighed portion of distilled water (250 mg) into the bed of diesel-coated clay in the extraction cell.

Method of calibration and preparation of calibrant solutions

To evaluate the SFE recovery, the peak areas of the *n*-alkanes in the SFE extracts, normalized to the appropriate internal standard peak area, were compared with those generated by directly injecting a calibration solution of SRM 1624. Calibration solutions were prepared gravimetrically from SRM 1624 and a solution of internal standards, biphenyl and anthracene. Approximately 25 ml of SRM 1624 were drawn up into a 50-ml syringe. The syringe was weighed, and then its contents were injected into 2 ml of 5% (v/v) methylene chloride in hexane solution. The syringe was then reweighed, and the weight of SRM 1624 delivered was determined by difference. Because, in this study, the absolute recoveries of specific analytes extracted from the clay samples were to be measured (as opposed to the amount actually contained in the original clay samples), the internal standards were added to the samples after extraction.

SFE extraction procedure

Samples were extracted using an automated SFE instrument using SFE-grade carbondioxide. All 1-g

samples were extracted in 7.5 cm × 1.1 cm I.-D. stainless-steel extraction cells having an internal volume of 7 ml. After each sample had been loaded into the cell, the excess cell volume was filled by placing a 6 cm × 1.0 cm glass rod in the portion of the cell below the sample bed (Fig. 1). The extraction cells were sealed and the samples were extracted immediately to avoid evaporative losses. Samples were extracted using the conditions shown in Table I. After depressurization through an adjustable stainless-steel (SS) orifice, the extracted sample components were collected on an octyldecylsilane (ODS) trap and then eluted from the trap with two 1-ml portions of 5% (v/v) methylene chloride in hexane into 1.8-ml chromatography vials. The trap temperature was maintained at 10°C during analyte collection and at 40°C during analyte elution. After extraction, the two 1-ml trap eluates were combined with a weighed portion (440 mg) of a toluene solution containing the biphenyl and anthracene internal standards.

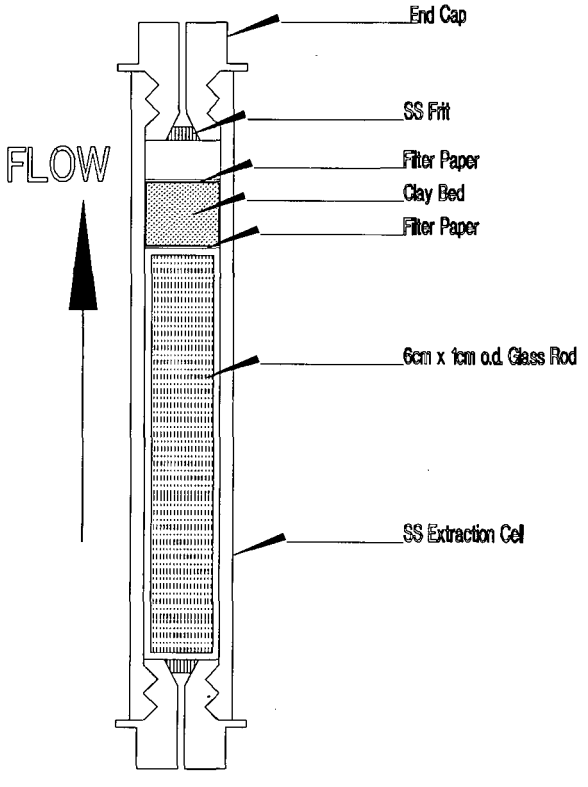

Fig. 1. Schematic diagram of extraction cell.

Soxhlet extraction procedure

Cellulose extraction thimbles were pre-extracted for 4 h in methylene chloride and charged with 1.0-g samples of diesel-coated montmorillonite clay. Triplicate samples were extracted for 6 h with 100 ml of methylene chloride. The resulting extracts were concentrated with argon to 0.5 ml using an automated evaporative concentrator. The concentrates were reconstituted to 2 ml with 5% (v/v) methylene chloride in hexane and the internal standards were added. Instead of adding internal standards before concentration, an evaporation blank was run. A weighed portion of the SRM 1624 was added to 100 ml of methylene chloride, which was then similarly concentrated and reconstituted to determine if any sample loss occurred during evaporation of the Soxhlet extracts.

Gas chromatographic (GC) analysis

The extracted diesel oil samples were analyzed using a gas chromatograph equipped with an autosampler and a flame ionization detector. The diesel analytes were separated on a 60 m × 0.25 mm I.D. immobilized methylsilicone column with a film thickness of 0.25 mm. The injection volume was 3 ml and the split ratio was 30:1. The carrier gas was helium at a flow-rate of 1 ml/min. The column oven was held at 100°C for 5 min, then programmed at 4°C/min to 280°C and held there for 5 min. The injector and detector temperatures were set at 280°C. Integration was performed using a PC-based data acquisition system. The reported recoveries represent the mean values of at least three individual GC analyses of each extract.

RESULTS AND DISCUSSION

The initial extraction and collection conditions [5 min, low pressure and temperature (P/T)] are shown in Table I and were determined by evaluating the recoveries of n-C_{11} to n-C_{22} Alkanes in SRM 1624 from the spiked filter paper samples. A chromatogram of SRM 1624 is shown in Fig. 2, and the results of the spiked filter paper studies are shown in Fig. 3. Quantitative extraction of SRM 1624 from the non-adsorptive filter paper matrix occurred after the passage of as few as 2.2 column volumes of carbon dioxide through the extraction cell. This observation suggests that once the ana-

TABLE I

SUPERCRITICAL FLUID EXTRACTION CONDITIONS

Parameter	5 min, low P/T	20 min, low P/T	20 min, high P/T
Extractant	CO_2	CO_2	CO_2
Extractant density	0.8 g/ml	0.8 g/ml	0.8 g/ml
Extractant pressure	19.1 MPa (189 atm)	19.1 MPa (189 atm)	37.0 MPa (365 atm)
Extractant flow-rate	1 ml/min	1 ml/min	2 ml/min
Extraction temperature	45°C	45°C	80°C
Extraction time	5 min	20 min	20 min
Cell volumes swept	2.2	8.8	17.6

lytes are desorbed from the sample matrix, the extracted components are efficiently swept out of the cell without excessive mixing and are quantitatively retained on and then eluted from the ODS trap.

No organic material was found in extracts of the blank clay samples, and therefore the clay was used as received without further clean-up. Although the 5 min, low P/T extraction conditions provided greater than 95% recovery of each of the alkanes from the non-adsorptive filter paper, these conditions were not adequate for quantitative extraction from the spiked clay samples, being *ca.* 90% for C_{14} to as low as 80% for C_{22}, indicating that physical and/or chemical interactions were occurring be-

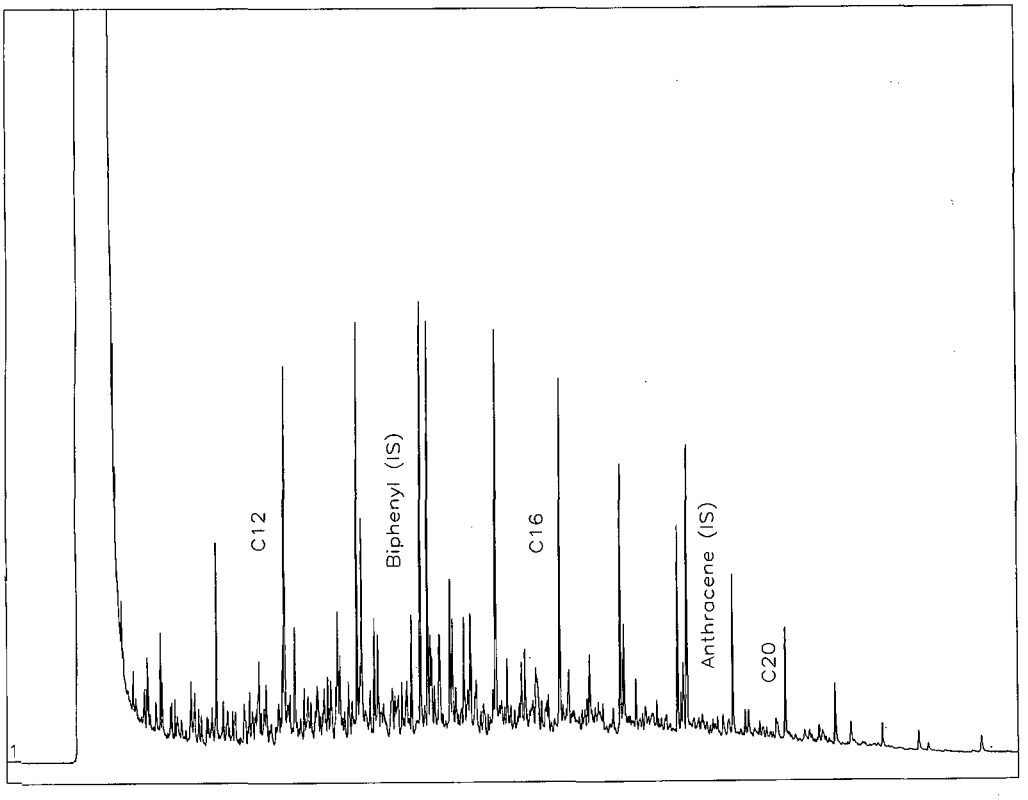

Fig. 2. GC of SRM 1624 diesel fuel oil. GC conditions: column, 60 m × 0.25 mm I.D. DB-5 with 0.25-μm film thickness; carrier gas, helium (1 ml/min); split ratio, 30:1; column temperature, 100°C for 5 min, increased at 4°C/min to 280°C; held for 5 min; flame ionization detection.

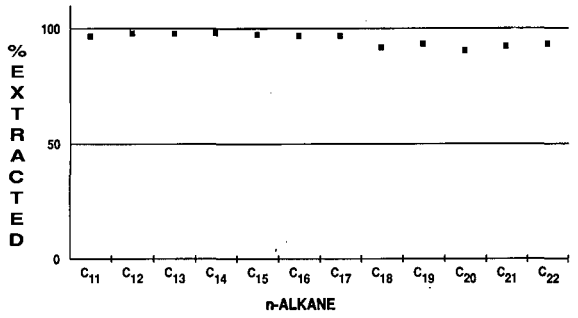

Fig. 3. Recoveries of *n*-alkanes in SRM 1624 from spiked filter paper following supercritical fluid extraction. CO_2: 0.8 g/ml at 1.0 ml/min. Conditions: 19.1 MPa (189 atm) and 45°C for 5 min.

tween the alkanes and the clay matrix. However, essentially quantitative recovery (>95%) of each of the sample components from each of the adsorptive clay matrices was achieved by increasing the number of column volumes of carbon dioxide swept through the extraction cell using 20-min extraction times (see Table I).

The 20 min, low P/T conditions were used to extract the illite and kaolinite clays. The recovery results are shown in Fig. 4. Recoveries >95% were achieved for each of the alkanes in SRM 1624 from the spiked illite and kaolinite samples. The apparent low recoveries of *n*-C_{11} to *n*-C_{13} alkanes in the coated samples were shown by the Soxhlet experiments to be evaporative losses that occurred during coating of this material and were found not to be due to inefficient SFE extraction. Because of these losses, the maximum recovery and the mean replicate deviation reported for each experiment apply only to *n*-C_{14} to *n*-C_{22} alkanes. The high recoveries from both the spiked and coated samples indicate a weak alkane–clay interaction. Both illite and kaolinite possess strong interlayer bonding of the silicate sheets (Table II), as reflected by their basal spacings. As a result, penetration and adsorption of the alkanes by the clay matrices would be expected to be difficult [6].

TABLE II

CLAY PROPERTIES [4,7,10]

Clay	Basal spacing (nm)	Average surface area (m^2/kg)
Illite	1.0	100
Kaolinite	0.7	10
Montmorillonite	1.8	800

Results for the spiked and coated sodium montmorillonite clay are presented in Fig. 5. The recoveries of the alkanes from the spiked sodium mont-

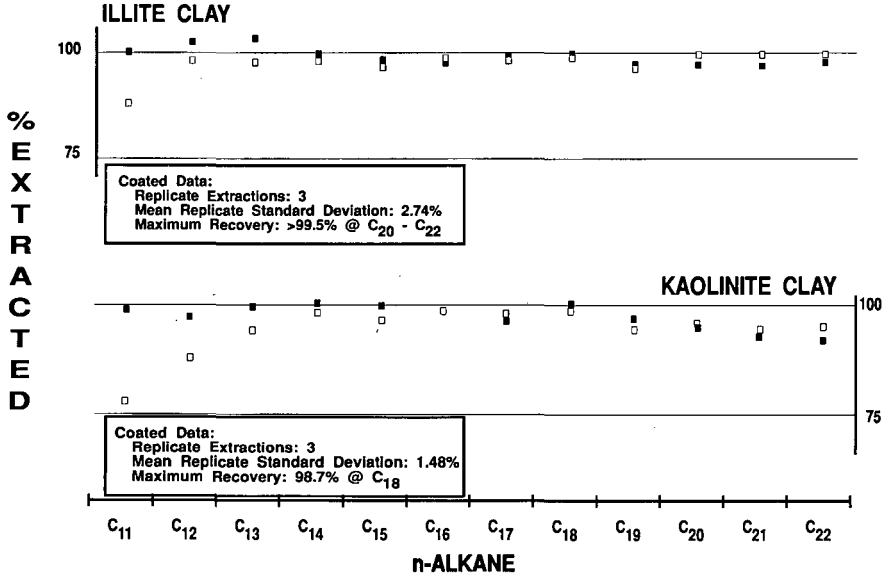

Fig. 4. Recoveries of *n*-alkanes in SRM 1624 from illite clay and kaolinite clay following supercritical fluid extraction. CO_2: 0.8 g/ml at 1.0 ml/min. Conditions: 19.1 MPa (189 atm) and 45°C for 20 min. ■ = spiked; □ = coated.

morillonite samples were significantly greater than those from the coated material. This effect is probably attributable to the extremely large internal surface area (approaching 750 m^2/kg) accessible to the alkanes in this freely expandable clay. The large internal surface area is due to large basal spacings that result from weak interlayer bonding of the silicate sheets of the clay matrix [7]. Lower recoveries of the higher molecular weight alkanes extracted from the clay may be due to the greater Van der Waals sorption forces of these compounds with the clay matrix [8], the lower solubility of these species in the extracting fluid [9] and the lower diffusivities of these compounds through the clay matrix [10].

Additional samples of the coated sodium montmorillonite material were extracted using the 20 min, high P/T conditions (Table I). The number of cell volumes of carbon dioxide swept through the extraction cell was increased to 17.6 as its flow-rate was doubled. The extraction cell temperature was increased to 80°C while maintaining a constant density of 0.8 mg/ml, causing the extractant fluid pressure to increase to 37.0 MPa. The greater recoveries achieved using these conditions may result from the increased mobility of the alkanes and their increased solubility in the carbon dioxide. The recoveries for each of the analytes using the modified clay conditions are shown in Fig. 5.

As seen in Fig. 5, even under conditions near the pressure limit of the instrument, quantitative recovery of the higher-molecular-weight alkanes was not possible using pure carbon dioxide as the extractant. To determine if exhaustive extraction of all of the alkanes could be achieved, 1-g samples of montmorillonite clay coated with SRM 1624 were extracted using a classical Soxhlet apparatus. The Soxhlet extraction data, corrected for any evaporative losses are shown in Fig. 6. The results of the Soxhlet extraction study indicate that the SRM material was not irreversibly adsorbed and could be recovered. The Soxhlet extraction results also confirmed that the losses of n-C_{11} to n-C_{13} alkanes occurred during preparation and not extraction. There was significantly greater imprecision (8–9%) of the "recovered" low-molecular-weight alkanes that may have been caused by irreproducible losses in the Soxhlet extraction process and the final evaporative concentration step. Because the imprecision of the SFE recoveries for these alkanes was observed to be lower (2–3%), SFE appears to be a more precise method for extracting these volatile compounds.

Spiked and coated samples of the calcium form of montmorillonite were also studied further to investigate matrix effects with respect to diesel fuel recovery. Although calcium montmorillonite clay is

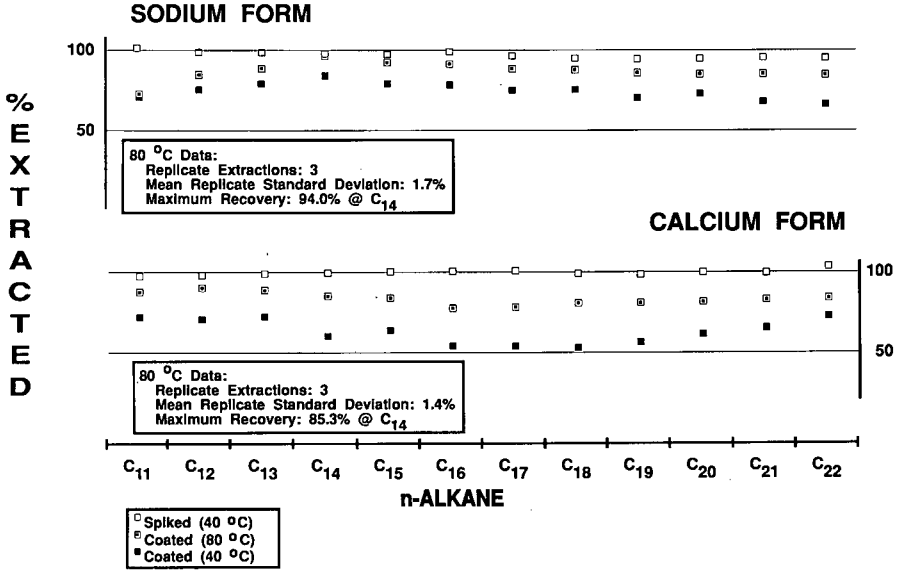

Fig. 5. Recoveries of n-alkanes in SRM 1624 from sodium montmorillonite clay and calcium montmorillonite clay following supercritical fluid extraction. CO_2: 0.8 g/ml at 2.0 ml/min. Conditions: 37.0 MPa (365 atm) and 80°C for 20 min.

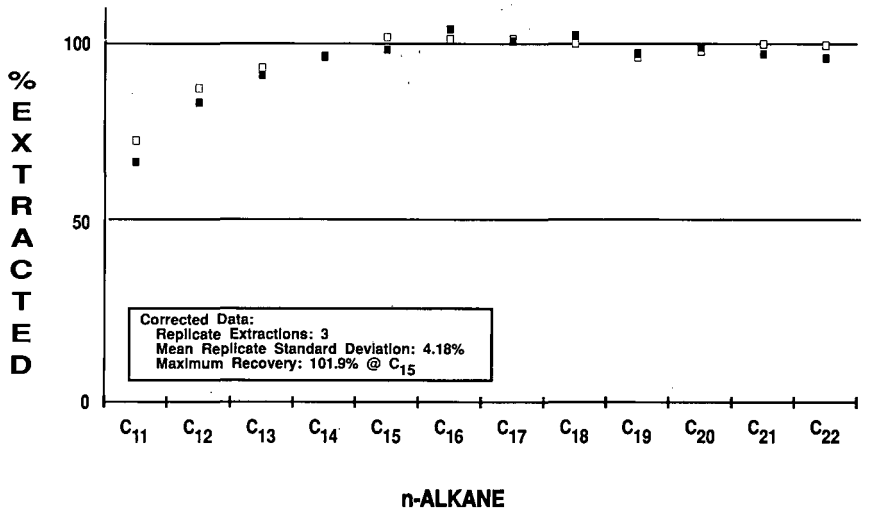

Fig. 6. Recoveries of *n*-alkanes in SRM 1624 from sodium montmorillonite clay following Soxhlet extraction (6h, methylene chloride). □ = Corrected for losses due to evaporative concentration; ■ uncorrected.

not as readily expanded by solvents as the sodium form of the clay [11], the calcium form, because of the greater energy of hydration of the calcium ion, is more adsorptive than its sodium counterpart [12]. SFE extraction recoveries were lower for the calcium form than those for the sodium form of the clay, as shown in Fig. 5. Unlike the other clay materials that were studied where the alkane recovery tended to decrease with increasing molecular weight, the recovery data for the calcium montmorillonite clay exhibited a parabolic trend with respect to carbon number such that the mid-range alkanes were most strongly retained. This suggests that a size-exclusion effect, possibly due to the more structured interlayers in the calcium montmorillonite clay matrix [13], in addition to adsorption effects may influence the interaction of the diesel fuel with the clay matrix.

Sodium montmorillonite samples, with added water, were also analyzed using the 20 min, high

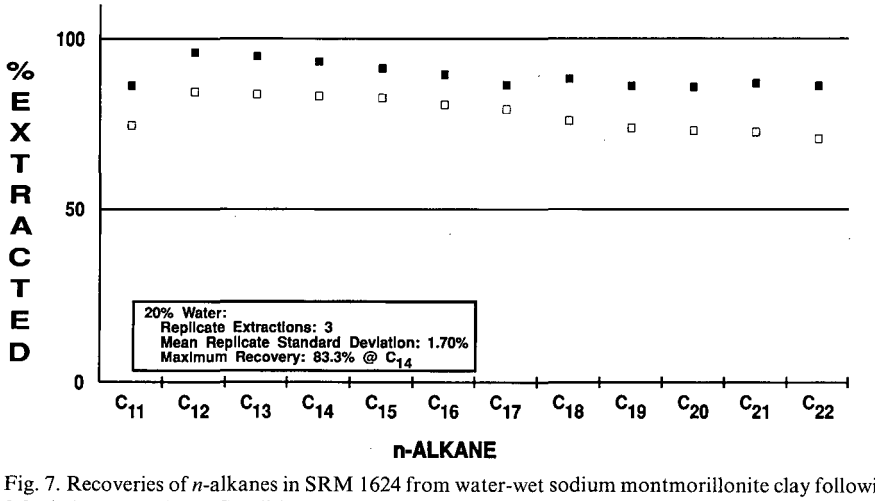

Fig. 7. Recoveries of *n*-alkanes in SRM 1624 from water-wet sodium montmorillonite clay following supercritical fluid extraction. CO_2: 0.8 g/ml at 2.0 ml/min. Conditions: 37.0 MPa (365 atm) and 80°C for 20 min. ■ = Coated, no added water; □ = coated, 25% added water.

P/T conditions. The recoveries for all of the alkanes were lower than those from dry diesel-coated clay, as shown in Fig. 7. When the clay matrix is swollen by the presence of water, the mass transfer of the analytes out of the matrix can be reduced. Addition of water can act to trap analytes physically within channels in the clay particles. Chemical changes, such as intra-cation exchange reactions, can also occur which affect the basal spacings within the clay by creating cavities that can cause the collapse of all or part of the lattice structure of the clay [7]. Further, the water film may also reduce the surface area available for penetration of the extractant.

As a result of this study, it was found that recovery of the *n*-alkanes from the clay matrices depended on the nature of the alkane and the matrix. While clays were used as model matrices to evaluate diesel recovery, the aim was to apply these results to the study of diesel-contaminated soil. Preliminary investigation of diesel-contaminated soils indicate that, while the highly adsorptive pure clays readily sorb and retain the diesel material, soils were quantitatively extracted using the 20 min, high P/T extraction conditions.

CONCLUSIONS

The SFE technique was easy to perform, rapid and required small amounts of solvents. We found that, unlike in the more accepted Soxhlet extraction and sonication procedures, the SFE extraction conditions must be optimized for the analyte and the matrix in order to achieve quantitative extractions. The SFE results showed that diesel oil recovery is influenced by the adsorptive behaviour of the individual clay matrix. The large internal surface areas of both of the montmorillonte clays enabled them to adsorb and retain more diesel material than the illite and kaolinite clays. Similarly, calcium montmorillonite retained more material than sodium montmorillonite. The recovery of the diesel oil was reduced when water was added to coated sodium montmorillonite clay, possibly because of changes in the matrix that may trap some of the adsorbed diesel, making it inaccessible to the extracting fluid. In all instances, the recovery was improved by increasing the length, temperature and pressure of the extraction.

As the result of the study, a reliable SFE–GC method was developed that can be used successfully to extract diesel oil from illite and kaolinite clay, and also from the highly adsorptive sodium montmorillonite (wet or dry) and calcium montmorillonite clays. In all instances, diesel fuel recoveries were $>75\%$ with a precision of 2–3%, making this method a candidate for survey analysis.

ACKNOWLEDGEMENTS

We acknowledge the Consortium for Automated Analytical Systems for financial support and Hewlett-Packard for the loan of the SFE instrumentation.

REFERENCES

1 W. Park and G. G. Eichholz, *Waste Manage.*, 10 (1990) 125–139.
2 M. van der Waarden, W. M. Groenewoud and A. L. A. M. Bridie, *Water Res.*, 11 (1977) 359–365.
3 M. T. Galceran, R. Rubio, G. Rauret and L. Alonso, *Waste Manage.*, 10 (1990) 261–268.
4 I. Barshad, in F. E. Bear (Editor), *Chemistry of the Soil*, Reinhold New York, 2nd ed., 1964, p. 1.
5 R. C. MacKenzie, in J. E. Gieseking (Editor), *Soil Components, Vol. 1, Inorganic Components*, Springer, New York, 1975, p. 8.
6 L. G. Morrill, B. C. Mahilum and S. H. Mohiuddin, *Organic Compounds in Soils: Sorption, Degradation and Persistance*, Ann Arbor Sci. Publ. Ann Arbor, M_I, 1982, p. 40.
7 P. B. Attewell and I. W. Farmer, *Principles of Engineering Geology*, Wiley, New York, 1976, p. 17.
8 D. P. Salisbury and N. S. Walker, *Spectroscopy*, 1, No. 3 (1989) 44–47.
9 A. W. Francis, *J. Phys. Chem.*, 58 (1954) 1099–1114.
10 R. M. Barrer, *Zeolites and Clay Minerals as Sorbants and Molecular Sieves*, Academic Press, London, 1978, pp. 407–466.
11 E. Czarnecka and J. E. Gillott, *Clays Clay Miner.*, 28 (1980) 197–203.
12 B. F. G. Theng, *The Chemistry of Clay–Organic Reactions*, Adam Hilger, London, 1974, pp. 6–130.
13 P. L. Hall, in M. J. Wilson (Editor), *A Handbook of Determinative Methods in Clay Minerology*, Chapman and Hall, New York, 1987, pp. 1–15.

Journal of Chromatography, 606 (1992) 229–235
Elsevier Science Publishers B.V., Amsterdam

CHROM. 24 314

Determination of aminoglycoside antibiotics in pharmaceuticals by capillary zone electrophoresis with indirect UV detection coupled with micellar electrokinetic capillary chromatography

M. T. Ackermans, F. M. Everaerts and J. L. Beckers

Laboratory of Instrumental Analysis, Eindhoven University of Technology, P.O. Box 513, 5600 MB Eindhoven (Netherlands)

(Received March 19th, 1992)

ABSTRACT

Aminoglycoside antibiotics can be determined by capillary zone electrophoresis (CZE) with indirect UV detection in the anionic mode with a reversed electroosmotic flow (EOF) by addition of FC 135 to the background electrolyte. The effective mobilities of thirteen aminoglycoside antibiotics were determined as a function of pH. Applying CZE with indirect UV detection in the anionic mode and reversed EOF coupled with micellar electrokinetic capillary chromatography with the cationic surfactant cetyltrimethylammonium bromide, both neutral and charged antibiotics can be determined in combined pharmaceuticals. As an example, neomycin and hydrocortisone were determined in Otosporin eardorps.

INTRODUCTION

Capillary zone electrophoresis (CZE) has proved to be a highly efficient separation method, generally applicable for the determination of charged components. Using a UV detector, non-UV-absorbing components can also be detected in the indirect UV mode. Neutral components can be separated by micellar electrokinetic capillary chromatography (MECC), a hybrid technique, combining both chromatographic and electrophoretic separation principles. Since the introduction of MECC [1,2] and CZE [3,4], many components of pharmaceutical interest have been determined [5–10] using these techniques. No attention has been paid, however, to analyse for aminoglycoside antibiotics. So far, the non-UV-absorbing aminoglycoside antibiotics have been determined by, *e.g.*, ion-pair reversed-phase high-performance liquid chromatography using a refractive detector [11,12] and spectrometric methods using derivatization reagents [13].

Combined pharmaceuticals often contain both charged and neutral compounds, which may or may not be UV absorbing. In this work, we studied the possibilities of applying CZE with indirect UV detection for the determination of aminoglycoside antibiotics and CZE with indirect UV detection coupled with MECC for the determination of aminoglycoside antibiotics and neutral components in combined pharmaceuticals. In Fig. 1 the structural formulae of some representative aminoglycoside antibiotics are given.

EXPERIMENTAL

Instrumentation

For all experiments a P/ACE System 2000 HPCE instrument (Beckman, Palo Alto, CA, USA) was used. All experiments were carried out in a fused-

Correspondence to: Dr. J. L. Beckers, Laboratory of Instrumental Analysis, Eindhoven University of Technology, P.O. Box 513, 5600 MB Eindhoven, Netherlands.

0021-9673/92/$05.00

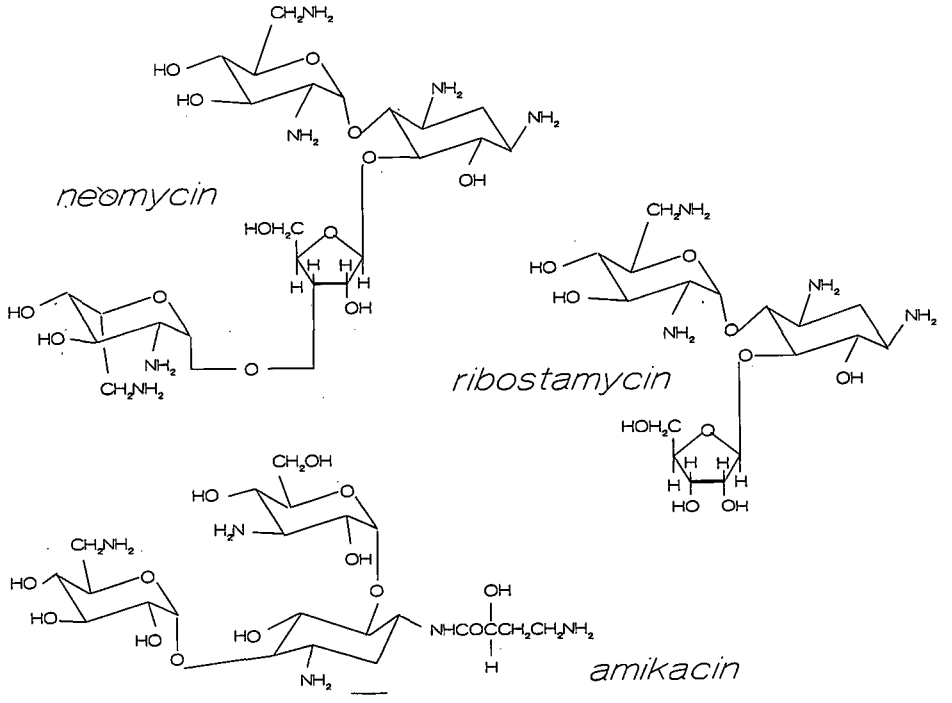

Fig. 1. Structural formulae of aminoglycoside antibiotics.

silica capillary from Siemens (Karlsruhe, Germany) of 50 μm I.D., total length 27 cm, distance between injection and detection 20 cm, or total length 67 cm, distance between injection and detection 60 cm. The wavelength of the UV detector was set at 214 nm. Data analysis was performed using the laboratory-written data analysis program CAESAR.

Chemicals

Amikacin dihydrate, gentamycin sulphate, streptomycin sulphate and tobramycin were obtained from Fluka (Buchs, Switzerland), butirosin disulphate salt, dibekacin sulphate salt, dihydrostreptomycin sesquisulphate salt, kanamycin B sulphate salt, lividomycin sulphate salt, neomycin sulphate, paromomycin sulphate, ribostamycin sulphate salt and sisomycin sulphate salt from Sigma (St. Louis, MO, USA), paracetamol from Merck-Schuchardt (Hohenbrunn, Germany), dexamethasone No. 85G30-50971 from De Onderlinge Pharmaceutische Groothandel (Utrecht, Netherlands), dapsone was donated by the State Institute for Quality Control of Agricultural Products (Wageningen, Netherlands), the fluorochemical surfactant FC 135 was obtained from Fluorad/3M (Leiden, Netherlands) and hydrocortisone from Aldrich (Brussels, Belgium).

Standard solutions

Standard solutions of the aminoglycoside antibiotics were prepared by weighing accurately 50.0 mg of the standards and dissolving them in 50.0 ml of a 100 m*M* cetyltrimethylammonium bromide (CTAB) solution (the stock solution of CTAB was stored at 30°C). For calibration, dilutions of this stock solution were used at concentrations of 1.0, 0.8, 0.6, 0.4, 0.2 and 0.1 mg/ml. For the determination of neomycin and hydrocortisone in Otosporin eardrops, a stock solution of 0.2 mg/ml of hydrocortisone and 0.1 mg/ml neomycin was prepared (in 100 m*M* CTAB) and six dilutions were prepared spread between one- and tenfold dilution, so that the concentration of the sample is near the middle of the linear range of the calibration graph.

Sample preparation

Otosporin eardrops (Wellcome Foundation, London, UK), labelled to contain 10 mg/ml of hydrocortisone and 5 mg/ml of neomycin, were diluted 100-fold with distilled water. This dilution was used for the injection without further pretreatment.

RESULTS AND DISCUSSION

Determination of aminoglycosides by CZE with indirect UV

Aminoglycoside antibiotics are non-UV-absorbing components, positively charged in their protonated form at pH 3–8. Isotachophoretic (ITP) experiments showed that they migrate at intermediate pH with effective mobilities of $20 \cdot 10^{-5}$–$50 \cdot 10^{-5}$ $cm^2/V \cdot s$ with positive charges of 2^+ to 5^+, as could be concluded from their response factors [14]. In the first instance the aminoglycoside antibiotics were determined using CZE in the cationic mode (cathode at the detection side) with the indirect UV mode. Very bad peak shapes, due to strong attractive forces between the highly positively charged components and the negatively charged capillary wall, and a low resolution were the result. Because higher separation numbers [15] can be obtained at low apparent mobilities and to suppress the attractive forces between the analytes and the capillary wall, experiments were carried out in the anionic mode (anode at the detection side) with a reversed electroosmotic flow (EOF) by the addition of FC 135 to the background electrolyte [16]. All aminoglycoside antibiotics now migrated in the upstream mode [17]. With the addition of FC 135, values for the mobility of the electroosmotic flow (m_{EOF}) can easily be obtained down to $-90 \cdot 10^{-5}$ $cm^2/V \cdot s$.

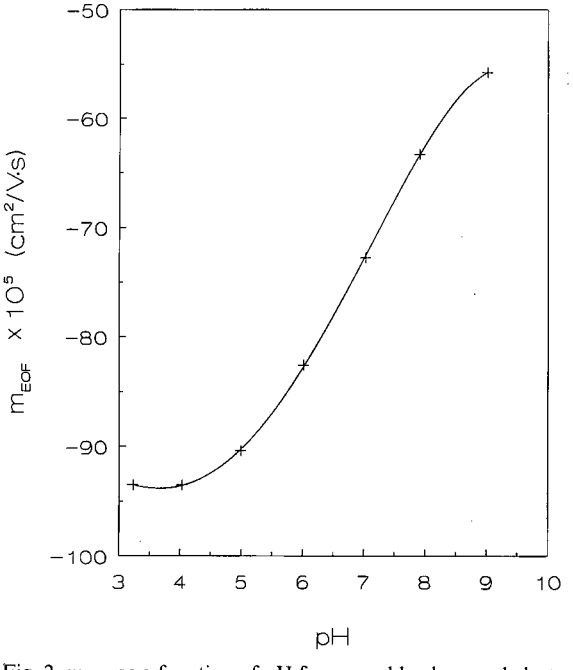

Fig. 2. m_{EOF} as a function of pH for several background electrolytes with 50 μg/ml of FC 135 added.

In Fig. 2, the m_{EOF} values as a function of the pH of the background electrolyte are shown for the background electrolytes with FC 135. In Table I, the compositions of all the background electrolytes are given. As can be seen from Fig. 2, the absolute values of m_{EOF} increase with decreasing pH, in contrast to the m_{EOF} values in background electrolytes without FC 135, which increase with increasing pH. This can be easily understood as follows. In fused silica the negative charge of the capillary wall increases with increasing pH (higher ζ-potential, higher m_{EOF}). An adsorbing layer of FC 135 molecules shields this negative charge. At high pH this shielding is less effective, resulting in a lower $|m_{EOF}|$.

Owing to this effect, the peak shape of the aminoglycosides in the reversed mode will also be the best at low pH, and will deteriorate at higher pH values. In Fig. 3 an example of the separation of a mixture of amikacin, dihydrostreptomycin, kana-

TABLE I

COMPOSITIONS OF BACKGROUND ELECTROLYTES AT DIFFERENT pH VALUES

All buffers were prepared by adding the buffering counter ion to the cations until the desired pH was reached. To all buffers, FC 135 was added at a concentration of 50 μg/ml.

Cation	Buffering counter species	pH
0.01 *M* imidazole	Formic acid	3.3
0.01 *M* imidazole	Formic acid	4.0
0.01 *M* imidazole	Acetic acid	5.0
0.01 *M* imidazole	MES[a]	6.0
0.02 *M* imidazole	Acetic acid	7.0
0.02 *M* imidazole	Acetic acid	7.9
0.02 *M* benzylamine	Acetic acid	9.0

[a] 2-(N-Morpholino)ethane sulphonic acid.

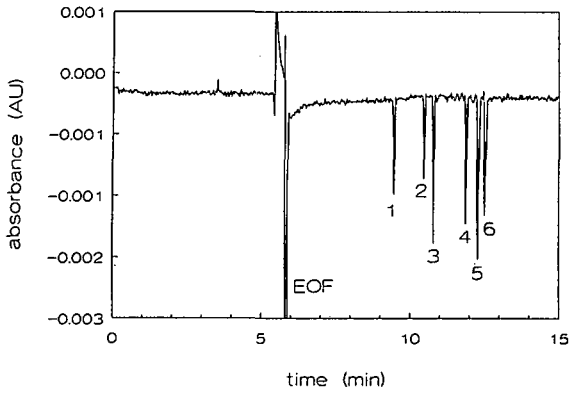

Fig. 3. Electropherogram for the separation of (1) dihydrostreptomycin, (2) lividomycin, (3) amikacin, (4) kanamycin, (5) tobramycin and (6) sisomycin (all 0.1 mg/ml) in the anionic mode with reversed EOF applying a background electrolyte of 0.01 *M* imidazole acetate at pH 5.0 containing the additive FC 135 (50 μl/ml). Capillary length, 67 cm; applied voltage, 12.5 kV; pressure injection time 2 s; UV detection wavelength, 214 nm.

mycin, lividomycin, sisomycin and tobramycin (all at a concentration of 0.1 mg/ml), obtained by applying a background electrolyte of 0.01 *M* imidazole at pH 5.0 adjusted by adding acetic acid with the additive FC 135 (50 μg/ml), is given [16]. The effective mobilities of the aminoglycoside antibiotics were determined as a function of pH. In Table II all the determined effective mobilities of the aminoglycoside antibiotics are given (see Table I for the background electrolyte composition). From Table II and Fig. 3, it can be concluded that aminoglycosides can easily be determined in the anionic CZE mode with reversed EOF by the addition of FC 135 with indirect UV detection at an optimum pH of about 5, although not all components can be separated at this pH.

Coupled capillary zone electrophoresis and micellar electrokinetic capillary chromatography

Pharmaceuticals often contain both neutral and charged components. In order to determine simultaneously both charged and neutral components, a micelle-forming surfactant has to be added to the background electrolyte.

Applying a coupled CZE and MECC system, negative, positive and neutral components can migrate in any order depending on their effective mobilities and capacity factors. As an illustration, a schematic representation of the different migration possibilities is given in Fig. 4. In Fig. 4a the original situation is shown, where the capillary is filled with background electrolyte containing a cationic surfactant. The cathode is placed at the injection side (i). In Fig. 4b the situation after some time is shown and Fig. 4c shows the corresponding electrophero-

TABLE II

CALCULATED EFFECTIVE MOBILITIES, $m \cdot 10^5$ ($cm^2/V \cdot s$), OF AMINOGLYCOSIDE ANTIBIOTICS AT DIFFERENT pH VALUES

For the composition of the background electrolytes, see Table I.

Component	pH					
	3.23	4.03	4.99	6.01	7.02	7.90
Amikacin	42.76	42.31	41.68	40.01	34.15	30.11
Butirosin	43.08	42.74	41.05	37.85	34.27	32.07
Dibekacin	52.35	51.46	48.45	46.34	40.26	34.33
Dihydrostreptomycin	35.31	35.00	34.58	35.26	32.51	31.47
Gentamycin	50.39	49.03	46.39	44.81	40.34	35.93
Kanamycin	50.31	49.31	46.18	43.30	35.37	27.90
Lividomycin	42.73	42.05	40.03	36.34	28.91	23.78
Neomycin	51.28	50.22	47.99	46.39	39.98	32.53
Paromomycin	47.52	46.94	44.51	41.50	34.68	28.00
Ribostamycin	46.05	44.85	41.10	39.14	34.52	28.54
Sisomycin	51.41	50.71	48.15	45.53	39.94	33.86
Streptomycin	34.99	39.94	34.70	34.92	33.22	32.36
Tobramycin	51.34	50.67	47.51	45.04	38.21	30.73

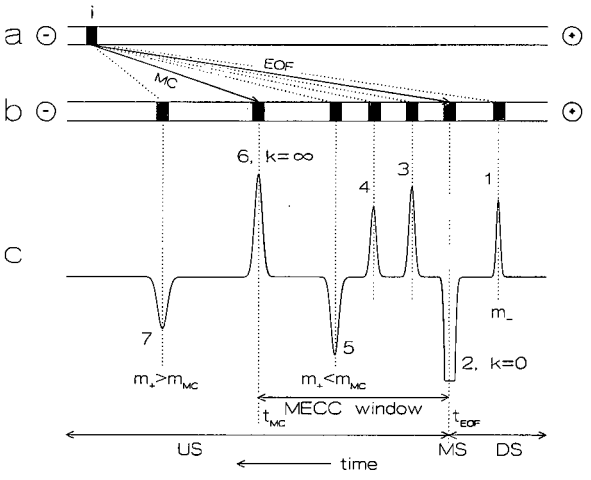

Fig. 4. Schematic representation of several migration modes in CZE with indirect UV detection in the anionic mode with reversed EOF coupled with MECC with a cationic surfactant. (a) Original situation; (b) separation after some time; (c) electropherogram of components migrating in different modes. Components 1, 3, 4, 6 are UV absorbing, components 5, 7 are non-UV-absorbing. For further explanation, see text.

gram. In this electropherogram, component 1 is negatively charged and migrates in the downstream mode (DS) in front of a water dip (midstream mode, MS), that can act as an EOF marker [17]. A non-solubilized neutral component can also act as an EOF marker (with a capacity factor $k = 0$) if the component absorbs UV radiation. The completely solubilized component 6 acts as a micelle (MC) marker ($k = \infty$). The time window for neutral components migrating in the MECC mode is demarcated by t_{MC} and t_{EOF} and, *e.g.*, a neutral component (4) migrates in the MECC mode. Component 3, negatively charged but partially solubilized, migrates behind the EOF marker. Component 5, without UV absorption, is a positive component with a mobility smaller than that of the micelles, whereas the positive component 7, without UV absorption, with a mobility larger than that of the MC marker migrates behind the MC marker.

For the determination of neutral components simultaneously with aminoglycoside antibiotics in the anionic mode with reversed EOF, in first instance sodium dodecyl sulphate (SDS) was used. As the additive FC 135 probably solubilized in the SDS micelles, the mobility of the reversed EOF strongly decreased, as a result of which the aminoglycoside

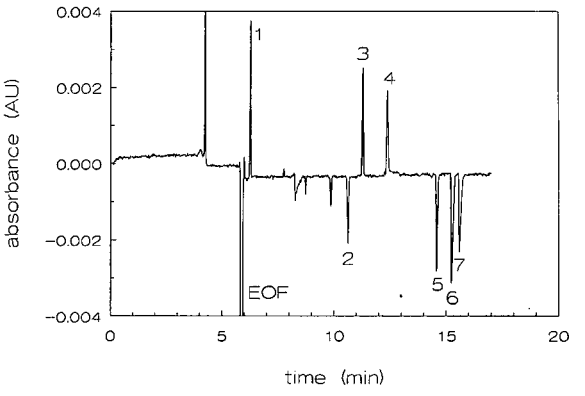

Fig. 5. Electropherogram for the separation of (1) paracetamol, (2) dihydrostreptomycin, (3) dapsone, (4) dexamethasone, (5) kanamycin, (6) tobramycin and (7) sisomycin obtained by applying a coupled CZE–MECC system consisting of 0.01 *M* imidazole acetate at pH 5.0 containing FC 135 (50 μl/ml) and 100 m*M* CTAB. Capillary length, 67 cm; applied voltage, 15 kV; pressure injection time, 5 s; UV detection wavelength 214 nm.

antibiotics could no longer be detected in the anionic mode. For this reason the cationic surfactant CTAB was tried as a micelle-forming surfactant causing, moreover, a reversed EOF. Good results in the separation of aminoglycoside antibiotics and several neutral components could be obtained with the addition of CTAB (100 m*M*) and FC 135 (50 μg/ml).

In Fig. 5 an example is given of the separation of a mixture of the UV-absorbing neutral components paracetamol and dapsone (0.02 mg/ml) and dexamethasone and the aminoglycoside antibiotics dihydrostreptomycin, kanamycin, tobramycin and sisomycin (all 0.1 mg/ml). The background electrolyte consisted of 0.01 *M* imidazole at pH 5.0 adjusted by adding acetic acid with the additives 50 μg/ml FC 135 and 100 m*M* CTAB. In order to

TABLE III

REGRESSION COEFFICIENTS, *r*, AND LIMITS OF DETECTION, LOD, FOR THE CALIBRATION GRAPHS OF DIHYDROSTREPTOMYCIN, SISOMYCIN, PARACETAMOL AND DAPSONE

Component	*r*	LOD (μg/ml)
Dihydrostreptomycin	0.9998	23.38
Sisomycin	0.9995	35.89
Paracetamol	1.0000	9.87
Dapsone	0.9997	29.84

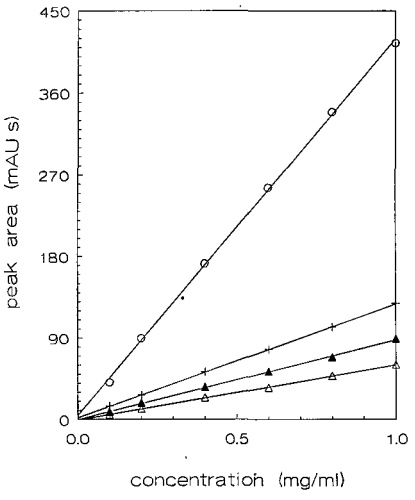

Fig. 6. Calibration graphs for peak area (mAUs) *versus* injected concentration (mg/ml) for (△) dihydrostreptomycin, (▲) sisomycin, (+) paracetamol and (○) dapsone. For separation conditions, see Fig. 5.

check quantitative aspects of separations using a coupled CZE–MECC system, calibration graphs of peak area *versus* injected concentration (5-s pressure injection) were set up for the aminoglycoside antibiotics dihydrostreptomycin and sisomycin and the neutral components paracetamol and dapsone in the same background electrolyte. The qualitative abilities of this separation were checked by measuring the effective and pseudo-effective mobilities of the separate components [15], and comparing them with the effective and pseudo-effective mobilities in the mixture. In Fig. 6 the calibration graphs are presented and in Table III all regression parameters are given, showing a linear relationship between peak area and injected concentration for both charged and neutral components.

As an application, we determined neomycin and hydrocortisone in Otosporin eardrops. The sample was measured four times. In Table IV the regression coefficients of the calibration graphs of the two components and the labelled and determined concentrations of the components in the sample are given. As can be seen, the determined and the labelled values agree well.

TABLE IV

REGRESSION COEFFICIENTS, r, FOR THE CALIBRATION GRAPHS OF NEOMYCIN AND HYDROCORTISONE, AND THE LABELLED AND MEASURED CONCENTRATIONS OF THESE COMPONENTS IN OTOSPORIN EARDROPS

Component	r	Concentration (mg/ml)	
		Labelled	Measured
Neomycin	0.9997	5.00	5.42
Hydrocortisone	0.9990	10.00	10.56

CONCLUSIONS

The determination of aminoglycoside antibiotics in the cationic mode is difficult owing to attractive forces between the positively charged aminoglycoside antibiotics and the negative charged capillary wall. By addition of FC 135 to the background electrolyte, resulting in a reversed wall charge, the aminoglycoside antibiotics could easily be determined in the anionic mode with reversed EOF. The effective mobilities of thirteen aminoglycoside antibiotics were measured as a function of pH. Charged and neutral components can be determined simultaneously by applying coupled CZE and MECC. By the application of an electrolyte consisting of 0.01 *M* imidazole adjusted to pH of 5.0 by adding acetic acid and the additives FC 135 (50 μg/ml, for reversed EOF) and CTAB (100 m*M*, as micelle-forming surfactant), the aminoglycoside antibiotics (in the anionic mode with reversed EOF with indirect UV detection) and neutral components (reversed MECC mode) could be simultaneously determined. The values obtained for neomycin and hydrocortisone in eardrops agreed with the labelled values.

REFERENCES

1 S. Terabe, K. Otsuka, K. Ichikawa, A. Tsuchiya and T. Ando, *Anal. Chem.*, 56 (1984) 113.
2 S. Terabe, K. Otsuka and T. Ando, *Anal. Chem.*, 57 (1985) 834.
3 F. E. P. Mikkers, F. M. Everaerts and Th. P. E. M. Verheggen, *J. Chromatogr.*, 169 (1979) 1.
4 J. W. Jorgenson and K. K. Lukacs, *Anal. Chem.*, 53 (1981) 1298.
5 M. T. Ackermans, F. M. Everaerts and J. L. Beckers, *J. Chromatogr.*, 585 (1991) 123.
6 M. T. Ackermans, J. L. Beckers, F. M. Everaerts and I. J. G. A. Seelen, *J. Chromatogr.*, 595 (1992) 341.
7 M. T. Ackermans, J. L. Beckers, F. M. Everaerts, H. Hoogland and M. J. H. Tomassen, *J. Chromatogr.*, 596 (1992) 101.

8 A. Wainright, *J. Microcol. Sep.*, 2 (1990) 166.
9 H. Nishi, N. Tsumagara and S. Terabe, *Anal. Chem.*, 61 (1989) 2434.
10 S. Fujiwara and S. Honda, *Anal. Chem.*, 59 (1987) 2773.
11 G. Inchauspe and D. Samain, *J. Chromatogr.*, 303 (1984) 277.
12 G. Inchauspe, P. Delrieu, P. Dupin, M. Laurent and D. Samain, *J. Chromatogr.*, 404 (1987) 53.
13 S. S. Sampath and H. H. Robinson, *J. Pharma. Sci.*, 79, (1990) 428.
14 J. L. Beckers and F. M. Everaerts, *J. Chromatogr.*, 470 (1989) 277.
15 J. L. Beckers, F. M. Everaerts and M. T. Ackermans, *J. Chromatogr.*, 537 (1991) 407.
16 A. Emmer, M. Jansson and J. Roeraade, *J. Chromatogr.*, 547 (1991) 544.
17 F. M. Everaerts, A. A. A. M. van de Goor, Th. P. E. M. Verheggen and J. L. Beckers, *J. High Resolut. Chromatogr.*, 12 (1989) 28.

Journal of Chromatography, 606 (1992) 237–247
Elsevier Science Publishers B.V., Amsterdam

CHROM. 24 275

Fast capillary electrophoresis–ion spray mass spectrometric determination of sulfonylureas

Frederick Garcia* and Jack Henion

Drug Testing and Toxicology, New York State College of Veterinary Medicine, Cornell University, 925 Warren Drive, Ithaca, NY 14850 (USA)

(First received January 27th, 1992; revised manuscript received April 14th, 1992)

ABSTRACT

This paper describes the use of a simple, laboratory-made capillary electrophoresis (CE) system equipped with relatively short (25–35 cm) capillaries that may be coupled to a pneumatically assisted electrospray (ion spray) interface for separations with on-line mass spectrometric (MS) detection. Sulfonylurea crop protection chemicals were used as model compounds to demonstrate the utility of the CE–MS system described. By using 35-cm fused-silica capillaries the CE–MS determination of an eight-component mixture of these compounds was accomplished within 5 min. In addition, on-line CE–MS under tandem mass spectrometric conditions (CE–MS–MS) was shown to give full-scan collision-induced mass spectra from 30-pmol levels of these compounds.

INTRODUCTION

Sulfonylurea crop protection chemicals play an important role in today's agricultural arena [1]. These compounds have use rates substantially less than those of previous herbicides and are rapidly and efficiently metabolized in plants, animals and soil [2]. Because of their polarity and chemical instability, their analytical determination is particularly challenging. They are very sensitive to thermal degradation caused by the elevated temperatures common to capillary gas chromatography (GC)–mass spectrometry (MS) and they cannot be analyzed intact by this technique. Liquid chromatography (LC)–thermospray MS typically does not give significant molecular ion abundances for the sulfonylurea compounds when the vaporizer temperature is optimized for maximum sensitivity. However, characteristic fragment ions may be obtained which can be monitored for the trace determination of sulfonylureas and their polar metabolites [3].

Recent developments in mild ionization conditions amenable to LC–MS include continuous-flow fast atom bombardment (CF-FAB) [4] and electrospray [5]. These techniques do not expose the analyte to excessive heat during either the separation or ionization process, and provide very mild ionization conditions that ensure molecular weight determination. It should be noted that FAB ionization usually produces some fragmentation along with molecular weight determination while the electrospray process produces essentially no fragmentation with the formation of abundant singly or multiply charged ions indicative of the molecular weight of the compound.

A recent report has described the packed capillary LC–MS determination of sulfonylureas using the CF-FAB technique [6]. Low nanogram levels of these compounds and their metabolites isolated from environmental samples could be identified. Analysis times were typically 30 min, and some use-

Correspondence to: Dr. J. Henion, Drug Testing and Toxicology, New York State College of Veterinary Medicine, Cornell University, 925 Warren Drive, Ithaca, NY 14850, USA.

* Visiting scientist from Rhone-Poulenc Recherches, Lyon, France. Present address: CECA SA, 22 Place des Vosges Cedex 54, 92062 Paris La Defense 5, France.

0021-9673/92/$05.00

ful fragment ions were observed that facilitated metabolite characterization studies of these compounds. These and related CF-FAB reports continue to demonstrate new advances in the utility of FAB-MS.

It is our view [7], however, that the alternative electrospray technique provides an easier, more analytically rugged approach to analytical problem solving via on-line separation using chromatography or electrophoresis [8–14]. When electrospray is coupled with on-line separation techniques such as high-performance and capillary electrophoresis (CE), its utility appears to be increased by assisting the "spray" aspect of the process by pneumatic assistance [15] or a coaxial sheath-flow of organic solvent such as 2-propanol or 2-methoxyethanol [16]. We prefer the former approach and have demonstrated the utility of the ion spray device coupled with a variety of modern separation techniques [7].

Following the lead of Reiser and co-workers' LC–CF-FAB-MS studies of sulfonylureas [2,3,6], we have investigated the analytical utility of open-tubular CE–MS via the liquid-junction–ion spray interface combination [11] for the determination of sulfonylurea compounds. Although CE–MS does not at present appear well suited for trace analysis studies, the speed of analysis, mild analysis and ionization conditions and the structural information available via CE–MS combined with tandem mass spectrometry (CE–MS–MS) suggest that this approach has come worthwhile analytical merits. In this paper we show that a mixture of eight important sulfonylurea compounds may be separated and identified within 5 min by on-line CE–MS with detection limits down to at least 600 fmol of injected components in the selected ion monitoring (SIM) mode of detection. Structural information is also available via tandem MS from on-line CE–MS–MS product ion scans of the $[M+H]^+$ precursor ions.

EXPERIMENTAL

Materials

The reference sulfonylurea compounds were kindly provided by R. W. Reiser of DuPont (Wilmington, DE, USA). All buffer and sample solutions were prepared fresh and filtered through nylon filter units of 0.2-μm pore size (Schleicher & Schuell, Keen, NH, USA). The buffer solutions were vacuum degassed by suction filtration and the samples were kept at 4°C when not in use. Optima-grade acetonitrile and methanol were obtained from Fisher Scientific (Fairlawn, NJ, USA). Water was purified in-house with a Barnstead Nanopure system; all other reagents were of electrophoresis grade and used without further purification.

Capillary electrophoresis instrumentation

The fused-silica capillary columns used in this work were made from polyimide-clad fused-silica capillaries (Polymicro Technologies, Phoenix, AZ, USA). They were 75 μm I.D. and ranged in length from 1 m to 35 cm. No external cooling or temperature control of the capillary column was utilized.

The commercial CE system used during the early stages of this work was a P/ACE 2000 (Beckman, Palo Alto, CA, USA). This system was modified for CE–MS operation as described previously [12]. This included on-line UV detection 20 cm from the inlet of the separation capillary with the standard P/ACE 2000 UV detector [12,13], and passage of the capillary through the wall of the capillary cartridge holder with extension to the liquid junction coupling and ion spray interface [11,14].

The other CE system used in this work was constructed in-house from readily available materials. The system design goals included (a) small CE instrument "foot print", (b) pressure injection capability and (c) robotic operation of the capillary inlet for sample loading and conditioning of the inside capillary surface, and utilization of 35-cm separation capillaries. The simple CE system constructed for this work is shown in Fig. 1. It consists of a plastic desiccator cabinet equipped with a rubber o-ring seal between the lid and the cabinet (Item H42053-0000; Bel-Art Products, Pequannock, NJ, USA), a security switch (J) that shuts off the high-voltage power supply if the lid is opened while the high voltage is on (A), a gas inlet fitting, for pressurizing the device with nitrogen (0.5 p.s.i) for pressure injection during free solution CE techniques, and a remote battery-operated (C) sample vial–running buffer vial lifting and switching mechanism for transferring the capillary inlet from running buffer to the sample vial. The latter was obtained from the "dump" and "steering" mechanisms of a toy dump truck (Model 60-2309, Radio Shack, Fort Worth, USA). After timed pressure sample injection, the

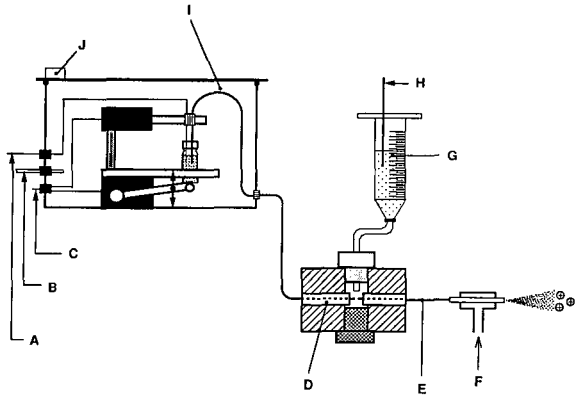

Fig. 1. Capillary electrophoresis–liquid junction–ion spray device. A = Capillary electrophoresis high-voltage supply lead running to anode buffer vial; B = pressurization inlet for pressurized injection and flushing of capillary column; C = battery-powered supply to activate lifting actuator mechanism for sample vial–running buffer vial placement of capillary inlet; D = exit end of capillary electrophoresis column placed in the liquid junction device; careful alignment of a 10-μm grap is required between the capillary exit and the corresponding 75 μm *i.d.* capillary transfer line leading to the ion spray interface; E = 6 cm × 75 μm I.D. transfer capillary connecting the liquid junction and ion spray devices; F = nitrogen inlet of ion spray interface; G = liquid junction reservoir; H = high-voltage lead for ion spray interface (2.5–4.0 kV); I = capillary electrophoresis column, typically 35–50 cm × 75 μm I.D.; J = safety switch that opens the capillary electrophoresis high-voltage supply when the pressurized box device is opened.

capillary inlet was moved to the running buffer by battery-powered remote control. A positive high-voltage potential (A) (30–38 kV or 300–1000 V/cm) was then applied across the capillary column to commence the CE separation. The capillary column exit could either be connected directly to a modified Waters Model 440 micro-UV detector (Waters Chromatography Division, Milford, MA, USA), or to the liquid junction coupling–ion spray devices (D–H) for mass spectrometric detection. The UV detector was not used in series with MS detection in order to minimize the effective size of the combined CE–MS system.

The positive polarity high voltage for CE was supplied by a Model RHR60P30 high-voltage reversible polarity 60-kV power supply (Spellman, Plainview, NY, USA). The capillary column (I) passes through an adaptor fitting installed in the wall of the plastic dessiccator cabinet and the capillary inlet immersed into the running buffer vial while the exit is connected to the liquid junction (D) coupling (see below). The CE system is placed on a Lab-Jack to facilitate adjustment of the liquid level of the inlet buffer vial to the same height as the level of the make-up buffer in the liquid junction reservoir. This simple, inexpensive device provided a desirable feature not incorporated in our commercial CE system. This pertains to its reduced size so it can be placed close to the ion sampling region of the mass spectrometer. This allows the use of short (35–50-cm) capillaries for CE–MS which can provide a five fold decrease in CE–MS analysis times compared with separations using 100-cm capillaries.

Mass spectrometry

The mass spectrometer used in this work was a Sciex TAGA 6000E tandem triple quadrupole system upgraded to an API III (Sciex I., Thornhill, Ontario, Canada). The capillary end from the CE system was coupled to the atmospheric pressure sampling region of the mass spectrometer via a liquid junction coupling and a pneumatically assisted electrospray (ion spray) interface [14]. This interface has been described previously [11,14]. The only modification in this work was that the inner capillary in the ion spray interface consisted 5 cm × 75 μm I.D. polyimide-clad fused silica instead of stainless steel [14]. During CE–MS operation the liquid junction along with the ion spray interface may be floated at +3 kV and the mass spectrometer operated in the positive-ion detection mode. When the high voltage is maintained at 30–38 kV, the 3 kV potential maintained on the ion spray interface produces a potential difference across the separation capillary of 27–35 kV. Using this configuration, organic cations in solution are introduced into the gas phase at atmospheric pressure by the ion evaporation mechanism prevailing in the electrospray process [17].

Gas-phase ions generated from the ion spray interface via the ion evaporation mechanism are sampled into the mass spectrometer by a potential difference of about 2.5 kV set between the ion spray interface and the ion sample orifice. The sampling orifice is a 100-μm diameter hole in the end of a conical skimmer extended towards the atmosphere. To minimize solvent cluster formation, this system utilizes a curtain of ultrapure nitrogen applied to the atmospheric side of the skinner. For full-scan

CE–MS work, the first quadrupole (Q1) was scanned repetitively from m/z 300 to 700 in 5 s with a scan step of 1 u. For CE–MS–MS work, ultrapure argon (AIRCO, BOC Group, Murray Hill, NJ, USA) was used as the collision gas and introduced into the collision cell (Q2) at a target gas thickness of $200 \cdot 10^{12}$ atoms/cm^2. The collision energy used for the MS–MS experiments was 50 V (laboratory frame). Both the first and third quadrupole analyzers were operated at unit mass resolution in this work. The mass spectrometer data system was a standard Macintosh IIcx-based data acquisition and software package provided by Sciex for the API III system.

Methods

Sequential rinsing and conditioning of the capillary between analyses was typically performed by pressurizing the corresponding inlet vial to 20 p.s.i. for 2 min with distilled water and then with the electrophoretic buffer. This procedure is beneficial not only for conditioning the capillary wall surface, but also for cooling it from the Joule heating produced by the applied 1000 V/cm and for refilling the capillary with fresh running buffer. The running buffer used for all the separations described in this work consisted of ammonium acetate–acetonitrile (75:25) adjusted to pH 5 with 17% acetic acid. Although methanol behaves similarly to acetonitrile as an organic modifier in these applications, the latter was chosen because it produces slightly improved peak shapes and separation efficiencies, as we have reported previously [12]. For full-scan and SIM CE–MS determinations, 7 and 1 pmol per component were injected in 15 and 5 nl of running buffer respectively. Injection was accomplished by pressurizing the sample vial at 0.5 in.Hg for 10–15 s followed by transfer of the capillary inlet into a vial containing the running buffer. The high-voltage potential applied across the separation capillary was typically 300 V/cm, but for the fastest separations 1000 V/cm was used. For those CE–MS analyses accomplished with the commercial CE system, the separation capillary was 100 cm × 75 μm I.D., whereas for those CE–MS analyses performed with the laboratory-made CE system the separation capillary was 35 cm × 75 μm I.D.

RESULTS AND DISCUSSION

Our initial observations focused on the relatively short analysis times observed resulting from CE–UV method development for the separation of a synthetic mixture of the eight sulfonylurea compounds available in this study (Fig. 2). Preliminary CE studies were initiated without sulfometuron methyl (compound **2**) because this compound was not initially available to us. As shown in Fig. 3A, the seven-component mixture containing *ca.* 7 pmol of each compound could be separated and detected by UV at 254 nm with the commercial P/ACE 2000 system, within about 9 min using a running buffer of 5 m*M* ammonium acetate–acetonitrile (75:25), pH adjusted to 5 with acetic acid, with 300 V/cm across a 100 cm × 75 μm I.D. capillary column. However, as shown in Fig. 3B, on-line detection by SIM mass spectrometry where the analytes migrated through an additional 80 cm of the capillary column and the liquid junction–ion spray coupling required *ca.* a 40-min total analysis time. When the

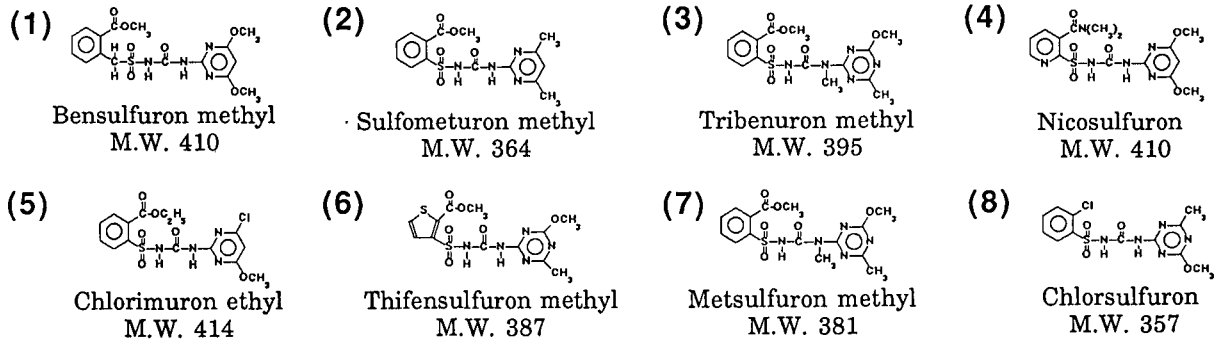

Fig. 2. Structures, names and molecular weights of sulfonylurea compounds studied.

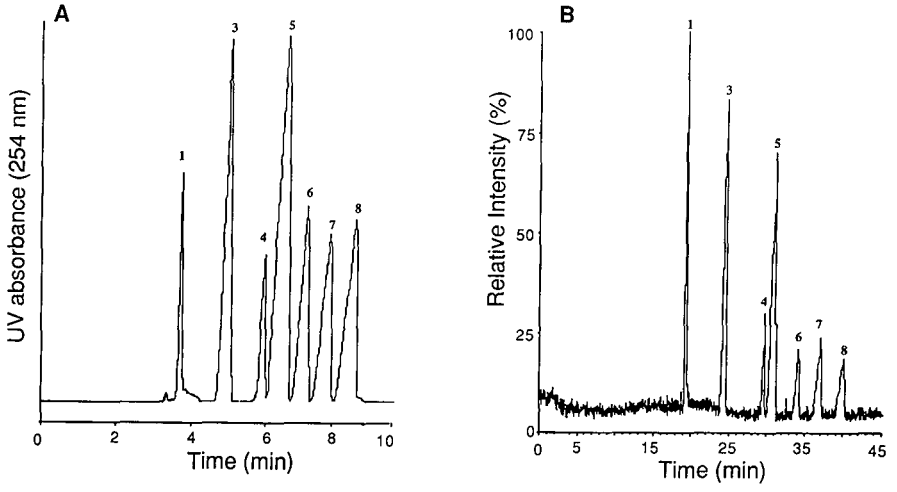

Fig. 3. Capillary electrophoresis analysis of a seven-component synthetic mixture containing sulfonylurea crop protection chemicals (compound **2**, sulfometuron methyl, was not present in this mixture). (A) CE–UV electropherogram containing *ca.* 7 pmol of each compound. The running buffer consisted of 5 m*M* ammonium acetate–acetonitrile (75:25), pH adjusted to 5 with acetic acid, with 300 V/cm across a 100 cm × 75 μm I.D. capillary column that produced 15 μA current. (B) SIM CE–MS total selected ion current electropherogram after the analytes migrated through an additional 80 cm of the capillary column and through the liquid junction–ion spray coupling.

data in Fig. 3A and B are compared, it is clear that a better separation is achieved, for example, between the last three components in the mixture under these conditions with MS detection than with UV detection. This is easily explained, however, by the fact that the analytes are detected in Fig. 3B after traversing a much longer (80 cm) portion of the capillary compared with Fig. 3A. Therefore, if one is interested in simply achieving baseline separation for these compounds, the full 100 cm of capillary column is not necessary.

One limitation of many commercial CE instruments is their large physical size, which restricts their placement very close to the ion sampling source region of a mass spectrometer. Therefore, in most instances a longer than necessary capillary column is used not only to achieve the required separation efficiency for a particular application, but rather simply to "reach" the mass spectrometer. The results shown in Fig. 3 are representative of this situation. We have constructed a small, simple CE device that allows the use of shorter capillary columns for close coupling to the ion sampling region of an atmospheric pressure ionization mass spectrometer [18]. The system is depicted in Fig. 1. It incorporates a pressurization feature that allows both "conditioning" and cooling of the capillary with running buffer and solvents between analyses and the loading of sample, or injection, by pressurization. These features are useful for the CE–MS system described here because it obviates dismantling the capillary exit from the carefully aligned liquid junction coupling as would be required if suction techniques were used to serve these purposes. Robotic placement of the capillary inlet into either a sample or a running buffer vial is provided by the electronic actuator system described in the Experimental section. The clear plastic desiccator box facilitates observation of the robotic mechanism relative to the vials inside and its small size (length 22.5 × width 16 × height 20 cm) allows its placement immediately in front of the mass spectrometer ion sampling region. On-line UV and MS detection is not utilized with this simple laboratory-made system because of the extra column length that would be required to accomplish this task. However, a modified Waters Model 440 UV detector may be used in place of the mass spectrometer when only UV detection is needed.

Fig. 4 shows the on-line full-scan CE–MS total ion current profile (TIC) obtained using the laboratory-made CE system described above. This

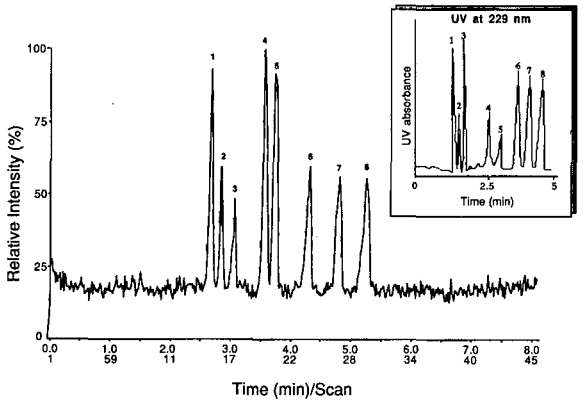

Fig. 4. On-line full-scan CE–MS total ion current profile (TIC) obtained using the laboratory-made CE system and a 35-cm capillary column described in Fig. 1. The running buffer consisted of 5 m*M* ammonium acetate–acetonitrile (75:25), pH adjusted to 5 with acetic acid, with 1000 V/cm across a 35 cm × 75 μm I.D. capillary column. This mixture contained the eight sulfonylurea compounds shown in Fig. 2 with *ca.* 7 pmol of each compound loaded into the capillary column and detected by the mass spectrometer operated in the positive-ion mode of detection while scanning repetitively from *m/z* 300 to 700. The inset is the UV electropherogram obtained with the same system when the mass spectrometer and the liquid junction–ion spray system were replaced with the micro-UV detector.

mixture contains the eight sulfonylurea compounds shown in Fig. 2 with *ca.* 7 pmol of each compound loaded into the capillary column and detected by the mass spectrometer operated in the positive-ion mode of detection while scanning repetitively from *m/z* 300 to 700. Scanning below *m/z* 300 was not done as no analyte ions were observed in this region. The running buffer consisted of 5 m*M* ammonium acetate–acetonitrile (75:25) adjusted to pH 5 with acetic acid, with 1000 V/cm across a 35 × 75 μm I.D. capillary column. Thus the shorter analysis time is accomplished both by shortening the length of the capillary column and increasing the voltage per unit length (300 *vs.* 1000 V/cm). The inset in Fig. 4 is the UV electropherogram obtained with this same system when the mass spectrometer and the liquid junction–ion spray system were replaced with the micro-UV detector. These data reveal the similarity of the sulfonylurea peak shapes and separation efficiency. The slightly longer analysis time observed in the CE–MS TIC compared to the CE–UV electropherogram is believed to be due to the *ca.* 6 cm greater distance that the separated components must travel through the liquid junction–ion spray system in contrast to on-column UV detection in the CE–UV experiment.

The poor electrophoretic peak shape for slower migrating sulfonylurea components (in particular peaks 6–8) observed throughout this work remains a problem. The last three peaks seen in both the CE–UV and CE–MS electropherograms in Figs. 3 and 4 show considerable "fronting". Several attempts to eliminate this behavior were largly unsuccessful. Although conditioning and treatment of the inside surface of the fused-silica capillary occasionally seemed to reduce the problem, it is possible that the injected levels used in this work (1–15 pmol) were sufficiently high to cause overloading of the capillary by localized electrical effects in the fused-silica capillary that produces the observed fronting. Another possible problem is the Joule heating caused by the 1000 V/cm potential (15 μA) used in this work in the absence of any capillary column cooling. These conditions caused considerable variation in migrating times from one run to the next, and would benefit from external cooling of the capillary. However, this feature is not easy to incorporate during CE–MS experiments because of the need to extend the column from the CE system to the mass spectrometer. In any case, these compounds appear to be particularly susceptible to this behavior and elimination of this problem may require either more efficient surface treatment of the fused silica or more sensitive MS detection, or both. As both the UV and MS detectors appeared to give the same behavior, it is unlikely this is a detector phenomenon.

In contrast to LC–FAB-MS results [6], the mass spectra obtained from the electrospray process used in this work display only molecular weight information with no fragmentation. Fig. 5 shows the full-scan CE–MS mass spectra for nicosulfuron (peak 4) and chlorsulfuron (peak 8) obtained from the corresponding CE–MS TIC observed in Fig. 4. From these data it is evident that the predominant ion observed for each compound is the $[M+H]^+$ ion with some evidence for an ammoniated molecule such as $[M+NH_4]^+$. Hence the ion spray CE–MS system described here appears to provide sufficiently mild separation and ionization conditions to produce no detectable breakdown of these labile compounds.

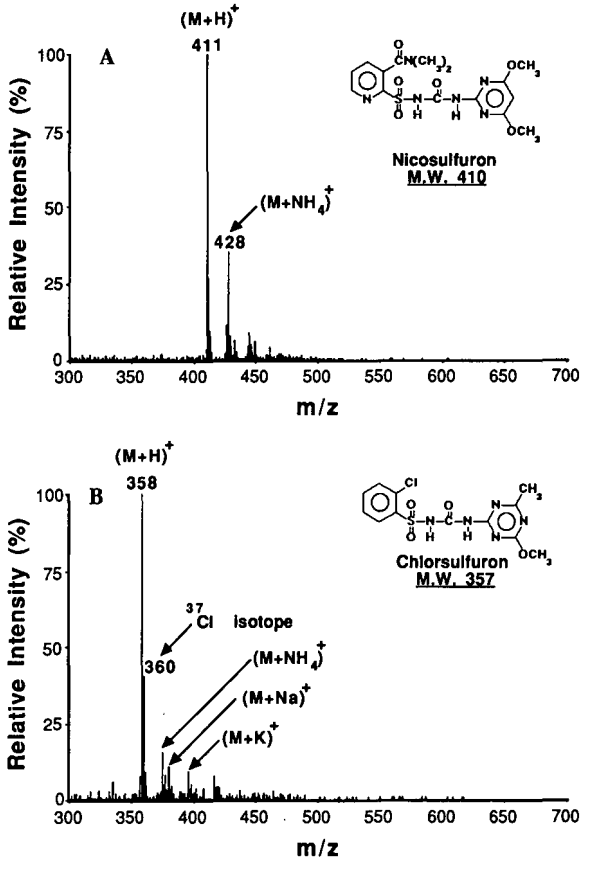

Fig. 5. Representative full-scan CE–MS mass spectra for peaks 4 and 8 in Fig. 4.

Although some variation in electrophoretic peak shape and migration time persisted through this work, we were able to obtain the shortest analysis times with reduced variation in migration time for the last three components (peaks 6–8) by utilizing the pressurization feature of the laboratory-made CE system to implement a form of "flow programming" during the CE–MS analysis. Fig. 6A shows the total selected ion current profile from the SIM CE–MS analysis of 1 pmol per sulfonylurea component under conditions optimized for the shortest analysis time. These include a running buffer consisting of 5 m*M* ammonium acetate–acetonitrile (75:25), pH adjusted to 5 with acetic acid, and 1000 V/cm across 35 × 75 μm I.D. capillary column. The $[M+H]^+$ ion for each sulfonylurea was monitored sequentially using a dwell time of 200 ms for each ion with mass spectral acquisition commencing with application of high voltage across the CE capillary column.

The total selected ion current electropherogram shown in Fig. 6A displays relatively good peak shape for peaks 1–5, but broad, well separated peaks for peaks 6–8. To compensate for this behavior, the results shown in Fig. 6B were obtained by repeating the same experiment, but applying a 0.5 p.s.i. pressurization of the desiccator box immediately following the elution of the fifth component at *ca.* 3.8 min. This procedure essentially increases the bulk, electroosmotic flow by *ca.* 7 nl/min, and "pushes" the remaining three components through

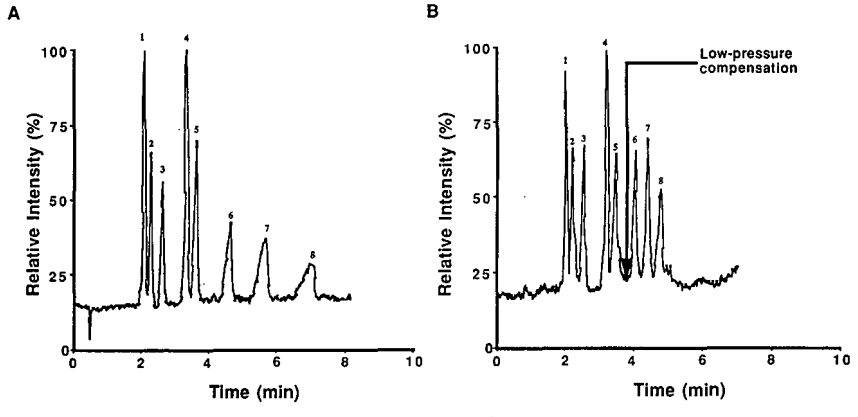

Fig. 6. SIM CE–MS total selected ion current electropherograms for a synthetic mixture containing the eight sulfonylurea compounds, (A) without pressure compensation and (B) with pressure compensation. The latter is accomplished by applying a 0.5 p.s.i. pressurization of the desiccator box immediately following the elution of the fifth component at *ca.* 3.8 min. See text for experimental details.

the capillary to the mass spectrometer. Although this procedure certainly decreases the separation efficiency for these components, it does reduce the analysis time by more than 2 min and improves the "apparent" peak shape for these components. This procedure may not be of general use, but could be useful in those instances where interfering components are not observed and rapid analyses are required.

Tandem mass spectrometry

It was noted above that CE–MS analysis of the target sulfonylurea compounds using the ion spray interface provides abundant molecular weight information for these compounds, but no fragment ions to facilitate their structural characterization. The mild ionization conditions common to electrospray provide an ideal scenerio for tandem mass spectrometry (MS–MS) [19]. Thus, on-line CE–MS–MS analysis of the sulfonylurea mixture can produce a full-scan collision-induced dissociation (CID) spectrum for each component in the mixture that contains fragment ions indicative of their molecular structures. This experiment may be conducted in a manner similar to those described above, but with some important exceptions. First, we chose to slow down the CE separation to provide wider electrophoretic peaks to allow scanning the full mass range (m/z 50–700) at a rate sufficient to provide good ion statistics for each scan. The same 35 cm × 75 μm I.D. capillary column and 5 mM ammonium acetate–acetonitrile (75:25) adjusted to pH 5 with 17% acetic acid, but an 800 V/cm potential on the capillary were used in this example. Pressure compensation following, in this case, peak 6, was utilized to minimize the otherwise slow migration of the last two sulfonylurea compounds (peaks 7 and 8).

The tandem triple quadrupole mass spectrometer was operated in the product ion scan mode [19] by focusing the protonated molecule precursor ion in the first quadrupole mass analyzer (Q1) and scanning the third quadrupole (Q3) through the mass range inclusive of the precursor ion and m/z 50. This is done for each component in sequence according to its migration time, while the collision quadrupole (Q2) is pressurized with argon at a target gas thickness of $200 \cdot 10^{12}$ atoms/cm^2.

Fig. 7 shows an overlay of the TICs for each of the eight target sulfonylurea compounds obtained from the on-line CE–MS–MS analysis of a synthetic mixture containing *ca.* 30 pmol per component dissolved in 15 nl of the running buffer that was loaded onto the capillary by pressure injection. These relatively high levels were required owing to the inherent ion transmission losses in the MS–MS mode. Although it has been reported that MS–MS techniques significantly reduce both the chemical and electrical noise [20], the absolute level of analyte ion current is also significantly reduced relative to a single MS scan such that the available ion current signal may be too weak to produce a good CID mass spectrum.

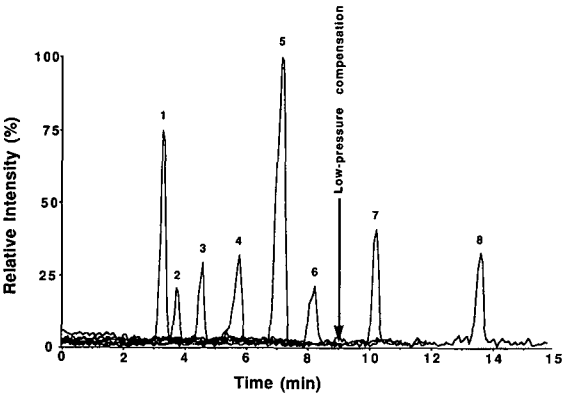

Fig. 7. An overlay of the full-scan TICs for each of the eight target sulfonylurea compounds obtained from the on-line CE–MS–MS analysis of the synthetic mixture containing *ca.* 30 pmol per component dissolved in 15 nl of the running buffer that was loaded on to the capillary by pressure injection. A 35 cm × 75 μm I.D. capillary column containing 5 mM ammonium acetate–acetonitrile (75:25) adjusted to pH 5 with 17% acetic acid, but 800 V/cm potential on the capillary, was used in this example to slow the separation and allow better ion statistics during this CE–MS–MS analysis.

Representative full-scan CID mass spectra are shown in Fig. 8 that display important structural features common to the target analytes. For example, Fig. 8A shows the base peak at m/z 149 indicative of cleavage of the benzylic–sulfonamide bond in benzsulfuron methyl (peak 1). The other major fragmentation process observed for benzsulfuron methyl appears to be dictated by the tendency for carbonyl carbon α-cleavage of the urea portion of the compound to give an ion of m/z 182. Related fragmentation processes appears in Fig. 8B and C to give their corresponding base peaks at m/z 155

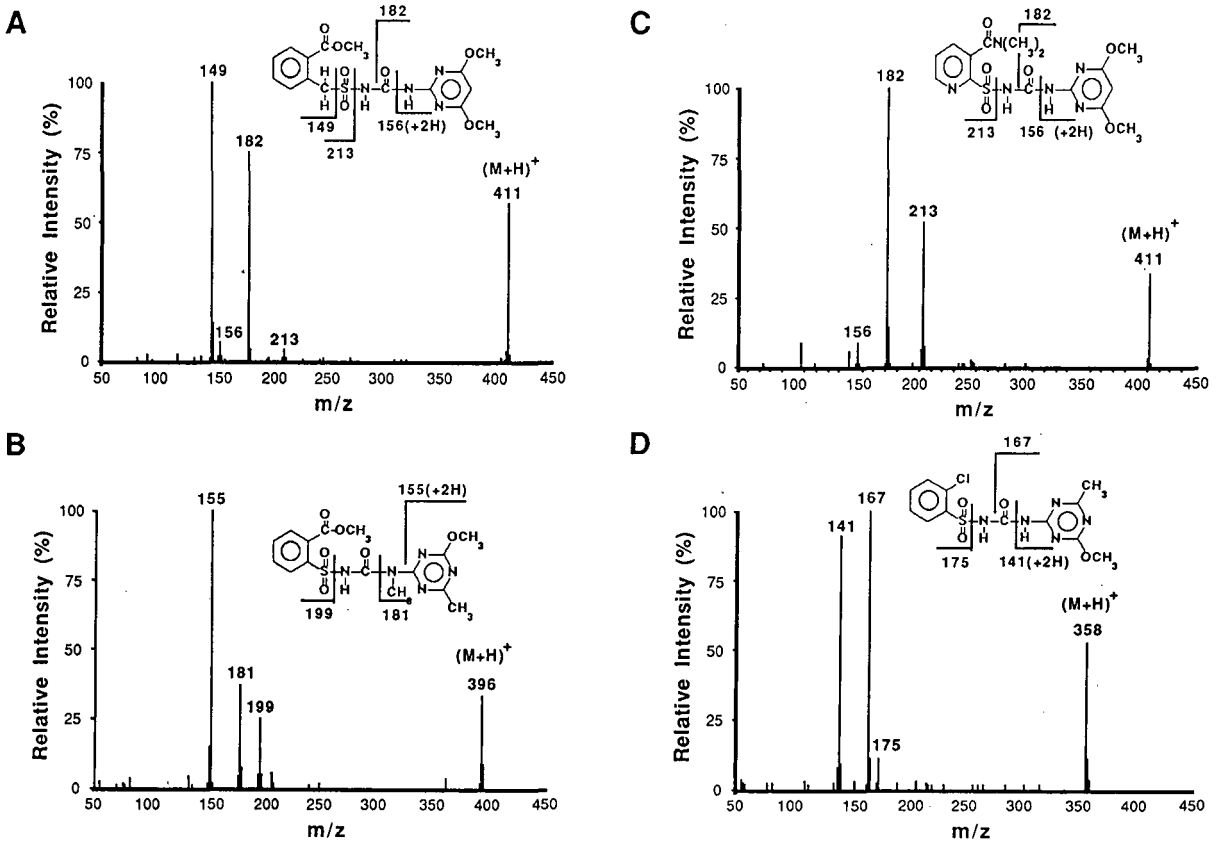

Fig. 8. CID mass spectra obtained from the CE–MS–MS results shown in Fig. 7. (A) Peak 1, bensulfuron methyl, M.W. 410; (B) peak 3, tribenuron methyl, M.W. 395; (C) Peak 4, nicosulfuron, M.W. 410; (D) chlorsulfuron, M.W. 357.

and 182, respectively. This prevalent cleavage α to the sulfonyl group is common to this class of compounds and generally is indicative of this functional group. Chlorsulfuron (Fig. 8D, peak 8) displays its base peak at *m/z* 167 as a result of the competing process due to cleavage α to the carbonyl carbon in the "bridge" [2,3] urea portion of this compound. The *m/z* 141 ion again appears to originate from α cleavage of the urea carbonyl carbon in this compound.

As a final example, the implementation of CE–MS–MS for the determination of sulfonylurea compounds in a *Fargo* soil extract was investigated. The TIC for the full-scan CE–MS–MS analysis of a spiked soil extract (*Fargo*) is shown in Fig. 9A. The soil extraction procedure has been described previously [6]. In this instance the extract of *Fargo* soil (5 g) was fortified with Bensulfuron methyl at a level of 411 ng/μl and 15 nl (15 pmol) were injected into the capillary column by pressure injection. This concentration of sulfonylurea in soil is much higher than the low nanograms per gram (ppb) level usually observed in soil samples. However, an elevated level was used in this case owing to the low injection volume required by CE and the limited detection limit of the CE–MS–MS technique described here. The TIC shown in Fig. 9A was obtained by tuning Q1 to transmit the $[M+H]^+$ ion for bensulfuron methyl at *m/z* 411 into the argon-pressurized Q2 region whereupon CID occurred to produce the full-scan CID spectrum shown in Fig. 9B. From these data it is evident that the migration time for bensulfuron methyl is 2.9 min under these conditions, and no other significant *m/z* 411 species are detected in the soil extract. Inspection of the full-scan CID spectrum obtained from the electropho-

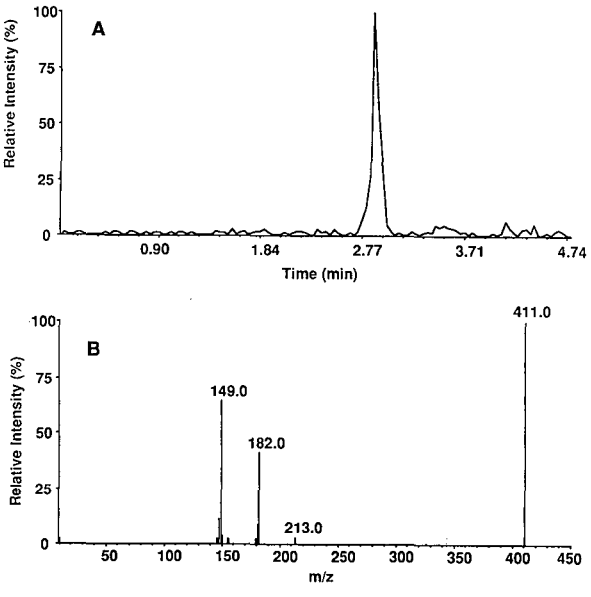

Fig. 9. CE–MS–MS analysis of a *Fargo* soil extract fortified with bensulfuron methyl (compound **1**, Fig. 2). The extract of soil contained this analyte at a level of 411 ng/μl, and 15 nl (15 pmol) of sample were injected into the capillary column by pressure injection. Experimental conditions as in Fig. 8. See text for details.

retic peak maximum shown in Fig. 9A gives the mass spectrum shown in Fig. 9B. These combined data provide unique selectivity and good analytical support for the identification of bensulfuron methyl in this fortified sample. In those instances where high levels of sulfonylurea compounds are present, this CE–MS–MS approach offers unique analytical utility. However, significant improvement in MS detection limits will be required to use this combination of techniques routinely for the determination of the low ppb levels of these compounds in environmental samples. We plan to investigate the feasibility of coupling an ion spray–ion trap system with on-line CE in an effort to achieve improved capability in this regard [2].

CONCLUSIONS

The CE–MS and CE–MS–MS results described here suggest that relatively rapid analysis times may be obtained for the separation and identification of sulfonylurea crop protection chemicals using shortened capillary columns and high-voltage potentials across the separation capillary. It is not straightforward to implement the use of short capillaries (less than 50 cm) for CE–MS with many commercial CE instruments because of the relatively large size and configuration of these instruments. The simple, laboratory-made system described here does not have the versatility of commercial units, but does provide the basic requirements for the work described. It should be noted that the use of high-voltage potentials (800–1000 V/cm) does create considerable Joule heating, which can generate excess heat in the separation capillary. The use of external cooling of the capillary (not implemented in this work) would facilitate this approach, but is difficult to implement in practice while coupled to the mass spectrometer. When the liquid junction coupling and the ion spray interface described in this work are properly adjusted, the system is relatively routine to use.

It should also be noted that CE–MS detection limits are not yet entirely satisfactory. The very low levels of analytes that are typically loaded into a CE column often require SIM CE–MS techniques and sometimes even then there is insufficient sensitivity. Efforts are being made to improve this situation using a benchtop ion trap mass spectrometer.

ACKNOWLEDGEMENTS

We thank Waters Chromatography Division for the modified micro-UV cell for the Model 440 UV detector and Beckman Instruments for the loan of a P/ACE 2000 capillary electrophoresis instrument. We also thank Drs. R. Reiser and L. Shalaby of DuPont for helpful discussions and providing samples. F. G. thanks Rhone-Poulenc Recherches for financial support during his stay at Cornell.

REFERENCES

1 E. M. Beyer, M. J. Duffy, J. V. Hay and D. D. Schleuter, *Herbicides: Chemistry, Degradation and Mode of Action*, Vol. 3, Marcel Dekker, New York, 1987, Ch. 3.
2 L. M. Shalaby and R. W. Reiser, in C. N. McEwen and B. S. Larsen (Editors), *Mass Spectrometry of Biological Materials*, Marcel Dekker, New York, 1990, Ch. 11.
3 L. M. Shalaby, in J. D. Rosen (Editor), *Applications of New Mass Spectrometry Techniques in Pesticide Chemistry, Vol. 91, Chemical Analysis*, Wiley-Interscience, New York, 1987, p. 161.
4 R. M. Caprioli, *Anal. Chem.*, 62 (1990) 477A.

5 J. B. Fenn, M. Mann, Ch. K. Meng, S. F. Wong and C. M. Whitehouse, *Science (Washington, D.C.)*, 246 (1989) 64.
6 R. W. Reiser, A. C. Barefoot, R. F. Dietrich, A. J. Fogiel, W. R. Johnson and M. T. Scott, *J. Chromatogr.*, 554 (1991), 91.
7 T. Wachs, J. D. Conboy, F. Garcia and J. D. Henion, *J. Chromatogr. Sci.*, 29 (1991) 357.
8 E. D. Lee, W. Mück, T. R. Covey and J. D. Henion, *J. Chromatogr.*, 458 (1988) 313.
9 E. D. Lee, W. Mück, T. R. Covey and J. D. Henion, *Biomed. Environ. Mass Spectrom.*, 18 (1989) 253.
10 W. M. Mück and J. D. Henion, *J. Chromatogr.*, 495 (1989) 41.
11 E. D. Lee, W. Mück, J. D. Henion and T. R. Covey, *Biomed. Environ. Mass Spectrom.*, 18 (1989) 844.
12 I. M. Johansson, E. C. Huang, J. Zweigenbaum and J. D. Henion, *J. Chromatogr.*, 554 (1991) 311.
13 I. M. Johansson, R. Pavelka and J. D. Henion, *J. Chromatogr.*, 559 (1991) 515.
14 A. P. Bruins, T. R. Covey and J. D. Henion, *Anal. Chem.*, 59 (1987) 2642.
15 A. P. Bruins, L. O. G. Weidolf and J. D. Henion, *Anal. Chem.*, 59 (1987) 2647.
16 R. D. Smith, C. J. Barinaga and H. R. Udseth, *Anal. Chem.*, 60 (1988) 1948.
17 B. A. Thomson and J. V. Iribarne, *J. Chem. Phys.* 71 (1979) 4451.
18 F. Garcia and J. D. Henion, *Proceedings of the 39th ASMS Conference on Mass Spectrometry and Allied Topics, Nashville, TN, May 19–24, 1991*, p. 312.
19 K. L. Bush, G. L. Glish and S. A. McLuckey, *Mass Spectrometry/Mass Spectrometry: Techniques and Applications of Tandem Mass Spectrometry*, VCH, New York, 1988.
20 R. A. Yost and D. D. Fetterolf, *Mass Spectrom. Rev.*, 2 (1983), 1.
21 S. A. McLuckey, G. J. van Berkel, G. L. Glish, E. C. Huang and J. D. Henion, *Anal. Chem.*, 63 (1991) 375.

Journal of Chromatography, 606 (1992) 248–250
Elsevier Science Publishers B.V., Amsterdam

CHROM. 24 353

Short Communication

Influence of pressure on solute retention in liquid chromatography

Georges Guiochon and Michael J. Sepaniak

Department of Chemistry, University of Tennessee, Knoxville, TN, 37996-1600 and Division of Analytical Chemistry, Oak Ridge National Laboratory, Oak Ridge, TN (USA)

(First received February 26th, 1992; revised manuscript received May 14th, 1992)

ABSTRACT

Confirming recent, independent experimental results, simple considerations of thermodynamics show that the logarithm of the retention factors of solutes vary linearly with increasing pressure, in the pressure range most commonly used (0–200 atm). The coefficient of this dependence increases linearly with the difference between the partial molar volumes of the solute in the stationary and the mobile phases. For homologues, this coefficient increases linearly with the number of carbon atoms and with the difference, ΔV_{CH_2}, between the partial molar volumes of a CH_2 group in the two phases. The pressure dependence of the retention factor may be significant because for a C_{18}–methanol system $\Delta V_{CH_2}/V_{CH_2}$ is of the order of 6%.

In the early days of liquid chromatography, Martire and Locke [1] suggested and Bidlingmeyer and Rogers [2] reported that important retention and even selectivity changes can be observed at very high pressures. Conventional wisdom has it so far, however, that pressure-induced changes in retention data are negligible under conventional experimental conditions (*i.e.*, at pressures below 5000 p.s.i.). In a recent paper, McGuffin and Evans [3] reported experimental results illustrating the significant pressure dependence of the retention factors of the components of a homologous series in reversed-phase liquid chromatography. Although their interpretation of their results in terms of the unified theory of retention developed by Martire and Boehm [4] is correct, it should be noted that simple, general results of solution thermodynamics permit the derivation of the same conclusions using the limited set of data available.

We know from thermodynamics [5] that the change, dG, in the Gibbs free energy of 1 mol of a component is related to the changes dp and dT in the pressure and temperature, respectively, of the system by

$$dG = Vdp - SdT \quad (1)$$

where V is the molar volume and S the molar entropy. Applied to a component in equilibrium between two different phases, eqn. 1 gives

$$d(\Delta G) = \Delta V dp - \Delta S dT \quad (2)$$

where ΔG, ΔV and ΔS are the differences in the molar Gibbs free energy, the molar volume and the molar entropy, respectively, which are associated with the passage of the component from one phase to the other. We derive from eqn. 2 that

Correspondence to: Professor G. Guiochon, Department of Chemistry, University of Tennessee, Knoxville, TN 37996-1600, USA.

0021-9673/92/$05.00

$$\frac{\partial}{\partial p} \cdot \Delta G = \Delta V \tag{3}$$

The retention factor, k', is related to the change in the molar Gibbs free energy of phase change by

$$\Delta G = RT \ln K = RT \ln \phi k' \tag{4}$$

where R is the universal ideal gas constant, K is the thermodynamic constant of the phase equilibrium studied (based on mole fraction and activity coefficient [6]), and ϕ is the phase ratio. Combination of eqns. 3 and 4 gives

$$\frac{\partial}{\partial p} \ln k'_n = \frac{\Delta V_n}{RT} - \frac{1}{\phi} \cdot \frac{\partial \phi}{\partial p} \tag{5}$$

where k'_n is the retention factor of the homologue with n carbon atoms in its linear alkyl chain and ΔV_n is the change in partial molar volume associated with the passage of this homologue from one phase to the other.

It is reasonable to assume that, for the components of a homologous series, the molar volume, V_n, increases linearly with increasing carbon number. The unit increase in molar volume is the contribution, V_{CH_2}, to the molar volume of the addition of one CH_2 group to the molecule, hence

$$V_n = V_0 + nV_{CH_2} \tag{6a}$$

where V_0 is the contribution of the functional group to the partial volume of the homologue, and

$$\Delta V_n = \Delta V_0 + n\Delta V_{CH_2} \tag{6b}$$

where ΔV_{CH_2} represents the difference $\Delta V_{n+1} - \Delta V_n$. Then, eqns. 5 and 6b can be combined to predict the linear dependence of the logarithm of the retention factor on the pressure:

$$\frac{\partial}{\partial p} \ln k'_n = -\frac{1}{\phi} \frac{\partial \phi}{\partial p} + \frac{\Delta V_0}{RT} + \frac{\Delta V_{CH_2}}{RT} \cdot n \tag{7}$$

provided that the term $\partial\phi/\partial p$ is either negligible or constant and that ΔV_0 and ΔV_{CH_2} are independent of the pressure. The experimental results of McGuffin and Evans [3] exhibit a quadratic dependence. However, a linear dependence would be consistent with the experimental results if the data point at the highest pressure were omitted, *i.e.*, up to a pressure of *ca.* 3000 p.s.i. (Fig. 4 in ref. 3). The observed deviation from the linear dependence is easily explained by the pressure dependences of the differences between the partial molar volumes of each of the homologues in the two phases, *i.e.*, of ΔV_0 and ΔV_{CH_2}. These parameters are pressure dependent, a fact which is taken into account in the more sophisticated model derived by Martire and Boehm [4]. We also note that eqn. 6 is linear in n. The rate of variation of $\ln k'_n$ with increasing pressure increases linearly with increasing carbon number, n, again in agreement with the experimental results of McGuffin and Evans [3].

Finally, if k'_n and k'_{n+1} are the retention factors of two successive homologues, and $\alpha_{n+1/n} = k'_{n+1}/k'_n$, we have

$$\frac{\partial}{\partial p} \ln \alpha_{n+1/n} = \frac{\Delta V_{CH_2}}{RT} \tag{8}$$

As the molar volumes of homologues increase linearly with increasing carbon number of the chain, the difference between the molar volumes of two successive homologues is constant and equal to the contribution of one CH_2 group. Hence it is expected that the increase in the separation factor for a given increase in the column average pressure will be constant. This is confirmed by the experimental results, and the value reported by McGuffin and Evans [3] for two successive homologues with an even carbon number is $\Delta\alpha/\alpha = 0.026\ (\pm 0.0083)$ for $\delta p = 3500$ p.s.i. or $\partial \ln \alpha/\partial p \approx 1.04 \cdot 10^{-4}$. Obviously, as $\ln k'$ actually increases as a quadratic function of the pressure, so does $\ln \alpha$. The precision of the experimental data [3] does not permit the investigation of this dependence, however.

If we introduce the numerical result of McGuffin and Evans [3] into eqn. 8, and note that what they call α is what we have defined above as $\alpha_{n+2/n} = \alpha^2_{n+1/n}$, we obtain

$$\Delta(\Delta V_{CH_2}) = 0.0001\ RT = 2.5\ (\pm 0.8)\ \text{ml} \tag{9}$$

(with $RT = 22\,400T/273$), assuming the measurements were made at 20°C. Hence the experiments of McGuffin and Evans permit the direct determination of the difference between the partial molar volumes of the CH_2 group in solution in methanol and adsorbed on the surface of the C_{18}-bonded silica. This difference is significant and of the order of 6%, as the volume occupied by a CH_2 group in a pure alkane is *ca.* 14/0.7 = 20 ml (assuming a density of 0.7 for the liquid alkane). It is noteworthy that the partial molar volume of a CH_2 group is larger when

adsorbed in the chemically bonded C_{18} phase than in solution in methanol. This probably reflects a lower density of the bonded phase and some hindrance of the immobilized alkyl chains, more than any peculiarity of the methanol solution.

From the results obtained, it could further be expected that the pressure dependence of ln k' for the components of other homologous series will be very similar. As the volume occupied by a CH_2 group is relatively independent of the chemical structure of the functional end-group, we can predict that the slope of the plot of $\partial \ln k'/\partial p$ *versus* n will be very close for all homologous series studied in a given phase system, and that the value of $\alpha_{n+1/n}$ will be nearly the same for all successive couples of all these series. These values should depend only on the nature of the phase system selected, through the values of ϕ and ΔV_0, and their pressure dependences.

As expected, these relationships are similar to and consistent with those which have been abundantly demonstrated previously, and which are commonly found in gas or liquid chromatography [7,8] between the number of carbon atoms and the retention indices or ln k' in homologous series. Likewise, the additivity of group contributions to the Gibbs free energy of phase equilibria should not cause any surprises: those relationships are the application to a new experimental problem of the classical Martin principle of linear contributions to phase equilibrium constants [1,7–9].

The changes in the partial molar volumes of the solutes may result from the compressibility of either phases, from variations in the energy of molecular interactions or from the energy density of interactions. As always with a purely thermodynamic approach, no information is available regarding the mechanism(s) or the interaction(s) involved at the microscopic or molecular level. Studies of the possible mechanisms can be made only through the use of microscopic models, such as that provided by the unified theory of retention [4]. These studies will require more abundant, and probably more precise, experimental data.

In conclusion, the paper by McGuffin and Evans [3] provides both a warning to analysts that the influence of the pressure (and hence of the flow-rate) on the retention factors, and therefore on the resolution of mixtures, is far from negligible, and reminds us of a useful tool for the study of the thermodynamics of solutions and of phase equilibria [1,2].

REFERENCES

1 D. E. Martire and D. C. Locke, *Anal. Chem.*, 39 (1967) 921.
2 B. A. Bidlingmeyer and L. B. Rogers, *Sep. Sci.*, 7 (1972) 131.
3 V. L. McGuffin and C. E. Evans, *J. Microcol. Sep.*, 3 (1991) 513.
4 D. E. Martire and R. E. Boehm, *J. Phys. Chem.*, 91 (1987) 2433.
5 J. C. Giddings, *Unified Separation Science*, Wiley, New York, 1991, Ch. 2.
6 W. J. Moore, *Physical Chemistry*, Prentice Hall, Englewood Cliffs, NJ, 4th ed., 1972, p. 317.
7 B. L. Karger, L. R. Snyder and Cs. Horváth, *An Introduction to Separation Sciences*, Wiley, New York, 1973, pp. 55–57.
8 G. Guiochon and C. Guillemin, *Quantitative Gas Chromatography*, Elsevier, Amsterdam, 1988, pp. 508–515.
9 A. J. P. Martin, *Biochem. Soc. Symp.*, 3 (1949) 4.

Journal of Chromatography, 606 (1992) 251–254
Elsevier Science Publishers B.V., Amsterdam

CHROM. 24 341

Short Communication

High-performance liquid chromatographic study of acenaphthaleno[1,2-*e*]pyrene, phenanthro[9,10-*e*]pyrene and their dihydro derivatives

Yee-Hing Lai, Siau-Gek Ang and Hwee-Chze Li

Department of Chemistry, National University of Singapore, Kent Ridge, Singapore 0511 (Singapore)

(First received February 5th, 1992; revised manuscript received May 4th, 1992)

ABSTRACT

The high-performance liquid chromatographic study of acenaphthaleno[1,2-*e*]pyrene, phenanthro[9,10-*e*]pyrene and their dihydro derivatives is reported. The main factor which determines the retention order is the degree of staggering of the two *ortho*-fused moieties. The degree of staggering in the fully unsaturated systems is dependent on the bay-region steric interactions and that in the dihydro derivatives is determined by the geometric demand of the saturated bridge.

INTRODUCTION

The polycyclic aromatic compounds (PACs) are now routinely analysed by chromatographic methods [1,2]. High-performance liquid chromatography (HPLC), for example, is most useful for the analysis of the higher benzenoids with low volatility. Results reported previously indicate that effective HPLC separations of PACs depend on the number of rings and shape as well as the degree of planarity [3–5] of the PACs. The deviation from planarity studied so far is mainly the result of intramolecular steric strain arising from interaction between aromatic protons in various bay regions. We have recently prepared [6–8] acenaphthyleno[1,2-*e*]pyrene (**1**), phenanthro[9,10-*e*]pyrene (**2**) and their respective dihydro derivatives (**3** and **4**). The spectral data of **3** and **4** indicated a large deviation from planarity of the two fused moieties in each molecule. There are no detailed reports on comparative chromatographic studies of PACs and their corresponding dihydro derivatives and thus it would be interesting to investigate the chromatographic behaviour of **1**–**4** collectively. The PACs are environmental pollutants that perhaps represent the largest class of suspected chemical carcinogens. However, the chemical analysis of large PACs has sometimes been limited owing to lack of standard reference compounds. Our study was aimed at providing some analytical data for the PACs (**1**–**4**) concerned.

Correspondence to: Dr. Y.-H. Lai, Department of Chemistry, National University of Singapore, Kent Ridge, Singapore 0511, Singapore.

EXPERIMENTAL

Syntheses of the investigated PACs, **1** [6], **2** [7], **3** [6] and **4** [8], have been achieved in our laboratory.

0021-9673/92/$05.00

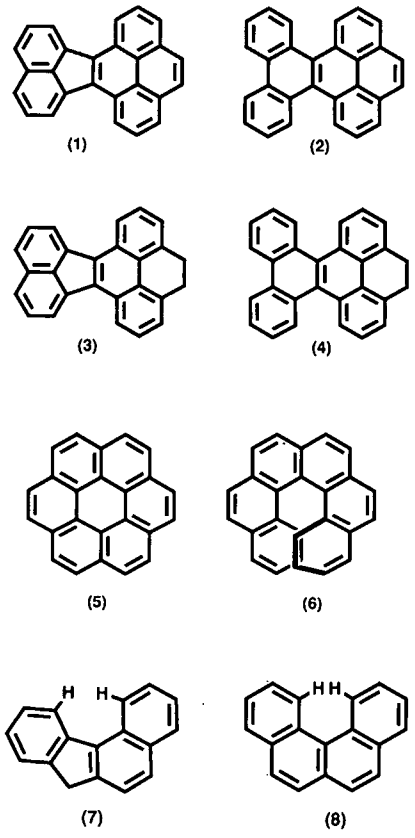

Chromatographic studies were performed on a Shimadzu LC-6A binary gradient liquid chromatograph equipped with a Shimadzu SPD-6AV UV–Vis spectrophotometric (254 nm) detector and a Shimadzu SCL-6A system controller. A Partisil 5 ODS-3 reversed-phase C_{18} column (30 cm × 3.9 mm I.D.) was used for chromatographic separations. HPLC-grade acetonitrile and dichloromethane were purchased from Fisher Scientific and J. T. Baker, respectively. Water was purified with a Milli-Q system (Millipore, Bedford, MA, USA).

The chromatographic condition employed was a linear gradient or 40–100% acetonitrile in water at 0.5%/min and 1 ml/min with a maximum pressure of 500 kgf/cm^2.

RESULTS AND DISCUSSION

Satisfactory resolution (Fig. 1) of both pairs of compounds, **1** and **3** or **2** and **4**, was observed under the chromatographic conditions employed in our study. In the chromatographic study [9] of the planar coronene **5** and the non-planar phenanthro[3,4-*c*]phenanthrene **6** a slot model of retention was used to account for the retention order. In each pair of **1** and **3** or **2** and **4**, the dihydro derivative was always eluted first. Observation from appropriate molecular models suggests that the geometric demand of the saturated bridge in **3** and **4** leads to more severe

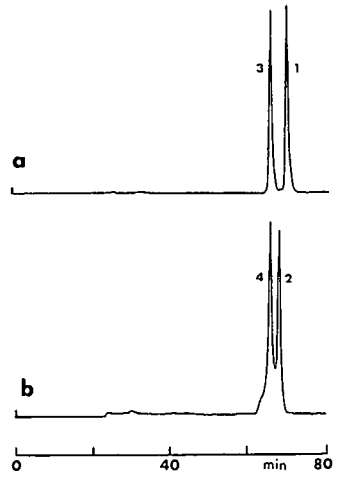

Fig. 1. High-performance liquid chromatograms of (a) **1** and **3**; (b) **2** and **4**. The approximate concentration of each sample was 0.5 mg/ml in dichloromethane.

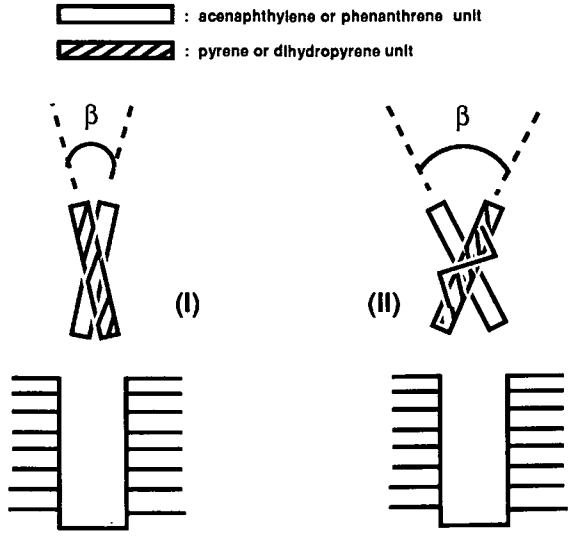

Fig. 2. Representation of the slot model of retention showing the differences in ease of fitting into the gaps in the stationary phase.

(Fig. 2; larger angle β) puckering of the dihydropyrene ring and the staggering of the two fused moieties as represented in Fig. 2 (II), compared with that of the corresponding parent PACs as shown in Fig. 2 (I). The less planar **3** and **4** thus could not fit readily into the "gaps" of the stationary phase, resulting in a weaker interaction with the bonded phase, and they eluted earlier than **1** and **2**, respectively.

In the chromatographic study (Fig. 3) of a mixture of acenaphthylene, phenanthrene, pyrene and compounds **1**–**4**, the higher benzenoids, **1**–**4**, eluted much more slowly, as expected. However, the separation of **1** and **2** could be affected by several factors. Based on the number of π electrons or double-bond equivalents [10–12], acenaphthylenopyrene **1** (with 13 pairs of π electrons) is expected to elute before phenanthropyrene **2** (with 14 pairs of π electrons). Differences in retention owing to the shape of the molecules [9,13,14] have been described in terms of the length-to-breadth ratio (L/B). Approximate measurements from molecular modelling (Fig. 4) gave **1** a slightly larger L/B ratio than **2**, again suggesting that **1** would elute before **2**. The result from our work (Fig. 3) however clearly indicates that **1** eluted after **2**, in contrast to the prediction made from the above-mentioned factors. It is believed that the governing factor is in fact the

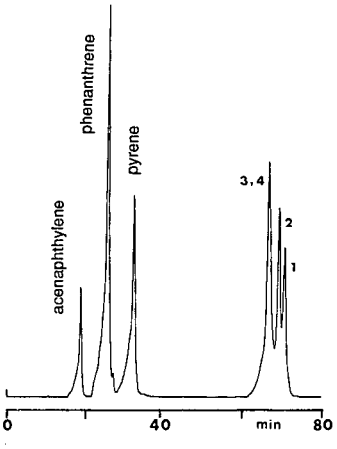

Fig. 3. High-performance liquid chromatogram of a mixture of **1**–**4** and three reference PACs. Approximate concentrations in dichloromethane: acenaphthylene, 2.0 mg/ml; phenanthrene, 0.75 mg/ml; pyrene, 1.5 mg/ml; **1**–**4**, 0.25 mg/ml. Retention times observed in order are 19.1, 26.2, 33.0, 68.0, 68.0, 70.7 and 72.2 min, respectively.

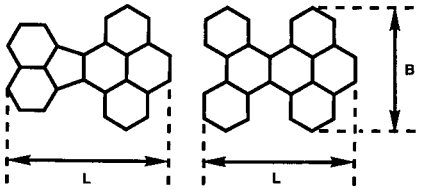

Fig. 4. The longest axis, L, and its longest perpendicular axis, B, for the consideration of the L/B ratio.

degree of staggering [see Fig. 2 (I)] of the two fused moieties in **1** and **2**. The steric interactions experienced in **1** and **2** are expected to be similar to those of the corresponding four-sided bay regions in benzo[*c*]fluorene **7** and benzo[*c*]phenanthrene **8**, with the latter known to deviate more significantly from planarity. A similar argument would suggest a larger angle β in I (Fig. 3) for **2** than for **1**. Based on the permeation effect, **1** would then penetrate more readily into the "slots", interact more strongly with the stationary phase and thus elute after **2**.

The dihydro compounds, **3** and **4**, unexpectedly were not resolved in our study (Fig. 3). With the introduction of the saturated bridges, steric interactions in bay regions in **3** and **4** are no longer significant because of molecular puckering. However, the degree of staggering of the two fused moieties is governed mainly by the geometric demand of the bridge. Thus a similar angle β in Fig. 2 (II) is expected of both **3** and **4** resulting in similar retention and no separation of the two compounds as described in our chromatographic study.

CONCLUSIONS

The PACs investigated in this work have a unique structural feature in having two smaller benzenoid units *ortho* fused. Retention of these PACs seems to depend largely on the degree of staggering of these two fused moieties. In fact, this is the main factor involved, making others such as the double-bond equivalent and the L/B ratio less important. This staggering effect determined by the geometric demand of the saturated bridge is more significant in the dihydro derivatives but it results in less satisfactory separation of the dihydro-PACs with similar dihydro bridges.

ACKNOWLEDGEMENT

The authors thank the National University of Singapore for financial support (RP860606 and RP880603).

REFERENCES

1 M. L. Lee, M. V. Novotny and K. D. Bartle, *Analytical Chemistry of Polycyclic Aromatic Compounds*, Academic Press, New York, 1981.
2 T. Vo-Dinh, *Chemical Analysis of Polycyclic Aromatic Compounds*, Wiley, New York, 1989.
3 J. C. Fetzer and W. R. Biggs, *J. Chromatogr.*, 295 (1984) 161.
4 J. C. Fetzer and W. R. Biggs, *J. Chromatogr.*, 322 (1985) 275.
5 J. C. Fetzer and W. R. Biggs, *J. Chromatogr.*, 386 (1987) 87.
6 P. Chen, *Ph.D. Dissertation*, National University of Singapore, Singapore, 1992.
7 Y.-H. Lai and S.-M. Lee, *J. Org. Chem.*, 53 (1988) 4472.
8 Y.-H. Lai, S.-G. Ang, H.-C. Li and S.-Y. Wong, *J. Chem. Soc. Perkin Trans. 2*, (1992) in press.
9 S. A. Wise,and L. C. Sander, *J. High Resolut. Chromatogr. Chromatogr. Commun.*, 8 (1985) 248.
10 P. L. Grizzle and J. S. Thomson, *Anal. Chem.*, 54 (1982) 1071.
11 D. Karlesky, D. C. Shelley and I. M. Warner, *J. Liq. Chromatogr.*, 6 (1983), 471.
12 K. Jinno and K. Kawasaki, *Chromatographia*, 18 (1984) 44.
13 S. A. Wise, W. J. Bonnett, F. R. Guenther and W. E. May, *J. Chromatogr. Sci.*, 19 (1980) 457.
14 L. C. Sander and S. A. Wise, *Adv. Chromatogr.*, 25 (1986) 139.

Journal of Chromatography, 606 (1992) 255–259
Elsevier Science Publishers B.V., Amsterdam

CHROM. 24 335

Short Communication

Separation of aglucones, glucosides and prenylated isoflavones by high-performance liquid chromatography

Hubert Gagnon, Satoshi Tahara*, Ernst Bleichert and Ragai K. Ibrahim

Plant Biochemistry Laboratory, Department of Biology, Concordia University, 1455 De Maisonneuve Boulevard West, Montréal, Québec H3G 1M8 (Canada)

(First received January 23rd, 1992; revised manuscript received May 5th, 1992)

ABSTRACT

A high-performance liquid chromatography (HPLC) method was developed for the separation of lupin isoflavones, which consist of genistein and 2'-hydroxygenistein, their 7-O-glucosides and their respective 6-, 8-, 3'-mono- and 6,3'-diprenylated derivatives, as well as two coumaronochromones, lupinalbin A and B. HPLC was carried out with a Merck reversed-phase C_{18} LiChrospher 100 column using 45% solvent A (0.5% methanolic acetic acid) in 55% solvent B (0.5% aqueous acetic acid) for 2 min, followed by a gradient increase to 100% solvent A in 78 min then maintaining isocratic conditions for a further 10 min. The order of elution of the isoflavonoid derivatives was inversely proportional to their degree of polarity, with the 2'-hydroxygenistein glucoside eluting first and the 6,3'-diprenyl genistein eluting last.

INTRODUCTION

Simple isoflavones (Fig. 1; **1**, **1a**) are key intermediates in the biosynthesis of the isoflavonoid phytoalexins [1]. The latter are known to be synthesized *de novo* by members of the Leguminosae family in response to attack by microorganisms [2], or elicitation by biotic or abiotic elicitors [3]. In addition, several isoflavonoids have been reported to have antifungal [4], oestrogenic [5] and spasmolytic [6] activity and to be inducers of common *nod* genes in *Bradyrhizobium japonicum* [7] and inhibitors of the peroxidase-catalysed oxidation of lignin precursors [8].

Whereas most legumes accumulate simple isoflavones and their glucosides [9], white lupin (*Lupinus albus*) has a remarkable ability for the constitutive expression of a variety of prenylated isoflavones [10–12] as well as small amounts of several pyrano, dihydroxypyrano and dihydrofurano derivatives [13]. These compounds seem to replace the phytoalexins which commonly occur as antimicrobial defence compounds in many other legumes [2,3].

Previously used methods for the separation and determination of isoflavonoids are thin-layer and column liquid chromatography [14], or gas chromatography of the trimethylsilyl derivatives [15,16]. However, the poor resolution observed with the former procedures, and the need for derivatization in the latter, make these methods cumbersome. Fur-

Correspondence to: Professor Ragai K. Ibrahim, Plant Biochemistry Laboratory, Department of Biology, Concordia University, 1455 De Maisonneuve Boulevard West, Montréal, Québec H3G 1M8, Canada.

* Permanent address: Department of Agricultural Chemistry, Faculty of Agriculture, Hokkaido University, Sapporo 060, Japan.

0021-9673/92/$05.00

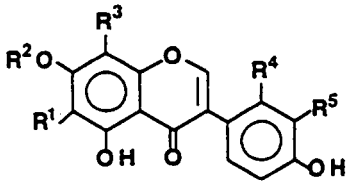

Isoflavonoids

1 R^1= R^2= R^3= R^4= R^5= H, genistein

1a R^1= R^2= R^3= R^5= H, R^4= OH, 2'-hydroxygenistein

2 R^1= R^3= R^4= R^5= H, R^2= glucosyl, genistein 7-O-glucoside

2a R^1= R^3= R^5= H, R^2= glucosyl, R^4= OH, 2'-hydroxygenistein 7-O-glucoside

3 R^1= $CH^2CH{=}C(Me)^2$, R^2= R^3= R^4= R^5= H, wighteone

3a R^1= $CH_2CH{=}C(Me)_2$, R^2= R^3= R^5= H, R^4= OH, luteone

4 R^1= R^2= R^4= R^5= H, R^3= $CH_2CH{=}C(Me)_2$, lupiwighteone

4a R^1= R^2= R^5= H, R^3= $CH_2CH{=}C(Me)_2$, R^4= OH, 2,3-dehydrokievitone

5 R^1= R^2= R^3= R^4= H, R^5= $CH_2CH{=}C(Me)_2$, isowighteone

5a R^1= R^2= R^3= H, R^4= OH, R^5= $CH_2CH{=}C(Me)_2$, licoisoflavone A

6 R^1= R^5= $CH_2CH{=}C(Me)_2$, R^2= R^3= R^4= H, lupalbigenin

6a R^1= R^5= $CH_2CH{=}C(Me)_2$, R^2= R^3= H, R^4= OH, 2'-hydroxylupalbigenin

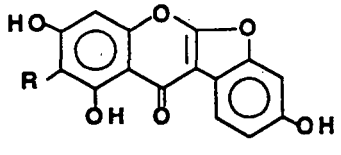

Coumaronochromones

7 R= H, lupinalbin A

8 R= $CH_2CH{=}C(Me)_2$, lupinalbin B

Fig. 1. Isoflavonoid derivatives of white lupin. Me = Methyl.

thermore, the complexity of the isoflavonoid composition of some plant tissues, *e.g.* lupin roots [10–13], can require multiple chromatographic steps for their analysis and, therefore, the possibility of artifacts arising during fractionation and derivatization.

High-performance liquid chromatography (HPLC) has also been successfully applied to the determination of isoflavonoid compounds [14,17–23]. These compounds include the simple isoflavones, genistein and 2'-hydroxygenistein, and their 6-prenyl derivatives in white lupin hypocotyls [8]; genistein, daidzein and their glucosides in soybean (*Glycine max*) [17–21]; genistein, formononetin and

biochanin A in *Ononis spinosa* [22]; formononetin and biochanin A in chickpeas (*Cicer arietinum*) [23]; and the prenylated isoflavones jamaicin and lisetin in Jamaican dogwood (*Piscidia erythrina*) [24]. White lupin roots accumulate a complex mixture of isoflavonoids based on the aglucones genistein (**1**) and 2′-hydroygenistein (**1a**), their respective 7-O-glucosides (**2a**, **2b**), as well as the 6-, 8-, 3′-monoprenyl (**3**–**5**, **3a**–**5a**), 6,3′-diprenyl (**6**, **6a**) derivatives, and two related coumaronochromones (**7**, **8**) as major constituents [10–13] (Fig. 1). Such a variety of isoflavonoids with different substitution patterns and a wide range of polarity required the development of an HPLC protocol for their optimum separation, which is the subject of this paper.

EXPERIMENTAL

Chemicals

All isoflavonoid compounds were from our laboratory collection. These were previously isolated from white lupin roots and characterized by spectroscopic methods [10–13]. Chromatographic solvents were of analytical-reagent grade. They were passed through a 0.45-μm membrane filter (Type HA, Millipore) and degassed before use. All solvent ratios were on a volume basis.

Equipment

A Waters HPLC system (Millipore) was used equipped with an M45 solvent delivery system, and M441 absorbance detector (at 254 nm), a 7010 Rheodyne sample injector (20-μl loop) and an SIM interface module for data acquisition. Data were processed using Waters Baseline 810 software. Isoflavonoids were chromatographed on a Merck reversed-phase C_{18} LiChrosper 100 column, 250 × 4 mm I.D. (particle size 5 μm). Samples were passed through 3 mm diameter filters (pore size 22 μm) before injection through the column.

Extraction of isoflavonoids from tissue samples

Tissue extracts were prepared by homogenizing fresh filtered cells with three aliquots of aqueous 80% methanol (1:5, w/v) at room temperature. The combined methanolic extracts were evaporated *in vacuo* at 30°C to about 30% of their original volume and the aqueous residue was extracted twice with ethyl acetate (5:1, vol/tissue wt.). The organic layers were stirred with anhydrous sodium sulphate before being evaporated to dryness. The residue was dissolved in 80% aqueous methanol and stored at −20°C until analysed. This method gives an efficient extraction of the isoflavonoid aglucones, glucosides and prenylated derivatives, but not the malonylated glucosides which are usually soluble in 50% aqueous methanol [25,26].

Chromatography

For the determination of isoflavonoids in cell cultures, samples consisted of 20 μl in 80% aqueous methanol, which were equivalent to *ca.* 150 mg of fresh tissue. Chromatography was carried out at a flow-rate of 1 ml/min using 45% solvent A (0.5% methanolic acetic acid) in 55% solvent B (0.5% aqueous acetic acid) for 2 min. This was followed by a gradient increase to 100% solvent A in 78 min and isocratic conditions were maintained for a further 10 min. Equilibration of the column was achieved using 45% solvent A for 15 min before injection of a new sample. For quantitative analysis, known amounts of authentic compounds were injected to generate standard reference curves. Linearity was observed within a concentration range 10 ng to 5 μg of the reference compounds used (Fig. 2). Isoflavonoids in cell cultures were identified and determined using the software, based on their retention times

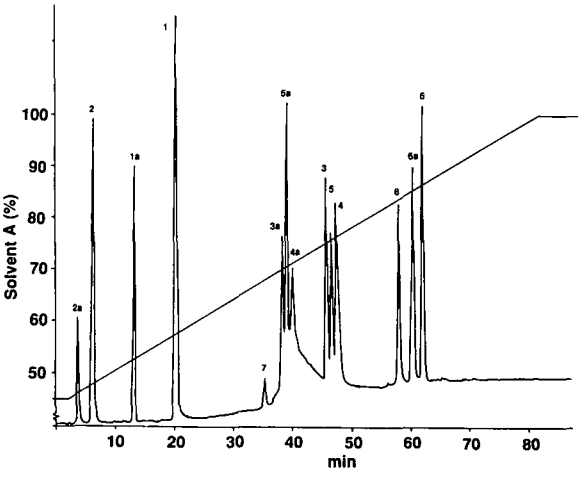

Fig. 2. HPLC profile for the elution pattern of authentic samples of the isoflavone (**1**–**6**, 1a–**6a**) and coumaronochromone (**7**, **8**) derivatives (Fig. 1). Amounts of isoflavonoids injected were: 1 μg each of compounds **2a**, **4a** and **7**: 2 μg of **2**, **3**, **3a** and **8**; 2.5 μg of **1a**, **5** and **6a**; 3 μg of **4**, **5a** and **6**; 4 μg of **1**.

and the calibration graphs generated with the standard compounds, respectively. Whereas the retention times of isoflavonoids may vary slightly during different runs (*ca.* 0.05–0.5 min), they did not affect the relative positions of their peaks on the chromatogram.

RESULTS AND DISCUSSION

Separation of authentic isoflavonoids

The solvent gradient of choice was defined after extensive examination of various solvent combinations, flow-rates, and different linear and non-linear gradients. The elution procedure used gave an optimum and reproducible separation of the fourteen isoflavonoids of interst (Fig. 2). The inclusion of acetic acid in, and elimination of acetonitrile from, the mobile phase [24,27] allowed separation of the three monoprenylated isomers of genistein and 2'-hydroxygenistein (**3–5** and **3a–5a**, respectively) which could not otherwise have been resolved.

Several workers have used aqueous methanol in the separation of simple isoflavonoids [17–23], including some prenylated derivatives [8,24], but with limited success. However, this is the first report in which several isoflavonoid derivatives, with a wide range of polarity, have been resolved in a single chromatographic run (Fig. 2). As expected, the isoflavone glucosides (**2**, **2a**) eluted first, followed by the parent aglucones (**1**, **1a**) and then the monoprenylated (**3–5**, **3a–5a**) and diprenylated (**6**, **6a**) derivatives. Isoflavonoids prenylated at position 6 eluted first, followed by those prenylated at positions 3', and 8. Whether they were glucosides, aglucones or prenylated compounds, the 2'-hydroxygenistein derivatives (**1a–6a**) eluted before those derived from genistein (**1–6**) and in the same relative order (Fig. 2). The coumaronochromones lupalbin A (**7**) and lupalbin B (**8**), however, had intermediate polarity and eluted before and just after the monoprenylated derivatives of genistein, respectively (Fig. 2).

Separation of isoflavonoids in lupin cell culture

The isoflavonoid profile of a cell culture derived from lupin radicle [28] is shown in Fig. 3. This profile shows all the major compounds known to occur in lupin roots [10–13], as well as a number of other unidentified peaks. The baseline drift observed during their separation is partly due to the increasing concentration of methanol in the gradient (Fig. 3), as well as the nature of the tissue analysed, especially for members of the Leguminosae family [21].

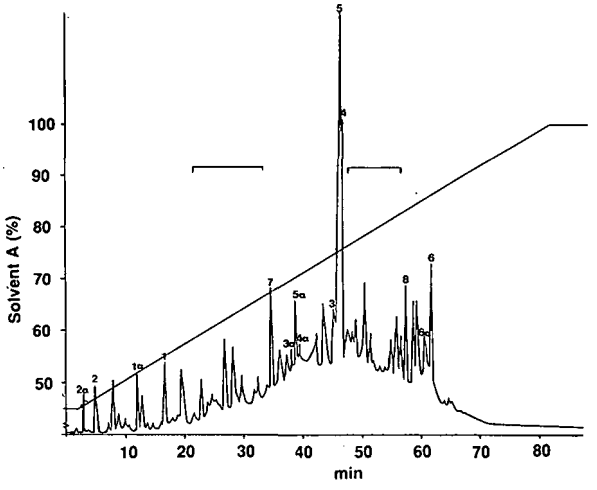

Fig. 3. HPLC profile for the elution pattern of isoflavonoid and coumaronochromone derivatives of a two-week old lupin cell suspension culture. Brackets indicate unidentified peaks.

TABLE I

AMOUNTS OF ISOFLAVONOIDS IN LUPIN CELLS AT DIFFERENT STAGES OF CULTURE GROWTH

Isoflavonoids[a]	Concentration of isoflavonoids (nmol/g fresh tissue)[b]		
	1-week culture	2-week culture	3-week culture
1	18.7	23.2	69.6
1a	16.9	33.1	132.5
2	85.2	68.6	12.8
2a	79.5	44.7	16.5
3	9.7	26.5	39.7
3a	8.6	12.5	37.6
4	38.5	60.3	167.3
4a	1.9	4.6	65.7
5	42.1	96.6	218.5
5a	6.9	12.8	66.7
6	15.6	49.9	89.6
6a	18.3	36.2	75.8
7	16.7	26.8	69.5
8	19.8	66.2	180.5

[a] Numbers correspond to compounds listed in Fig. 1.
[b] Average of two determinations with variations of 2–6%.

However, it is interesting to note the significant variations in the amounts of individual compounds accumulated within the cells, especially the decrease in the amount of glucosides and increased prenylated derivatives with culture growth (Table I). This clearly indicates the state of flux in metabolite production by cultured lupin cells, considering that a significant amount of the lipophilic, prenylated compounds (*ca.* 20%) is released into the nutrient culture medium [28]. In addition, several unidentified compounds (Fig. 3) were consistently observed in cell culture extracts and tend to increase in amount during culture growth. Their identity is currently being under investigation.

ACKNOWLEDGEMENTS

This work was supported in part by operating grants from the Natural Sciences and Engineering Research Council of Canada and the Department of Higher Education, Government of Québec. We thank Didier Hallard for his excellent assistance.

REFERENCES

1 P. M. Dewick, in J. B. Harborne (Editor), *The Flavonoids, Advances in Research Since 1980*, Chapman & Hall, London, 1988, Ch. 5, p. 125.
2 R. A. Dixon and C. J. Lamb, *Annu. Rev. Plant Physiol. Plant Mol. Biol.*, 41 (1990) 339.
3 J. L. Ingham, in W. Herz, H. Grisebach and G. W. Kirby (Editors), *Progress in the Chemistry of Organic Natural Products*, Springer, New York, 1983, pp. 1.
4 S. Tahara, S. Nakahara, J. Mizutani and J. L. Ingham, *Agric. Biol. Chem.*, 48 (1984) 1471.
5 E. W. K. Cheng, L. Yoder, C. D. Strong and W. Borroughs, *Science (Washington, D.C.)*, 120 (1954) 575.
6 S. Shibata, M. Harada and T. Murakami, *Yakugaku Zasshi*, 79 (1959) 863.
7 R. M. Kosslak, R. Bookland, J. Barkei, H. E. Paaren and H. E. Appelbaum, *Proc. Natl. Acad. Sci., USA*, 84 (1987) 7428.
8 M. A. Ferrer, M. A. Pedreno, A. A. Calderon, R. Munoz and A. R. Barcelo, *Physiol. Plant.*, 79 (1990) 610.
9 P. M. Dewick, in J. B. Harborne and T. J. Mabry (Editors), *The Flavonoids, Advances in Research*, Chapman & Hall, London, 1982, Ch. 10, p. 535.
10 J. B. Harborne, J. L. Ingham, L. King and M. Payne, *Phytochemistry*, 15 (1976) 1485.
11 J. L. Ingham, S. Tahara and J. B. Harborne, *Z. Naturforsch., C: Biosci.*, 38 (1983) 194.
12 S. Tahara, J. L. Ingham, S. Nakahara, J. Mizutani and J. B. Harborne, *Phytochemistry*, 23 (1984) 1889.
13 S. Tahara, S. Orihara, J. L. Ingham and J. Mizutani, *Phytochemistry*, 28 (1989) 901.
14 C. A. Williams and J. B. Harborne, in J. B. Harborne (Editor), *Methods in Plant Biochemistry*, Vol. 1, Academic Press, London, 1989, Ch. 12, p. 421.
15 M. Naim, B. Gestetner, I. Kirson, Y. Birk and A. Bondi, *Phytochemistry*, 12 (1973) 169.
16 M. Strobiecki and P. Wojtaszek, *J. Chromatogr.*, 508 (1990) 391.
17 R. E. Carlson and D. Dolphin, *J. Chromatogr.*, 198 (1980) 193.
18 P. A. Murphy, *J. Chromatogr.*, 211 (1981) 166.
19 A. C. Eldridge, *J. Chromatogr.*, 234 (1982) 494.
20 Y. Kitada, Y. Ueda, M. Yamamoto, M. Ishikawa, H. Nakazawa and M. Fujita, *J. Chromatogr.*, 366 (1986) 403.
21 T. L. Graham, *Plant Physiol.*, 95 (1991) 584.
22 P. Pietta, P. Mauri, E. Manera and P. Ceva, *J. Chromatogr.*, 513 (1990) 397.
23 S. Z. Dziedzic and J. Dick, *J. Chromatogr.*, 234 (1982) 497.
24 P. Pietta and C. Zio, *J. Chromatogr.*, 260 (1983) 497.
25 Y. Shibuya, S. Tahara, Y. Kimura and J. Mizutani, *Z. Naturforsch., C*, 46 (1991) 513.
26 J. Berlin, L. Fecker, C. Rügenhagen, C. Sator, D. Strack, L. Witte and W. Wray, *Z. Naturforsch., C: Biosci.*, 46 (1991) 725.
27 P. G. Pietta, P. L. Mauri, E. Manera, P. L. Ceva and A. Rava, *Chromatographia*, 27 (1989) 509.
28 D. Hallard, E. Bleichert, H. Gagnon, S. Tahara and R. K. Ibrahim, *Z. Naturfosch., C: Biosci.*, 47 (1992) 19.

Journal of Chromatography, 606 (1992) 260–263
Elsevier Science Publishers B.V., Amsterdam

CHROM. 24 198

Short Communication

Sulphur compounds

CLVII.* Determination of cysteine-*S*-sulphonate by ion-pair chromatography and its formation by autoxidation of cysteine persulphide

Ralf Steudel and Angela Albertsen

Institut für Anorganische und Analytische Chemie, Technische Universität Berlin, Sekr. C 2, D-1000 Berlin 12 (Germany)

(First received January 27th, 1992; revised manuscript received March 24th, 1992)

ABSTRACT

Chromatographic analyses and UV spectra show that alkaline aqueous solutions of cystine (or homocystine) and sulphide contain the anions HS^-, RS^-, RSS^-, and $RSSO_3^-$ (R = alanyl). The latter species originates from the autoxidation of the persulphide RSS^- by air. Under special conditions, $S_2O_3^{2-}$ and R_2S_3 are observed in addition.

INTRODUCTION

Cystine is an important constituent of most proteins. Its disulphide bond links neighbouring parts of the amino acid chains and it is therefore responsible for the conformation of the protein. Reductive or nucleophilic cleavage of the disulphide bridge changes the chemical and physical properties of the protein considerably, as is used, for instance, in the treatment of hair and wool. The two most important nucleophiles in this context are probably sulphide (S^{2-} and HS^-) and sulphite, which react with organic disulphides according to eqns. 1 and 2:

$$RSSR + HS^- \rightleftharpoons RSS^- + RS^- + H^+ \quad (1)$$

$$RSSR + SO_3^{2-} \rightleftharpoons RSSO_3^- + RS^- \quad (2)$$

In the case of cystine (bis-alanyldisulphane), the "persulphide" RSS^- (alanyldisulphide) formed in reaction 1 has been detected by its UV absorption spectrum, which is characterized by a maximum at 335 nm in 0.2 *M* sodium hydroxide solution [2]. According to Rao and Gorin [2], reaction 1 is relatively slow ("half-life" of *ca.* 12 min at concentrations of 0.0185 *M* for cystine and 0.069 *M* for sulphide at 25°C) and does not go to completion. Lipoic acid also reacts with sulphide in 0.1 *M* NaOH to form a persulphide absorbing near 335 nm [3,4]. Reaction 2 is also relatively slow in the case of cystine at pH 7 and 20°C, taking *ca.* 15 min for completion [5]. Because of its importance for the chemistry of proteins this reaction has been studied extensive-

Correspondence to: Professor Dr. R. Steudel, Institut für Anorganische und Analytische Chemie, Technische Universität Berlin, Sekr. C 2, D-1000 Berlin 12, Germany.

* For Part CLVI, see ref. 1.

0021-9673/92/$05.00

ly; at pH > 9 reaction 2 is reversible [5–10].

Cysteine-*S*-sulphonate is also formed on treatment of cysteine with thiosulphate at pH 7–7.4 (eqn. 3) [11]:

$$RSH + S_2O_3^{2-} \rightleftharpoons RSSO_3^- + HS^- \quad (3)$$

A convenient preparation of the sodium salt of cysteine-*S*-sulphonate from cysteine and sodium tetrathionate has been reported [12]; the product obtained was shown by X-ray crystallography to have the composition $C_3H_6O_5NS_2Na \cdot 3/2\ H_2O$ [13].

Inorganic sulphide (HS^-), polysulphide (S_x^{2-}), sulphite (SO_3^{2-}), thiosulphate ($S_2O_3^{2-}$) and polythionate ($S_nO_6^{2-}$) anions can be separated and determined by ion-pair chromatography [14–18]. This method uses an inert organic stationary phase and a water–acetonitrile mixture containing tetrabutylammonium ions and a buffer as a mobile phase. We have now applied this analytical technique to study reactions 1 and 2.

EXPERIMENTAL

The experimental conditions were similar to those described in ref. 18, and the same chromatographic and spectroscopic equipment was used. The UV detector (variable wavelength) was operated at 210 or 215 nm. A PLRP-S column (Polymer Laboratories, 120 mm × 4 mm I.D., particle size 8 μm) was used. The eluent compositions used for the results shown in Figs. 1, 3 and 4 were in the following range: 91.5–93.0% water (doubly distilled), 7.0–8.5% (v/v) acetonitrile, 2 mmol/l tetra-*n*-butylammonium hydroxide, 1 mmol/l Na_2CO_3. The eluent was degassed, and in some cases oxygen-free helium was bubbled through the eluent; but even in this case it was not possible to detect RSS^- chromatographically.

Cysteine, cystine (both from Merck; biochemical standards), homocysteine and homocystine (both from Fluka, purum) were used as delivered. $Na_2S \cdot 7H_2O$ (Merck) was recrystallized weekly from deoxygenated water to remove thiosulphate, sulphite and polysulphide [18]. Sodium cysteine-*S*-sulphonate (Bunte salt of cysteine) prepared after Inglis and Liu [12] gave excellent analytical data (C, H, N, S).

The sodium salt of alanylthiosulphate, $RSSO_3Na$ $3/2\ H_2O$, prepared by the published procedure [12], was used to determine the calibration function shown in Fig. 1; this function is linear up to at least 3 mmol/l provided the peak height is used.

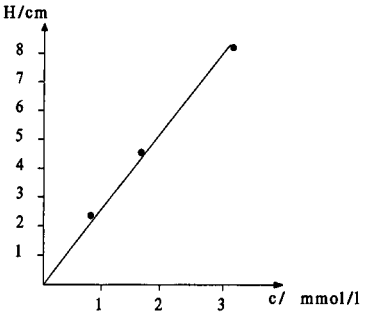

Fig. 1. Calibration function (peak height *H versus* concentration of sodium cysteine-*S*-sulphonate (detected at 210 nm, flow 1 ml/min, sample loop 50 μl).

All solutions were prepared with exclusion of oxygen unless stated otherwise. $Na_2S \cdot 7H_2O$ was dissolved in oxygen-free water and RSH or R_2S_2 in dilute NaOH of pH 11.0–13.0. The clear solutions were then mixed in appropriate ratios.

RESULTS

When D,L-cystine, dissolved in aqueous NaOH at pH 13.0, was treated with aqueous Na_2S in a molar ratio of 1:1 at 20°C, the above-mentioned UV absorption maximum at 335 nm appeared (Fig. 2a). A similar spectrum was obtained when homocystine was used at the same molar concentration (peak maximum at 335 nm). To check the air sensitivity of the alanyldisulphide (RSS^-) oxygen was bubbled into a solution of cystine and Na_2S at pH 13.0 (molar ratio 19:1): Fig. 2b demonstrates that the persulphide absorption disappeared almost completely within 45 min.

Both the unoxidized and the oxygenated persulphide solutions were analysed by ion-pair chromatography. Fig. 3a shows the chromatogram of the same solution as used to record the UV spectrum of Fig. 2a (curve 3). The expected components HS^-, RS^- and R_2S_2 (R = alanyl) are well separated (peaks 1, 2 and 3). In addition, two minor peaks were observed which could definitely be assigned to the trisulphane R_2S_3 [19] and the Bunte salt anion $RSSO_3^-$. All peaks were assigned on the basis of

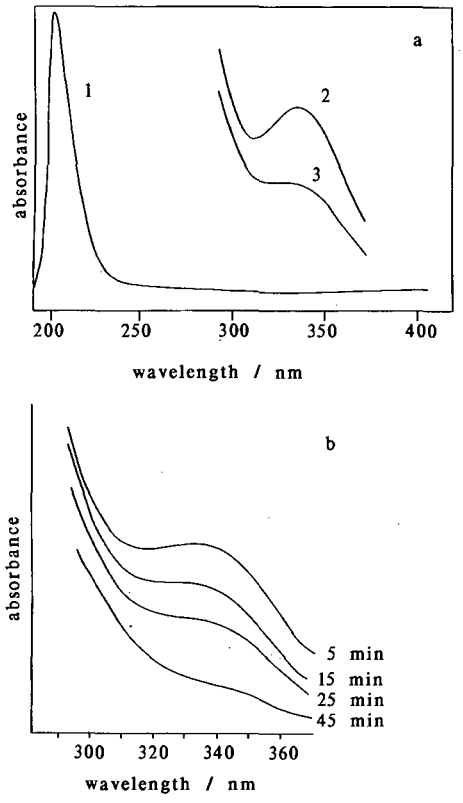

Fig. 2. (a) UV absorption spectra of cysteine persulphide (curve 3), homocysteine persulphide (curve 2) and cysteine-*S*-sulphonate (curve 1). Curves 2 and 3 were recorded by a conventional spectrometer (solvent: water–sodiumhydroxide). Curve 1 applies to the solvent acetonitrile–water (8.5/91.5, v/v) recorded by a diode-array detector after chromatographic separation; peak maximum at 200 nm. (b) Spectral changes when oxygen was bubbled into a solution of cysteine persulphide for the time indicated (0.038 mol/l cystine, 0.002 mol/l Na_2S in water–sodiumhydroxide of pH 13.0 at 20°C; solution prepared with exclusion of oxygen).

their retention times and UV spectra (recorded on-line using a diode-array detector) by comparison with chromatograms and spectra obtained with authentic samples. No peak for the persulphide RSS^- was observed and the UV spectra of the substances causing the large peaks 2 and 3 did not show any UV absorption near 335 nm, which would indicate that RSS^- was obscured by either RS^- or R_2S_2. Obviously, the persulphide concentration was too small for chromatographic detection owing to the secondary reactions 4 and 5 which remove persulphide:

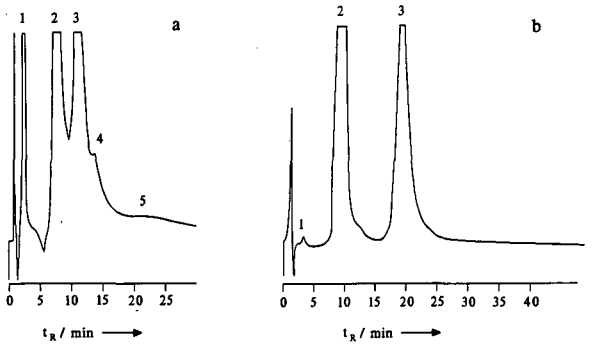

Fig. 3. (a) Ion-pair chromatogram of a solution of 1.00 mmol of cystine and 1.04 mmol of Na_2S in dilute NaOH (pH 13.0) with exclusion of oxygen; peaks: 1 = HS^-; 2 = RS^-; 3 = R_2S_2; 4 = R_2S_3; 5 = $RSSO_3^-$; R = alanyl. (b) Chromatogram of a solution of 0.20 mmol of cystine and 0.25 mmol of Na_2S at pH 11.0 after exposure to air for 48 h at 20°C; peaks: 1 = HS^-; 2 = R_2S_2; 3 = $RSSO_3^-$.

$$RSS^- + 3/2\ O_2 \rightarrow RSSO_3^- \quad (4)$$

$$RSS^- + R_2S_2 \rightleftharpoons RS^- + R_2S_3 \quad (5)$$

Reaction 4 is analogous to the well-known autoxidation of inorganic polysulphide yielding thiosulphate, eqn. 6 [20]:

$$S_2^{2-} + 3/2\ O_2 \rightarrow S_2O_3^{2-} \quad (6)$$

When an alkaline cystine solution was treated with Na_2S in a molar ratio of 1:1.25 (pH 11.0) and kept in air for 48 h, the chromatogram shown in Fig. 3b was obtained. It reveals cystine and the Bunte salt as the main constituents (peaks 2 and 3); the UV spectrum of peak 3 (Fig. 2a, curve 1) is identical to the UV spectrum of cysteine-*S*-sulphonate prepared from cysteine and tetrathionate [12].

The peak for the cysteine-*S*-sulphonate was also observed when cystine was treated with sulphite at pH 9.5 and 20°C (0.025 mmol of cystine and 0.05 mmol of sulphite in 10 ml of water, reaction time 1–24 h).

When aqueous cystine was treated with Na_2S at 20°C in a molar ratio of 1:5 (pH 11.0), the products found were dependent on whether or not air had access to the solution. In Fig. 4a the chromatogram of the mixture which was kept under nitrogen for 150 min is shown. Besides HS^-, the presence of RS^- and R_2S_2 is evident. Fig. 4b, on the other hand, demonstrates that the same mixture stored in

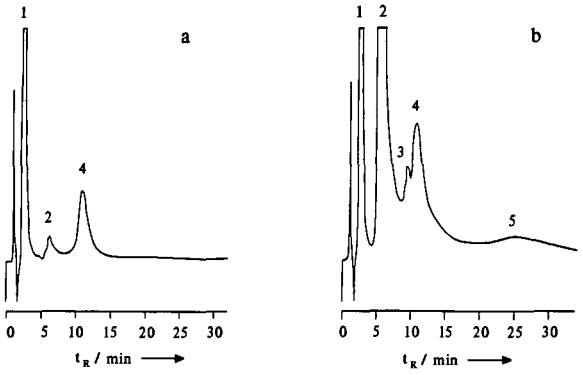

Fig. 4. Chromatograms of aqueous solutions prepared from 0.025 mmol of cystine and 0.125 mmol of Na_2S at pH 11.0. (a) Exclusion of oxygen; (b) exposure to air for 150 min. Peaks: 1 = HS^-; 2 = RS^-; 3 = $S_2O_3^{2-}$; 4 = R_2S_2; 5 = $RSSO_3^-$.

air for 150 min was composed of HS^-, R_2S_2, $S_2O_3^{2-}$ and $RSSO_3^-$, originating from reactions 1, 4, 6 and 7:

$$RSS^- + HS^- \rightleftharpoons RS^- + S_2^{2-} + H^+ \quad (7)$$

Another explanation for the presence of thiosulphate may be the oxidation of HS^- by oxygen, which is known [18] to produce $S_2O_3^{2-}$, S_x^{2-}, SO_3^{2-} and, finally, SO_4^{2-}.

CONCLUSION

Cysteine, homocysteine, cystine, homocystine and cysteine-*S*-sulphonate can be separated by ion-pair chromatography. Reaction of sulphide with cystine produces the persulphide, which reacts with oxygen to give the *S*-sulphonate and with cystine to give the trisulphide.

ACKNOWLEDGEMENTS

This work was supported by the Deutsche Forschungsgemeinschaft and the Verband der Chemischen Industrie.

REFERENCES

1 R. Steudel, in R. Steudel (Editor), *The Chemistry of Inorganic Ring Systems*, Elsevier, Amsterdam, 1992, Ch. 13.
2 G. S. Rao and G. Gorin, *J. Org. Chem.*, 224 (1959) 749.
3 M. Villarejo and J. Westley, *J. Biol. Chem.*, 283 (1963) 4016.
4 G. Bosser, J. Paris and V. Plichon, *J. Chem. Soc., Chem. Commun.*, 1988, 720.
5 J. R. McPhee, *Biochem. J.*, 64 (1956) 22.
6 H. T. Clarke, *J. Biol. Chem.*, 97 (1932) 235.
7 R. Cecil and J. R. McPhee, *Biochem. J.*, 60 (1955) 496.
8 J. L. Bailey and R. D. Cole, *J. Biol. Chem.*, 234 (1959) 1733.
9 N. J. J. van Rensburg and O., A. Swanepoel, *Arch. Biochem. Biophys.*, 108 (1967) 531.
10 N. J. J. van Rensburg and O. A. Swanepoel, *Arch. Biochem. Biophys.*, 121 (1967) 729.
11 T. W. Szczepkowski, *Nature (London)*, 182 (1958) 934.
12 A. S. Inglis and T.-Y. Liu, *J. Biol. Chem.*, 245 (1970) 112.
13 R. Steudel, A. Zahn, M. Kustos and J. Pickardt, in preparation.
14 S. B. Rabin and D. M.Stanbury, *Anal. Chem.*, 57 (1985) 1130.
15 J. Weiss and M. Göbel, *Fresenius' Z. Anal. Chem.*, 320 (1985) 439.
16 R. Steudel and G. Holdt, *J. Chromatogr.*, 361 (1986) 379.
17 R. Steudel, G. Holdt, T. Göbel and W. Hazeu, *Angew. Chem.*, 99 (1987) 143; *Angew. Chem., Int. Ed. Engl.*, 26 (1987) 151.
18 R. Steudel, G. Holdt and T. Göbel, *J. Chromatogr.*, 475 (1989) 442.
19 T. Göbel, *Dissertation*, Technische Universität, Berlin, Berlin, 1988.
20 R. Steudel, G. Holdt and R. Nagorka, *Z. Naturforsch., B: Anorg. Chem., Org. Chem.*, 41 (1986) 958.

Journal of Chromatography, 606 (1992) 264–271
Elsevier Science Publishers B.V., Amsterdam

CHROM. 24 378

Short Communication

Determination of alkaline phosphatase aggregation by size exclusion high-performance liquid chromatography with low-angle laser light scattering detection

D. J. Magiera and I. S. Krull

Department of Chemistry, The Barnett Institute, 341 MU, Northeastern University, 360 Huntington Avenue, Boston, MA 02115 (USA)

(First received January 23rd, 1992; revised manuscript received May 26th, 1992)

ABSTRACT

The formation of aggregates of alkaline phosphatase (AP) is examined in two different buffer systems: phosphate-buffered saline and modified protein buffer, using isocratic size-exclusion chromatography combined with low-angle laser-light scattering, ultraviolet spectroscopy, and a modified differential refractive index detector, all in series. The effects of buffer conditions, concentrations, and different batch preparations of alkaline phosphatase, as obtained from a manufacturer, were examined.

INTRODUCTION

Low-angle laser-light scattering (LALLS) has been interfaced with an ultraviolet (UV) and a differential refractive index (DRI) detector to collect on-line weight-average molecular mass (M_w) information of protein molecules separated by a prior high-performance liquid chromatography (HPLC) separation technique, the most popular technique being size-exclusion chromatography (SEC) [1–5]. Over the past twenty years, LALLS has been used to measure the molecular masses of various polymers. Static or traditional LALLS was used during the past 15 years for measuring synthetic polymer characteristics, such as M_w, second virial coefficients (A_2) and the degree of copolymer branching. Recently, our group and others [6–8] have focused on using LALLS to measure the M_w of biopolymers, as long as the refractive index (n) of the solvent and dn/dc (where c is concentration) of the biopolymer in solution are known [9–11]. An on-line system consisting of HPLC technique followed by LALLS, UV and DRI detectors, connected in series, was developed in our laboratory and used to calculate on-line M_w and dn/dc, with excellent reproducibility [12]. A detailed description of LALLS theory can be found in approaches to SEC–LALLS [13].

The tri-detection system described above is very useful for detecting protein aggregation in salt containing buffer solutions. We have compared the extent of aggregation of alkaline phosphatase (AP) in two different types of salt buffer systems, phosphate-buffered saline (PBS) and a surfactant-en-

Correspondence to: Professor I. S. Krull, Dept. of Chemistry, The Barnett Institute, 341 MU, Northeastern University, 360 Huntington Avenue, Boston, MA 02115, USA.

0021-9673/92/$05.00

hanced modified protein buffer (MPB). SEC was used to separate the aggregates formed from the monomer unit of AP. Because LALLS provides absolute M_w values, no recalibration of the SEC columns was required. The purity of AP from three different batch preparations was analyzed and compared, in order to observe different degrees of aggregation as a function of protein concentration and batch-to-batch preparation.

EXPERIMENTAL

Apparatus

The SEC–LALLS–UV–DRI system consisted of a ConstaMeteric II analytical metering pump (LDC Analytical/Thermo Instruments, Riviera Beach, FL, USA) operated at 0.7 ml/min, a Rheodyne (Cotati, CA, USA) Model 7125 20-μl injection loop, a medium TSK-PW 6000 size-exclusion column (30 cm × 8 mm I.D.) or a TSK-PWXL 3000 size-exclusion column (30 cm × 8 mm I.D., from Supelco/Division of Rohm & Haas, Bellefonte, PA, USA), a 0.22-μm (GV membrane) on-line filter apparatus (LDC), a Chromatrix KMX-6 (HeNe equipped laser operating at a wavelength 632.8 nm) LALLS photometer (LDC) equipped with a 10-μl flow through cell, a UV–visible (VIS) spectroMonitor-D (LDC) variable-wavelength absorbance detector operating at a 280 nm wavelength (0.2 AUFS at 10 mV full scale) and a modified refractoMonitor IV DRI detector (LDC), operated at $0.2 \cdot 10^{-3}$ RI units (10 mV full scale). The modifications to the DRI enabled dn/dc measurements to be made on-line at *ca.* 650 nm, as discussed elsewhere [12]. A Soltec (Sun Valley, CA, USA) Model 1242 strip chart recorder operating at 10 mV full-scale for UV or DRI outputs and 1 V full scale for LALLS output, at a recording speed of 15 cm/h was used to record raw chromatograms from LALLS and UV or DRI detectors. All detector outputs were connected to a PCI 2000 analog-to-digital converter (Burr Brown, Palo Alto, CA, USA) for computer data acquisition (CompuAdd 810, CompuAdd, Austin, TX, USA) and graphics/data manipulation. Software packages for simultaneously collecting data from the three detectors for calculating molecular weights were obtained from LDC, version PCLALLS. In-house software was developed [12] on LOTUS-123 to calculate on-line dn/dc measurements and percent recoveries. RI measurements were made as described previously [9].

Mobile phases

All water used to make the PBS and MPB buffers was deionized by a Nanopure System (Millipore, Bedford, MA, USA) and filtered with a 0.22-μm nylon membrane (Millipore) and degassed under vacuum before use as HPLC solvent. PBS was made with 150 mM sodium chloride, 25 mM monobasic sodium phosphate and 25 mM dibasic sodium phosphate pH 6.8 at room temperature, $n = 1.33$ at 633 nm. MPB was composed of 18 mM N-2-hydroxyethylpiperazine-N-2-ethanesulfonic acid (HEPES), 7 mM imidazole, 1 mM ethylenediaminetetraacetic acid (EDTA), 3 mM sodium azide, 200 mM sodium acetate, 0.5 mM non-ionic surfactant, octaethylene glycol-mono-N-dodecyl ether (Sigma, St. Louis, MO, USA), $n = 1.335$ at 633 nm, pH 7.0 at room temperature.

Chemicals and supplies

Bovine human AP was received from Sigma without further purification and stored immediately in the freezer (−20°C). Three different batch preparations of AP were analyzed as provided by the supplier. All solutions were made daily and stored in the refrigerator (5°C) in-between analyses or injections. All refrigerated samples were allowed to equilibrate to room temperature for 30 min before chromatographic analysis.

Ammonium acetate was reagent grade and obtained from EM Science (Gibbstown, NJ, USA). Imidazole, 99% pure, was used without further purification as obtained from Aldrich (Milwaukee, WI, USA). ACS reagent-grade chemicals EDTA, monobasic sodium phosphate, dibasic sodium phosphate and HEPES were obtained from Sigma. Sodium acetate, HPLC reagent grade, was obtained from Fisher. Sodium azide, used for a bacterial group repressor, was obtained from Eastman Kodak (Rochester, NY, USA).

Procedures

SEC–LALLS–UV–DRI studies. The columns for SEC analysis were equilibrated with buffer for 1 h before analysis at a flow-rate of 0.5 ml/min. The column was washed out at the end of each day's analysis with deionized water at a flow-rate of 0.5

ml/min for 1 h and then the flow-rate was lowered to 0.2 ml/min overnight.

Medium-resolution SEC study. A batch of AP, corresponding to lot 3 in Table I, was analyzed by medium-resolution SEC in the two different buffer systems, by weighing out the sample and adding it to the buffer solution to provide concentrations ranging from 1–3 mg/ml. The theoretical M_w of the monomer species was 68 000. A second batch of AP, lot 1, was analyzed by medium-resolution SEC; but only in the MPB buffer system to compare the purity of different batches of AP. An off-line dn/dc value of 0.146 was used for AP M_w calculations, as measured previously [9] for both MPB and PBS buffer systems. The percent recoveries (calculated by comparing computer collected UV areas at the same concentrations injected) were in the ranges of 60% for PBS and 50% for MPB.

High-resolution SEC study. For this study two different batches of AP, lots 1 and 2, were chromatographed on a high-resolution system. The first batch of AP, lot 3, was not used because of sample limitations for this study and was also unobtainable from the supplier, as it was out of stock. The same procedures described above were used for sample storage and HPLC analysis, except for the column, which was replaced with a high-resolution TSK-PWXL gel SEC column. Injections were made in both buffer systems, MPB and PBS, at concentrations ranging from 1.0–14.0 mg/ml (n = 3). All samples were prepared for injection by adding 1 ml of buffer to a weighed mass of lyophilized protein, always avoiding foaming.

The percent recoveries were calculated by measuring the molar absorptivity off-line of AP, dissolved in MPB and PBS buffers, by flow injection analysis. The procedure involved plotting the peak height versus concentration for three different dilutions of the injection solution (n = 3). A least-squares fit of this line provided the molar absorptivity (ε) of the protein, as the slope. The final percent recovery determined on-line was then calculated by using the in-house developed Lotus software [13]. The average percent recovery on the high-resolution

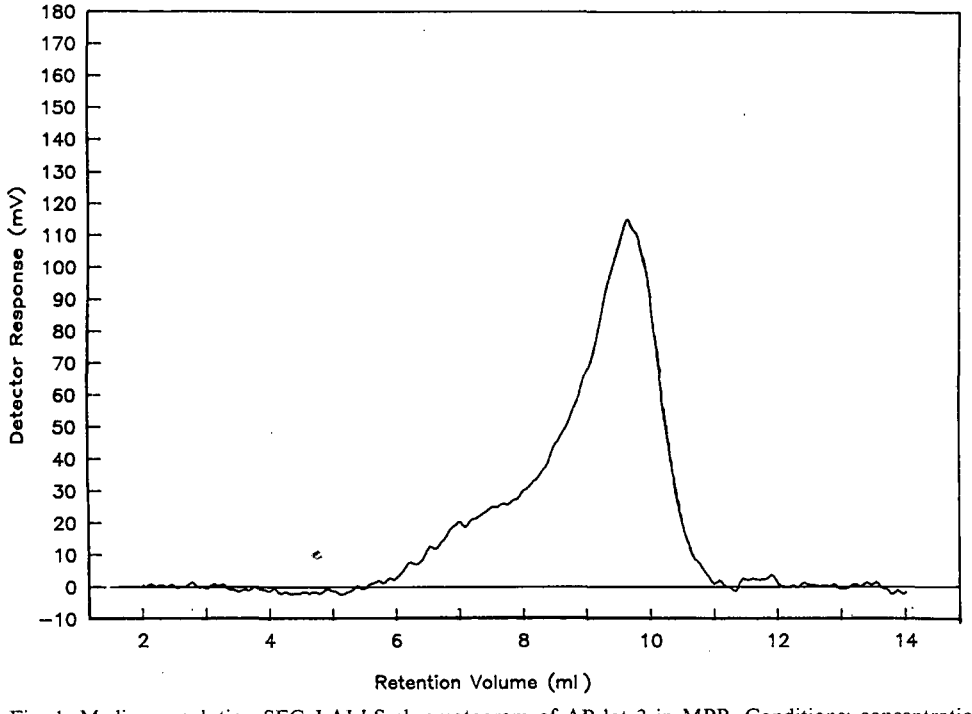

Fig. 1. Medium-resolution SEC–LALLS chromatogram of AP lot 3 in MPB. Conditions: concentration, 2.6 mg/ml; 100-μl loop; flow-rate, 0.7 ml/min.

column was *ca.* 90.0% in both buffer systems. An on-line calculated d*n*/d*c* for AP in MPB was 0.174, and in PBS 0.175 at *ca.* 5.0 mg/ml concentrations.

RESULTS AND DISCUSSION

PBS buffer was orginally thought to support aggregation of AP in solution. That is, as one increases the concentration of AP in an aggregating buffer solution, one would expect to see increased aggregation. The buffer components for PBS buffer, such as relatively high salt concentration, make it a suitable buffer to support the formation of AP aggregates. The aggregation of AP itself in PBS can be attributed to the weak dipole–dipole and hydrophobic forces of attraction, causing incomplete dissociation to the monomer species in solution. The next question that had to be answered was whether or not AP could be totally dissociated in any salt containing buffer solution.

A non-aggregating buffer solution was critical to this type of study because it served as the control. We have chosen to use an MPB buffer, which has not caused any aggregation of proteins upon dissolution [9–14].

The M_w results are listed in Table 1 for AP lot 3 in PBS and MPB buffers. The M_w calculated for lot 3 of AP dissolved in PBS buffer, approximately 78 400, was greater than the M_w corresponding to that calculated from the MPB buffer and suggested the existence of increased aggregation.

The existence of an aggregate was shown in the LALLS chromatograms (Figs. 1 and 2). Even though complete resolution of the species was not obtained, a reproducible M_w could still be obtained. The higher M_w calculated in the PBS buffer for lot 3 was compared to the M_w calculated for the same species at a similar eluate concentration dissolved in MPB.

High-resolution SEC–LALLS–UV–DRI was next used to obtain better resolution between the AP aggregate and monomer, which could discriminate between the different degrees of aggregation already present in the lyophilized samples. The AP aggregate was separated from the monomer species on the high-resolution SEC column (Figs. 3 and 4).

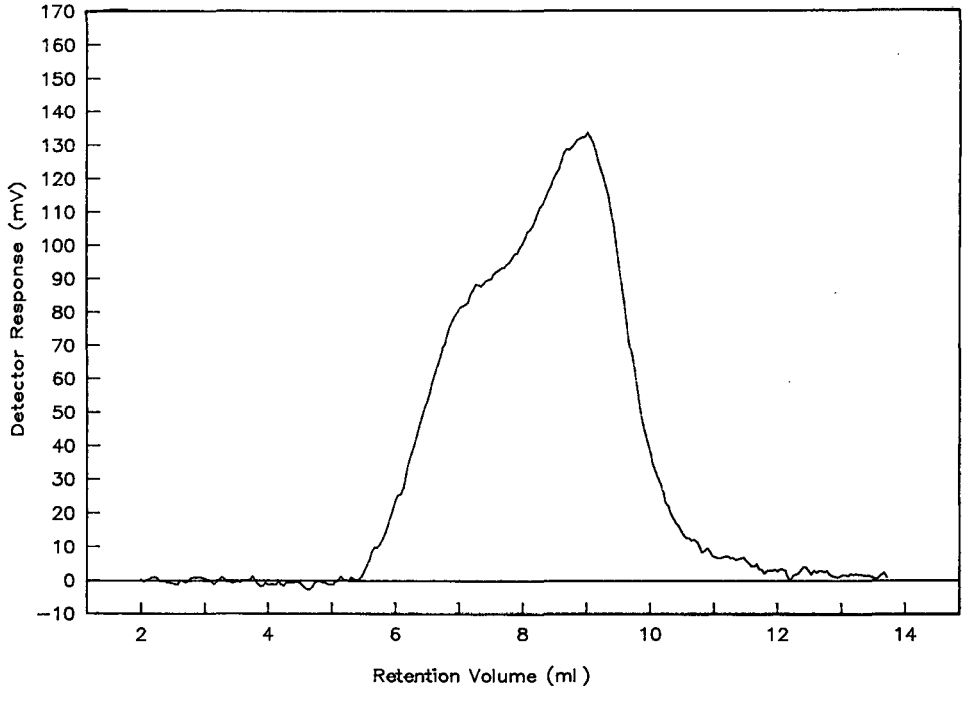

Fig. 2. Medium-resolution SEC–LALLS chromatogram of AP lot 3 in PBS. Conditions as in Fig. 1.

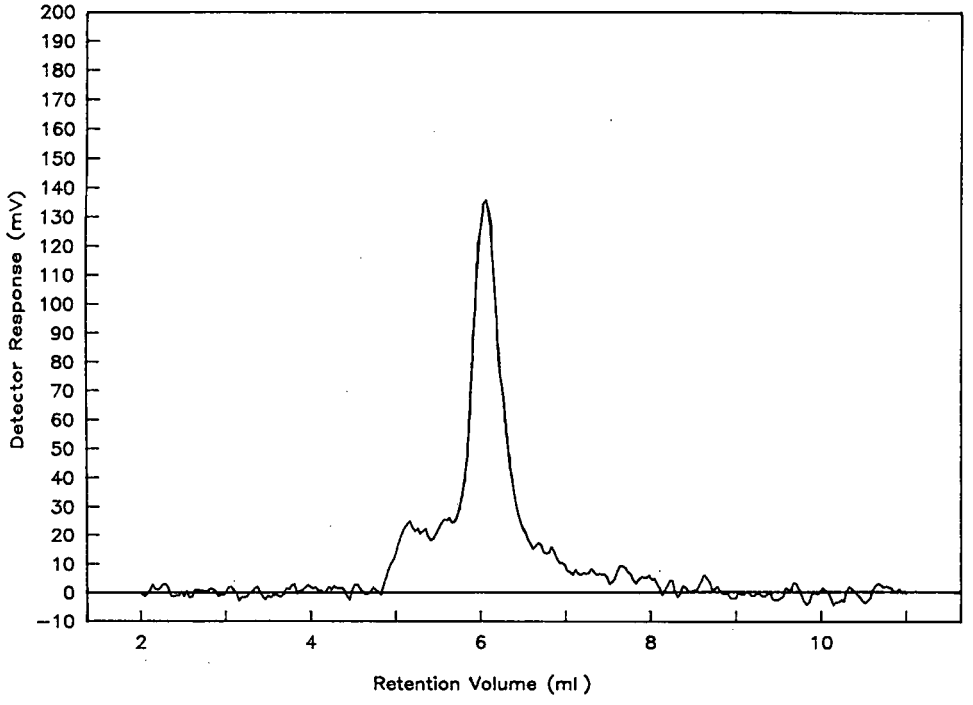

Fig 3. High-resolution SEC–UV chromatogram of AP lot 1 in PBS. Conditions: concentration, 1.33 mg/ml; 20-μl loop; flow-rate, 0.7 ml/min.

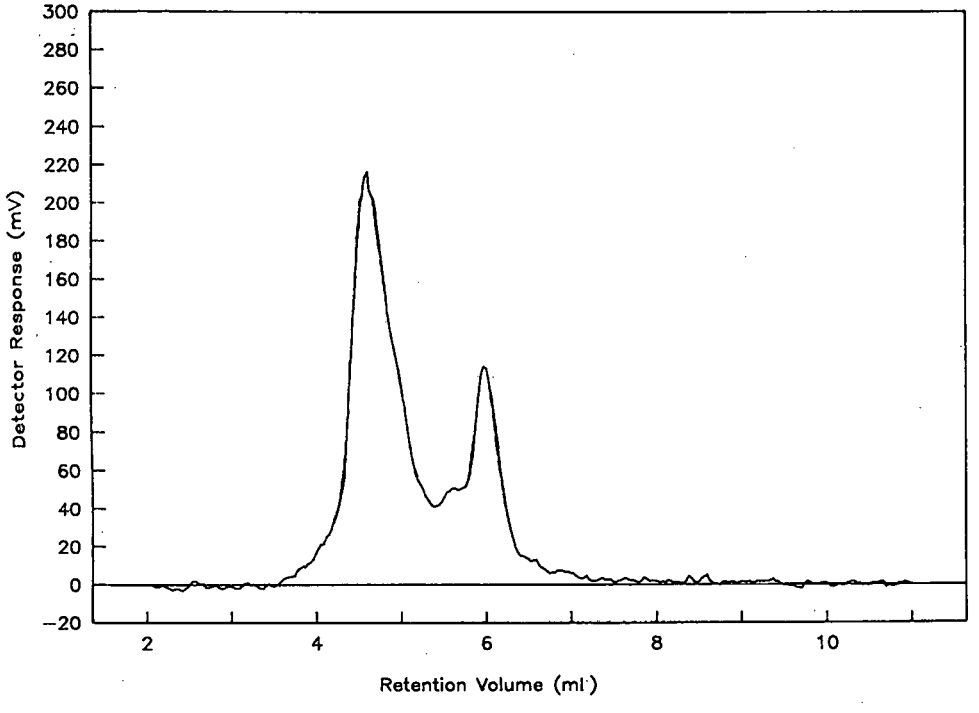

Fig. 4. High-resolution SEC–LALLS chromatogram of AP lot 1 in PBS. Conditions as in Fig. 3.

TABLE I

M_w OF ALKALINE PHOSPHATASE SAMPLES

A = Medium-resolution SEC–LALLS (n = 2); B = high-resolution SEC–LALLS (n = 3). SEC–LALLS–UV–DRI conditions: HPLC 20-μl loop for high-resolution and 100-μl loop for medium-resolution SEC; columns: TSK-PWXL 3000 for high resolution and TSK-PW 6000 for medium resolution; mobile phase PBS or MPB buffer, flow-rate 0.7 ml/min; UV = 280 nm; DRI = $1.0 \cdot 10^{-4}$ refractive index units; LALLS: LALLS attenuator constant (D) = $3.9223 \cdot 10^{-9}$, 6–7 degree annulus, 0.2 mm field stop, LALLS flow through cell system.

SEC–LALLS	AP sample (Lot No.)	Concentration (mg/ml)	Buffer	M_w	Average M_w	Relative S.D. (%)
A	3	2.8	PBS	82 500 – 80 000	81 300	
	3	2.6	PBS	77 800 – 73 200	75 500	
	3	1.50	MPB	70 700 – 70 500	70 600	
	3	2.7	MPB	73 400 – 67 900	70 700	
	1	1.24	MPB	76 400 – 78 600	77 500	
B	2	1.1	PBS	87 200		5.8
	2	5.5	PBS	87 600		5.8
	2	11.0	PBS	89 700		9.4
	1	1.3	PBS	76 600		5.8
	1	5.8	PBS	76 700		5.2
	1	11.7	PBS	79 100		11.2
	2	1.17	MPB	89 600		5.3
	2	5.1	MPB	89 600		2.5
	2	13.4	MPB	90 200		0.6
	1	1.7	MPB	81 800		8.2
	1	5.1	MPB	81 900		7.5
	1	10.0	MPB	81 200		2.8

On-line M_w analyses along with % recoveries and on-line dn/dc measurements are reported in Table I. The aggregate impurity was determined to be the dimeric species of AP, having a M_w of 136 000. The high-resolution SEC results are shown in Tables II and III for aggregate formation as the concentration of protein was increased in each buffer system, MPB and PBS, for lots 1 and 2. The graphs of % aggregate /% monomer *versus* concentration of AP in solution are shown in Figs. 5 and 6. The

TABLE II

HIGH-RESOLUTION SEC–LALLS–UV–DRI AP DEGREE OF AGGREGATION STUDY (MPB)

SEC–LALLS–UV–DRI conditions: HPLC: 20-μl loop for high-resolution SEC; column: TSK-PWXL 3000; mobile phase MPB buffer; flow-rate 0.7 ml/min; UV = 280 nm, DRI = $1.0 \cdot 10^{-4}$ refractive index units; LALLS: D = $3.9223 \cdot 10^{-9}$, 6–7 degree annulus, 0.2 mm field stop, LALLS flow through cell system.

AP Lot No. (n = 3)	Concentration (mg/l)	% Monomer	% Aggregate
1	1.7	79.69	20.30
	5.1	79.59	20.41
	10.0	80.23	19.56
2	1.17	68.12	31.87
	5.1	68.30	31.70
	13.4	67.34	32.66

TABLE III

HIGH-RESOLUTION SEC–LALLS–UV–DRI AP DEGREE OF AGGREGATION STUDY (PBS)

SEC–LALLS–UV–DRI conditions: HPLC: 20-μl loop for high-resolution SEC; column: TSK-PWXL 3000; mobile phase PBS buffer; flow-rate 0.7 ml/min; UV = 280 nm, DRI = $1.0 \cdot 10^{-4}$ refractive index units; LALLS: D = $3.9223 \cdot 10^{-9}$, 6–7 degree annulus, 0.2 mm field stop, LALLS flow through cell system.

AP Lot No. (n = 3)	Concentration (mg/l)	% Monomer	% Aggregate
1	1.3	87.42	12.58
	5.8	87.20	12.80
	11.7	83.70	16.30
2	1.1	71.85	28.15
	5.5	71.11	28.89
	11.0	68.16	31.84

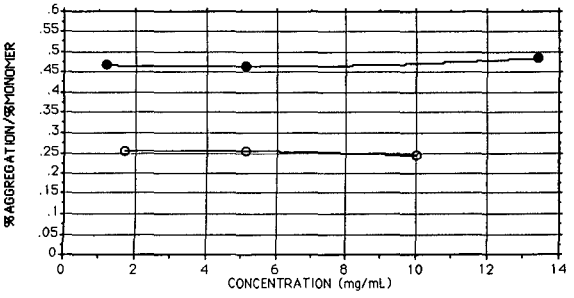

Fig. 5. Graph of % aggregate / % monomer *vs.* concentration for MPB. ○ = AP lot 1; ● = AP lot 2. SEC–LALLS–UV–DRI conditions as in Table II.

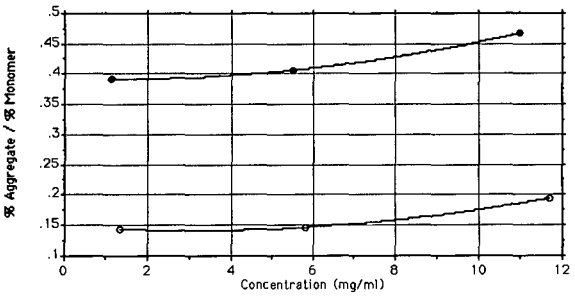

Fig. 6. Graph of % aggregate / % monomer *vs.* concentration for PBS. ○ = AP lot 1; ● = AP lot 2. SEC–LALLS–UV–DRI conditions as in Table III.

% monomer and % aggregate were determined by the ratio of their integrated UV areas to the total UV area collected by computer with the PCLALLS software. The degree of aggregation in PBS was shown to increase with increasing protein concentration for both lots 1 and 2.

The degree of aggregation observed in MPB did not increase with increasing protein concentration (Table II). The starting ratios of aggregate-to-monomer were almost the same as in PBS buffer at the 1.0 mg/ml concentration. But, as the concentration of AP was increased in the MPB solution, no increase in the aggregate-to-monomer ratio was seen over a broad concentration range (Fig. 5).

CONCLUSIONS

The degree of aggregation of AP has been studied using the SEC–LALLS–UV–DRI system in two different buffer systems, PBS and MPB. The monomer species was observed at M_w 68 000 and the dimer as an impurity at M_w 136 000. The degree of aggregation of AP in PBS increased with increasing protein concentration, and it may therefore be classified as an aggregating buffer system. The degree of aggregation in MPB remained constant and is probably present in the lyophilized powder before dilution. Therefore, it is concluded that since the ratios of dimer-to-monomer were constant over a broad range of increasing concentrations for all AP batches in MPB, the manufacturer had provided us with three differing purities.

ACKNOWLEDGEMENTS

Research funding, instrumentation donations and maintenance, and technical assistance were provided by LDC Analytical, Division of Thermo Instrument Systems, Riviera Beach, FL, USA. Additional funding for the SEC–LALLS program at Northeastern University has been provided by Merck Sharp and Dohme Research Laboratories, Inc., West Point, PA, USA (M. Brooks). We also wish to acknowledge the assistance of H. H. Stuting (Director of Analytical Chemistry, Roche Biomedical Laboratories, Raritan, NJ, USA), Wm. Mahn (LDC), C. Luckas (LDC), H. Kenny (LDC), and B. Howe (LDC) for their technical assistance. Several colleagues within Northeastern University provided stimulating discussions and support throughout this project, especially R. Mhatre, M. Szulc, J. Mazzeo, A. Quazi, A. J. Bourque, F.-X. Zhou and L. Dou.

This is contribution number 540 from The Barnett Institute at Northeastern University.

REFERENCES

1 W. Kaye, *Anal. Chem.*, 45 (1973) 221A.
2 P. L. Dubin (Editor), *Aqueous Size-Exclusion Chromatography (Journal of Chromatography Library*, Vol. 40), Elsevier, Amsterdam, 1988.
3 A. C. Ouano and W. Kaye, *J. Polym. Sci., Polym. Chem. Ed.*, 12 (1974) 151.
4 C. S. Wu and L. Sneak, *J. Liq. Chromatogr.*, 13 (1990) 851.
5 A. Huber, *J. Poly. Sci.*, (1992) in press.
6 T. Takagi, S. Maezawa and Y. Hayashi, *J. Biochem.*, 101 (1987) 805.

7 R. Mhatre, H. H. Stuting and I. S. Krull, *J. Chromatogr.*, 502 (1990) 21.
8 T. Takagi, *J. Chromatogr.*, 506 (1990) 409.
9 I. S. Krull, H. H. Stuting and S. C. Krzysko, *J. Chromatogr.*, 442 (1988) 29.
10 R. Mhatre, H. H. Stuting and I. S. Krull, *J. Chromatogr.*, 502 (1990) 21.
11 H. H. Stuting and I. S. Krull, *J. Chromatogr.*, 539 (1991) 91.
12 H. H. Stuting and I. S. Krull, *Anal. Chem.*, 62 (1990) 2107.
13 H. H. Stuting, I. S. Krull, R. Mhatre, S. C. Krzysko and H. G. Barth, *LC · GC*, 7 (1989) 402.

Journal of Chromatography, 606 (1992) 272–276
Elsevier Science Publishers B.V., Amsterdam

CHROM. 24 297

Short Communication

Determination of coenzyme Q by non-aqueous reversed-phase liquid chromatography

Sören Andersson

Research and Development Department, Kabi Pharmacia AB, S-112 87 Stockholm (Sweden)

(First received May 16th, 1991; revised manuscript received April 24th, 1992)

ABSTRACT

A non-aqueous reversed-phase liquid chromatographic method for determination of coenzyme Q_{10} in pharmaceutical formulations has been developed. The reversed-phase system provides better reproducibility and better selectivity for the separation of coenzyme Q_{10} analogues and degradation products than studied normal-phase systems. Furthermore, the non-aqueous mobile phase showed a very good solubility and provides a greater variety of work-up solvents for the lipophilic formulations than aqueous mobile phases. Validation studies showed detector response linearity over a concentration range of 0.2–100 μg/ml. The lower limit of detection was 2 ng on-column. The intra-assay precision (relative standard deviation) for a soy bean oil formulation was 2.0% (n = 11).

INTRODUCTION

Coenzyme Q_{10} (CoQ_{10}) (see Fig. 1) is a lipid-soluble quinone which is the active component of various pharmaceutical preparations used in the treatment of cardiomyopathy and angina pectoris [1,2].

The determination of CoQ_{10} in formulations is commonly performed by straight-phase liquid chromatography [3]. This paper describes the usefulness of a non-aqueous reversed-phase liquid chromatographic (LC) method for analysis of the drug in various formulations. The non-aqueous mobile phase shows good solubility and provides a greater variety of work-up solvents for the lipophilic formulations than aqueous mobile phases. The method was applicable to the quantitative analysis of CoQ_{10} in samples as diverse as raw material, soy bean oil formulations and micelle-based preparations.

Correspondence to: Dr. S. Andersson, Research and Development Department, Kabi Pharmacia AB, S-112 87 Stockholm, Sweden.

EXPERIMENTAL

Chemicals

Methanol and *n*-hexane were of LiChrosolv or analytical grade (Merck, Darmstadt, Germany). Coenzyme Q_9 was from Sigma (St. Louis, MO, USA) and coenzyme Q_{10} from Dai-Nippon Chemicals (Osaka, Japan). Ubichromenol was synthesized in the laboratory by basic catalysis of CoQ_{10} with a tertiary amine by use of a method described elsewere [4].

Apparatus

The liquid chromatograph consisted of a Shimadzu LC pump, LC-6A (Shimadzu, Kyoto, Japan), with a Shimadzu SIL-6A autoinjector and an ABI S-1000 diode-array detector (Applied Biosys-

0021-9673/92/$05.00

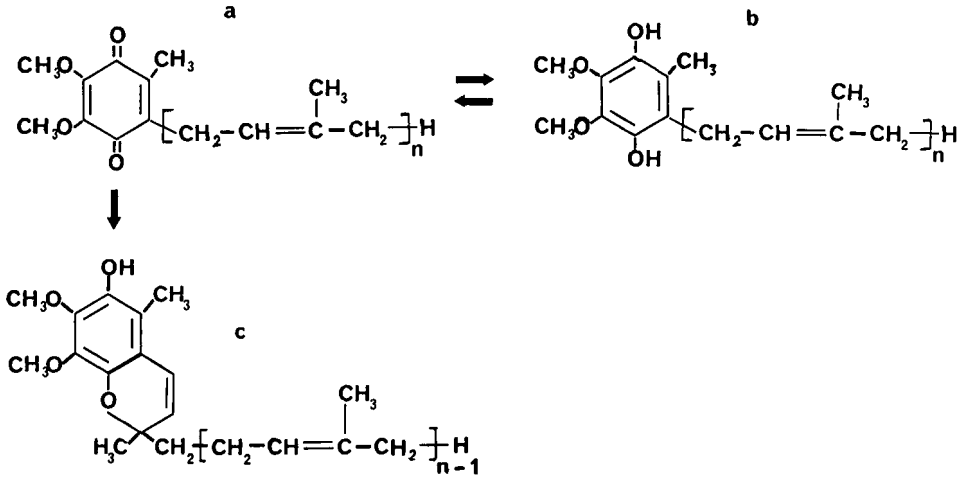

Fig. 1. (a) Chemical structure of CoQ_{10}, oxidized form, $n = 10$. (b) Chemical structure of CoQ_{10}, reduced form, $n = 10$. (c) Chemical structure of ubichromenol, $n = 10$.

tems, Foster City, CA, USA). For evaluation a Nelson 6000 chromatography data system (Perkin Elmer Nelson Systems, Cupertino, CA, USA) was used.

Sample preparation

(a) Soy bean capsules, 33 mg of CoQ_{10} (33.3 mg of CoQ_{10} suspended in soy bean oil). The capsule was opened with scalpel in a funnel over a 100-ml volumetric flask. The capsule was then transferred to the volumetric flask using forceps. The forceps, scalpel and the funnel were rinsed with hexane (the rinsing was performed by Pasteur pipette with 20 ml of hexane). The sample was ultrasonicated for 5 min and diluted to 100.0 ml with methanol and ultrasonicated again for another 2 min. A 2.00-ml aliquot of the sample was then diluted to 50.0 ml with methanol. A 20-μl aliquot was injected into the LC system.

(b) Mixed micelles, 4 mg/g CoQ_{10} (prepared from egg yolk lecithin/cholesterol and cholate). A 100-mg aliquot of the micelle preparation was dissolved in 100.0 ml of 20% *n*-hexane in methanol and ultrasonicated for 5 min. A 20-μl aliquot was injected into the LC system.

Chromatographic conditions

The analytical column (100 × 4.6 mm I.D.) contained Spherisorb ODS-2 material, 3-μm particles (Phase Separations, Queensferry, UK). The mobile phase, consisting of 10% *n*-hexane in methanol, was delivered at a flow-rate of 1.4 ml/min. The operative wavelength of the detector was 275 nm. The injected volume was 20 μl.

RESULTS AND DISCUSSION

The method uses an end-capped reversed-phase column with a mobile phase consisting of 10% *n*-hexane in methanol and UV detection at 275 nm. By using this non-aqueous LC method, problems associated with straight-phase liquid chromatography (*i.e.* non-reproducible retention times due to hydrogen bonding [5]) are avoided.

For the studied lipophilic formulations, which consisted of, for instance, triglycerides and phospholipids, this non-aqueous mobile phase showed a very good solubility compared with aqueous mobile phases, in which these components were poorly soluble.

Furthermore, this method provides better separation of CoQ analogues and major degradation products than straight-phase systems that have been studied. For instance, a heavily degraded CoQ_{10} solution gave very few, if any, extra peaks when it was analysed by the straight-phase method described by Palmer [5].

Fig. 2 shows the separation of oxidized and re-

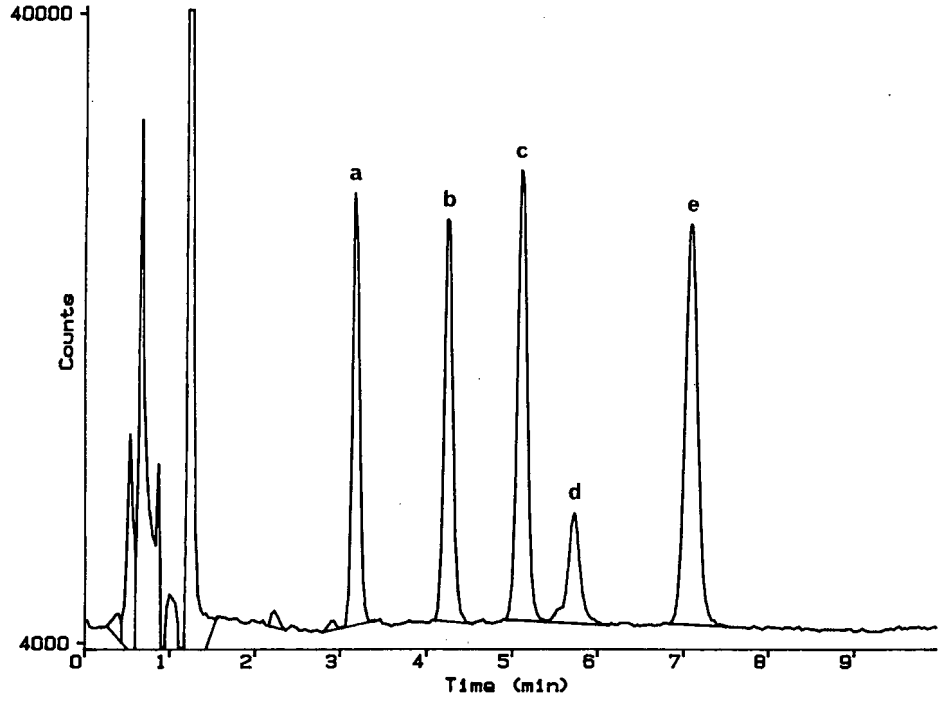

Fig. 2. HPLC separation of oxidized and reduced coenzyme Q_9, coenzyme Q_{10} and the major degradation compound ubichromenol. Peaks: a = CoQ_9, reduced form (100 μg/ml); b = CoQ_{10}, reduced form (100 μg/ml); c = CoQ_9, oxidized form (10 μg/ml); d = Ubichromenol (3.5 μg/ml); e = CoQ_{10}, oxidized form (10 μg/ml).

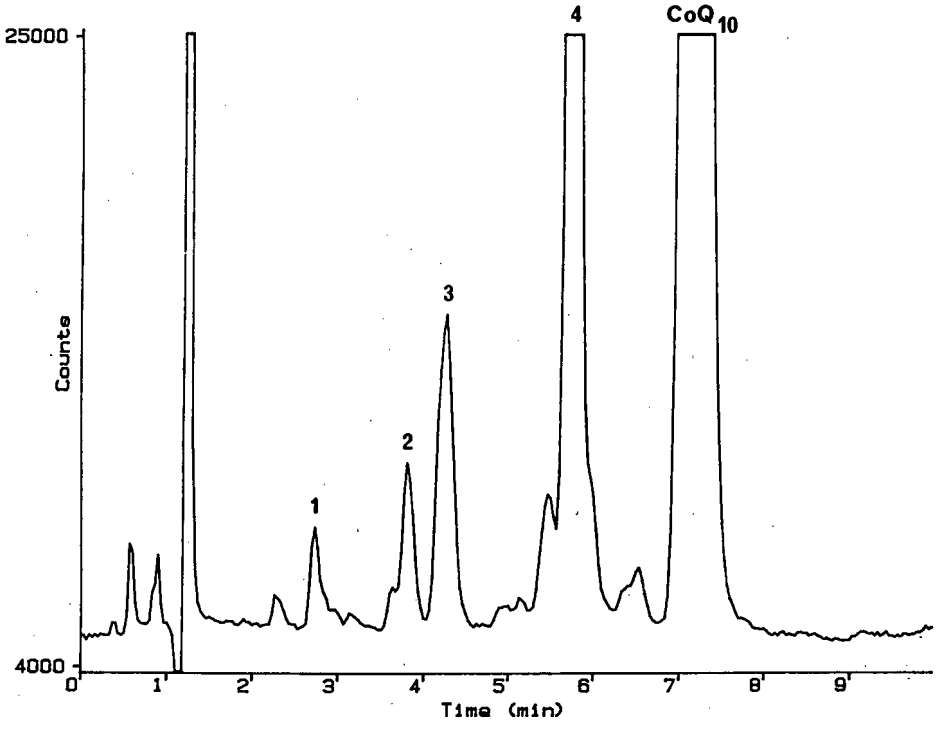

Fig. 3. Light-degraded raw material of CoQ_{10} after 20 h in daylight. Nominal content of CoQ_{10} was 500 μg/ml.

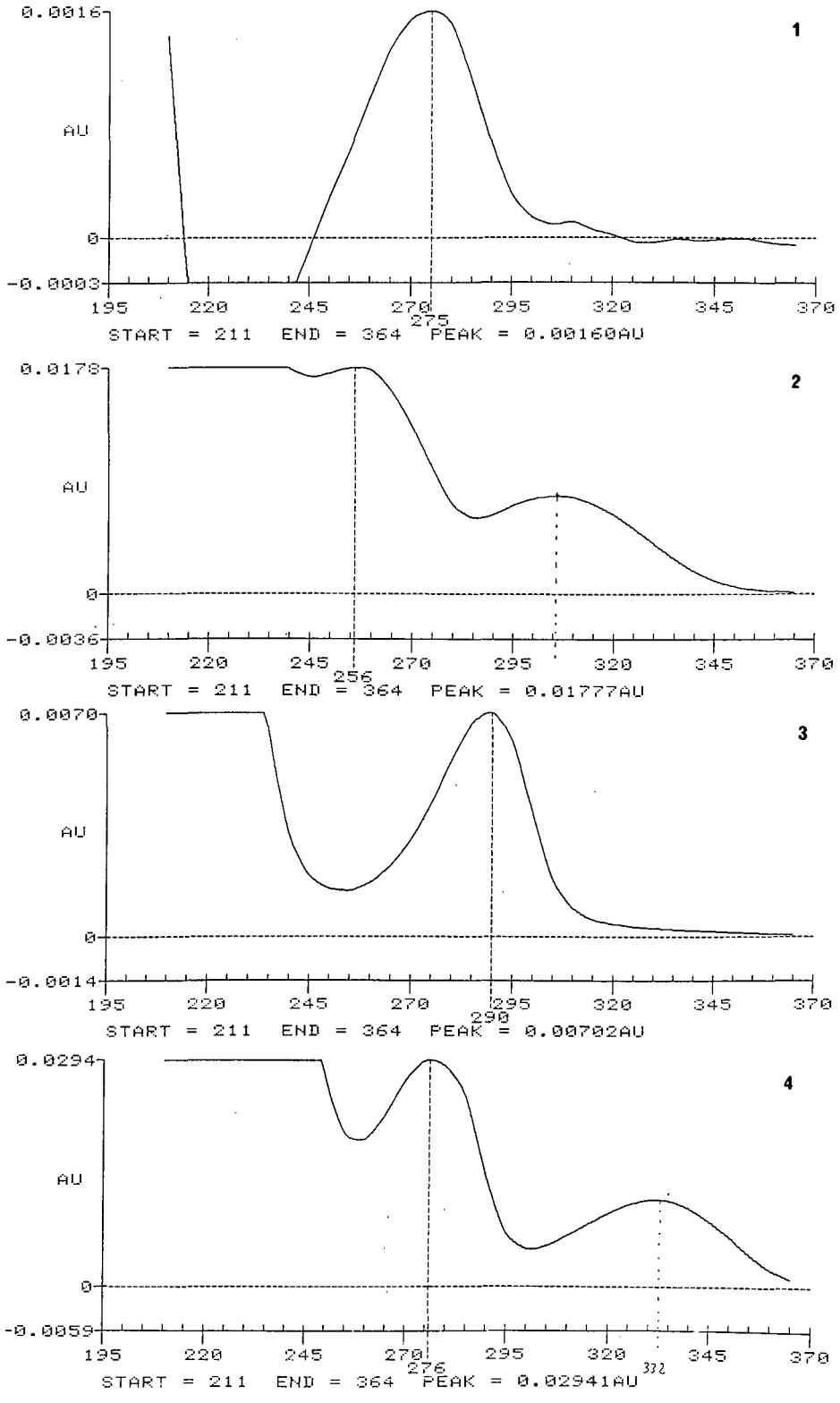

Fig. 4. UV spectra for some of the degradation products from the chromatogram in Fig. 3. 1 = Unknown; 2 = unknown; 3 = CoQ_{10}, reduced form; 4 = Ubichromenol.

duced CoQ_9, oxidized and reduced CoQ_{10} and the major degradation component ubichromenol (chemical structures in Fig. 1). These components could thus be easily quantitated within the same run.

In Fig. 3 a chromatogram from a light-degraded raw material is given. The identities of the unknown degradation products were checked using retention times and UV spectra. In Fig. 4, UV spectra for some of the unknown degradation products are shown.

For the studied formulations the determination of CoQ_{10} showed linear detector response in the concentration range 0.2–100 μg/ml. The lower limit of detection of CoQ_{10} at a signal-to-noise ratio of 3:1 (peak to peak) was 2 ng on-column. The intra-assay precision (relative standard deviation) of the method for soy bean capsules (5–20 μg/ml) was 2.0% (n = 11) and for micellar formulations (0.3–5.0 μg/ml) 2.6% (n = 6). The mean recovery of CoQ_{10} added to placebo capsules was 100.3 ± 1.9% (n = 6) and for CoQ_{10} added to a micelle vehicle was 99.7 ± 2.5% (n = 8).

REFERENCES

1 P. Michelle, *Annu. Rev. Biochem.*, 46 (1977) 996.
2 W. G. Nayler, K. Folkers and Y. Yamamura (Editors), in *Biomedical and Clinical Aspects of Coenzyme Q*, Vol. 2, Elsevier, Amsterdam, 1980, p. 409.
3 M. Ogawa, *Yakugaku Zasshi*, 97 (1977) 486.
4 I. Imada and H. Morimoto, *Chem. Pharm. Bull.*, 12 (1964) 1047.
5 D. N. Palmer, *Anal. Biochem.*, 140 (1984) 315.

Journal of Chromatography, 606 (1992) 277–280
Elsevier Science Publishers B.V., Amsterdam

CHROM. 24 285

Short Communication

Determination of ascorbic acid in elemental diet by high-performance liquid chromatography with electrochemical detection

Hiroshi Iwase

Ajinomoto Co., Inc., Kawasaki Factory, 1–1 Suzuki-cho, Kawasaki-ku, Kawasaki (Japan)

(First received February 13th, 1992; revised manuscript received April 24th, 1992)

ABSTRACT

Determination of ascorbic acid in a multi-component elemental diet was performed by high-performance liquid chromatography with electrochemical detection. This method is suitable for the routine determination of ascorbic acid in elemental diet because it is simple, rapid, sensitive, highly selective and reproducible. The calibration graph of ascorbic acid was linear in the range 0–1.0 μg. The recovery of ascorbic acid was over 95% by the standard addition method. There was good agreement between the concentrations of ascorbic acid stated and found.

INTRODUCTION

In a previous paper [1] the ultramicrodetermination of cyanocobalamin in an elemental diet (Elental, from Ajinomoto, Kawasaki, Japan), which contains 46 kinds of compounds (*e.g.*, amino acids, vitamins, organic acids, soybean oil, dextrin, minerals) [2] was reported. This paper deals with the routine determination of ascorbic acid (vitamin C) in Elental.

A simple, rapid, sensitive, highly selective and reproducible method for the determination of ascorbic acid in foodstuffs, drugs and biomedical samples is required for the purposes of process control, quality control and clinical chemistry aspects. Numerous methods have been developed for the determination of ascorbic acid, including iodimetry [3,4] and high-performance liquid chromatography (HPLC) [5–12]. Iodimetry is not suitable for complex sample matrices such as Elental.

The determination of ascorbic acid in biological fluids and foods has been investigated by HPLC with UV detection, electrochemical detection (ED) and fluorescence detection. Much effort has been directed to the development of specific and sensitive detection systems in HPLC. HPLC with ED is well recognized to be more sensitive than UV detection and as sensitive as fluorescence detection, and is extremely useful for the detection of trace compounds in complex matrices such as biological fluids because of the excellent sensitivity and selectivity provided [13]. ED has been widely used for phenolic compounds, in particular catecholamines and steroids in biological materials. Accordingly, the use of ED for the determination of ascorbic acid in Elental was undertaken in this study. However, HPLC could not be used for the routine determina-

Correspondence to: Dr. H. Iwase, Ajinomoto Co., Inc., Kawasaki Factory, 1–1 Suzuki-cho, Kawasaki-ku, Kawasaki, Japan.

0021-9673/92/$05.00

tion of ascorbic acid in Elental, because the experimental conditions for sample preparation, removal of interferences caused by the complex sample matrices and the relationship between the applied potential and the sensitivity of ascorbic acid and electrochemically active amino acids (cysteine, tyrosine and tryptophan) in Elental had not been investigated in detail.

This paper deals with the routine determination of ascorbic acid (97.5 ng/g) in Elental by HPLC–ED at 70 mV *versus* an Ag/AgCl reference electrode, which is highly specific for ascorbic acid. The determination of ascorbic acid in two other elemental diets, Elental P for paediatrics and Hepan ED for hepatic failure, is also described.

EXPERIMENTAL

Reagents and materials

Ascorbic acid was purchased from Tokyo Kasei (Tokyo, Japan). The reagent solution was freshly prepared prior to use. Other reagents were all of analytical-reagent or HPLC grade. Membrane filters (0.45 μm) were obtained from Advantec Tokyo (Tokyo, Japan).

Apparatus and conditions

A Model 655 A-11 high-performance liquid chromatograph (Hitachi, Tokyo, Japan) equipped with a Model E-502 electrochemical detector (IRICA, Kyoto, Japan) was used. The applied potential was set at 70 mV *versus* an Ag/AgCl reference electrode. The samples were applied with a Rheodyne Model 7125 sample loop injector with an effective volume of 20 μl. HPLC was carried out on a 25 × 0.46 cm I.D. column of Inertsil ODS-2 (5 μm) (GL Sciences, Tokyo, Japan) using 100 m*M* KH_2PO_4 (pH 3.0, adjusted with phosphoric acid) containing 1 m*M* ethylenediaminetetraacetic acid disodium salt (EDTA · 2Na) as the mobile phase. The flow-rate was 0.6 ml/min at ambient temperature. A Shimadzu UV-2100 variable-wavelength UV recording spectrophotometer (Shimadzu, Kyoto, Japan) was used to measure absorption spectra.

Sample preparation

Elental (1 g) was dissolved completely in 6% metaphosphoric acid (100 ml), the solution was filtered with a membrane filter (0.45 μm) and aliquots (20 μl) of the filtrate were injected into the chromatograph.

Elental P and Hepan ED solutions were also treated in the same manner.

RESULTS AND DISCUSSION

Chromatography

The relationship between applied potential and sensitivity of ascorbic acid and electrochemically active cysteine, tyrosine and tryptophan with concentrations at least 10–20 times higher than that of ascorbic acid, which might be considered to interfere in the determination of the latter, was examined. A typical hydrodynamic voltammogram is illustrated in Fig. 1. The current (peak height) at each applied potential was divided by the current at the most positive potential to obtain the relative current ratio. This value was plotted against the applied potential. The detector gave a linear response up to 900 or 1000 mV *versus* an Ag/AgCl reference electrode for cysteine, tyrosine and tryptophan.

Ascorbic acid in biomedical sampless has been determined by HPLC with ED at 800 mV *versus* Ag/AgCl [5,6]. When the applied potential was set at 800 mV *versus* Ag/AgCl, not only ascorbic acid, but also cysteine, tyrosine and tryptophan were de-

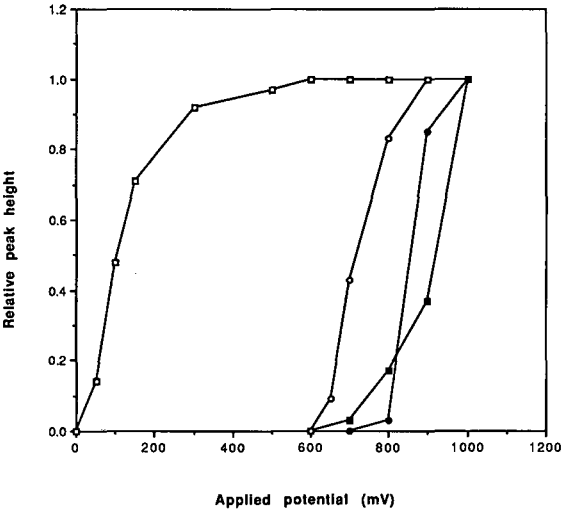

Fig. 1. Hydrodynamic voltammograms of (□) ascorbic acid, (○) cysteine, (●) tyrosine and (■) tryptophan.

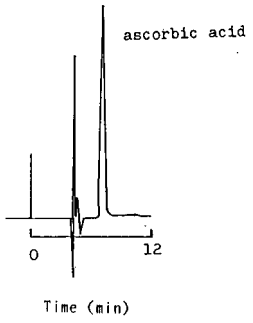

Fig. 2. Chromatogram of ascorbic acid in Elental with ED at 70 mV *versus* an Ag/AgCl reference electrode. Amount of ascorbic acid injected, 19.5 μg in 20 μl. HPLC was carried out on a 25 × 0.46 cm I.D. column of Inertsil ODS-2 (5 μm) using 100 m*M* KH_2PO_4 (pH 3.0, adjusted with phosphoric acid) containing 1 m*M* EDTA · 2Na as a mobile phase at a flow rate of 0.6 ml/min at ambient temperature.

tected. Complete elution took about 60 min after the retention time of ascorbic acid. In addition, further dilution of sample solution was needed because of the higher sensitivity. Ascorbic acid was unstable in the further diluted solution, and further dilution was not suitable for routine work because it was tedious and time consuming. On the other hand, the chromatography of ascorbic acid can be highly selective with rapid detection (retention time *ca.* 12 min) in the presence of other compounds using ED at a low applied potential of 70 mV *versus* Ag/AgCl. This allows routine analysis without clean-up. This procedure is simple and suitable for the routine work. A chromatogram of ascorbic acid in Elental is shown in Fig. 2.

The next effort was focused on UV detection of ascorbic acid. Ascorbic acid in biomedical samples has been determined by HPLC with UV detection [8–11]. Not only ascorbic acid, but also other vitamines, amino acids and organic acids absorb in the UV region. Ascorbic acid has an absorption at 265 and thiamine, riboflavin, nicotinamide, pyridoxine, folic acid, tyrosine, phenylalanine and tryptophan also show absorption at 265 nm.

Ascorbic acid was separated completely by monitoring at 265 nm. However, several unknown peaks were detected after the retention time of ascorbic acid and it took about 60 min for complete elution. Hence HPLC with UV detection is not suitable for routine analysis because it is not selective and the analytical time is long.

From the above results, it was concluded that the method established here was advantageous for the routine determination of ascorbic acid in Elemental, because it is simple, rapid and highly selective without the need for clean-up.

TABLE I

ACCURACY OF THE DETERMINATION OF ASCORBIC ACID ADDED TO ELENTAL

According to the label, Elental contains 9.75 mg of ascorbic acid per 100 g

Ascorbic acid (mg per 100 g)		Recovery (%)
Added	Found	
0	9.61	-
2.5	11.8	97.4
5.0	14.3	97.9
10.0	19.3	98.4
20.0	29.1	98.3

[a] R.S.D. = 0.5% (n = 7).

Determination of ascorbic acid

The calibration graph for ascorbic acid was constructed by plotting the peak height against the amount of ascorbic acid, and satisfactory linearity was obtained in the range 0–1.0 μg.

A known amount of ascorbic acid was added to Elental and the overall recovery was calculated by

TABLE II

ANALYTICAL DATA FOR ASCORBIC ACID IN THREE ELEMENTAL DIETS

Ascorbic acid concentration (mg per 100 g)			Recovery (%)
Sample	Stated	Found	
Elental	9.75	9.64	98.9
		9.61	98.6
		9.55	97.9
Elental P	35.8	35.7	99.7
		35.3	98.6
		35.3	98.6
Hepan ED	29.3	28.9	98.6
		28.3	96.6
		28.6	97.6

the standard addition method. As shown in Table I, the recovery of ascorbic acid was over 95% with a relative standard deviation (R.S.D.) of 0.5%.

The results in Table II show that the analytical data for ascorbic acid in Elental, Elental P and Hepan ED were excellent. There was good agreement between the ascorbic concentrations stated and found.

In conclusion, the proposed method is satisfactory with respect to selectivity, rapidity and accuracy. It is simple and convenient, and therefore applicable to the routine determination of ascorbic acid in elemental diets such as Elental, Elental P and Hepan ED.

REFERENCES

1 H. Iwase, *J. Chromatogr.*, 590 (1992) 187.
2 S. Ogoshi (Editor), *Elental Diet*, Nankodo, Tokyo, 1983.
3 *The United States Pharmacopeia, XXII Revision*, US Pharmacopeial Convention, Rockville, MD, 1990, p. 109.
4 *The Pharmacopeia of Japan*, Hirokawa, Tokyo, 12th Ed., 1992, p. C-37.
5 M. Yoshiura and K. Iriyama, *J. Liq. Chromatogr.*, 9 (1986) 177.
6 K. Iriyama, M. Yoshiura, T. Iwamoto and Y. Ozaki, *Anal. Biochem.*, 141 (1984) 238.
7 M. Yoshiura, T. Iwamoto and K. Iriyama, *Jikeiika Med. J.*, 32 (1985) 21.
8 R. C. Rose and D. L. Nahrwold, *Anal. Biochem.*, 123 (1982) 389.
9 R. R. Howard, T. Peterson and P. R. Kastl, *J. Chromatogr.*, 414 (1987) 434.
10 J. Cammack, A. Oke and R. N. Adams, *J. Chromatogr.*, 565 (1991) 529.
11 D. B. Dennison, T. G. Brawley and G. L. K. Hunter, *J. Agric. Food Chem.*, 29 (1981) 927.
12 J. T. Vanderslice and D. J. Higgs, *J. Chromatogr. Sci.*, 22 (1984) 485.
13 P. T. Kissinger, *Anal. Chem.*, 49 (1977) 477A.

Journal of Chromatography, 606 (1992) 281–284
Elsevier Science Publishers B.V., Amsterdam

CHROM. 24 384

Short Communication

Use of three molecularly toroid phases for the gas chromatography of some volatile oil constituents, and comparison with liquid crystal phases

T. J. Betts

School of Pharmacy, Curtin University of Technology, GPO Box U1987, Perth, W. Australia (Australia)

(First received January 24th, 1992; revised manuscript received June 1st, 1992)

ABSTRACT

A commercially available capillary, "Chiraldex-A-DA" and two 24-crown-8-ethers in packed columns, have been used in the gas chromatographic examination of some volatile oil constituents. They lose some selective-retaining properties at high temperatures. These molecular toroid phases show a characteristic elution sequence for aromatics: cuminal–anethole–safrole–thymol, different to liquid crystals. The Chiraldex and dicyclohexanocrown exhibit good retention of geraniol and caryophyllene; whereas the more polar dibenzocrown shows poor geraniol and good estragole retention, compared to other solutes.

INTRODUCTION

We have previously utilised liquid crystal substances as stationary phases for study by gas chromatography of volatile oil constituents in packed columns [1–4] and a commercially available capillary [2]. These phases could be used below [1,3] and above [2] their nematic or chiral nematic [4] temperature ranges. As these results should have been influenced by the molecular shapes of the solutes studied (in contrast to conventional stationary phases) it was of interest to investigate the effect of some molecularly toroid (ring) phases, which should respond in a different way to solute molecule shapes.

Correspondence to: Dr. T. J. Betts, School of Pharmacy, Curtin University of Technology, GPO Box U1987, Perth, W. Australia, Australia.

Crown (cyclic) ethers are one source of molecular rings, every third atom of which is oxygen; for example, eight ether bonds joining two-carbon units into a 24 (atom)-crown-8 (ether). Their properties can be influenced by including, on opposite sides of the ring, cyclic C_6 benzene or cyclohexane ring systems to form dibenzo- or dicyclohexano-crowns (see Fig. 1). The first crown ethers used for gas chromatography almost ten years ago by Ono [5] for dichlorophenols were the 18-crown-6s of smaller size. More recently, Ayyangar *et al.* [6] studied substituted aromatics both on this smaller dibenzo-18-crown-6, and on the two larger 24-crown-8 ethers. They found that on the larger crowns "nitrochlorobenzene and dimethylphenol isomers are separated very well", and as these two ethers are liquids well below the melting point of the 18-crown (which is about 153°C [6]) they were chosen for this study, along with the commercially available capillary to-

0021-9673/92/$05.00

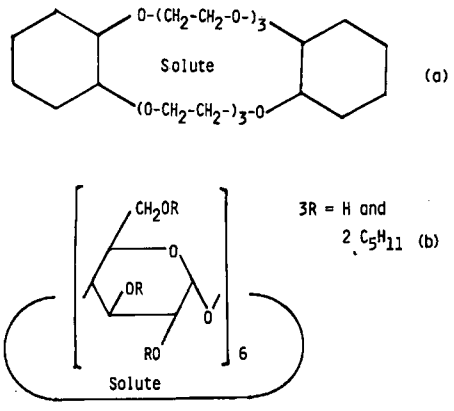

Fig. 1. Formulae of toroid phases used. (a) 24-Crown-8-ethers, with left and right hexagonal rings either dicyclohexano or dibenzo structure. (b) Chiraldex-A-DA.

roid phase "Chiraldex-A-DA". This lattermost consists of a di-O-pentylated α-cyclodextrin [7] and so retains an unsubstituted hydroxyl-group on each of its six α-glucose units which form a 30-atom ring (see Fig. 1). It is claimed to have a "hydrophobic surface" and "show pronounced selectivity differences based on the size, shape and functionality of the analyte" which "applies to both aromatic and nonaromatic enantiomers" with the warning that there is "critical temperature dependence for enantioselectivity" [7]. α-Cyclodextrin has the smallest cyclodextrin-ring system, and so is closest to the crown ether size.

Modified cyclodextrins in capillaries have been used recently to resolve enantiomers of terpene hydrocarbons by Konig *et al.* [8], but with fully tri-O-pentylated larger cyclodextrins. They have also been used in dilute mixture in polysiloxanes as stationary phases for mono- and sesqui-terpene hydrocarbons [9], which obviously leaves their contribution confused.

EXPERIMENTAL

Apparatus

For the capillary studies a Hewlett-Packard 5790A gas chromatograph was used, fitted with a flame ionisation detector, capillary control unit and splitter injection port in split mode. A Hewlett-Packard 3380A integrator/recorder was attached. For the packed column work a Pye-Unicam GCD gas chromatograph was used, fitted with a flame ionisation detector. A Pye wide-range amplifier and Hewlett-Packard 3390A integrator/recorder were attached.

A "Chiraldex-A-DA" capillary was used (Advanced Separation Technologies, Whippany, NJ, USA), 10 m × 0.25 mm I.D., only heated to 140°C or below at about 8°C min^{-1} and cooled slowly by switching the oven off. The injection port was maintained above 200°C. Helium was the mobile phase at 1.6 ml min^{-1}.

The packed columns were of glass, 1.5 m × 2 mm I.D. containing 3% (w/w) of the crown-ether on Chromosorb W AW, 80–100 mesh, prepared as in ref. 2, where details of the liquid crystal packed columns and capillary are also given. A high load 10% (w/w) crown ether column yielded very slowly emerging peaks, and was rejected, although used by Ayyangar *et al.* [6]. Reasonably high temperatures were needed.

Operating conditions are given in Table I, observing the GCD oven temperatures with a Technoterm 7300 probe. Nitrogen was the mobile phase for the packed columns at the high flow-rate of 40 ml min^{-1}.

Materials and methods

Di-benzo-24-crown-8 and di-cyclohexano-24-crown-8 were from Aldrich. Sources of solutes for injection are given in refs. 2–4. Injections were made from a microsyringe which had been filled, then "emptied".

RESULTS AND DISCUSSION

The polartity of the toroid phases was evaluated as before [4]. At 120° on Chiraldex-A-DA, 2-octyne emerged considerably after *n*-butanol and pyridine, indicating a very low polarity phase. In contrast, the dibenzo-crown ether released octyne together with butanol, well ahead of pyridine, typical of a quite polar phase. The dicyclohexano-crown ether had octyne eluting just ahead of pyridine, after butanol, indicating intermediate polarity; between the other two phases.

Once again, relative retention times to linalol were calculated, after subtracting holdup times [4], and were compared to results on liquid crystal phases obtained before. Average results are given in

TABLE I

RELATIVE RETENTION TIMES (LINALOL = 1.00) ON TOROIDAL AND LIQUID CRYSTAL PHASE COLUMNS

Average results. Values in italics are out of descending sequence, and could be shifted up or down the Table as indicated by their suffix arrows to the position of their abbreviation (G, etc.) Mobile phase details for toroids in this text, and for liquid crystals in refs. 1–4. Capillary shown by "cap" and packed column by "pac".

Solute	Gas chromatographic phases, used at various temperatures (°C), with liquid crystal condition shown											
	"Chiraldex-A-DA" cap			Dicyclohexano-crown pac		Dibenzo-crown pac		"MPMS" cap nematic [2]	$(MBT)_2$ pac		Cholesteryl acetate pac	
									Melted super-cool [1–3]	Unmelted	Chiral nematic [4]	Isotropic
	110	125	140	155	170	155	170	150	150	150	115	155
								A	A			
Thymol			10.00	10.51	9.00	10.75	9.18	6.20	6.60	4.71		5.65[a] Y
Geraniol (G)	4.60	4.04	*3.64*↓	*3.33*↓	*3.08*↓	*3.52*↓	*3.27*↓	*2.58*↓	*4.27*↓	3.85		2.40[a]↓
Safrole (S)	4.17	3.99	3.82	3.63 G	3.56	5.01	4.82	5.21	*4.58*↓	*2.67*↓		*3.48*↓
Anethole (A)	4.03	3.91	3.72 G	3.29	3.20 G	4.82	4.55	*7.60*↑	*8.26*↑	3.53		3.82
Caryophyllene (Y)	3.77	3.75	3.61	3.12	3.04	*2.43*↓	*2.52*↓	*3.26*↓	*2.18*↓	*2.87*↓		*5.08*[a]↑ S
Cuminal	3.25	3.28	3.22	2.69	2.68	4.30 G	4.21 GY	5.21 YG	5.01 SG	3.30 YS	2.79	2.69 G
α-Terpineol (T)	2.29	2.24	2.18	1.96	1.94	*2.30*↓	*2.32*↓	*2.54*↓	*2.43*↓	1.94	2.21	2.13
Estragole	2.03	2.05	2.04	1.86 P	1.84	2.44 YT P	2.42 T	3.03 T	2.83 TY P	1.70	2.02	1.97
γ-Terpinene	0.44			0.48		0.45			0.53	0.44	0.65 P	0.72 P
Cineole (N)	0.44			0.41		0.43			*0.41*↓	0.44 P	*0.46*↓	*0.58*↓
Limonene	0.39			0.40		0.37			0.49	0.40	0.54	0.63
p-Cymene (P)	0.38			*0.48*↑		*0.50*↑			*0.53*↑	*0.43*↑	*0.57*↑	*0.66*↑
α-Terpinene	0.32			0.36		0.35			0.43 N	0.38	0.48 N	0.59 N
α-Pinene	0.20			0.21		0.24			0.23	0.23	0.24	0.33

[a] New results, not in ref. 4.

Table I, and draw on some previous work [1–4], with some new observations included.

On all toroid phases the relative retention times of the linear aromatic estragole are almost constant despite column temperature changes. Two of these phases also show this near constancy for the branched side-chain aromatic cuminal, and the cyclic terpenoid α-terpineol. However, all three phases behave most distinctively at lower temperatures, losing some of their geraniol- or estragole-retaining property at 140°C for Chiraldex, and at 170°C for the crown-ethers. These are approaching maximum usable temperatures for the crowns [6], whilst higher temperatures for the Chiraldex might alter its character [7]. Under the conditions used, the Chiraldex capillary gave no sign of enantiomer resolution with racemic linalol or carvone.

All three toroid phases show the following elution sequence for this set of aromatics: cuminal (first)–anethole–safrole–thymol (long last). Thus

safrole is not ahead of anethole, as it is on liquid crystal phases [2,4]. On these, anethole is often last and safrole first, except for cholesteryl acetate [4]. The acyclic terpenoid geraniol is a variable amongst this aromatic set, being strongly retained on the low polarity Chiraldex capillary at lower temperatures (after safrole), and also at lower temperature on the intermediate polarity dicyclohexano-crown (but less strongly, ahead of safrole). This is unlike conventional phases. In contrast, its lack of affinity for the aromatic nature of dibenzo-crown sees geraniol emerge ahead of the aromatic solute set. The liquid crystal unmelted aromatic bis(methoxybenzylidineanilbitoluidine) [$(MBT)_2$] also strongly retains geraniol, whereas isotropic terpenoidal cholesteryl acetate shows low affinity for it. These results are the reverse of what might be expected, but neither phase is in the nematic state. The "MPMS" multi-aromatic liquid crystal capillary also shows a logical lack of affinity for geraniol, as does melted $(MBT)_2$.

A trio of mixed solutes, earlier than the aromatic set, shown on the lower polarity toroids Chiraldex and dicyclohexano-crown is: estragole–α-terpineol–caryophyllene (last); as it is also on unmelted $(MBT)_2$, isotropic cholesteryl acetate and nematic bis(methoxybenzilidineanilchloroaniline) [$(MBCA)_2$] [2]. This three-solute sequence is reversed on melted, supercooled $(MBT)_2$ [2] as the aromatic nature of the phase has become apparent by strongly retaining the aromatic estragole. The polar dibenzo-crown's aromaticity also delays estragole till last at 155°C. The non-polar large cyclic sesquiterpene hydrocarbon caryophyllene thus exhibits reasonable affinity for the Chiraldex and dicyclohexano-crown, appropriate strong retention on cholesteryl acetate, but little holdup on melted aromatics $(MBT)_2$ and azoxydiphenetole [2].

The Chiraldex capillary at 125°C or less thus shows similar responses in respect of good geraniol and caryophyllene retention to packed columns of dicyclohexano-24-crown-8 at 155°C and to unmelted $(MBT)_2$, although the capillary gives better chromatograms, or course. The six alcohol groups remaining in the Chiraldex-A-DA ring molecule (despite each sugar unit having dialkyl substituents) probably help to retain primary alcohols like geraniol, but not tertiary alcohols like α-terpineol. The packed column of dibenzo-24-crown-8-ether shows similar responses in respect of good estragole and poor geraniol retention to the "MPMS" liquid crystal capillary, and the latter is naturally the one to use, except for monoterpene hydrocarbons.

With regard to cyclic monoterpene hydrocarbons and substances of similar short retention times, the Chiraldex capillary cannot resolve cineole from γ-terpinene, nor limonene from *p*-cymene. Of the crown ethers these separations are surprisingly better on the polar dibenzo-crown as other overlaps appear on dicyclohexano-crown. A feature of both crown ethers is their strong affinity for *p*-cymene. This aromatic is also strongly retained by melted $(MBT)_2$ [10] and surprisingly well by isotropic cholesteryl acetate [4]. However, these two phases show low affinity for cineole, unlike the toroids.

ACKNOWLEDGEMENT

Thanks to Mr. B. MacKinnon for preparing the packed columns.

REFERENCES

1 T. J. Betts, C. A. Moir and A. I. Tassone, *J. Chromatogr.*, 547 (1991) 335.
2 T. J. Betts, *J. Chromatogr.*, 588 (1991) 231.
3 T. J. Betts, *J. Chromatogr.*, 587 (1991) 343.
4 T. J. Betts, *J. Chromatogr.*, 600 (1992) 337.
5 A. Ono, *Analyst (London)*, 108 (1983) 1265.
6 N. R. Ayyangar, A. S. Tambe and S. S. Biswas, *J. Chromatogr.*, 543 (1991) 179.
7 *Chiraldex Capillary GC Columns*, ASTED, Whippany, NJ 1990.
8 W. A. Konig, R. Krebber, P. Evers and G. Bruhn, *J. High Resolut. Chromatogr.*, 13 (1990) 328.
9 G. Takeoka, R. A. Flath, T. R. Mon, R. G. Buttery, R. Teranishi, M. Guntert, R. Lautamo and J. Szejtli, *J. High Resolut. Chromatogr.*, 13 (1990) 202.
10 T. J. Betts, *J. Chromatogr.*, 587 (1991) 343.

Journal of Chromatography, 606 (1992) 285–287
Elsevier Science Publishers B.V., Amsterdam

CHROM. 24 351

Short Communication

Gas chromatography–mass spectrometry method for the determination of the reducing end of oligo- and polysaccharides

Stanley F. Osman and Joanne O'Connor

US Department of Agriculture, ARS, Eastern Regional Research Center, 600 E. Mermaid Lane, Philadelphia, PA 19118 (USA)

(First received December 6th, 1991; revised manuscript received May 13th, 1992)

ABSTRACT

A gas chromatography–mass spectrometry (GC–MS) method for determining oligo- and polysaccharide reducing end-groups has been developed. This method, which is based on the monitoring of ions unique to the fragmentation of deuterated alditol acetates in mixtures also containing sugar acetates, can be used to identify the end-group and the degree of polymerization (DP). For the first time, GC–MS can be used in these types of analyses for polysaccharides of DP 100 or greater.

INTRODUCTION

An exopolysaccharide (EPS)-degrading enzyme isolated in our laboratory has the unusual property of not degrading the polymer to its basic subunit but to a lower-molecular-mass polysaccharide. In order to determine the specificity of this enzyme, and to confirm that it is indeed a polysaccharide depolymerase, it was necessary to determine the release of reducing end-groups in the depolymerization. End-groups have been determined by enzymatic, chromatographic and NMR methods, usually as a means of determining the degree of polymerization (DP) of polysaccharides. Use of enzymes is limited to those cases for which appropriate enzymes are available [1,2]. The chromatographic methods ultimately involve gas chromatographic (GC) separation of the alditol acetate (derived from $NaBH_4$ reduction of the reducing end) from a derivative, such as the aldononitrile acetate, of the internal sugars released on hydrolysis [3]. A GC–mass spectrometry (MS) method has been described that determines end-group by the sequence of reactions: sodium borodeuteride reduction, hydrolysis and sodium borohydride reduction [4]; the end-group/internal sugar ratio is then determined by the ratio of the deuterated ion, *m/z* 146, to the corresponding undeuterated ion, *m/z* 145, and retention time is used to determine the sugar. An NMR method [5] measures $NaBD_4$-reduced sugars before and after hydrolysis to get this ratio.

These analyses are often inaccurate when analyzing heteropolysaccharides, particularly when the relative concentration of end-groups to in-chain sugars is very small, which was the case for the polysaccharide we wished to analyze. The product of the

Correspondence to: Dr. S. F. Osman, US Department of Agriculture, ARS, Eastern Regional Research Center, 600 E. Mermaid Lane, Philadelphia, PA 19118, USA.

enzymatic treatment was still a relatively high-molecular-mass polymer (*ca.* 200 000), therefore it was necessary to characterize an end-group that was a minor fraction (*ca.* 1%) of the total mixture. The method described in ref. 3 could not be applied because it was impossible to resolve and observe the alditol peaks in the presence of the large amounts of glucose and galactose aldononitrile acetates; the small amount of alditols also precluded using a method that has been described for separating alditols by ion exchange prior to analysis [6]. The GC–MS method presented similar problems in that the intensity of the ion used to determine end groups, *i.e.*, 146, has a major contribution from the isotope peak of the ion at *m/z* 145. The method [4] is considered to be only reliable for oligosaccharides and therefore not suitable for our problem. For similar reasons, the NMR method was not applicable to our problem.

To overcome the drawbacks of the methods described, we have developed an end-group analysis that is based on GC–MS selective ion monitoring, but in contrast to the previously described GC–MS method, is not restricted by sugar composition and can be applied to polysaccharides with DP of *ca.* 100 or greater.

EXPERIMENTAL[a]

Materials

The isolation and characterization of *Pseudomonas marginalis* strain HT041B EPS has been described [7]. The EPS was depolymerized with an enzyme, to be described in a later publication, isolated from the same organism. The enzymatic depolymerization was monitored by measuring the change in viscosity of a solution of the EPS in aqueous 20 m*M* 4-(2-hydroxyethyl)-1-piperazineethanesulfonic acid (HEPES) buffer, pH 7.2.

Analysis

Polysaccharide solutions (*ca.* 1 mg/ml) were initially reduced with sodium borodeuteride (2 h at room temperature), neutralized with cation-exchange resin (Dowex 50W-X4) and then hydrolyzed for 1.5 h at 100°C with 0.5 *M* H_2SO_4 and then neutralized with $BaCO_3$ as previously described [7]. The hydrolysate was acetylated by reacting with pyridine–acetic anhydride (1:1, v/v) at 70°C for 30 min. The resultant deuterated alditol acetates were analyzed on a Hewlett-Packard 5995B GC–MS system, fitted with an SP-2330 (Supelco) capillary column (15 m × 0.25 mm I.D.), temperature programming the column for 150 to 250°C at 4°C/min. The ions at *m/z* 188 and *m/z* 218 in the mass spectrum were scanned to determine the presence of deuterated alditols.

[a] Mention of brand or firm names does not constitute an endorsement by the US Department of Agriculture over others of a similar nature not mentioned.

RESULTS AND DISCUSSION

The ions *m/z* 188 and *m/z* 218 are of relatively low intensity in the mass spectra of the deuterated alditol acetates (Table I) however they are not observed in the spectra of the corresponding aldose acetates. This feature makes it possible to detect very low concentrations of alditols in the presence of many fold excess of aldose acetates which is not possible with published methods, including the previously reported GC–MS method, for the reasons discussed in the introduction.

We have successfully used this method to determine the specificity of the enzymatic hydrolysis of an EPS, isolated from *P. marginalis* strain HT041B, which contains alternating glucose and galactose residues. The single-ion, co-chromatography GC–MS (Fig. 1a) unequivocally shows that enzymatic hydrolysis is at C-1 of glucose; *i.e.*, only deuterated glucitol acetate is present in the mixture after the reduction and derivatization of the hydrolysate as determined by the presence of *m/z* 188 and 218 at the retention time of glucitol acetate (end-group

TABLE I

ION INTENSITY (RELATIVE TO THE BASE PEAK = 100) OF DIAGNOSTIC IONS FOR DEUTERATED ALDITOL ACETATES

Deuterated alditol acetate	Relative ion intensity	
	m/z 188	*m/z* 218
Rhamnitol	12	8
Arabinitol	19	10
Glucitol	13	9

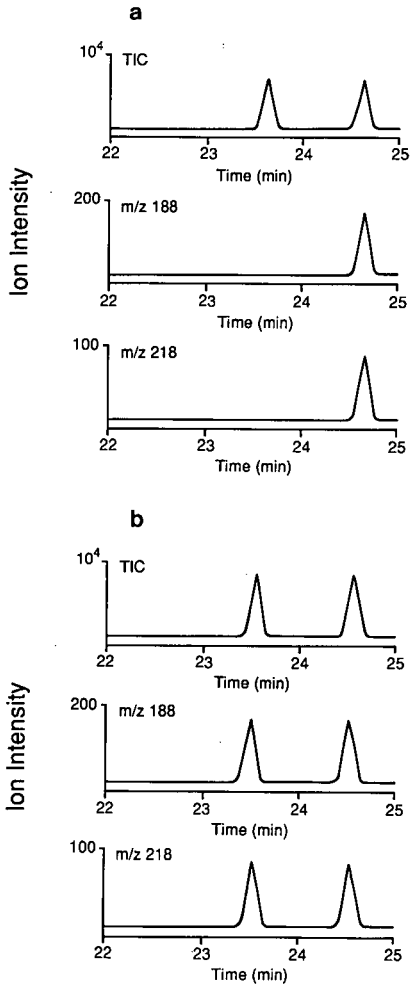

Fig. 1. GC–MS of (a) enzymatically and (b) chemically depolymerized *P. marginalis* EPS. Glucitol acetate retention time = 23.7 min, galactitol retention time = 24.6 min. TIC = Total ion current.

analysis for a partial chemical hydrolysis which yield, ultimately, deuterated glucitol and galactitol acetates is shown in Fig. 1b).

To determine the applicability of this method for determining molecular mass, a dextran molecular mass standard, (M_r = 20 000) was subjected to the analysis using a methyl silicone column for GC so that the separation of the sugar acetate anomers was eliminated, *i.e.*, the amount of internal sugar was determined by the measurement of only one peak (although one of the furanose anomers separated, it represents less than 1% of total sugar acetate mixture). The ratio of internal sugar to end-group was determined to be 127 which corresponds to a number-average molecular mass (M_n) of 20 592.

In conclusion, this relatively simple method can be used to characterize the reducing end of a polysaccharide without interference from the sugars within the polymer chain. The method is only limited in the determination of degree of polymerization by how accurately the deuterated alditol acetate/aldoze acetate ratio can be measured. For all the common sugars found in polysaccharides, identity of the alditol can be made unambiguously, on the basis of chromatographic retention time.

REFERENCES

1 D. J. Manners, J. Masson and R. J. Sturgeon, *Carbohydr. Res.*, 17 (1971) 109.
2 R. J. Sturgeon, *Carbohdr. Res.*, 30 (1973) 175.
3 I. M. Morrison, *J. Chromatogr.*, 108 (1975) 361.
4 A. Kamei, H. Yoshizumi, S. Akashi and K. Kagabe, *Chem. Pharm. Bull.*, 24 (1976) 1108.
5 W. J. Goux, *Carbohydr. Res.*, 173 (1988) 292.
6 H. Yamaguchi, S. Inamura and K. Kiyoshi, *J. Biochem. (Tokyo)*, 79 (1976) 299.
7 S. F. Osman and W. F. Fett, *J. Bacteriol.*, 171 (1989) 1760.

Journal of Chromatography, 606 (1992) 288–290
Elsevier Science Publishers B.V., Amsterdam

CHROM. 24 349

Short Communication

Application of enantioselective capillary gas chromatography in lipase-catalysed transesterification reactions in organic media

U. Bornscheuer, S. Schapöhler, Th. Scheper and K. Schügerl

Institut für Technische Chemie, Callinstrasse 3, W-3000 Hannover 1 (Germany)

W. A. König

Institut für Organische Chemie, Martin-Luther-King-Platz 6, W-2000 Hamburg 13 (Germany)

(First received February 18th, 1992; revised manuscript received May 13th, 1992)

ABSTRACT

The analysis of enantiomeric excesses of substrate and product during an enantioselective reaction can be performed easily with a chiral stationary phase based on γ-cyclodextrin. The transesterification of six related allylic alcohols to their corresponding acetates was catalysed by lipase from *Pseudomonas cepacia*.

INTRODUCTION

The determination of enantiomeric excesses is of great interest in the synthesis of enantiomerically pure pharmaceuticals. In addition to older methods such as the determination of the specific rotation, an increasing number of chiral stationary phases for gas and liquid chromatography and new chiral auxiliaries for NMR spectroscopy have been developed in recent years [1–3]. In the synthesis of enantiomerically pure compounds, the application of enzymes, especially lipases, in aqueous and organic solvents has also increased during recent years [4–8]. In our research, we investigated the enantioselective reaction of six related allylic alcohols and the influence of reaction conditions on the reaction progress and enantioselectivity [9]. The determination of enantiomeric excesses of substrate and product during the reaction was performed with a chiral stationary phase for gas chromatography (3-O-butyryl-2,6-di-O-pentyl-γ-cyclodextrin, Lipodex E) [10].

Correspondence to: Dr. U. Bornscheuer, Institut für Technische Chemie, Callinstrasse 3, W-3000 Hannover 1, Germany.

EXPERIMENTAL

The gas chromatograph used was an HRGC 5300 Mega series (Carlo Erba) with a 30-m Pyrex glass capillary coated with 3-O-butyryl-2,6-di-O-pentyl-γ-cyclodextrin (Lipodex E, Macherey–Nagel). Analysis conditions: injector temperature, 180°C; flame ionization detector temperature, 250°C; oven temperature, see Table II, carrier gas, hydrogen 55 kPa. Samples drawn during the reaction were centrifuged to separate them from the en-

0021-9673/92/$05.00

TABLE I

STRUCTURE OF THE ALLYLIC ALCOHOLS, COMPOUNDS **1–6**

Me = Methyl; Et = ethyl; *n*-Pr = *n*-propyl; Cyh = cyclohexyl; Ph = phenyl; CN = cyano; COMe = methoxy.

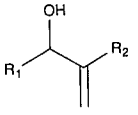

Compound	R_1	R_2
1	Me	CN
2	Et	CN
3	*n*-Pr	CN
4	Cyh	CN
5	Ph	CN
6	Me	COMe

zyme. The solution was then derivatized as follows: 200 μl of dichloromethane, 50 μl of trifluoroacetic acid (TFA) anhydride and 5 μl of the reaction solution were mixed. After evaporation of solvent and excess reagent, *n*-hexane was added for the analysis.

RESULTS AND DISCUSSION

The transesterification reactions were carried out with racemic allylic alcohols (Table I), cyclohexyl acetate as acyl donor and lipase from *Pseudomonas cepacia* at 40°C (for a detailed description, see ref. 9). The results of the analysis of enantiomeric excesses of the substrate (derivatized to the TFA ester) and corresponding acetates (product) are shown in Table II, the chromatogram of the analysis of compound **1** (TFA ester) is shown in Fig. 1. In the case of compounds **1-3**, both TFA ester and

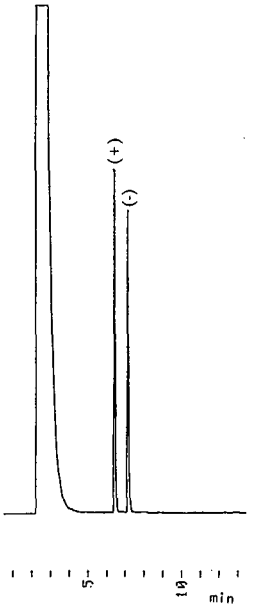

Fig. 1. Chromatogram of compound **1** (TFA ester) under the conditions described in the Experimental section with oven temperature 110γ and injection volume 0.2 μl.

TABLE II

α-VALUES, RETENTION TIMES AND ENANTIOMERIC EXCESSES OF THE SIX ALLYLIC ALCOHOLS (DETERMINED BY GC WITH LIPODEX E)

For compounds see Table I.

Compound	α-value		Retention time[a] [min (°C)]		Enantiomeric excess (%ee)		Acetate[c]
	TFA	Acetate	TFA[b]	Acetate[b]	TFA	Acetate	
1	1.118	1.258	6.23 (110)	9.13 (120)	11	98	(−)
2	1.390	1.262	7.18 (110)	11.05 (120)	5	63	(+)
3	1.428	1.238	8.33 (110)	12.90 (120)	21	75	(+)
4	1.075	–	8.34 (150)	–	9	[d]	(+)
5	–	1.023	–	19.60 (160)	8	76	(+)
6	1.147	–	10.78 (100)	–	25	86	(−)

[a] Retention time of first enantiomer.
[b] Oven temperature (isothermal).
[c] Specific rotation (determined by polarimetry).
[d] Not measured.

acetate could be separated into the enantiomers, resulting in high α-values using the enantioselective capillary gas chromatography. For compounds **4** and **6**, the separation of the acetate failed, compound **5** was only separated using the acetate.

The use of enantioselective capillary gas chromatography allows an effortless monitoring of the reaction progress. This is of great interest in the field of chemical engineering, especially for kinetic studies.

ACKNOWLEDGEMENTS

The authors thank Professor H. M. R. Hoffmann and his co-workers from the Institute of Organic Chemistry of the University of Hannover for providing them with the allylic alcohols.

REFERENCES

1 W. A. König, *Nachr. Chem. Tech. Lab.*, 37 (1989) 471.
2 R. Wiesner and H. Kühn, *GIT Supplement*, 3 (1989) 32.
3 R. Matusch and C. Coors, *Angew. Chem.*, 101 (1989) 624.
4 Z. F. Xie, H. Suemune and K. Sakai, *Tetrahedron Asymmetry*, 1 (1990) 395.
5 A. Kamal and M. V. Rao, *Tetrahedron Asymmetry*, 2(1991) 751.
6 P. A. Fitzpatrick and A. M. Klibanov, *J. Am. Chem. Soc.*, 113 (1991) 3166.
7 R. Bovara, G. Carrea, L. Ferrara and S. Riva, *Tetrahedron Asymmetry*, 2 (1991) 931.
8 K. Burgess and I. Henderson, *Tetrahedron Asymmetry*, 1 (1990) 57.
9 U. Bornscheuer, S. Schapöhler, T. Scheper and K. Schügerl, *Tetrahedron Asymmetry*, 2 (1991) 323.
10 W. A. König, R. Krebber and P. Mischnick, *J. High Res. Chromatogr.*, 12 (1989) 732.

Journal of Chromatography, 606 (1992) 291–296
Elsevier Science Publishers B.V., Amsterdam

CHROM. 24 276

Short Communication

Improvements in the method developed for performing isoelectric focusing in uncoated capillaries

Jeff R. Mazzeo and Ira S. Krull

Department of Chemistry, Barnett Institute, 341 MU, Northeastern University, Boston, MA 02115 (USA)

(First received January 7th, 1992; revised manuscript received April 6th, 1992)

ABSTRACT

Capillary isoelectric focusing run times were reduced from 30 to 5 minutes through reversing the polarity and shortening the separation distance. Complete resolution was only obtained by increasing the concentration of tetramethylethylenediamine in the sample solution. Problems previously seen with acidic proteins were shown to be due to anodic drift in the ampholyte gradient, and were minimized by increasing the concentration of phosphoric acid in the anode buffer. The inability of the method to tolerate protein samples with salt is also discussed.

INTRODUCTION

In a previous report [1], we described the development of a method for performing isoelectric focusing (IEF) in uncoated capillaries without the need for performing salt mobilization, as opposed to the traditional method of performing IEF in coated capillaries with salt mobilization [2–8]. This procedure relied upon the maintenance of some electroendosmotic flow (EOF), such that proteins spent sufficient time in the capillary to focus but were mobilized past a stationary detection point by residual EOF. Control of EOF was achieved by adding methyl cellulose to the sample–ampholyte mixture. Furthermore, it was necessary to supplement the pH 3–10 ampholytes with tetramethylethylenediamine (TEMED) so that basic proteins would focus in the region prior to the detection point, with the TEMED acting to block the region after the detection point [9,10]. A similar method has been reported by Thormann *et al.* [11], with the difference being that only a small plug of the sample–ampholyte mixture is introduced into the capillary filled with catholyte, as opposed to filling the whole capillary with the sample–ampholyte mixture, as in our case. In their method, it is not necessary to add TEMED to the ampholytes.

In this note, we wish to describe two improvements we have made to our capillary IEF (cIEF) method. Firstly, we will describe instrumental changes allowing run times to be decreased to less than 15 min with no sacrifice in resolution, and to about 5 min with some loss in resolution, compared to run times of about 30 min previously [1]. Furthermore, we will show that the problems with poor peak shape of acidic proteins are due to pH gradient decay, and can be improved by increasing the anode buffer concentration. We will also report the maximum concentration of salt in the sample which can be tolerated before serious loss in resolution is seen.

Correspondence to: Professor I. S. Krull, Department of Chemistry, Barnett Institute, 341 MU, Northeastern University, Boston, MA 02115, USA.

0021-9673/92/$05.00

EXPERIMENTAL

Chemicals

All chemicals, capillaries and instrumentation were as previously reported [1]. β-Lactoglobulin was from Sigma (St. Louis, MO, USA).

Capillary isoelectric focusing

In all cases, the sample was 0.5 mg/ml cytochrome *c*, chymotrypsinogen A, β-lactoglobulin A and 0.25 mg/ml myoglobin, 5% Pharmalyte 3–10 and 0.1% methyl cellulose TEMED concentration was in the range 0.5–1.6%. The catholyte was always 20 m*M* NaOH, while the anolyte varied from 10–100 m*M* H_3PO_4. In the salt concentration study, the sample was made 5, 10, 25 and 50 m*M* NaCl. The instrument, ISCO Model 3850 (Lincoln, NE, USA), was operated in the reverse polarity mode, such that the position of the cathode was 40 cm away from the detection point, and the anode was 20 cm further away. In all cases, the applied voltage was 24 kV, generating a field of 400 V/cm. Detection was at 280 nm.

RESULTS AND DISCUSSION

Decreasing migration time

The migration time of proteins in this method depends on which point in the capillary they are detected. Due to EOF, the migration direction is towards the cathode; the closer to the cathode they are detected, the longer the migration time. Thus, an apparently easy way to decrease migration time is to detect the proteins closer to the anode. However, there are several things which must be taken into account. First, wherever the detection point is in the capillary, it is required that all proteins focus on the anodic side of the window for them to be detected. The place where proteins focus in the capillary can be controlled by changing the concentration of TEMED. Higher concentrations of TEMED block more of the cathodic end of the capillary, causing proteins to focus closer to the anode. Secondly, it is important to detect the proteins at a point when they are completely focused. Otherwise, they will not be completely resolved. For any set of experimental conditions, there is a certain amount of time which is required to achieve complete focusing and resolution. In cases where the highest resolution is required, the total run time is limited to some time greater than this minimum amount of time. Of course, one can throw away some resolution in order to achieve faster run times.

In the previously reported separations [1], the total separation distance, that is, the distance from anode to detection point, was 40 cm, with a total capillary length of 60 cm. The instrument we are using requires a minimum capillary length of about 40 cm from the "hot" electrode (+ or −) to the detection point, and a minimum capillary length of 20 cm from the detection point to the ground electrode. Thus, shortening the separation distance and the run time could only be achieved by reversing the polarity and making the ground electrode the anode and the "hot" electrode the cathode. This leads to a separation distance of 20 cm, half of that previously used.

When the optimal conditions from the previous set-up are used in the reverse polarity set-up, the separation in Fig. 1 is obtained. Note that the migration time of the peak corresponding to p*I* 6.8, peak 4, is about 6 min, compared to 21 min in the previous set-up [1]. However, the peaks are broader than in the previous case and resolution is incomplete between the peaks corresponding to p*I* 7.2 and 6.8, peaks 3 and 4. Furthermore, chymotrypsinogen A, peak 2, shows up as only one peak, whereas before there were several minor peaks of lower p*I* just after the main peak. The broader peaks and lower resolution can be explained by assuming that the proteins have not yet fully focused. This suggests that the concentration of TEMED should be increased, with all other conditions the same.

Fig. 2. shows the same separation as in Fig. 1, with the exception that the TEMED concentration has been increased from 1.0 to 1.2%. Note that the migration time of the peak corresponding to p*I* 6.8, peak 4, has increased from 6 to 8.5 min, and that the peaks are much sharper and better resolved, as was expected. Theoretical plates for the peaks in Fig. 2 range from 200 to 400 000. However, since IEF is not an equilibrium-based separation technique, it is really inappropriate to report plates for the peaks.

When even higher concentrations of TEMED were used, better resolution and longer run times were achieved. At higher concentrations of TEMED, the proteins are focusing closer to the anode, further and further away from the detection

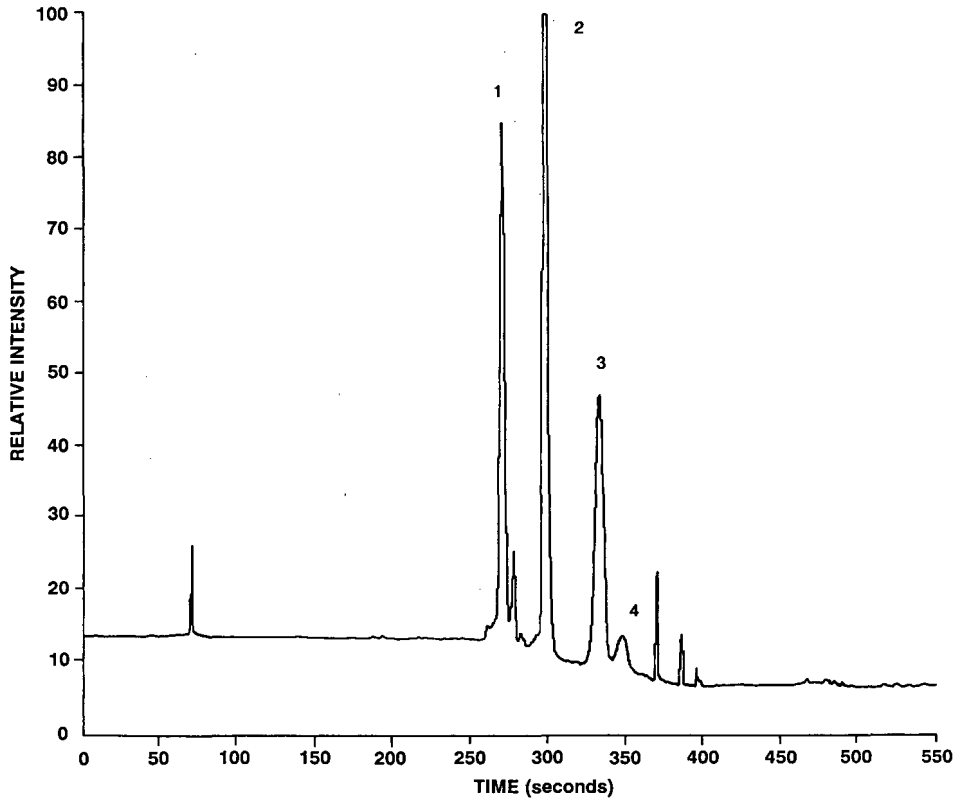

Fig. 1. cIEF of protein mixture using reverse polarity set-up. Capillary: 75 μm I.D., uncoated, 60 cm total length, 20 cm anode to detection. IEF: anolyte 10 m*M* H_3PO_4, catholyte 20 m*M* NaOH, voltage 24 kV. Detection: UV, 280 nm. Sample: 0.5 mg/ml cytochrome *c*, chymotrypsinogen A and β-lactoglobulin A, 0.25 mg/ml myoglobin, 5% Pharmalyte 3–10, 1.0% TEMED, 0.1% methyl cellulose. Peaks: 1 = cytochrome *c*, p*I* 9.6; 2 = chymotrypsinogen A, p*I* 9.1; 3 = myoglobin, p*I* 7.2; 4 = myoglobin, p*I* 6.8.

window. Thus, changing the TEMED concentration is a convenient way of changing run time and resolution. Faster run times can be achieved by lowering the concentration of TEMED, with a sacrifice in resolution. Better resolution can be achieved with higher concentrations of TEMED, at the expense of longer run times. However, there is a limited window of TEMED concentration which can be used. If the TEMED concentration is too low, some basic proteins may focus past the detection point. If the concentration is too high, excessive current will be generated, leading to problems with joule heating. We have found that TEMED concentrations of 0.5–1.6% can be employed with the 20-cm separation distance.

Improved separation of acidic proteins

In both Figs. 1 and 2, it is very difficult to determine which peak, if any, corresponds to β-lactoglobulin A, p*I* 5.1. One could argue that within the time frame monitored, β-lactoglobulin A did not migrate past the detection point. In Fig. 2, a plot of migration time *vs.* p*I* was linear with $r^2 = 0.997$. Based on the equation for this line, the expected migration time for β-lactoglobulin was 11 min. This assumes that all proteins are moving with the same velocity, which would be true if EOF was the sole source of mobilization in the capillary. However, as has been discussed and studied extensively [12–14], ampholyte gradients are known to suffer from pH gradient decay, whereby the basic end of the gradient migrates towards the cathode (cathodic drift)

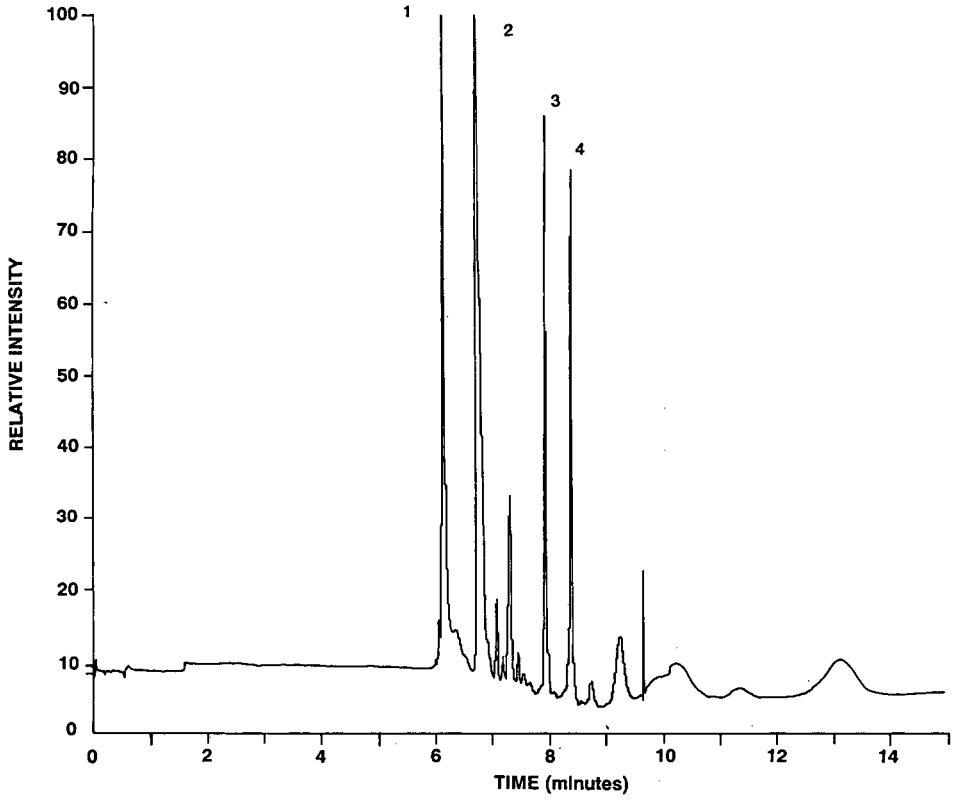

Fig. 2. cIEF of protein mixture using reverse polarity set-up, 1.2% TEMED. Conditions as in Fig. 1, except 1.2% TEMED. Peaks as in Fig. 1.

and the acidic end migrates toward the anode (anodic drift). We must assume that pH gradient decay is also occurring in our system [15]. Thus, the assumption that all proteins are migrating with the same velocity is not correct. Basic proteins will migrate with the additive sum of EOF and any cathodic drift, since they are in the same direction. Neutral proteins will migrate with EOF predominantly. Acidic proteins experience EOF toward the cathode and, in opposition to that, anodic drift toward the anode.

The clear solution to the problems with acidic proteins is to minimize any anodic drift. In a recent paper by Mosher and Thormann [12], it was pointed out that the extent of drift in ampholyte systems strongly depends on the phosphoric acid and sodium hydroxide concentrations. In all of our work, we have used 10 m*M* phosphoric acid and 20 m*M* sodium hydroxide, as was most commonly used in other cIEF separations [2–8]. According to the work of Mosher and Thormann, this ratio of concentrations leads to both cathodic and anodic drift, with the anodic drift being much worse. This would explain the poor peak shapes and inability to detect acidic proteins in our system. The solution, again according to the work of Mosher and Thormann, is to use higher concentrations of phosphoric acid, which will minimize anodic drift while increasing cathodic drift.

It is clear that the concentration of phosphoric acid must be optimized to successfully separate acidic proteins in our system. The concentration must be high enough to minimize anodic drift, but not so high that it increases cathodic drift to the point that basic proteins are detected when they have not yet fully focused and resolved.

Holding all other conditions the same as in Fig. 2, we have investigated phosphoric acid concentra-

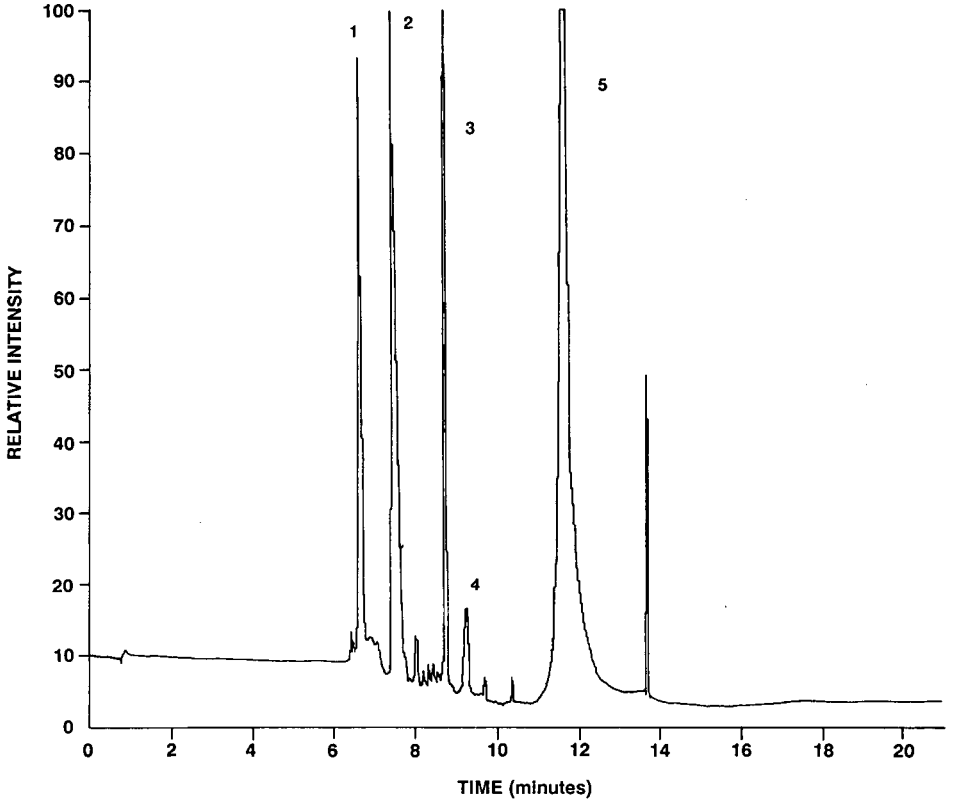

Fig. 3. cIEF of protein mixture using reverse polarity set-up, 25 m*M* H_3PO_4. Conditions as in Fig. 1, except 1.2% TEMED and 25 m*M* H_3PO_4. Peaks: 1 = cytochrome *c*, p*I* 9.6; 2 = chymotrypsinogen A, p*I* 9.1; 3 = myoglobin, p*I* 7.2; 4 = myoglobin, p*I* 6.8; 5 = β-lactoglobulin A, p*I* 5.1.

tions of 10, 15, 20, 25, 30, 50 and 100 m*M*. Fig. 3 shows the same separation in Fig. 2, with the exception that the concentration of phosphoric acid was 25 m*M*. A full scale peak at 12 min is now seen, peak 5, which corresponds to β-lactoglobulin A. We have found that concentrations of phosphoric acid ranging from 20 to 30 m*M* give about the same results, with lower concentrations giving no peak and higher concentrations leading to poor resolution in the basic region of the gradient.

Notice that the peak corresponding to β-lactoglobulin A is much broader than the basic and neutral protein peaks. This is most likely due to the fact that it is not moving with the same velocity as the other peaks, since the width of a peak in this system is a function of the speed with which a protein migrates past the detection point. At best, it would be expected that the fastest an acidic protein like β-lactoglobulin A could move is the speed of EOF. It is unlikely that a protein as acidic as β-lactoglobulin A would experience any cathodic drift, as the basic and neutral proteins do. From the data in Fig. 3, a plot of migration time *vs.* p*I* gave $r^2 = 0.951$ when the migration time of β-lactoglobulin A was included, and $r^2 = 0.997$ when not included. This also suggests that β-lactoglobulin is not migrating at the same speed as the other proteins.

This less than ideal peak shape and separation of acidic proteins is a problem which may be overcome by using capillaries which show EOF in the direction toward the anode, *i.e.*, capillaries which have been modified with a cationic sufactant. In this case, EOF and anodic drift will be in the same direction. However, then there will be a problem with basic proteins. Thus, using EOF-driven cIEF, it may never be possible to achieve optimal resolution throughout the entire pH gradient. Nevertheless, it is possible to do all proteins, acidic, neutral and

basic, using one set of experimental conditions. It is clear that cIEF is a unique and informative way to study the anodic and cathodic drift associated with ampholyte gradients.

Effect of salt concentration

In applying the method to samples of recombinant proteins for characterization, we have found that salt in the protein sample can greatly affect the separation, usually leading to higher initial focusing current and poor separation. It is well known that IEF is intolerant to salt. We wished to determine the maximum salt concentration which could be tolerated by our method. Using the same conditions in Fig. 3, we found that when the concentration of NaCl in the sample exceeded 10 m*M*, the separation was totally lost. Thus, it is imperative that samples be desalted prior to separation using this method. The same has also been said when using other cIEF methods [9].

CONCLUSIONS

We have described a simple way to decrease run times in the cIEF method from 30 min to as low as 5 min, with some sacrifice in resolution. Previous problems with the poor separation of acidic proteins have been shown to be due to anodic drift present in the ampholyte gradient, and were minimized by increasing the concentration of phosphoric acid. Finally, it has been shown that a maximum of 10 m*M* salt can be tolerated by this method.

ACKNOWLEDGEMENT

This work was supported, in part, by a grant from ISCO, Inc., as well as via donation of an ISCO HPCE instrument to Northeastern University. This is contribution number 538 from the Barnett Institute at Northeastern University.

REFERENCES

1 J. R. Mazzeo and I. S. Krull, *Anal. Chem.*, 63 (1991) 2852.
2 S. Hjertén and M. D. Zhu, *J. Chromatogr.*, 346 (1985) 265.
3 S. Hjertén, *J. Chromatogr.*, 347 (1985) 191.
4 S. Hjertén, J. L. Liao and K. Ya, *J. Chromatogr.*, 387 (1987) 127.
5 S. Hjertén, K. Elenbring, F. Kilar, J. L. Liao, J. C. Chen, C. Siebert and M. D. Zhu, *J. Chromatogr.*, 403 (1987) 47.
6 F. Kilar and S. Hjertén, *J. Chromatogr.*, 480 (1989) 351.
7 F. Kilar and S. Hjertén, *Electrophoresis*, 10 (1989) 23.
8 M. D. Zhu, D. L. Hansen, S. Burd and F. Gannon, *J. Chromatogr.*, 480 (1989) 311.
9 M. D. Zhu, R. Rodriguez and T. Wehr, *J. Chromatogr.*, 559 (1991) 479.
10 G. Yao-Jun and R. Bishop, *J. Chromatogr.*, 234 (1982) 459.
11 W. Thormann, J. Caslavska, S. Molteni and J. Chmelik, *J. Chromatogr.*, 589 (1992) 321.
12 R. A. Mosher and W. Thormann, *Electrophoresis*, 11 (1990) 717.
13 R. A. Mosher, W. Thormann and M. Bier, *J. Chromatogr.*, 351 (1986) 31.
14 R. Hagedorn and G. Fuhr, *Electrophoresis*, 11 (1990) 281.
15 J. R. Mazzeo and J. S. Krull, *J. Microcolumn Sep.*, 4 (1992) 29.

Journal of Chromatography, 606 (1992) 297–298
Elsevier Science Publishers B.V., Amsterdam

CHROM. 24 376

Book Review

Modern methods of polymer characterization, edited by H. G. Barth and J. W. Mays, Wiley-Interscience, New York, 1991, X + 561 pp., price US$ 186.00, ISBN 0-471-82814-9.

This volume forms Volume 113 of *Chemical Analysis: A Series of Monographs on Analytical Chemistry and its Applications*. The work consists of twelve chapters, the first three concerning various uses of size-exclusion chromatography (SEC). The first chapter details the characterization of polymers that are heterogeneous in more than one distributed property. It concentrates on techniques employing SEC and high-performance liquid chromatography where the added features of absorption and partition mechanisms extend the application of the procedures.

Chapter 2 considers the processing of data in SEC as applied to both simple and complex polymers while Chapter 3 summarises the current state of application of the technique to measurement of the variation of long-chain branching with molecular weight.

Chapter 4, Polymer analysis by field-flow fractionation (FFF), is offered as an alternative to SEC and two sub-techniques are considered namely thermal FFF and flow FFF. The retention mechanisms associated with general, thermal and flow FFF are described together with the fractionation range applicable. The chapter concludes with the characterization of polydisperse materials and a comparison of FFF and SEC.

Characterization by inverse gas chromatography forms Chapter 5 and following the theoretical basis and experimental techniques some applications are indicated with tabulation of determinations from the literature.

The use of Osmometry forms Chapter 6 and the basic properties of membrane and vapour pressure osmometry are indicated. The limited recent developments in the area are apparent from the bibliography, the latest references being almost a decade old. Dilute solution viscosity forms Chapter 7 and again details an old established technique and the chapter as indicated reviews the current status of viscometric characterization.

Chapter 8 concerns use of the ultracentrifuge and other light scattering methods which provide an absolute measure of molecular weight. While ultracentrifugal methods are time consuming some technique improvements have been developed, the availability of multicell apparatus from both American and European manufacturers and computer assisted data analysis has assisted utilization. Low-angle laser light scattering forms Chapter 9 developed during the 1970s has extended static light scattering methods and here its use as a detector for SEC is included. Theory and instrumentation form much of the contribution followed briefly by errors and some applications both to water-soluble and organosoluble macromolecules.

Photon correlation spectroscopy, quasielectric light scattering or dynamic light scattering forms Chapter 10. The chapter reviews these newer light scattering techniques as applied to polymer systems together with the theoretical background, the instrumentation and concluding with a comparison of results with those obtained using other techniques.

NMR characterization of polymers forms Chapter 11 and deals primarily with high resolution NMR. The basic techniques of ^{2}H and ^{13}C NMR are indicated and the determination of polymer microstructure, polymer mechanisms, polymer dynamics and interactions and morphology and structure property correlations are shown as the major applications of NMR to polymer systems.

The final chapter reviews the use of mass spec-

trometry (MS) in polymer characterization. Ionisation techniques have been developed by laser absorption, electrospray, thermospray and fast atom bombardment and these have increased the application to polymers. A number of examples of polymerization mechanisms by MS–MS, time resolved polymerization using Fourier transform MS and some high-performance liquid chromatography–MS analyses of antioxidants and epoxide oligomers completes the contribution.

The volume generally reviews the methods of polymer characterization and while new developments form the minority of the work it is certainly recommended as a worthy addition to the libraries of those working in the polymer area.

Kensington (Australia) J. K. Haken

Journal of Chromatography, 606 (1992) 299–300
Elsevier Science Publishers B.V., Amsterdam

CHROM. 24 364

Book Review

Rapid methods for analysis of food and food raw material, edited by W. Baltes, Technomic Publishing Co., Lancaster, 1990, 392 pp., price SFr. 143.00, ISBN 0-87762-794-0.

Twenty-three authors have contributed to this volume covering various aspects of food analysis. After a general review by K. Matissek on rapid methods for food analysis indicating the possibilities and limits and outlining the scope of the monograph, the topic moves to the description of rapid tests in food analysis (K. G. Schmidt) and a description of the equipment needed for rapid methods in food quality control (K. H. Torkler). Potentiometric methods and applications of ion-selective electrodes are described by F. Honold and K. Camman. Trace metal analysis is dealt with in the fifth chapter by H. J. Hoffmann.

Chromatographers, however, are more likely to be interested in the reviews written by Jork (Thin-layer chromatography, a screening method for food analysis), Engelhardt (High-performance liquid chromatography: reflections on application in food analysis) and Witkowski (Fast quality control by headspace analysis). The chapter written by Eichner (Characterization of changes during processing and storage by chromatographic determination of tracer substances) is also rich in chromatographic approaches.

Somewhat misplaced is the discussion by Schreier and Fröhlich of rapid sample preparation for instrumental analysis, which, in my opinion, is more general and should have been moved to somewhere at the beginning of the volume.

Other instrumental methods that can be seen in food analysis laboratories are adequately covered: infrared spectroscopic methods are dealt with by Rudzik, near-infrared by Zaeschman (although limited to dairy products only) and NMR by Barker.

Today, when everybody is looking for "natural" foods not affected (or contaminated) by all the chemistry used in agriculture and meat production, the chapter on rapid methods for drug and fattening substances in animals (Büning-Pfaue) will certainly be welcomed.

Methods of enzymatic analysis refer to the application of such procedures to carbohydrates, organic and inorganic acids and alcohols (Henniger).

It is interesting to see a chapter on isotachophoresis in this volume (by Offizorz); however, this chapter is limited to a general introduction only.

The final three chapters are devoted to methods of sensory analysis of foods (Fricker), methods of evaluating the reheology, particle size and consistency of foods (Windhab) and evaluation of the microbiological status of foods and food raw materials (Zschaler).

This book is certainly not an exhaustive treatise on food analysis methods. The Editor has rather selected some approaches that can be classified as rapid: in spite of the description on p. 18, this is a slightly vague definition, but nevertheless the methods used are indeed fast. Obviously the book has found its market as the reviewed English version is a translation of the German edition that was published some time ago. The approach to the subject is at the level of a textbook for an advanced graduate course. Chromatographers are likely to look for more details in the chromatographic procedures and, perhaps, they will miss some recent techniques such as capillary zone electrophoresis. On the other hand, one has to bear in mind that there is always a time lag between a methodological advance and its penetration into the various fields of application, of which food science is a typical example. The book is rich in reference data and also from this point of view it can serve as a good vade-mecum to graduate

students (this is probably one of the reasons for its commercial success in the German version).

Of course, as every book, including this one, has some features that can be classified as drawbacks and that the reviewer has to point out at least to prove that he really has read the book with meticulous care. What I personally disliked was the placement of some generally oriented chapters in the middle rather than at the beginning of the book (typically Chapter 9) and the quality of some figures (typically Fig. 1, p. 271; the greyish box shown there on a black background is not very instructive: I believe that an NMR spectrometer is presented here, but the instrument shown could be virtually anything). Also, I do not think that the separate numbering of figures in individual chapters starting always from "1" is desirable, although from the Editor's point of view certainly the easiest. The book would have benefited considerably from a subject index or, even better, an index of the food constituents dealt with. To answer the rather obvious question of what categories of compounds the rapid methods are used for is difficult with the presentation adopted.

In conclusion, I do not think that the shortcomings summarized above devalue the book; they are within the normal limits for a multi-author volume. Overall I enjoyed reading this monograph and I expect the English version to be as successful as its German predecessor.

Prague (Czechoslovakia) Zdenek Deyl

Author Index

Errata

J. Chromatogr., 585 (1991) 247–254

Page 249, right column, 14th line from the top: "0.05 *M* ammonium acetate buffer (pH 3.8)–acetonitrile (30:70, v/v)" should read "0.05 *M* ammonium acetate buffer (pH 3.8)–acetonitrile (70:30, v/v).

Page 250, left column, 13th line from the bottom: "0.05 *M* ammonium acetate buffer (pH 3.8)–acetonitrile solution (38:62)" should read "0.05 *M* ammonium acetate buffer (pH 3.8)–acetonitrile solution (62:38)".

Errata

J. Chromatogr., 603 (1992) 35–42 corrected 7 ottobre 35

Page 39, Table V:

Table heading, line below title should read:

...Eluent, methanol–water (methanol from 61 to 83%, v/v).

For Toluene, value under "Mean ± S.D." should read 3.45 ± 0.14.

For Nitrobenzene, value onder "3" should read 3.04.

Page 42, Table IX: please find below a a corrected version, with values for sodium nitrite and methanol interchanged.

TABLE IX

EFFECT OF DEAD TIME MEASUREMENTS ON *S* INDEX

Column, Polygosil-C_{18}; eluent, methanol–water. Dead times were measured using sodium nitrite and methanol as a non-retained compound. For experimental conditions, see text.

Compound	Non-retained compound	Methanol concentration (%, v/v)			*S*
		90	80	70	
Nitrobenzene	Sodium nitrite	0.35	0.64	1.26	2.75
	Methanol	0.29	0.55	1.08	2.84
Naphthalene	Sodium nitrite	0.81	1.80	4.55	3.75
	Methanol	0.73	1.64	4.12	3.77
Toluene	Sodium nitrite	0.61	1.25	2.77	3.29
	Methanol	0.54	1.12	2.48	3.33
Acenaphthene	Sodium nitrite	1.47	3.64	10.33	4.23
	Methanol	1.36	3.37	9.47	4.21

PUBLICATION SCHEDULE FOR 1992

Journal of Chromatography and *Journal of Chromatography, Biomedical Applications*

MONTH	O 1991–M 1992	J	J	A	S	O	N	D
Journal of Chromatography	Vols. 585–600	602/1 + 2 603/1 + 2 604/1	604/2 605/1 605/2 606/1	606/2 607/1 607/2	608/1 + 2 609/1 + 2			
Cumulative Indexes, Vols. 551–600		[a]						
Bibliography Section	610/1	610/2			611/1			611/2
Biomedical Applications	Vols. 573–577/1	577/2	578/1 578/2	579/1	579/2 580/1 + 2	[b]		

[a] Cumulative Indexes will be Vol. 601, to appear early 1993.
[b] The publication schedule for further issues will be published later.

INFORMATION FOR AUTHORS

(Detailed *Instructions to Authors* were published in Vol. 558, pp. 469–472. A free reprint can be obtained by application to the publisher, Elsevier Science Publishers B.V., P.O. Box 330, 1000 AH Amsterdam, The Netherlands.)

Types of Contributions. The following types of papers are published in the *Journal of Chromatography* and the section on *Biomedical Applications:* Regular research papers (Full-length papers), Review articles and Short Communications. Short Communications are usually descriptions of short investigations, or they can report minor technical improvements of previously published procedures; they reflect the same quality of research as Full-length papers, but should preferably not exceed five printed pages. For Review articles, see inside front cover under Submission of Papers.

Submission. Every paper must be accompanied by a letter from the senior author, stating that he/she is submitting the paper for publication in the *Journal of Chromatography*.

Manuscripts. Manuscripts should be typed in double spacing on consecutively numbered pages of uniform size. The manuscript should be preceded by a sheet of manuscript paper carrying the title of the paper and the name and full postal address of the person to whom the proofs are to be sent. As a rule, papers should be divided into sections, headed by a caption (*e.g.*, Abstract, Introduction, Experimental, Results, Discussion, etc.). All illustrations, photographs, tables, etc., should be on separate sheets.

Introduction. Every paper must have a concise introduction mentioning what has been done before on the topic described, and stating clearly what is new in the paper now submitted.

Abstract. All articles should have an abstract of 50–100 words which clearly and briefly indicates what is new, different and significant.

Illustrations. The figures should be submitted in a form suitable for reproduction, drawn in Indian ink on drawing or tracing paper. Each illustration should have a legend, all the *legends* being typed (with double spacing) together on a *separate sheet*. If structures are given in the text, the original drawings should be supplied. Coloured illustrations are reproduced at the author's expense, the cost being determined by the number of pages and by the number of colours needed. The written permission of the author and publisher must be obtained for the use of any figure already published. Its source must be indicated in the legend.

References. References should be numbered in the order in which they are cited in the text, and listed in numerical sequence on a separate sheet at the end of the article. Please check a recent issue for the layout of the reference list. Abbreviations for the titles of journals should follow the system used by *Chemical Abstracts*. Articles not yet published should be given as "in press" (journal should be specified), "submitted for publication" (journal should be specified), "in preparation" or "personal communication".

Dispatch. Before sending the manuscript to the Editor please check that the envelope contains four copies of the paper complete with references, legends and figures. One of the sets of figures must be the originals suitable for direct reproduction. Please also ensure that permission to publish has been obtained from your institute.

Proofs. One set of proofs will be sent to the author to be carefully checked for printer's errors. Corrections must be restricted to instances in which the proof is at variance with the manuscript. "Extra corrections" will be inserted at the author's expense.

Reprints. Fifty reprints of Full-length papers and Short Communications will be supplied free of charge. Additional reprints can be ordered by the authors. An order form containing price quotations will be sent to the authors together with the proofs of their article.

For Superior Chiral Separation

From Analytical to Semi-preparative column

HPLC column output is directly proportional to cross section

● Analytical column
0.46cmϕ×25cm

● Semi-preparative column
2cmϕ×25cm

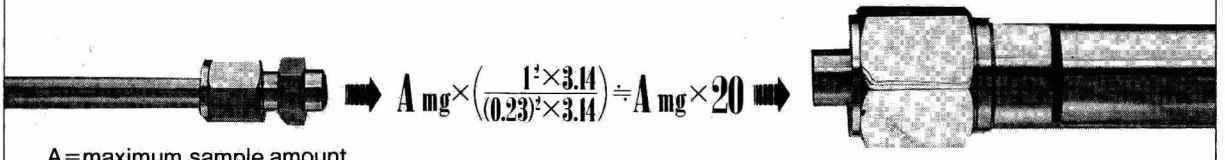

$$A\ mg \times \left(\frac{1^2 \times 3.14}{(0.23)^2 \times 3.14}\right) \div A\ mg \times 20$$

A=maximum sample amount of Analytical column

Analytical column

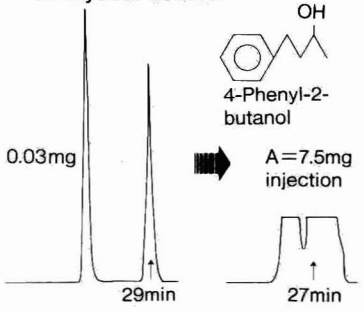

CHIRALCEL OD	column	CHIRALCEL OD
0.46cmϕ×25cm	column size	2cmϕ×25cm
10μm	Particle size	10μm
Hexane/IPA (9:1)	eluent	Hexane/IPA (9:1)
0.3ml/min.	flow rate	6ml/min.
UV 254nm	detection	UV 254nm
max 0.03mg→7.5mg	injection amount	7.5mg×20=150mg

Semi-preparative column

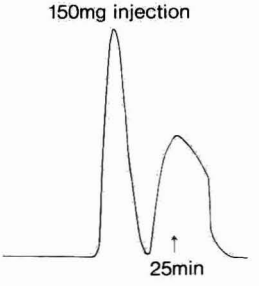

● Standard Available Column

● CHIRALPAK® /CHIRALCEL® (Particle size 10μm)

	I. D. Length
Analytical column	0.46cmϕ×25cm
Pre-column	0.46cmϕ× 5cm
Semi-preparative column	1cmϕ×25cm
	2cmϕ×25cm

● CROWNPAK™ (Particle size 5μm)

	I. D. Length
Analytical column	0.4cmϕ×15cm
Pre-column	0.4cmϕ× 1cm

CHIRAL TECHNOLOGIES, INC.
730 SPRINGDALE DRIVE
DRAWER I
EXTON, PA 19341
Phone: 215-594-2100
Fax: 215-594-2325

DAICEL (EUROPA) GmbH
Oststr. 22
4000 Düsseldorf 1, Germany
Phone: 49/211/369848
Telex: (41) 8588042 DCEL D
Fax: 49/211/364429

DAICEL CHEMICAL INDUSTRIES, LTD.
8-1, Kasumigaseki 3-chome, Chiyoda-ku, Tokyo 100, Japan
Phone: 81-3-3507-3151 Fax: 81-3-3507-3193